University of Wisconsin Milwaukee
UWM Digital Commons

December 2016

A Multi-Faceted Biogeochemical Approach to Analyzing Hypoxia in Green Bay, Lake Michigan

Shelby LaBuhn
University of Wisconsin-Milwaukee

Follow this and additional works at: https://dc.uwm.edu/etd

Part of the Biogeochemistry Commons, Environmental Sciences Commons, and the Fresh Water Studies Commons

A MULTI-FACETED BIOGEOCHEMICAL APPROACH TO ANALYZING HYPOXIA IN GREEN BAY, LAKE MICHIGAN

by

Shelby Lynne LaBuhn

A Dissertation Submitted in

Partial Fulfillment of the

Requirements for the Degree of

Doctor of Philosophy

in Freshwater Sciences

at

The University of Wisconsin-Milwaukee

December 2016

ABSTRACT

A MULTI-FACETED BIOGEOCHEMICAL APPROACH TO ANALYZING HYPOXIA IN
GREEN BAY, LAKE MICHIGAN

by

Shelby LaBuhn

The University of Wisconsin-Milwaukee 2016
Under the Supervision of Professor Dr. J. Val Klump

Green Bay, Lake Michigan is a large freshwater estuary that has experienced seasonal hypoxia

for decades. Hypoxia, or dissolved oxygen concentrations less than 2 mg L^{-1}, is a problem in

coastal ecosystems around the world because it has a negative impact on ecosystem health by

decreasing biodiversity and fisheries. In order to create adequate management policies for

hypoxia, it is important to understand the sources and sinks of oxygen within Green Bay. This

study utilizes a number of traditional and novel field methods to measure the production and

respiration of oxygen within lower Green Bay, defined as south of Chambers Island, which is the

area that experiences hypoxia. Primary production was measured using light-dark bottles and via

in-situ diel oxygen fluctuation calculations. The epilimnetic waters are slightly net autotrophic

during the summer months, meaning that they accumulate organic matter that can drive oxygen

respiration in the hypolimnion. Hypolimnetic oxygen consumption was calculated as the loss of

hypolimnetic oxygen inventories between two time periods. It was also determined that the two

major processes consuming oxygen within the hypolimnion are sediment oxygen demand (SOD)

and water column respiration (R_H). SOD was measured using core incubations and eddy

covariance. R_H was estimated as the difference between hypolimnetic oxygen consumption and

SOD. In shallow waters, close to the Fox River mouth, SOD dominates the oxygen consumption,

while in mid-bay waters oxygen respiration is divided between SOD and R_H. Based on natural

tracer results, cool bottom waters flows southward from the Lake Michigan-Green Bay gap and begins to lose oxygen once it reaches the mid-bay. This somewhat oxygen depleted water is further pushed down the bay into shallow waters where benthic respiration consumes more oxygen and drives water hypoxic.

^{222}Rn and CH_4 were also used as natural tracers to estimate advective flow in mid-bay bottom water and apparent methane production, respectively. Advective flow was estimated at ~3 km d^{-1}, which agrees with current profiler velocities of 1.8 km d^{-1}. This velocity can vary though, depending on upstream ^{222}Rn activity. Apparent methane production trends match apparent oxygen utilization trends, confirming that methane is produced when oxygen is depleted.

Finally, a biogeochemical model for Green Bay was created to predict what level of nutrient reductions would sufficiently reduce hypoxia, both now and under future scenarios. This biogeochemical model was part of an integrated modeling effort. The model was successfully formed and can be used to evaluate responses, although the baseline line model needs to be much better calibrated to better replicate observations.

TABLE OF CONTENTS

LIST OF FIGURES

LIST OF TABLES

ix

ACKNOWLEDGEMENTS AND DEDICATION

First, I would like to offer my sincerest gratitude to Dr. J. Val Klump for his unwavering support, guidance, and confidence in me. When I first met him I knew he was a man I wanted to work for and I haven't been disappointed. Val has taught me so much, but most importantly he has pushed me beyond limits I didn't know existed. The scientist that I am today, I owe to Val. His mentorship is invaluable and I cherish his leadership.

I would also like to thank my committee members for being influential in my graduate work. Sandra McLellan, Clare Reimers, James Waples, Hector Bravo, and Joseph DePinto- you have all taught me valuable lessons and have undoubtedly made me a much better scientist. I sincerely appreciate all of our conversations hope there are more to come.

My former lab members deserve acknowledgment for many, many things, but especially for making l8 hour days on the R/V Neeskay as bearable as possible, their encouraging words, and helping with data analysis and figure making. In particular, I need to thank Kim, Don and Brice, with whom I spent much of my time. Kim Weckerly is as skilled as making figures as she is at preparing for the field. Don Szmania is a guru at making a meal everyone enjoys and rigging field equipment in a way no one else could think of. Brice Grunert was the best student to share a lab with and I am truly thankful for my many ongoing conversations with him. Jeff Houghton and Dirk Koopmans round out the group and need to be recongized for all of their knowledge they have shared with me.

Several individuals deserve recognition for their contribution to the science presented here, through either data collection or sample analysis. The R/V Neeskay crew members, Greg Stamatelakys and Geoff Anderson, are some of the finest individuals to crew a boat that I have met. They care about the science and made sure that our work got done right. Pat Anderson was crucial in helping me complete analyses on a number of instruments in a timely fashion. Greg Barskey and Randy Metzger are wizards from the shop that made much of my work possible by creating and fixing various science contraptions.

There are numerous people to thank at the School of Freshwater Sciences who made graduate school as enjoyable as it can be. Harvey Bootsma, the Bootsma lab, John Janssen, Rebecca Klaper and Jerry Kaster always had an open door for me and helped me answer any questions

that I may have had, both science and non-science related. I especially have to thank the Bootsma lab, including Emily Tyner, Caroline Mosley, and Ben Turschak, for treating me as one of their own when I was the only student in my lab.

I would like to thank my parents for supporting me on this journey, even though they didn't quite understand why I wanted to do it. Their love and encouragement has made me try things that I had not imagined possible. They have taught me the value of working hard and have helped me accept my failures.

I need to thank my husband, Pete, for consoling me, cheering me on, and caring for me. You took care of my well-being and, for that, I can never tell you how appreciated it really was.

Finally, I would like to dedicate this body of work to my brother, Matthew Steven, who left this world far too soon. I can only imagine how wonderful life would be with you here. I miss you every day.

CHAPTER 1: INTRODUCTION

1.1 Hypoxia Overview

Hypoxia is a significant problem in many aquatic and marine environments, especially in coastal areas, with more than 400 known hypoxic zones around the world that span an estimated 245,000 km^2 (Diaz and Rosenberg 2008). The number of hypoxic areas has doubled each decade since the 1960s, and there is no indication that this is slowing down (Vaquer-Sunyer and Duarte 2008; Rabalais et al. 2014). Hypoxia is defined as a dissolved oxygen (O_2) concentration less than 2 mg L^{-1} (equivalent to 62.5 μM or 1.4 mL L^{-1}). This threshold was set following observations of fisheries collapses at oxygen concentrations below that level (Diaz and Rosenberg 1995; Renaud et al. 2007). Impacts can be varied and widespread in biological communities during hypoxic conditions include mortality, especially to sessile organisms which cannot evade the low-oxygen zones, reduced species richness (Conley et al. 2007), and altered organismal behavior or physiology (Ludsin et al. 2009). Typical movement patterns and habitat use is often disrupted for benthic invertebrate and vertebrate species during low O2 periods (Aku et al. 1997; Keister et al. 2000; Levin et al. 2009). Due to the general lack of benthic life in regions of hypoxia, the areas are also known as "dead zones."

The formation of hypoxia typically occurs after thermal stratification develops due to strong density differences between warm surface waters and cool bottom waters. The thermal gradient essentially eliminates atmospheric contact with the bottom water by reducing the ability of oxygen to mix into the bottom waters. Other causes of stratification can have the same effects with salinity gradients created by mixing of fresh and marine waters in estuaries being the most common. Thermal stratification is a seasonal phenomenon in temperate areas that forms during the summer months due to warming air and surface water temperatures. High wind speeds over shallow waters can cause water column mixing to occur, but in most systems the cooler

temperatures in autumn result in fall overturn, or full water column mixing. Some systems are meromictic, meaning they are permanently stratified. In all cases, the bottom layer of water could experience hypoxia.

Thermal stratification alone cannot cause depletion of oxygen within bottom, or hypolimnetic, waters. Oxygen consumption occurs when organic matter is remineralized by microbes, most typically characterized by the oxidation of glucose (Jurtshuk Jr. 1996):

$$C_6H_{12}O_6 + 6O_2 \leftrightarrow 6CO_2 + 6H_2O + energy \qquad \text{(Eqn. 1.1),}$$
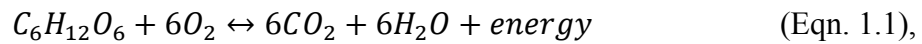
which chemically is the reverse of primary production. There are other possible stoichiometries for organic matter decomposition; however, in all these pathways the degradation of organic matter consumes oxygen in aerobic environments. In lakes and reservoirs, the organic material is either produced via primary production within the hypolimnion or introduced through dissolved and particulate organic carbon (DOC and POC, respectively) settling out of the eplimnion. Major oxygen sinks in the bottom water include sediment oxygen uptake and water column respiration. Oxygen may also be consumed within the hypolimnion via the oxidation of reduced chemical species, such as Fe^{2+} and methane that may be produced under anaerobic conditions within buried sediments or within the microenvironments inside particles.

Hypoxia can be a naturally occurring event, although the increase in hypoxic zones around the world is due to increasing human population in coastal cities and the subsequent increase in anthropogenic impacts in watersheds and coastal waters (Andersen et al. 2006; Howarth et al. 2011). Urbanization of watersheds, excessive nutrient application to agricultural areas, and deforestation result in increased runoff and nutrient loads to tributaries that feed coastal waters and lakes. Excessive nutrient loading to surface waters that results in algal production is defined

3

as eutrophication (Nixon 1995; Andersen et al. 2006). High levels of algal production can result in large concentrations of organic matter settling into the hypolimnion. This organic matter is either respired in the water column or deposited on the sediment surface, where it is also eventually respired or buried.

Oxygen depleted waters are often associated with other water quality impairments, besides eutrophication. One of the most noted issues for freshwater systems is when oxygen concentrations drop low enough, iron (Fe^{3+}) phases binding phosphate can be reduced to Fe^{2+} and the phosphate can subsequently be released to the bottom waters, which stimulates primary production (Petticrew and Arocena 2001; Matisoff et al. 2016). Furthermore, historical analysis of sediment cores shows that hypoxic periods can sustain cyanobacteria blooms through this mechanism of enhanced phosphorus recycling during low-O2 periods (Funkey et al. 2014). Other effects of hypoxic conditions include sulfide accumulation within bottom waters that leads to increased mortality of benthic communities (Vaquer-Sunyer and Duarte 2010).

There have been many attempts at creating management policies to reduce hypoxia, with the most common end goal of nutrient and organic matter load reductions to the water body (Mitsch et al. 2001; Carstensen et al. 2006). Marine ecosystem responses to decreased nutrient loads of Danish coastal systems were observed in the surface waters within just a few years, but have not yet been apparent in oxygen concentrations of bottom waters, even after 30 years of management (Riemann et al. 2016). It has been suggested that the full recovery of hypolimnetic biological communities affected by hypoxia can take years or even decades to occur (Pearson and Rosenberg 1978; Mee et al. 2005). The delay in recovery is due to loss in ecosystem buffers which provide resilience to hypoxia in a number of ways, such as the loss of benthic invertebrate communities, which can increase oxygen penetration into sediments by bioturbtation and

4

bioirrigation (Steckbauer et al. 2011). With decreased oxygen penetration, there is a shift towards anaerobic metabolic pathways that can exacerbate biological impacts of hypoxia (Vaquer-Sunyer and Duarte 2010) and can also cause release of sediment stocks of nutrients. Once these buffers have been compromised, hypoxia tends to be retained by the ecosystem until a normal oxic state is present long enough to allow for restoration of biological communities and biogeochemical cycles (Steckbauer et al. 2011).

The slow recovery of hypoxic zones in regions that have implemented nutrient loading targets has been partially attributed to effects of climate change (Riemann et al. 2016). Warming air temperatures and, in some cases, reduced wind speeds results in strengthened stratification and a longer stratified season. This means that while there may have been a positive response to nutrient reductions in the hypolimnion, it was masked by increased duration of stratification. Warming bottom water temperature, another climate change impact, can stimulate microbial metabolism which increases oxygen consumption rates and reduces oxygen solubility which lowers the amount of oxygen available (Conley et al. 2007).

1.2 Water Quality and Hypoxia in Lower Green Bay

Green Bay, located in northwest Lake Michigan (Fig. 1), is a freshwater estuary that represents ~7% of the surface area of the lake at ~4200 km^2. The Lower Fox River, the major entering

5

Figure 1: Map of Green Bay, Lake Michigan with the sampling grid generally used by University of Wisconsin-Milwaukee. The inset shows the area of the Lower Fox Watershed. Figure made by K. Weckerly.
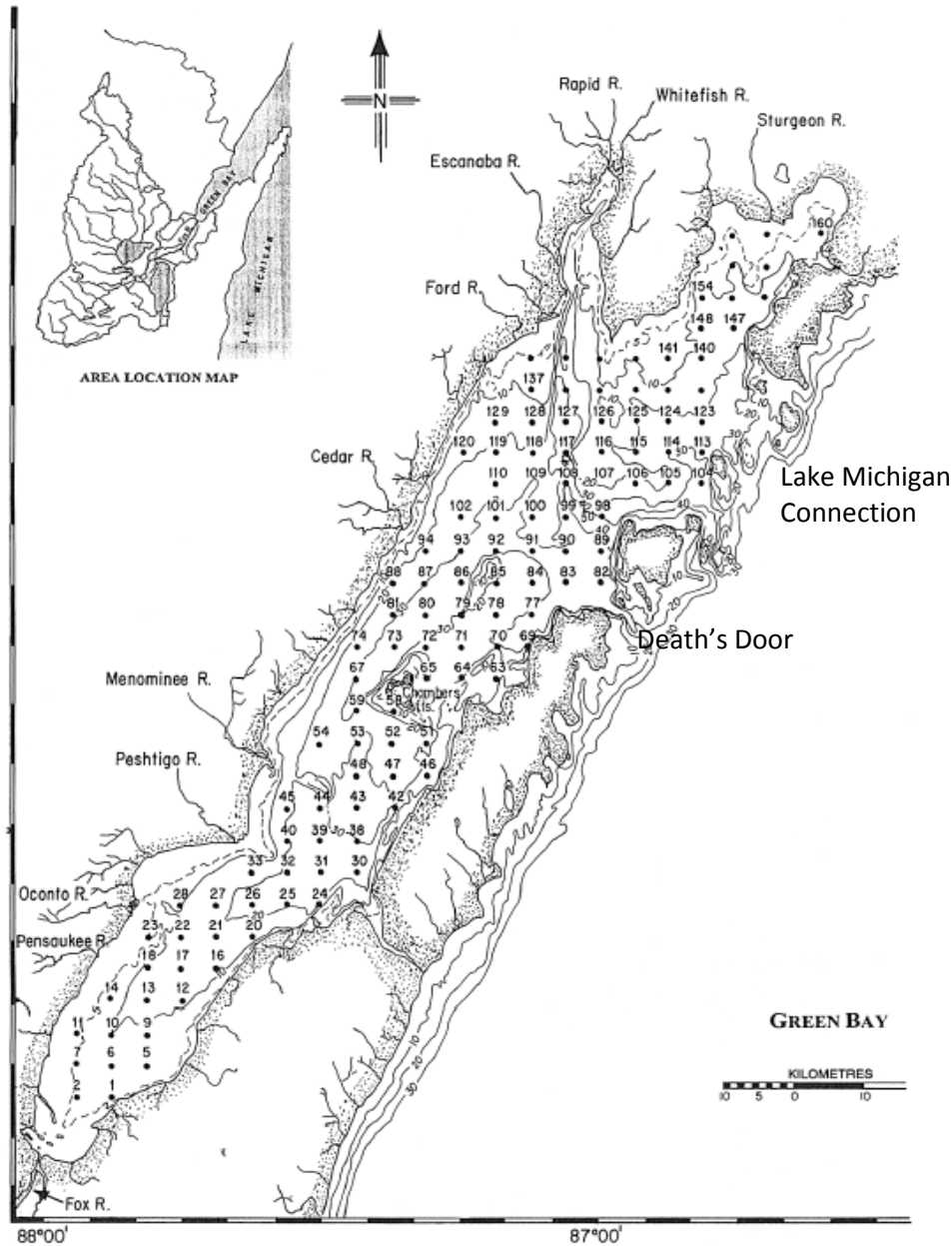
Green Bay at the southern end, near the City of Green Bay, was once one of the most polluted rivers in the world due to a combination of industrial and waste water discharge. In 1932, Bay Beach, located near the mouth of the Fox River, was the first public beach to be closed for swimming in the Great Lakes due to insufficient water quality (Conley 1983). Discharges from the pulp and paper mills along the lower Fox River had high loads of biological oxygen demanding (BOD) materials. This discharge was thought to be the cause of depleted oxygen conditions as early as 1928 that resulted in fish kills on the Fox River (Pollution 1939). Surveys in the lower Fox River and lower Green Bay in 1966-67 also noted hypoxic conditions under the ice during winter months (Schraufnagel et al. 1968). These depressed oxygen conditions resulted in declines of important water quality indicator species, such as the mayfly, or *Hexagenia*, and general loss of benthic diversity (Howmiller and Beeton 1971). Commercial fisheries also suffered from reduced diversity and declining fish populations (Smith et al. 1988).

Hypoxic conditions are still observed in Green Bay, but they are no longer limited to the area of the Fox River mouth or Lower Green Bay. Kennedy (1982) observed hypoxia within the mid-bay (defined as the Entrance Light to the Sturgeon Bay entrance). The hypoxic areas have been mapped by Klump et al. (in prep) through a 6 year survey of bottom water oxygen concentrations (Fig. 2). The areal extent of depleted oxygen concentration (<5 mg L^{-1}) ranges up to 500 to 600 km^2, or ~ 24% to 29% of the total area south of Chambers Island.

Green Bay hypoxia is generally attributed to high nutrient loading from the Fox-Wolf River watershed. The Fox River watershed is the 3rd largest for Lake Michigan and delivers 70% of the total phosphorus load to Lake Michigan. Currently, the watershed is primarily used for agriculture (Fig 3), which results in high nutrient and sediment loads to the Fox River. It is

7

Figure 2: Examples of bottom water oxygen concentration distribution in Green Bay. Figure from Klump et al. (in prep).
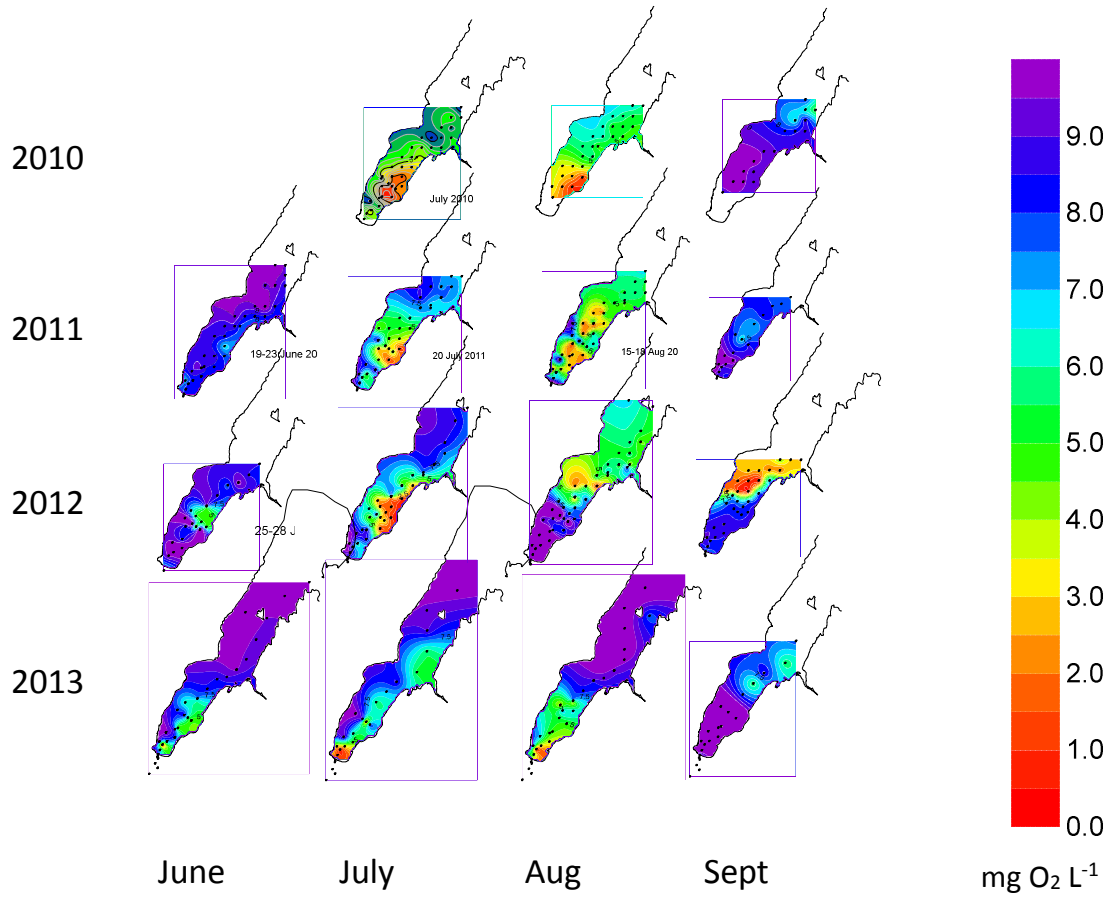
Figure 3: Fox-Wolf basin watershed and land uses. Figure from UW-Green Bay Watershed Monitoring Program.
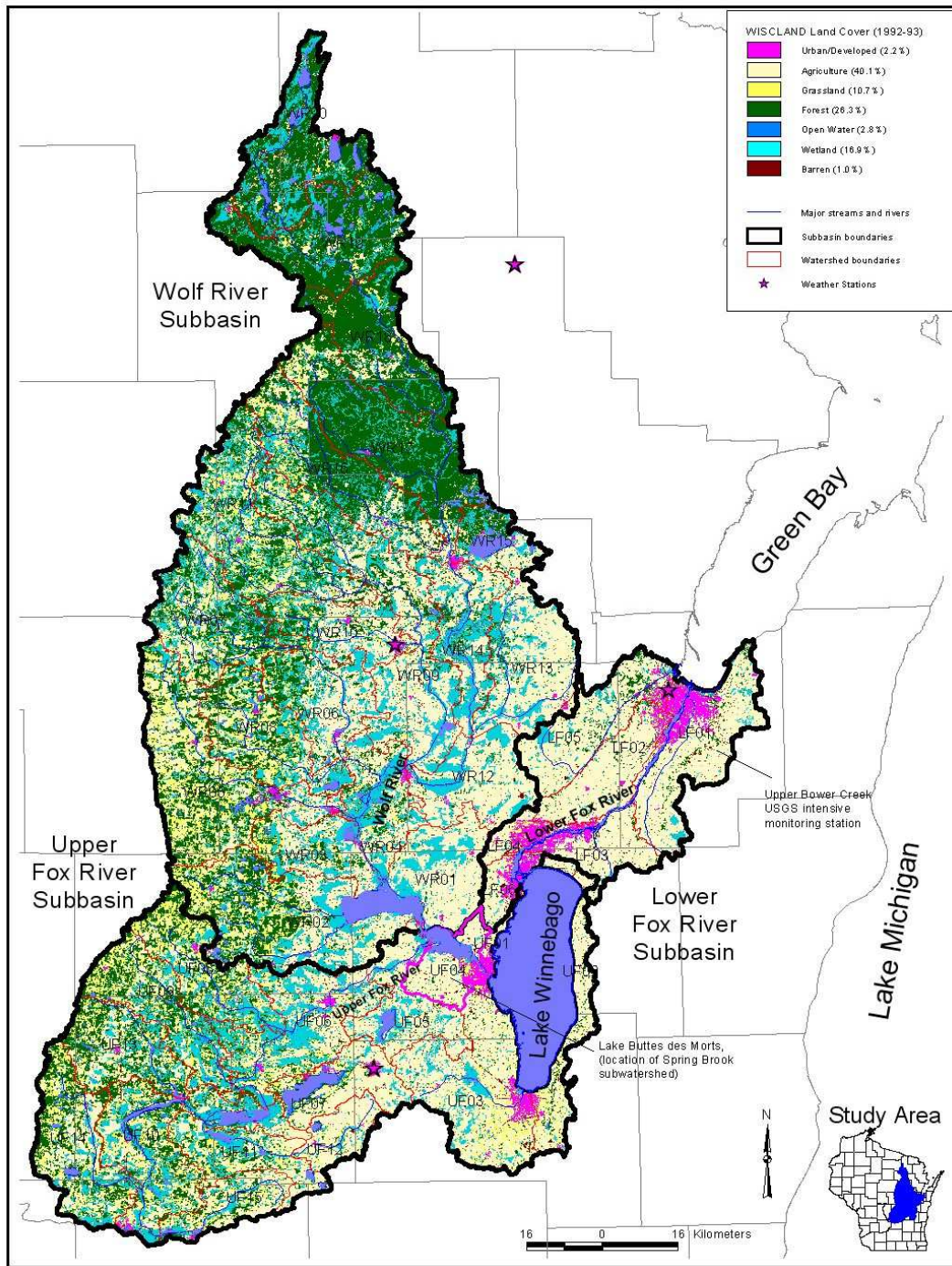
estimated that the Fox River delivers ~70,000 tons of carbon (Klump et al. 2009) and ~700 tons of phosphorus (Klump et al. 1997a) to lower Green Bay every year (Fig. 4). Approximately 70-90% of those nutrients are retained within Green Bay sediments (Klump et al. 1997a, 2009). The Fox River organic matter and nutrient load drives algal production in the surface waters, while efficient trapping of nutrients in the sediment can also stimulate growth under certain conditions. The combination of these two processes ultimately contributes to hypoxia that is now observed in the mid-bay (Klump et al. in prep).

1.3 Circulation of Green Bay

The physics within Green Bay have been identified as favorable for development of hypoxia, through both its hydrodynamics and resultant thermocline development (Bravo et al. 2015; Hamidi et al. 2015). The hydrodynamics within Green Bay have been well-studied and modeled due to implications that water mass movements have had for dispersion of pollutants (e.g. PCBs) from the Fox River in the mid-20th century and now for development of hypoxia. Modlin and Beeton (1970) used the differences in specific conductivity between the Fox River and Lake Michigan to study mixing dynamics between these two major water sources within Green Bay. They determined that due to the Lake Michigan-Green Bay exchange, the actual flushing rate of Green Bay was only 6 months, compared to 2 years, calculated from river inflow alone. Lake Michigan water was found to flow southward into Green Bay along the bottom, while Fox River water flows northeast in the surface water, resulting in a 2-layer flow dynamic (Mortimer 1978; Kennedy 1982). In the summer the general circulation of bottom water within the bay is counter clockwise, with Lake Michigan water moving into Green Bay through Death's Door Passage,

10

southward along the western shore, then moving northward along the eastern shore (Miller and Saylor 1985).

The cool Lake Michigan water in the hypolimnion and warm Fox River water in the epilimnion, combined with absorption of shortwave radiation in the surface, creates a strong thermal gradient within the bay during summer months (June-September). Since the stratification in Green Bay is driven, in part, by the underlying hydrodynamics, the thermal gradient can develop quickly. Stratification can also rapidly re-develop if a mixing event occurs, which favors hypoxia by reducing the amount of time bottom water has to re-oxygenate. The prevailing wind direction can have a major influence on the Lake Michigan-Green Bay exchange and a subsequent effect on biogeochemical cycling of oxygen and methane (Waples and Klump 2002). More recently a hydrodynamic model for Green Bay was completed (Hamidi et al. 2013, 2015) that more thoroughly investigated the development of stratification in Green Bay and its controlling factors (e.g. wind, water depth).

Figure 4: Historical phosphorus loading to lower Green Bay divided by its source (from D. Robertson, USGS).
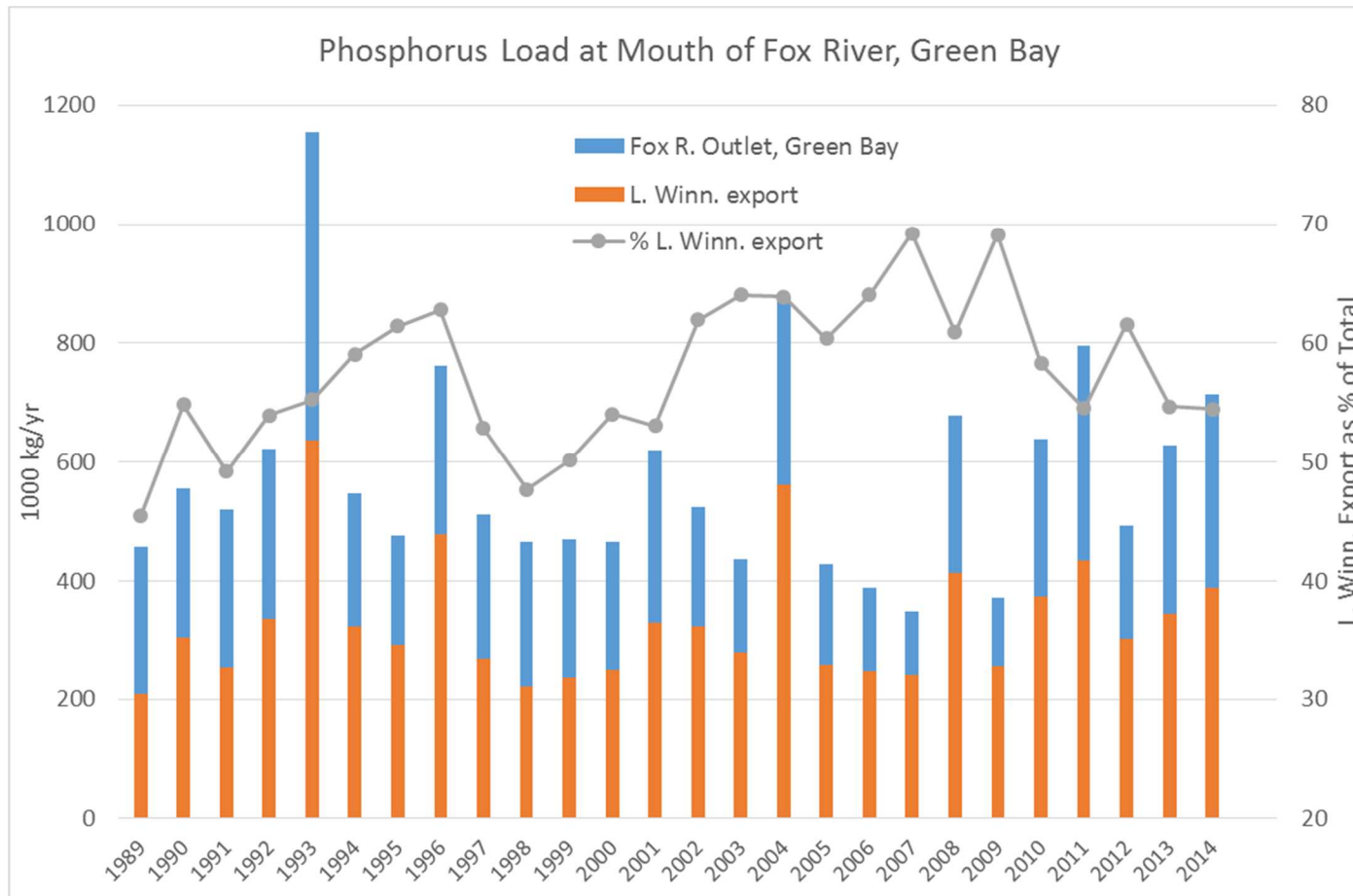
1.4 Management of Hypoxia

The reduction of hypoxia in Green Bay has been a management goal for many decades. The crash of fisheries in the 1960's and discovery of polychlorinated biphenyls (PCBS) accumulation in the fish during the early 1970's resulted in a call-to-action by stakeholders and increased research efforts by the Wisconsin Sea Grant (Smith et al. 1988). More formally, the Clean Water Act of 1972 set a suite of quality standards for waterbodies, including a O2 standard of 5 mg O_2 L^{-1} for all "immersion waters" and warmwater or coldwater fisheries (Williamson and Carter 2001). Due to violation of this standard (and others), Lower Green Bay and the Lower Fox River were designated as an area of concern (AOC) by the US Environmental Protection Agency. A remedial action plan (RAP) was developed in 1988 as one of the initial steps in delisting the Green Bay AOC (Persson et al. 1988). This RAP called for 120 remedial actions, including point source reductions of nutrients and solids. In 1993 and 2011 the RAP was updated (WIDNR 1993, 2011) to further establish goals of setting TMDL's for the Fox River and nutrient reductions from non-point sources. In 2012 the Lower Fox River TMDL published a report that requires a 59% reduction in total phosphorus loads from in-basin sources to achieve a target concentration of 0.10 mg P L^{-1} (Cadmus 2012).

An international agreement, known as the Great Lakes Water Quality Agreement (GLWQA; United States - Canada 2013) between the states and provinces of US and Canada that share the Great Lakes was signed in 1972. One of the major goals of the GLWQA is to restore beneficial uses to all regions of the Great Lakes. The GLWQA has been updated 3 times- in 1983, 1987, and most recently in 2012. The 2012 GLWQA update included 10 Annexes to focus on specific issues and required actions to reconcile those issues (United States - Canada 2013). Annex 4, in

13

particular, focuses on remediating the extremely poor water quality conditions of Western and Central Lake Erie. One of these goals is reduction of hypoxic area in the Central Lake Erie basin to values typical of the mid-1990s. Annex 1 of the updated agreement addresses AOCs and outlines provisions for implementation of RAPs. If Green Bay continues to experience hypoxia, which violates AOC delisting criteria and could have additional water quality implications, it is likely that criteria will be set for Green Bay through Annex 1 and/or Annex 4. The potential for additional regulation of Green Bay water quality adds an additional incentive for alleviating seasonal hypoxia.

A compounding factor on reducing oxygen depletion in the bottom waters is the unknown effects of climate change. Regional climate change projections vary substantially for the Green Bay area, although most include increased air temperature of 2 to 5 degrees Celsius by the end of the 21st century (WICCI, 2011). This will result in lengthening of the stratified season by up to 6 weeks, meaning that the O2 concentrations within the hypolimnion will be separated from the atmosphere for additional month or more (Qualls et al. 2013). Other projections include increased precipitation and more frequent large storm events. Increased precipitation means greater runoff from the watershed, potentially increasing nutrient load (Robertson et al. 2016), while increased storm events could induce water column mixing events. Changes in wind direction can also play an important role as it has been noted that wind fields shifting to a more southerly storm track over Green Bay results in decreased water exchange with Lake Michigan and a subsequent decrease in hypoxia (Waples and Klump 2002). All of these factors, along with unknown effects, make effective management of hypoxia extremely difficult.

In order to adequately manage hypoxia, both under current and future conditions, it is important to fully understand the oxygen dynamics within the system. While there have been thorough

14

mass balances performed for carbon, nitrogen and phosphorus (Klump et al. 2009, 1997a), before this work there has not been a comprehensive understanding of the sources and sinks of oxygen within the bay. Major questions that needed research included:

1) Are surface waters net sources or sinks of autochthonous organic matter?
2) What are the major biogeochemical processes responsible for oxygen consumption in the hypolimnion?
3) Does cool, bottom water from the northern bay contribute substantially to hypoxia?
4) What level of nutrient load reductions from the watershed will result in acceptable decrease of hypoxia?
    a. Will this amount of reduction be adequate in the future?

To answer these questions, a comprehensive study of oxygen processes within Green Bay, south of Chambers Island, was performed and the essential fluxes that contribute to oxygen mass balance were studied (Fig. 5), which is the primary focus of this dissertation.

Chapters 2 and 3 use diel oxygen cycles from seasonal buoys to calculate primary production and respiration rates of the epilimnetic waters in Green Bay to address Question 1. Chapter 2 (also LaBuhn and Klump, 2016) thoroughly discusses methods and presents a comprehensive 4-year dataset from NOAA45015 at GB17. Chapter 3 utilizes a historical dataset (1986-2013) from Green Bay Metropolitan Sewerage District that includes nutrient concentrations and bottom water oxygen levels to evaluate possible correlations with primary production.

Oxygen sinks within the hypolimnion are presented in Chapter 4 by using sediment incubation experiments, loss of oxygen inventories, and apparent oxygen utilization, all of which help address Question 2. Sediment core incubation experiment rates are compared against eddy

covariance measurements (Chapter 4), which is a novel and non-invasive technique to measure benthic metabolism.

A suite of natural tracers, including $D_2^{18}O$ (Chapter 4 and 6), ^{222}Rn, and CH_4 (Chapter 6), were used in attempt to understand whether cool bottom water from the northern bay is biogeochemically important in the lower bay, which would answer Question 3. The mixing percentages between Lake Michigan and Fox River sourced waters were calculated using $D_2^{18}O$ isotopes. A combination of methane and radon porewater profiles and water column profiles were evaluated for use as a tracer of horizontal advection, too.

Finally, a biogeochemical model was created as part of an integrated modeling project for Green Bay and is presented in Chapter 7. This model was used to evaluate the response of different parameters within the bay to nutrient reduction and climate change scenarios. A management analysis tool was created from model outputs for use by stakeholders around Green Bay. The model and the management analysis tool answer Question 4.

Figure 5: Oxygen mass balance framework for Lower Green Bay, where J is that atmospheric-surface water flux, P is production, R is respiration, D is thermocline diffusion, A is advection and SOD is sediment oxygen demand.
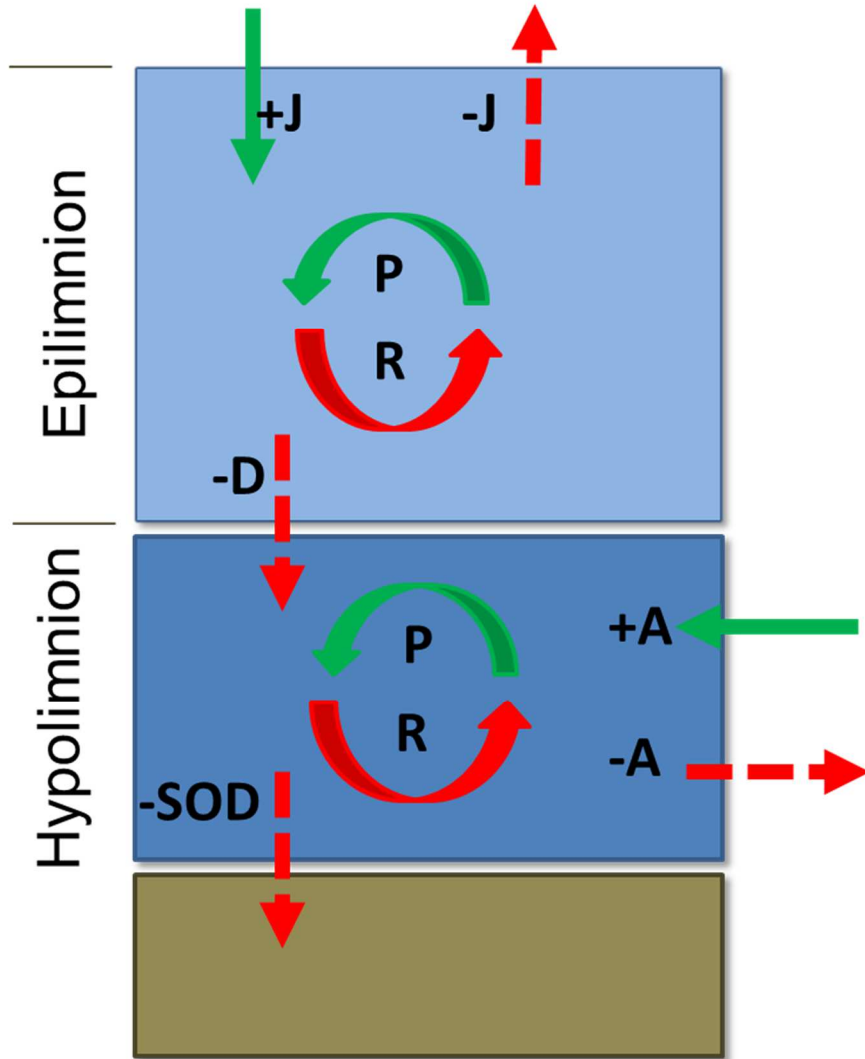
CHAPTER 2: ESTIMATING SUMMERTIME EPILIMNETIC PRIMARY PRODUCTION VIA *IN SITU* MONITORING IN AN EUTROPHIC FRESHWATER EMBAYMENT, GREEN BAY, LAKE MICHIGAN

2.1 Abstract

Quantifying the rates of primary production and respiration is fundamental to understanding ecosystem function. This study utilized high frequency time series buoy-based sensor data to estimate daily primary production and respiration rates during the summers of 2012- 2015 in southern Green Bay, Lake Michigan. Highly coherent diel oscillations of dissolved oxygen concentrations in epilimnetic waters were commonly observed at 30 minute time intervals from the GLOS buoy (NOAA 45014) sensor array for much of the summer. Corrections for air-sea exchange based upon wind speed derived gas exchange coefficients and saturation state, when combined with mixing depth, allow calculation of day time net oxygen production and night time respiration. Thermistor string observations at 1-meter depth intervals over the 13 meter water depth showed the onset of thermal stratification, development of the thermocline, and occasional mixing events. For the summers of 2014 and 2015, during which a nearly continuous sensor record exists, gross primary production (GPP) and respiration (R) were estimated to be 342 ± 117 and 318 ± 83 mmol O_2 m^{-2} d^{-1} for GPP and -325 ± 120 and -306 ± 66 mmol O_2 m^{-2} d^{-1} for R, respectively. These results indicate that during most of the summer southern Green Bay tends towards net autotrophy with production on average exceeding respiration by $9\pm6\%$ (SD). Cumulative net ecosystem production during 2014 and 2015 summer periods were estimated to be 3.2 and 1.3 mol C m^{-2} (118 and 113 days, respectively), and is sufficient to drive a significant portion of benthic respiration, the principal cause of seasonal bottom water hypoxia.

Keywords: Primary production; net ecosystem production; respiration; diel oxygen; observing systems

2.2 Introduction

Gross primary production (GPP), ecosystem respiration (R) and net ecosystem production (NEP) have served as indicators of ecosystem function for many decades (Odum 1957; Woodwell and Whittaker 1968; Richey et al. 1978; Strayer 1988). GPP is generally defined as the creation of biomass through carbon fixation by autotrophs over a given length of time (i.e. productivity), and ecosystem respiration as the fraction of this fixed carbon that is used by primary producers and remineralized back to carbon dioxide during cellular respiration (Odum 1956). NEP, or the balance between production and respiration, is a measure of the net gain (or loss) in biomass for the ecosystem in question. Quantitatively, in aquatic ecosystems, GPP, R and NEP are commonly estimated from the production and consumption of dissolved oxygen during diel cycles of photosynthesis and respiration (D'Avanzo et al. 1996; Staehr et al. 2010b; Collins et al. 2013).

Modern sensor technology has made it increasingly easier to collect *in situ* data for studying ecosystem processes, such as that required to calculate GPP and NEP. The measurements can now be made essentially continuously over an entire season and at multiple locations within one body of stratified water with a much lower investment in the time and expense usually needed for field sampling. Observing systems, such as the Great Lakes Observing System (GLOS; data.glos.us/obs), are increasingly being deployed as sensor platforms (Read et al., 2010). These systems collect long-term datasets that provide insights into temporal dynamics at significantly higher temporal resolution than previously possible. These observing systems are especially useful in highly variable systems in which isolated time points over a season are often a poor indication of mean conditions. The use of permanent moorings, such as GLOS buoys, has the

20

potential to provide data relevant to understanding short term (minutes to days), seasonal, and long term (interannual) dynamics.

Such time series data has widespread application, particularly in eutrophic coastal regions, where human activities have accelerated the delivery of nutrients, stimulating excessive primary production, deteriorated water quality, nuisance algal blooms, and hypoxia (Zhou et al. 2013, 2014). One such area is Green Bay, Lake Michigan, an environment that has suffered hypereutrophic conditions for several decades, and has led, in part, to its designation as an Area of Concern (AOC). Loading data tabulated over 1967 to 2008 indicates that nutrient and sediment loading from the Fox River supports 70% of the annual nutrient and sediment inputs to the bay and ~1/3 of the total phosphorous load to the entire Lake Michigan basin (Dolan and Chapra 2012; Klump et al. 2009). These inputs drive a steep gradient in water quality from hyper-eutrophic conditions in the AOC to meso- to oligotrophic conditions at the northern, deeper portion of the bay that connects directly to Lake Michigan. Water quality varies along this gradient with Secchi depths ranging from less than 1 meter to over 10 meters and dissolved inorganic phosphorus concentrations ranging from ~1000 nmol L^{-1} in the lower Fox River to < 20 nmol L^{-1} in northern Green Bay (Auer and Canale, 1986; Qualls et al., 2007; GBMSD, unpubl). Light-extinction coefficients, range from 1.3 m^{-1} in the southern end to 0.31 m^{-1} in the mid-upper region (Grunert 2013). These relatively high light-extinction coefficients limit primary production for much of the bay south of Chambers Island and are a likely cause of the benthic environment's minor contribution to the total primary production (Althouse et al. 2014). Quantifying the linkages among nutrient inputs, pelagic primary production and water clarity is an important management consideration in this system with one of the principal goals of the Remedial Action Plan (RAP) for the bay the improvement in water clarity through reductions in

algae and suspended sediment concentrations (WIDNR, 1988). Furthermore, as a consequence of the decomposition of both autochthonous and allochthonous organic matter southern Green Bay also experiences seasonal hypoxia (Qualls et al. 2013; Valenta 2013) typically during late summer (Qualls et al., 2013; Valenta, 2013; Klump et al., in prep).

Hyper-eutrophication and hypoxia concerns have led to two complimentary research areas – understanding the development of excessive algal production in regions of the Great Lakes (.e.g. western Lake Erie, Saginaw Bay, and Green Bay (Davies and Hecky 2005; Malkin et al. 2010; Maccoux et al. 2013)) and the deployment and use of long-term monitoring systems to understand ecosystem dynamics (Consi et al. 2007; Read et al. 2010; Watras et al. 2015; Rigosi et al. 2015). The main focus of this paper is the application of high-frequency *in situ* time series data from a buoy to investigate rates of primary production and respiration over summer season deployments in southern Green Bay between 2012 and 2015.

2.3 Methods

Study Site and buoy based measurements

Automated, *in situ* observations of dissolved oxygen, water temperature, conductivity, turbidity and standard meteorological parameters, including wind speed and direction, solar radiation and air temperature, were generated at 30-minute intervals during portions or all of the period from early June to October in 2012, 2013, 2014 and 2015 using a Great Lakes Observing System (GLOS) buoy at a southern location in Green Bay¸ Lake Michigan. The buoy is a CB-1500 coastal monitoring buoy from Fondriest Environmental (Dayton, OH) with a 2 meter-tall met senor array, solar power system, and cellular communications for real time data access. The buoy is anchored on a 2-point mooring holding a relatively constant directional orientation.

22

This GLOS buoy, also listed as NOAA 45014 (position 44º48.0'N, 87º45.6'W), is located in 13 meters of water and is approximately 70 km northeast of the city of Green Bay, WI (Fig. 6). The buoy represents one of a series of standard GLOS deployments within the Great Lakes (Read et al., 2010) and is equipped with the following instruments: YSI 6600 series multi-parameter sonde measuring temperature, pH, turbidity, dissolved oxygen and conductivity; Lufft WS501-UMB Compact Weather Station (Santa Barbara, CA) measuring temperature, relative humidity, global radiation, air pressure, mean wind speed and direction (over a 2 minute period) and wind gust speed; a Nexsens (Dayton, OH) temperature string with thermistors every 1 m from 2-12 m; Nortek acoustic Doppler current profiler (ADCP) measuring x, y, and z velocities and amplitudes in 1 meter bins. The sonde sensors, including oxygen and temperature sensors used here, are located ~1 meter below the surface. Data is transmitted hourly to Nexsens iChart6 desktop software via a machine-to-machine cellular modem.

Meteorological and temperature data from NOAA 45014 are available on line through the GLOS web site Data Portal or Observation Explorer tools (see: http://glos.us/data-tools/observations-explorer). Sonde data is being made available at fwwat.adc4gis.com.

The NOAA 45014 buoy is currently deployed during the recreational summer season, typically June through October for July 2012 to October 2015 (GLOS.org). Sondes were calibrated approximately monthly for dissolved oxygen (polarographic electrodes and optodes), pH, conductivity, and turbidity following the manufacturer's protocol, and were checked against

23

Figure 6: At GB17 (box) a Great Lakes Observing System (GLOS) buoy has been deployed seasonally since 2012.
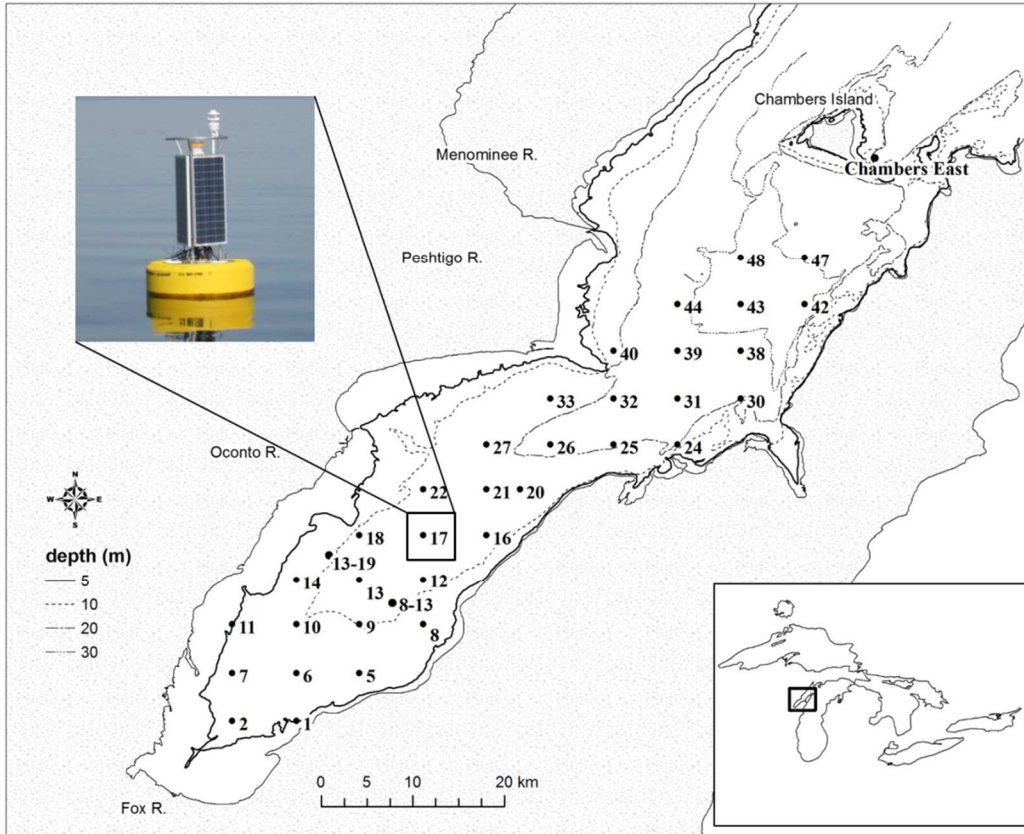
separate measurements with sondes used for profiling on monthly buoy servicing cruises. Sensor failure, fouling or buoy communication issues resulted in periods during which data were deemed unreliable and were excluded from calculations. GPP and R calculations were also only carried out for periods where O2 concentrations exhibited coherent diel fluctuations indicating near steady state conditions in the epilimnion not confounded by advection or mixing (Fig. 7). For the purpose of this study, the relative change in oxygen concentrations is more critical than absolute change. Therefore, if the oxygen sensor is capturing the change between concentrations adequately even if a small amount of drift in calibration has occurred, the rates of production and respiration calculated are not significantly affected. Corrections for drift were insignificant in 2014 and 2015 when optical oxygen sensors were employed.

Diel-based primary production rates

Rates of ecosystem productivity were estimated from the continuous YSI sonde data using the free-water accounting method outlined by Staehr et al. (2010) with minor adaptations.

The general equation for changes in dissolved oxygen over a daily basis is

$$\frac{\Delta O_2}{\Delta t} = GPP - R - J_{atm} \pm A \qquad \text{(Eqn. 2.1)}$$

where *GPP* is gross primary production, *R* is respiration, and *J_{atm}* is the atmospheric oxygen flux (defined as positive from the water to the atmosphere). *A* is a net term inclusive of other processes, e.g. advection. *A* is generally assumed to be negligible relative to other sources (Odum 1956) and is not included in these calculations. All of the remaining terms in Eqn. 1, except GPP, can be calculated with data measured on the buoy.

A classic GPP definition gives:

Figure 7: An example of the data received from the buoy over a 5-day period in July 2014. The diel O2 cycles are used to calculate primary production and respiration rates over the day. Daylight hours are determined from solar radiation values.
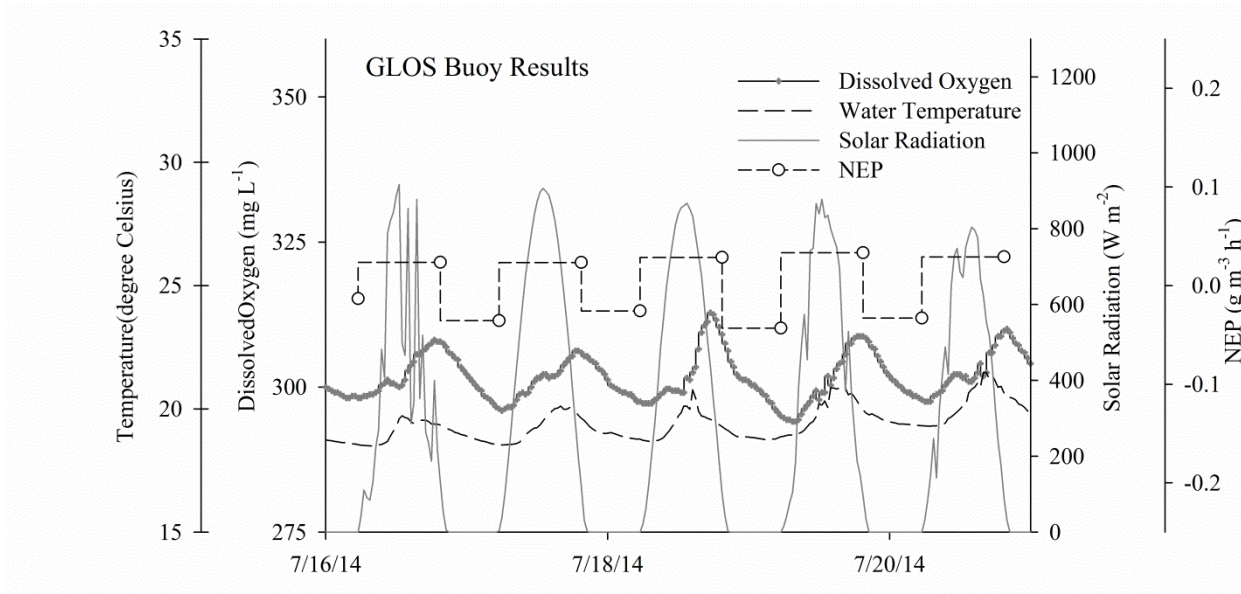
$$GPP = NEP + R \qquad \text{(Eqn. 2.2)}$$

where the net ecosystem production (NEP) can be calculated after substitution into Eqn. 1 for each time step using

$$NEP = dO_2/dt + J_{atm}/z_{mix} \qquad \text{(Eqn. 2.3)}$$

where z_{mix} is the depth of the epilimnion, which was determined from monthly temperature profiles and defined as the top of the thermocline in this study. Throughout the epilimnion dissolved oxygen concentrations are relatively constant, meaning the water column in this region is well mixed and the sonde is assumed to be representative of the entire epilimnion.

Dissolved oxygen concentrations (O_{2meas}), collected at 30 minute intervals at 1 meter depth, were used to calculate dO_2/dt. J_{atm} is determined as:

$$J_{atm} = k(O_{2meas} - O_{2sat}) \qquad \text{(Eqn. 2.4)}$$

where k is the piston velocity, or coefficient of gas exchange between the water surface and atmosphere (Weiss 1970) and O_{2sat}, the saturated oxygen concentration, is based on water temperature and atmospheric pressure. Piston velocity is calculated

$$k = k_{600}(\frac{Sc}{600})^{-1/2} \qquad \text{(Eqn. 2.5)}$$

where

$$k_{600} = (2.07 + .215U_{10}^{1.7})/100 \qquad \text{(Eqn. 2.6)}$$

(Cole and Caraco 1998) and

$$Sc = -0.0476T^3 + 3.7818T^2 - 120.1T + 1800.6 \qquad \text{(Eqn. 2.7)}$$

27

(Wanninkhof 1992). U_{10} is wind speed at 10 meters above the water surface and T is temperature in degrees Celsius. Wind speed was measured on the buoy at 2 meters above the water surface at 30 minute intervals, then transformed using

$$U_{10} = 1.4125 \times U_z \times z^{-0.15} \qquad \text{(Eqn. 2.8)}$$

(Smith 1985) where U_z is wind speed at z height in meters.

NEP_{hr} was calculated for every 30 minute time step using Eqn. 3. NEP_{day} and R_{day} were calculated using NEP_{hr} and the number of daylight hours, or continuous periods of solar irradiance greater than 0.0 W m^{-2}, over a 24-hour period, as taken from the solar irradiance measurements on the buoy.

$$NEP_{day} = mean\ NEP_{hr}\ during\ daylight\ \times\ hours\ daylight \quad \text{(Eqn. 2.9) and}$$

$$R_{day} = mean\ NEP_{hr}\ during\ darkness\ \times hours\ daylight \qquad \text{(Eqn. 2.10)}$$

(Staehr et al., 2010). We follow the usual assumption that NEP during the night represents the respiration rate for the entire 24-hr period, although we recognize this may not always hold true (Tobias et al. 2007; Hotchkiss and Hall 2014). There are also predictive model methods that use additional variables (e.g. photosynthetically active radiation, chlorophyll α) to better calculate daytime-respiration rates (Hanson et al. 2008; McNair et al. 2013).

GPP can be computed using Eqns. 2.2, 2.9 and 2.10. NEP, GPP and R values are initially calculated as volumetric rates, which can be converted to areal rates by multiplying by the epilimnetic mixed layer depth. The depth of the thermocline was taken from thermistor string data, monthly sonde profiles or estimated from previous observations, when temperature and sonde data was lacking.

28

This study also assumes that changes in oxygen concentration due to advection and loss of oxygen through the thermocline are negligible. Thermocline diffusivities are assumed to be low ($\sim10^{-8}$ m^2 s^{-1}, Edwards et al., 2005) because the thermocline is typically very steep (Hamidi et al. 2012). Oxygen diffusion into the thermocline would result in additional losses of oxygen from the mixed layer, making respiration seem larger than it actually is. To capture horizontal gradients in oxygen and spatially variable dynamics, such as advectively introduced water masses with differences in oxygen, a matrix of sensors would be needed (Van de Bogert et al. 2007). Average surface water velocities, measured by an ADCP on NOAA45014, are ~ 2.5 cm s^{-1}. Over an hour (two sampling time points), this corresponds to a sampling "footprint" for the sensor of just under 100 meter radius or $\sim25,000$ m^2. Cumulative NEP (NEP_{cum}) is the sum of daily NEP values and is also reported as monthly rates (Table 1). During those time periods when daily data is missing (2012 and 2013) average rates across the time period were used to estimate monthly rates. NEP_{cum} values were converted from mol O_2 m^{-2} to mol C m^{-2} using the molar ratio 138 mol O_2: 106 mol C (Redfield et al. 1963).

Light-dark bottles

Light-dark bottle experiments were carried out at a range of stations during summers of 2013 as simple independent estimates of primary production rates. Water was collected in 20L carboys from 1-2 meters in depth, thoroughly mixed and distributed into triplicate standard 300 mL BOD bottles. In some instances when samples were collected late in the day, water was held in the carboy and aerated at ambient temperature overnight before incubation in light-dark bottles. Initial and final oxygen, temperature, and atmospheric pressure measurements were made using a YSI ProODO handheld sensor, calibrated in air immediately before initial readings. Bottles were placed in a circulating surface water bath continuously flushed in a flow-through system from the

ship's surface water sampling pump to maintain *in situ* surface water temperature conditions. Bottles were incubated for eight to twelve hours during daytime in direct sunlight.

"Light" samples were incubated under 3 ambient light levels, 100%, 30% and 11% by screening with multiple layers of nylon window screening. Dark samples were incubated in black coated BOD bottles and used to estimate respiration rates. Rates are given as averages over the entire incubation period. Gross primary production is calculated as follows:

$$GPP = NPP + R \qquad\qquad \text{(Eqn. 2.11)}$$

where NPP is the productivity rate from light bottles and R is the respiration rate from dark bottles. All bottle incubations were conducted on triplicate, sometimes quadruplicate subsamples. Light intensity for the various shading levels were measured using a HOBO Temperature and Light Logger that was attached to the neck of the bottles and placed under screening.

2.4 Results and Discussion

The periods of data used for the free water calculations and some of the corresponding NOAA 45014 data are given in Table 1. The years 2012 and 2013 yielded partial results, approximately 77% and 57% of the deployment time period respectively. For 2014 and 2015, the entire season (early June - September/October) of data was usable (Fig. 8). For months when data was discontinuous the values from different periods were time-weight averaged to approximate a monthly value.

Air-water gas exchange

Table 1: GLOS buoy information for GB17 including sampling interval, number of samples (n) per time period, average wind speed (WS) ± standard deviation, range of wind speeds and average daily irradiance. * indicates that the value was taken from a different buoy than the GLOS buoy.

Time Period	Sampling Interval	n	Thermocline depth (m)	WS (m s^{-1})	Range (m s^{-1})	Irradiance (W m^{-2})
8/21/12-8/31/12	6 min	2471	9.667	4.1*		n/a
9/1/12-9/8/12	6 min	1750	9.667	4.1*		n/a
9/26/12-9/30/12	30 min	203	9.667	4.24*		n/a
6/1/13-6/26/13	30 min	1210	11	4.26±2.16	0-15.8	273.4
8/1/13-8/11/13	30 min	524	10	4.18±1.70	0-11.4	408.9
8/20/13-8/27/13	30 min	357	6	4.83±2.06	0-16.8	418.0
8/29/13-8/31/13	30 min	191	6	3.83±2.21	0-8.7	353.3
9/1/13-9/7/13	30 min	334	12	5.37±1.92	0.4-11.1	352.6
9/10/13-9/25/13	30 min	742	9.667	5.29±2.23	0-11.3	331.6
6/4/14-6/30/14	30 min	1271	10	4.90±2.40	0-13.6	419.8
7/1/14-7/31/14	30 min	1487	9	4.97±2.29	0-12.3	427.4
8/1/14-8/31/14	30 min	1487	11	4.17±2.17	0-13.3	360.6
9/1/14-9/30/14	30 min	1439	12	5.40±2.60	0-14.8	284.1
6/3/15-6/30/15	30 min	1357	10	4.34±2.13	0-12.1	424.8
7/1/15-7/31/15	30 min	1488	10	4.73±2.10	0-13.8	496.5
8/1/15-8/31/15	30 min	1345	8	4.83±2.32	0-16.7	345.7
9/1/15-9/30/15	30 min	1440	10	4.77±2.20	0-12.4	314.0

Figure 8: Measurements of dissolved oxygen, at GB17 from the GLOS buoy, that were used for data analysis during (from top) 2012, 2013, 2014 and 2015.
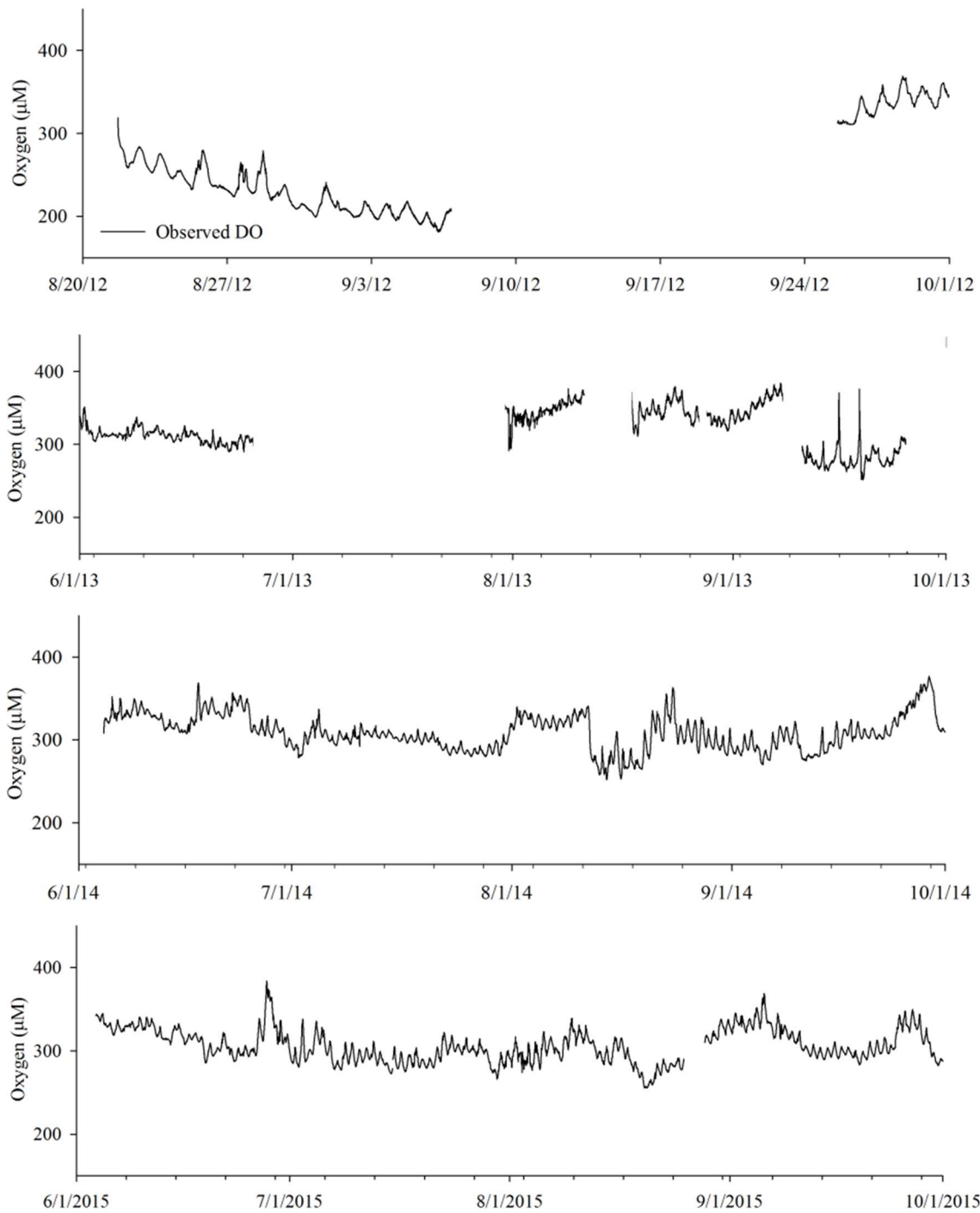
For the 2013, 2014, and 2015 calculations, observed wind velocities were taken directly from the buoy anemometer. Average wind speeds were remarkably similar for all three years. In the first year of deployment, 2012, the meteorological station was not functioning properly, so wind speeds were acquired from the northern Lake Michigan buoy, NOAA Buoy 45002 (ndbc.noaa.gov) and average values applied for the two time periods of data. The northern Lake Michigan buoy has been shown to be a reasonable surrogate for determining wind fields in Green Bay (Waples 1998; Waples and Klump 2002). The 2013 average wind speed over the useable data was 4.69 ± 0.5 m s^{-1}, with maximum speeds ranging from 11.1 to 16.8 m s^{-1}. In 2014 the average wind speed from June 4 to Sept. 30 was 4.86 ± 0.5 m s^{-1} (Fig. 9), with the monthly maximums ranging from 13.6 to 18.8 m s^{-1}. In 2015 the average wind speed was 5.00 ± 2.3 m s^{-1} from June 3-October 27 and the monthly maximums ranged from 14.2 to 28.8 m s^{-1}. The resulting piston velocities (k, eqn. 2.5) ranged from 0.013 to 0.28 m hr^{-1} in 2014 (Fig. 9) and from 0.011 to 0.289 m hr^{-1} in 2015, using Eqn. 2.6.

Over much of the 2013, 2014 and 2015 summertime deployments, oxygen concentrations in surface waters were at or above atmospheric equilibrium, driving gas exchange fluxes outward (positive), i.e. from the water to the atmosphere. Averaged atmospheric exchange (J_{atm}) ranged from -0.64 to +3.31 mmol O_2 m^{-2} h^{-1}. Only two time periods, both in late summer, exhibited average inward (negative) fluxes. These periods coincided with periods of water column mixing (Fig. 10), entraining hypoxic, hypolimnetic water with epilimnetic waters, lowering the overall oxygen saturation state of surface water below equilibrium with the atmosphere. Waples (1998) observed a similar trend in Green Bay for CO_2 uptake occurring throughout the summer, followed by a release during mixing and turnover in the fall.

Figure 9: Measured solar radiation (top), wind speed (middle) and calculated piston velocity (bottom) in 2014 from the GLOS buoy data, with daily averaged values in bold lines.
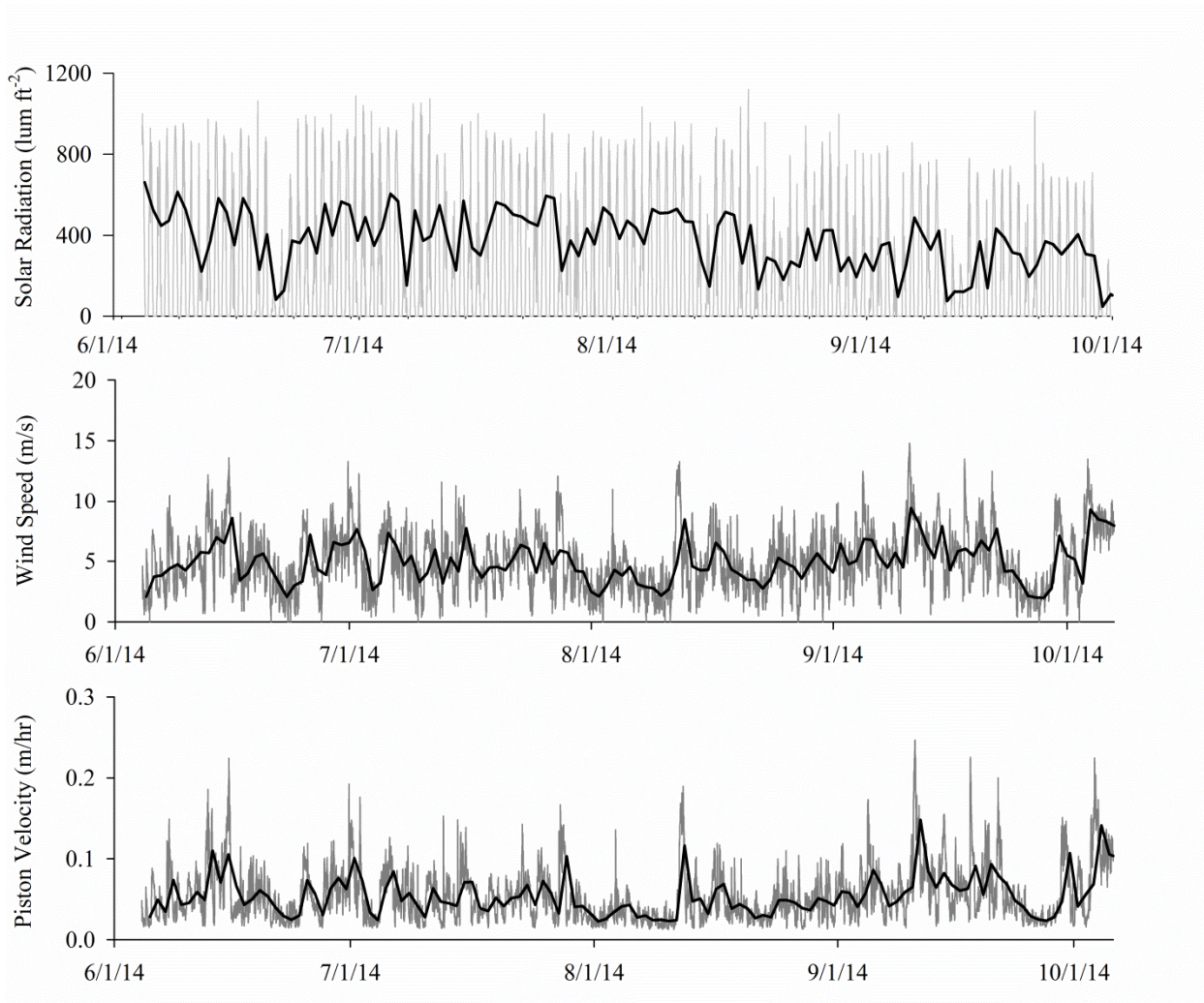
Figure 10: 2014 comparisons of surface temperature (red), water column temperature (contour plot below), dissolved oxygen saturation (green) and atmospheric oxygen flux (black). The periods of inward, or negative, atmospheric flux coincide with periods of water column mixing.
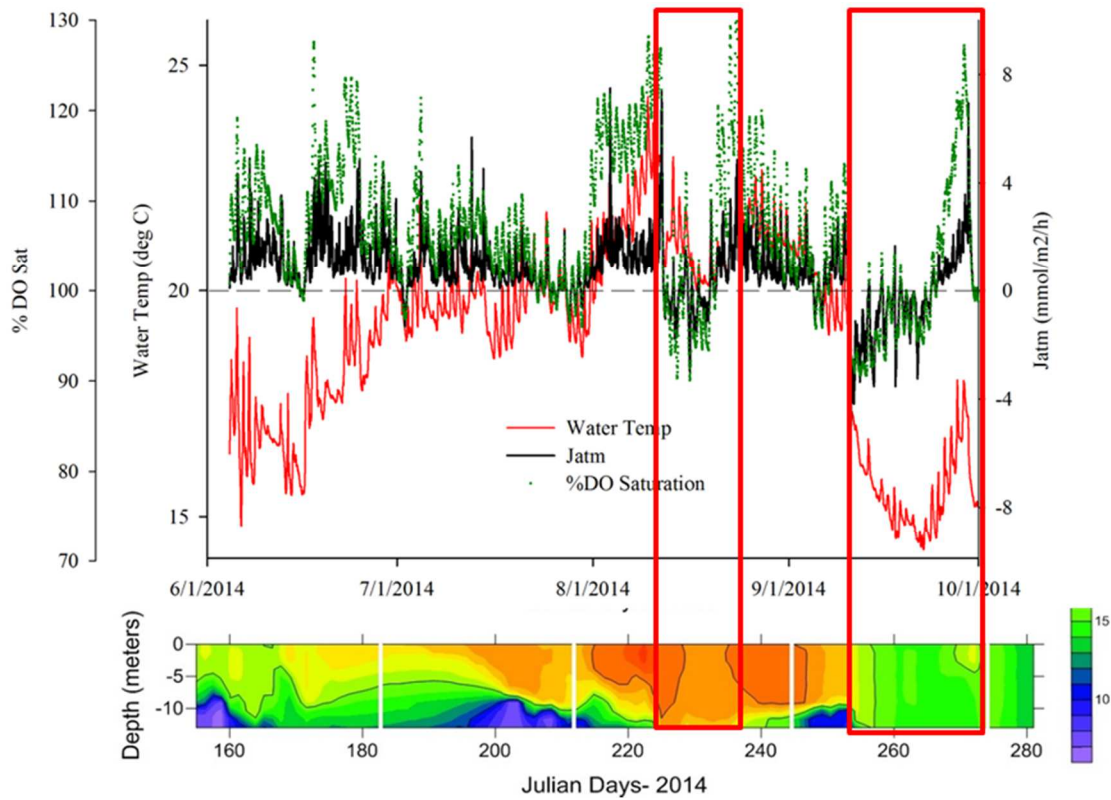
In lower productivity waters, atmospheric exchange has the potential to contribute a relatively large fraction of O_2 flux to/from the overall surface water reservoir (Howarth et al. 1992; Caffrey 2004) and choosing an appropriate piston velocity model can be quantitatively important. However, J_{atm} was generally less than 1% of the GPP; therefore, the choice of formulation for calculating piston velocity (e.g. Collins et al. 2013) would have less than 3% contribution to on the overall magnitude of GPP or R rates observed in Green Bay.

Monthly Results

August and September sonde data were available for all 4 years of this study, allowing year to year comparisons for these two months. Over the 4 year period the areal monthly NEP rate remained consistently close to zero, ranging from -80 to 77 mmol O_2 m^{-2} d^{-1} (Table 2). The epilimnion was slightly autotrophic in August and September, with net production ranging from 3.0±64 to +9.9±48 mmol O_2 m^{-2} d^{-1}, respectively. The August-September averages indicate that Green Bay tends towards net autotrophy during this period, although GPP and R are nearly balanced.

Daily GPP and R rates are relatively consistent over this 4 year deployment (Fig. 11). Both average GPP and R rates appear to decline slightly as the summer progresses from August to September. This decrease is possibly due to declining phytoplankton growth due to shorter day length, cooler water temperatures, nutrient depletion, changes in nutrient availability, sedimentation and/or grazing (Lohrenz et al. 1999; Wetzel 2001). Regardless, despite a few outliers, these rates were remarkably constant over the course of the summer and from year to year. Primary production rate estimates from this oxygen monitoring system compare well with and generally fall within the range of similar regions within the Great Lake and estuarine systems (Table 3). It should be noted that several experiments have shown that direct comparisons of GPP and R measurements by various techniques (e.g. ^{14}C, light-dark bottles and free water O_2) yield varying results (Bender et al. 1987; Ostrom et al. 2005). However, carbon and oxygen measured fluxes are more likely to reach equilibrium as time periods approach phytoplankton generation time (Ostrom et al., 2005). Additionally, Hanson et al. (2003) found that over broad ranges in TP and DOC in aquatic systems there was almost a 1:1 change in diel O_2 and CO_2 changes. GPP:R ratios are sometimes used to indicate the extent of external vs. internal sources of organic matter. Major inputs of allochthonous organic matter can drive a

Table 2: Monthly averaged net ecosystem production (NEP), gross primary production (GPP) and respiration (R). An average for August and September is also given to compare those 2 months which were present in the 4 years of the study. These values represent averages over an incomplete dataset.

	June	July	August	September	Avg for Aug & Sept
GPP (mmol O_2 m^{-2} d^{-1})					
2012	----	----	477*	472*	*474.6**
2013	204	----	146	258	*202.0*
2014	360	244	499	263	*380.8*
2015	312	438	254	271	*262.8*
Respiration (mmol O_2 m^{-2} d^{-1})					
2012	----	----	-557*	-438*	*-497.2**
2013	-207	----	-69	-193	*-131.0*
2014	-305	-209	-493	-293	*-392.5*
2015	-278	-398	-245	-302	*-273.8*
NEP (mmol O_2 m^{-2} d^{-1})					
2012	----	----	-80*	34*	*-75.2**
2013	-3	----	77	65	*68.2*
2014	55	33	6	-29	*16.3*
2015	34	40	9	-31	*12.9*

37

Table 3: Gross primary production (GPP) comparisons between this study and other studies in both similar systems and other Great Lakes.

GPP Value mmol O2/m2/d	System	Method	Year	Reference
31.5	Lake Superior	Carbon-14	Summers 2006-08	Sterner, 2010
40.6-65.1	Saginaw Bay	C14 into a model	1989-1993	Fahnenstiel et al., 1995
64.1	Lake Michigan	Carbon-14	1970	Fee, 1973
73.4	Lake Michigan	Carbon-14	July to Sept 07-08	Fahnenstiel et al., 2010
65.1	Mid Green Bay, Lake Michigan	Carbon-14	June-August 1988	Millard and Sager, 1994
94-122	Sandusky Bay, Lake Erie	Light-Dark Bottles	July-August 2003	Ostrom et al. 2005
156	Colne Estuary - UK	Carbon-14	Aug-95	Calculated from Kocum et al., 2002
168	Mid-Green Bay	Model		Auer and Canale, 1986
193	Long Island Sound	Diel O2	May-Aug 2010	Collins et al. 2013
195	Lake Mendota	Carbon-14	Summer 1979-81	Brock, 2012
203	**GB17**	**Diel O2**	**June-Sept 2013**	**This Study**
342	**GB17**	**Diel O2**	**June-Sept 2014**	**This Study**
319	**GB17**	**Diel O2**	**June-Sept 2015**	**This Study**
358-412	Gulf of Mexico	Carbon-14	Jul-Aug 1990	Lohrenz et al. 1999
358 - 1258	Green Bay- Nearshore	Diel O2	2010-2011	Althouse et al. 2014
691-1071	Chesapeake Bay	Carbon-14	Summer 1969-70	Taft et al., 1980

38

system to net heterotrophy and result in GPP:R ratios less than 1 (del Giorgio and Peters 1993).

For 2013-2015 the monthly averaged GPP to monthly averaged R ratio is ~1.09±0.06 (SD),

indicating net autotrophy at this site from June to September. On an annual basis, however,

Figure 11: Daily GPP versus R for the days included in the data analysis from 2012-2015.
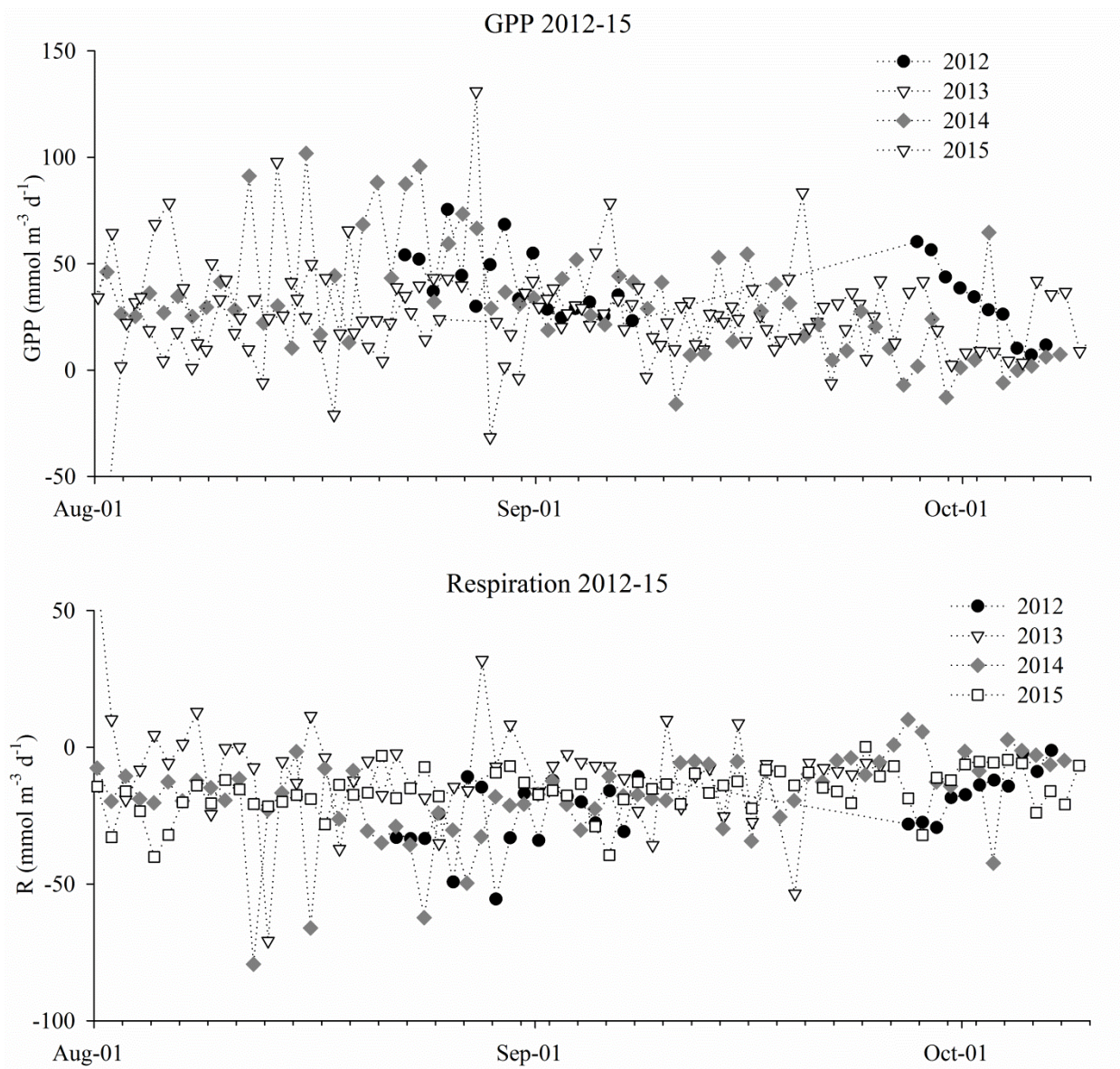
southern Green Bay tends towards net hetero

trophy and carbon budgets are significantly influenced by organic matter inputs from the Fox

River (Robertson and Saad, 2011, Klump et al., 2009; Waples, 1998).

Light-dark bottle incubation experiments conducted in 2013 with water from the same station as

NOAA 45014 compare reasonably well to the monthly averaged *in situ* sonde data rates. August

Figure 12: Results of light-dark bottle experiments and diel sonde measurements in 2013. In each set of bottle treatments there are 3 dates, represented by letters above the bars. Jn: 6/26/13, Jl: 7/31/13 and A: 8/25/13. The daily sonde values (rightmost bars) are from Jn: 6/25/13, Jl: 81/1/13, A: 8/25/13.
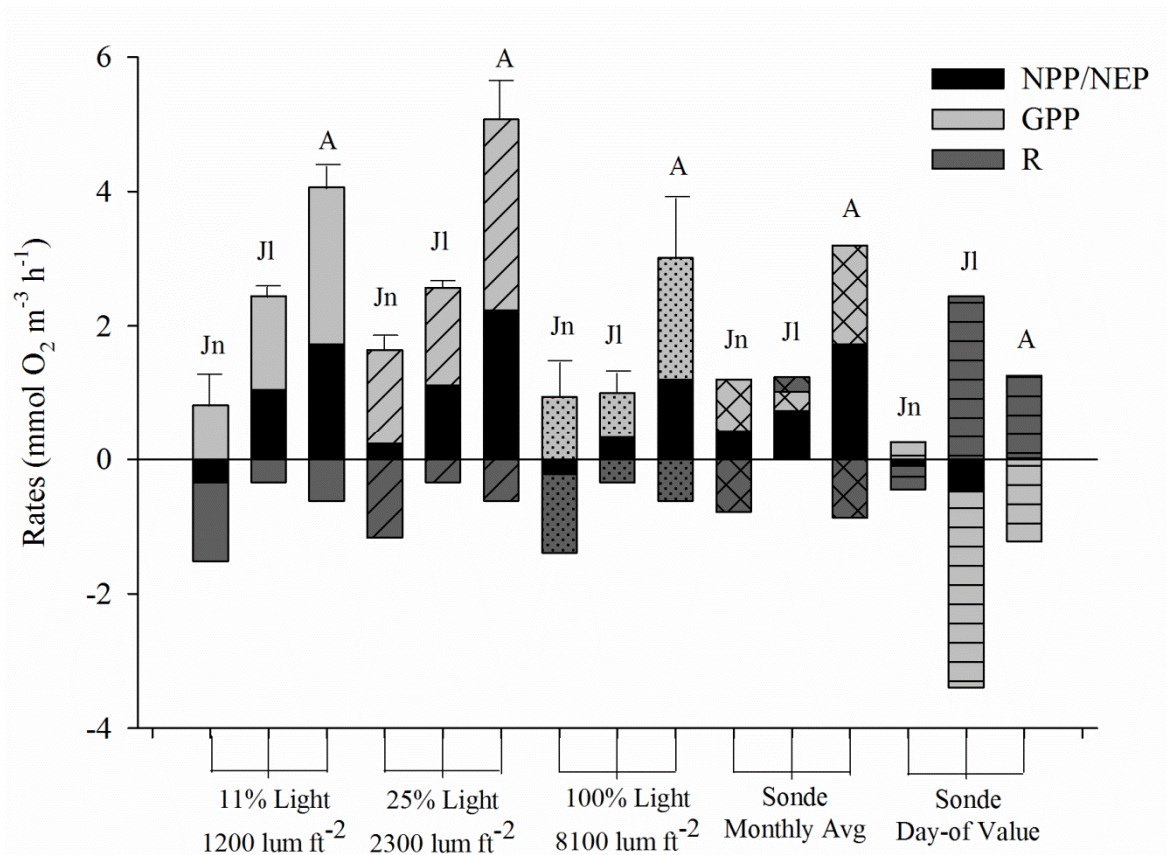
rates (GPP ~ 1.5-2.8 mmol m^{-3} h^{-1}) were higher for both bottle and *in situ* estimates than rates measured in June and July (~0.5-1.5 mmol m^{-3} h^{-1}, Fig. 12). Rates were also highest in the attenuated 25% ambient light bottles and lowest in the 100% ambient light bottles, probably as a result of photo-inhibition. In general both 12% and 25% ambient light incubations gave similar results with slightly higher rates at the higher light level. The *in situ* diel-O$_2$ measured rates agree most closely with the 100% ambient light bottle incubations; however the *in situ* rates were averaged over a longer time period and the bottle incubations only represent 1 day. The monthly averaged *in situ* diel-O$_2$ calculated rates agree more closely with light/dark bottle incubations than the same day *in situ* rates, probably because diel calculated rates are relatively constant over periods of days to weeks. Individual days are subject to perturbations in mixing and short term dynamics that often obscure a simple coherent diel signal that may be missed when a water sample is isolated in a bottle incubation.

Linking NEP and the benthos

The coupling between benthic and pelagic systems is a key process in understanding ecosystem function particularly in shallow aquatic environments (Schindler and Scheuerell 2002; Renaud et al. 2008). Evidence suggests that recently deposited, relatively fresh organic matter settling out of the water column is largely responsible for driving benthic respiration resulting in steep oxygen gradients and oxygen depletion within millimeters of the sediment-water interface (Klump et al., 2009, unpub). Assuming the total net amount of organic material produced within the epilimnion (ΣNEP) settles through the thermocline and reaches the bottom, the extent of benthic respiration that can be supported from production within the overlying water, can be estimated from aerobic benthic carbon metabolism assuming the Redfield stoichiometry for respiration in which 138 moles of oxygen are consumed for every 106 moles of carbon

41

remineralized.   Excess organic matter that is not respired, may be exported, stored within the sediments or remineralized anaerobically.

Over periods of deployment in 2014 and 2015 where a continuous record exists, cumulative NEP production is estimated as 4120 and 1660 mmol O_2 m^{-2} in 2014 (118 days) and 2015 (113 days) respectively for the period of June through September (Fig. 13). There is a relatively constant increase in net production throughout the season, with the exception of when mixing events occur, such as in August 2014. These cumulative production amounts do not capture the total net production in this system, since significant primary production likely occurs during fall, winter and spring months that were not monitored here. Nevertheless, comparisons to other components of the carbon and oxygen budget of the bay may be made as a means of placing these measurements within the context of system mass balances. Klump et al (2009) concluded that southern Green Bay was a net heterotrophic system that is subsidized by significant loading of fixed carbon from upstream reservoirs. It is estimated that 50-60% of the total phosphorus loading delivered to the mouth of the Fox River is derived from the Lake Winnebago system, a highly eutrophic system in its own right, and delivered largely as fixed phosphorus in the form of algae (Dale Robertson, pers. comm.).

 Cumulative net ecosystem production, i.e. that portion of primary production that may be lost from the epilimnion via deposition or advection is estimated at 3.2 and 1.3 mol C m^{-2} over the periods from June through September of 2014 and 2015 respectively or ~ 26.8 and 11.0 mmol C m^{-2} d^{-1}. The mean oxygen consumption rate within the sediments of southern Green Bay during summer is estimated to be approximately 12 mmol O_2 m^{-2} d^{-1} (LaBuhn et al. in prep.). Rates measured at station 17 average 9.1 mmol O_2 m^{-2} d^{-1}.This translates to a benthic carbon aerobic remineralization rate ~7 mmol C m^{-2} d^{-1}.

Figure 13: Top: Cumulative net ecosystem production for 2014 (black) and 2015 (gray) in 30 minute intervals, with bold lines showing the 3-day running average. Bottom: Weekly average NEP accumulation. *marks water column mixing event.
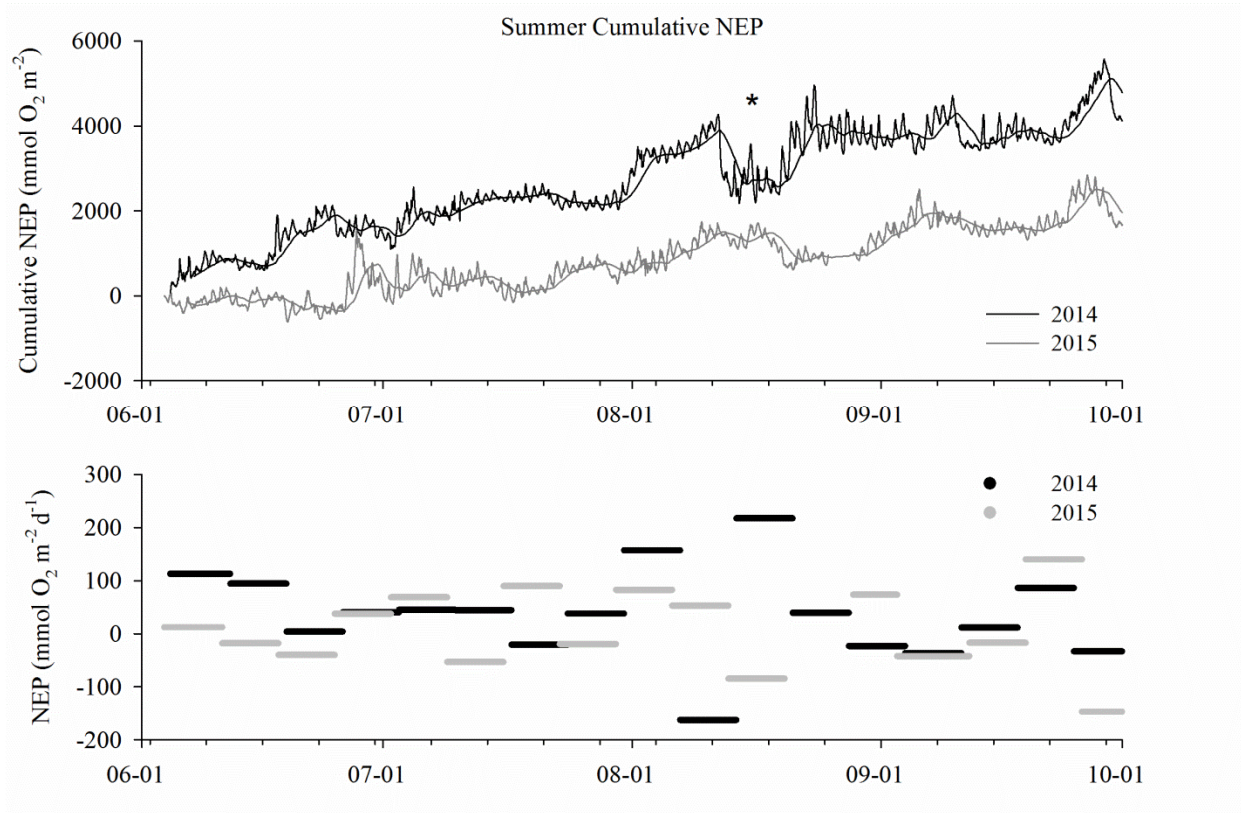
Largely because of its morphology, Green Bay is an extremely efficient sediment trap, sequestering 70-80% of the total nutrient input in rapidly accumulating sediments mostly south of Chambers Island (Klump et al., 1997, 2009). Particle settling rates are also high (meters per day), and algal detritus can reach the sediments within hours to days, particularly under stratified conditions. The implication is that NEP helps fuel benthic respiration, and summertime carbon production could potentially support a significant fraction of the measured sediment respiration rates at this station. This is also consistent with the indirect calculations based upon hypolimnetic oxygen depletion conducted by Valenta (2013) based upon repeated profiling at numerous stations during the summer.

2.5 Conclusions

This study focused on using buoy-based, continuous, real time *in situ* monitoring data collected as part of the GLOS observing network for the estimation of ecosystem primary production in the eutrophic waters of Green Bay. Daily GPP, R and NEP rates were calculated over portions of the summer for 4 years (2012-15), with a majority of the data collected in August and September. General trends include a tendency towards net autotrophy in the epilimnion, based on the August-September average NEP rate, although this was quite variable and the values remained close to zero. Primary production and respiration tended to be greater in August than in September, although this was not always the case.

Primary production rates will undoubtedly vary depending upon location within the trophic gradient, light attenuation, nutrient concentrations, algal speciation, and seasonal succession. In fact, it seems reasonable that a gradient in autotrophy/heterotrophy exists within the bay with distance from the major nutrient input at the mouth of the Fox River (Auer and Canale 1986).

44

Inherent limitations also exist when inferring whole lake production or metabolism from a single spatial location, despite having multiple time points. There can also be shifts in process rates with changes in depth that cannot be captured from a single point measurement. However, the estimated rates and fluxes in this study do imply that the water column and sediments are tightly coupled, and the system is efficient in turning over primary production through respiration and metabolism both in the water column and at the sediment-water interface.

Future work will include linking environmental drivers via ecosystem models to primary production, algal abundance and the formation of hypoxia. Evaluating the role and form of external loading from the lower Fox River and Lake Winnebago would also be insightful since they are major contributors of total phosphorus to Green Bay. Although previous data suggests that perhaps as much as ~75% enters as fixed P (Klump et al. unpub) that may be changing with changing land use practices, especially in agriculture. Since water quality conditions vary greatly in Green Bay, single point estimates of primary production are somewhat limited spatial application or extrapolation. However, in conjunction with other observations, e.g. satellite imagery, nutrient loading, etc. buoy based observations are extremely useful in verifying and calibrating hydrodynamic (Hamidi et al. 2015) and ecological models aimed at projecting the response of the system to changes in landscape processes and climate and informing ecosystem restoration efforts.

Continuous buoy based observations give high frequency temporal datasets that are unobtainable in any other fashion and are extremely helpful in identifying system processes and variability that occurs in highly dynamic coastal systems. These observations are also valuable because they integrate broader scale processes than individual station by station point in time measurements or

experiments. The advent of this technology should reveal unobserved temporal dynamics and assist in evaluating patterns and trends in environmental change.

Acknowledgements

CHAPTER 3: LONG-TERM MEASUREMENTS OF PRIMARY PRODUCTION AND RESPIRATION AT THE ENTRANCE LIGHT

3.1 Introduction

Green Bay Metropolitan Sewerage District (GBMSD), now known as NEW Water, developed a Green Bay Water Quality monitoring program in 1986 under the direction of John Kennedy. Through this program a suite of water quality parameters are measured and continuous moorings are deployed. Weekly grab samples for monitoring water quality parameters are taken around the Lower Fox River, East River, and Lower Green Bay. GBMSD has recently expanded sampling to mid-Green Bay, as well (Fig. 14). Some of the parameters that are measured from the grab samples include total phosphorus, ortho-phosphate, nitrate, nitrite, turbidity, total suspended solids, volatile suspended solids, and chlorophyll-*a* (GBMSD, unpub).

The other component of this water quality monitoring program is the deployment of two YSI 6600 Sondes (Yellow Springs, OH) that measure dissolved oxygen, temperature and conductivity. The sondes are deployed at the Entrance Light station, where the "X" is on Figure 14. One of the sondes is placed 1-meter from the surface and the other is mounted 1-meter from the bottom.

Due to the advantages of calculating primary production and respiration from *in-situ* moorings discussed in LaBuhn and Klump (2016) (i.e. Chapter 2), it was logical to use this dataset to work towards understanding epilimnetic sources and sink of oxygen, one of the goals of this dissertation. The long-term monitoring dataset from GBMSD was used to 1) calculate seasonal gross primary production (GPP), respiration ('R), and net ecosystem production (NEP) and 2) to examine potential trends and drivers of seasonal GPP and R.

48

Figure 14: A map of sampling stations used by Green Bay Metropolitan Sewerage District's Water Quality Monitoring Program. The "X" designates the location of the Entrance Light mooring.
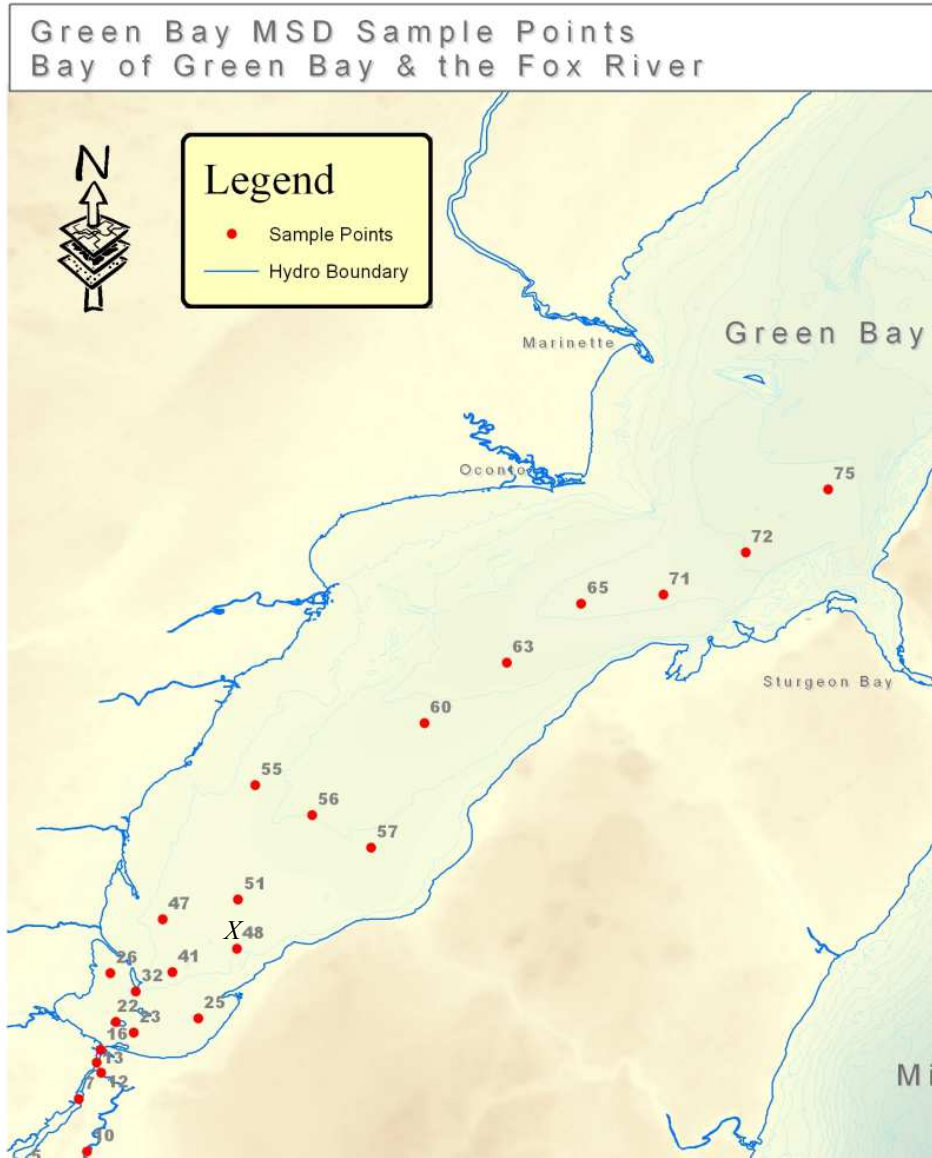
3.2 Methods

GPP, R and NEP

The same general approach was used to calculate GPP, R and NEP as was used in section 2.2 of Chapter 2. Dissolved oxygen (O_2) concentrations and water temperature were measured in 15-minute intervals at 1-meter depth, generally from May to September of each year. The years of data analyzed were 1986-1994, 2004, and 2007-2013. Data was quality checked and provided by GBMSD. Also, since this technique only works over periods of steady-state, only data that exhibited diel O_2 fluxes, indicative of steady-state, were used for calculations of GPP, R, and NEP.

Corresponding wind speed was not available at the site, as it was for the GLOS buoy data in Chapter 2. Therefore, wind data was from NOAA buoy 45002 in northern Lake Michigan was used from 1986 through 2008. In August 2008 a meteorological station was placed on Chambers Island (CBRW3), so that wind data was used from 2009-2013. Wind data from NOAA45002 and CBRW3 was collected in 10-minute intervals. In order to match sonde data collections, the data was transformed to 15-minute intervals using an interpolation technique in R.

The approach was the same as used in Chapter 2. Briefly, wind data was used to calculate piston velocity, which was then used to determine atmospheric flux of oxygen. For ease of calculation, the epilimnetic depth was assumed to be 4 meters 6/1 to 7/15 and 5.5 meters for any date after 7/15. These depths are based on 5-6 water column profiles of temperature over the course of a summer sampling period (i.e. June through September). NEP was estimated:

$$NEP = \frac{dO_2}{dt} + J_{atm} \qquad \text{(Eqn. 3.1)}$$

where J_{atm} is the atmospheric flux and dO_2 is the different in oxygen concentrations between time points, dt. The day and night components of NEP were separated (see Staehr et al. 2010) and NEP_{night} was used as the respiration rate. Respiration was assumed to be equal during the day and night periods, then GPP could be calculated as:

$$GPP = NEP_{day} + R_{day} \qquad \text{(Eqn. 3.2)}$$

where NEP_{day} is the NEP over daylight hours and R_{day} is the R over daylight hours. Then, NEP was calculated last as GPP less R.

Monthly average values of GPP, R and NEP were time-weighted by the number of days each time period contributes. If a time period fell between two months, the value from that period was used in each month. The exception to this was if the time period started on the last day of a month, then the value was only used for the following month (e.g. 7/31-8/2, value only used in August).

Cumulative NEP was calculated for each month based on the average NEP rate for each month. The averaged-monthly NEP in a daily rate was then multiplied by the days of each month to get an estimated cumulative-NEP for each month.

Ancillary Data

The nutrient and bottom sonde data were also provided by GBMSD. The nutrients were analyzed by employees of GBMSD and the data were quality checked. The nutrient data for lower Green Bay stations were averaged together into "Zones" to compare with GPP and NEP from the Entrance Light. Zone 1 nutrients represent the average of GBMSD22 and GBMSD32 samples; Zone 2 nutrients represent GBMSD41-GBMSD51 samples; Zone 3 nutrients represent the

average of GBMSD55-57 samples. The bottom sonde oxygen and temperature data from the Entrance Light was analyzed and provided V. Klump (UWM). This data is part of Klump et al.'s (in prep) discussion of hypoxia in Green Bay.

3.3 Results and Discussion

GPP, NEP and R

There were a total of 124 individual time-periods analyzed for GPP, NEP and R (Table 4). The summertime-averaged GPP (June-September) ranged from 192 to 657 mmol O_2 m^{-2} d^{-1}, with an average production rate of 465 ±120 mmol O_2 m^{-2} d^{-1} (n = 16; Fig. 15). In general, August experienced the highest amounts of productivity (591 ± 198 mmol O_2 m^{-2} d^{-1}; n = 15), followed by July (542 ± 252 mmol O_2 m^{-2} d^{-1}; n = 16). The average summertime respiration was -421 ±125 mmol O_2 m^{-2} d^{-1} and the average net ecosystem production was +46 ± 69 mmol O_2 m^{-2} d^{-1} (Table 5). NEP values were generally positive for June through August and negative in September. Positive values indicate a tendency towards net autotrophy, or net production of organic matter, and negative NEP values indicate net heterotrophy. The overall positive NEP for the summer agrees with results from LaBuhn and Klump (2016), which shows slight net autotrophy ~18 km north of this station. There were a few years (1987, 1990, 1992, and 2007) that had an overall negative average NEP.

The results (i.e. GPP>R and highest production in August) from the Entrance Light station show a similar trend to those observed at GB17 (GBMSD station 63), but larger in magnitude. There are only two years of overlap between the two datasets for further comparisons are not performed. The greater productivity at the Entrance Light could be attributed to either better access to nutrients from the Fox River mouth or to more frequent mixing events at the shallower

station that mixes in nutrient rich bottom water to the surface. Figure 16 demonstrates the historical changes in July primary production and change in phosphate concentrations between June and July. There is some indication that when phosphate is drawn down from June to July there is an increase in primary production ($r^2 = 0.29$). Therefore, the drawdown of phosphorus, the limiting nutrient of this system, is presumably due to increased organic matter formation, which corresponds to increased productivity.

Seasonal net ecosystem production was considered over the historical record. There seems to be an increase in cumulative NEP since 1986 (Fig. 17), although 2012 and 2013 cumulative production were among the lowest. Some years (e.g. 1987-1988) only had NEP rates for 3 out of the 4 months used to calculate the summer cumulative NEP. This likely underestimates NEP for those months, making this a conservative look at potential net production for each year. Since the GPP has remained relatively constant since 1986, the increased NEP must result from decreased respiration. Another explanation could be that increased wind speeds in the lower bay have increased the periods of non-steady state. Therefore, the steady-state time periods that were chosen for the calculations had to have a higher dO_2/dt value to be selected from the noise. Predominant wind direction could also affect how much of the nutrient-rich Fox River water was reaching the Entrance Light station. For instance, winds out of the west would force the Fox River plume to hug the eastern shore of Green Bay and a majority of the nutrients may "by-pass" the sensor. The differing source of wind data (i.e. NOAA45002 vs CBRW3) is not likely to have influenced these results since average summertime wind speeds from 2009-2012 were higher at NOAA54002 than CBRW3 (Table 6) and higher winds actually results in greater NEP. For example, 7/6-7/9, 2009 a wind speed increase by a factor of 1.8 results in NEP of 285 mmol O_2

53

m^{-2} d^{-1} (compared with 190 mmol O$_2$ m^{-2} d^{-1} before). Therefore, if wind data from NOA54002

was used, the NEP rates

Table 4: Entrance Light data time periods that were analyzed for GPP, NEP and R (mmol O$_2$ m^{-2} d^{-1}).

Year	Month	Date Range	GPP	NEP	R
1986	June	6/18-6/20	551	101	-450
1986	July	7/6-7/8	218	56	-161
1986	July	7/16-7/19	356	86	-270
1986	August	7/31-8/2	294	-58	-352
1986	August	8/6-8/8	445	67	-378
1986	August	8/15-8/17	321	148	-174
1986	August	8/19-8/21	333	122	-210
1986	September	9/24-9/26	591	-134	-727
1987	July	7/17-7/20	265	3	-261
1987	July	7/26-7/28	223	-21	-242
1987	August	7/31-8/2	237	-28	-265
1987	August	8/11-8/14	438	91	-347
1987	August	8/19-8/24	199	-103	-303
1987	September	9/2-9/10	450	-55	-505
1988	July	7/1-7/5	439	40	-399
1988	July	7/11-7/13	283	-16	-299
1988	July	7/22-7/27	904	62	-840
1988	August	7/31-8/3	347	95	-253
1988	August	8/12-8/14	708	0	-708
1988	September	9/9-9/12	237	31	-206
1988	September	9/14-9/16	296	-65	-359
1989	July	7/1-7/4	269	73	-196
1989	July	7/14-7/18	928	158	-772
1989	July	7/22-7/26	1224	270	-954
1989	August	8/7-8/11	861	29	-834
1989	August	8/26-8/28	863	89	-773
1989	September	9/13-9/18	254	-57	-311
1990	June	6/24-6/27	475	-11	-488
1990	July	7/15-7/22	679	21	-657

54

1990	August	7/31-8/3	421	-132	-552
1990	August	8/22-8/25	481	-93	-574
1990	September	9/1-9/3	354	-256	-610
1992	June	6/24-6/28	306	55	-251
1992	July	7/24-7/28	832	-62	-894
1992	August	8/2-8/7	863	-81	-944
1992	August	8/14-8/17	1272	67	-1205
1992	August	8/19-8/21	1219	-81	-1301
1992	September	9/3-9/6	168	-83	-249
1992	September	9/10-9/13	222	-65	-287
1993	June	6/12-6/14	509	15	-494
1993	June	6/28-7/4	274	48	-226
1993	July	6/28-7/4	274	48	-226
1993	July	7/14-7/17	1298	237	-1059
1993	August	8/12-8/14	670	-36	-706
1993	August	8/25-8/27	681	46	-634
1994	June	6/21-6/23	255	6	-249
1994	July	7/3-7/5	280	-15	-296
1994	July	7/20-7/23	385	115	-270
1994	July	7/26-7/28	409	26	-385
1994	August	8/15-8/18	404	2	-402
1994	August	8/25-8/27	476	168	-306
1994	September	9/23-9/25	416	-74	-488
2004	June	6/4-6/8	463	120	-343
2004	June	6/26-6/30	116	25	-91
2004	July	7/18-7/21	897	284	-614
2004	July	7/23-7/28	1105	158	-947
2004	August	7/31-8/2	648	186	-461
2004	August	8/6-8/8	823	52	-770
2004	August	8/14-8/16	691	29	-663
2004	September	9/3-9/5	414	131	-284
2007	June	6/24-6/27	150	13	-138
2007	July	7/3-7/5	213	-59	-338
2007	September	9/27-9/30	213	28	-186
2008	June	6/25-6/27	279	124	-155
2008	July	7/4-7//6	989	193	-796
2008	July	7/23-7/25	605	72	-533

2008	August	7/31-8/2	308	81	-227
2008	August	8/4-8/6	400	62	-339
2008	August	8/11-8/17	815	79	-736
2008	August	8/20-8/22	579	58	-523
2008	August	8/29-9/4	457	34	-425
2008	September	8/29-9/4	457	34	-425
2009	June	6/21-6/24	171	104	-68
2009	July	7/4-7/6	429	190	-239
2009	July	7/9-7/11	315	199	-116
2009	August	8/21-8/25	430	229	-201
2009	August	8/26-8/29	565	108	-457
2009	September	9/2-9/8	555	112	-443
2010	June	6/16-6/19	333	119	-213
2010	July	7/7-7/11	158	6	-150
2010	July	7/16-7/18	211	201	-10
2010	July	7/25-7/30	359	210	-151
2010	August	8/1-8/5	473	266	-206
2010	August	8/9-8/13	605	249	-356
2010	August	8/21-8/23	622	438	-184
2010	August	8/26-9/3	500	282	-220
2010	September	8/26-9/3	500	282	-220
2010	September	9/18-9/20	679	107	-574
2010	September	9/25-9/30	455	101	-354
2011	June	6/12-6/15	413	106	-306
2011	June	6/29-7/2	455	193	-263
2011	July	6/29-7/2	455	193	-263
2011	July	7/3-7/5	334	189	-145
2011	July	7/6-7/12	334	116	-218
2011	July	7/15-7/17	883	474	-411
2011	July	7/29-8/1	375	29	-345
2011	August	8/3-8/7	803	134	-669
2011	August	8/16-8/21	650	70	-581
2011	August	8/25-8/30	528	88	-440
2011	September	9/6-9/11	571	22	-548
2011	September	9/15-9/17	418	62	-356
2012	June	6/23-6/27	258	30	-229
2012	July	7/8-7/16	281	39	-243
2012	July	7/20-7/26	646	70	-576

2012	July	7/28-8/5	782	19	-763
2012	August	7/28-8/5	782	19	-763
2012	August	8/6-8/8	710	91	-619
2012	August	8/12-8/14	481	-69	-550
2012	August	8/18-8/22	495	-12	-507
2012	August	8/27-8/30	715	40	-675
2012	September	8/31-9/5	442	15	-426
2012	September	9/14-9/16	375	-2	-376
2012	September	9/18-9/25	162	-7	-168
2013	June	6/19-6/21	279	15	-264
2013	June	6/24-6/27	300	56	-233
2013	July	7/2-7/8	454	104	-351
2013	July	7/11-7/15	476	106	-371
2013	July	7/30-8/4	440	22	-418
2013	August	7/30-8/4	440	22	-418
2013	August	8/6-8/9	792	67	-725
2013	August	8/10-8/13	486	-29	-516
2013	August	8/14-8/21	844	65	-779
2013	August	8/26-8/30	373	10	-363
2013	September	9/3-9/7	392	-7	-399
2013	September	9/9-9/12	378	-22	-400
2013	September	9/22-9/28	234	-53	-287

Figure 15: Gross primary production separated by monthly averages. Red dots indicate the summer average.
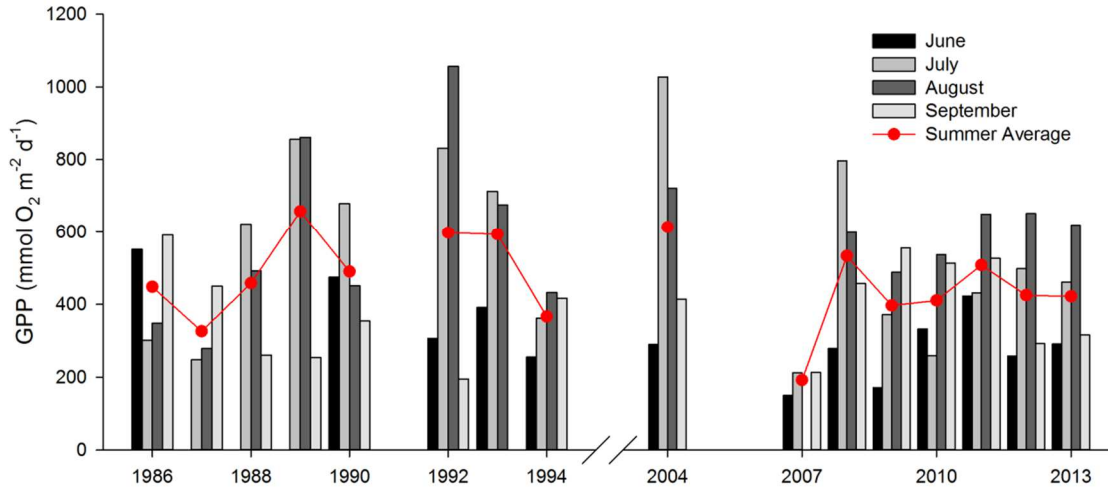
Table 5: GPP, NEP, and R average rates (mmol O_2 m-2 d-1) over June-September.

	GPP	NEP	R
1986	448	28	-420
1987	326	-13	-356
1988	458	30	-428
1989	657	56	-602
1990	490	-90	-579
1992	597	-29	-627
1993	593	55	-538
1994	366	13	-353
2004	613	124	-488
2007	192	-6	-220
2008	533	89	-444
2009	397	147	-250
2010	411	175	-236
2011	508	106	-402
2012	425	23	-402
2013	422	35	-386
Overall Average	465	46	-421
Standard Deviation	120	69	125

Figure 16: (Top) Historical comparisons between average July primary production (GPP) and the loss of phosphate from June to July. (Bottom) Scatterplot of the GPP and phosphate loss with linear regression.
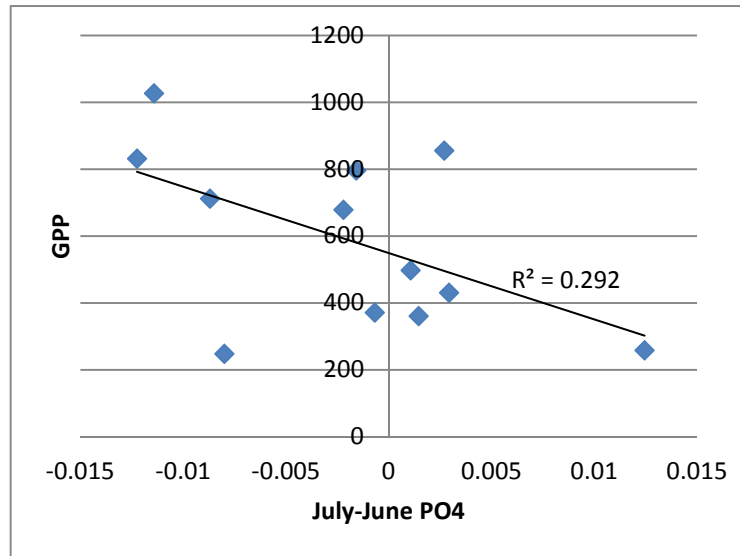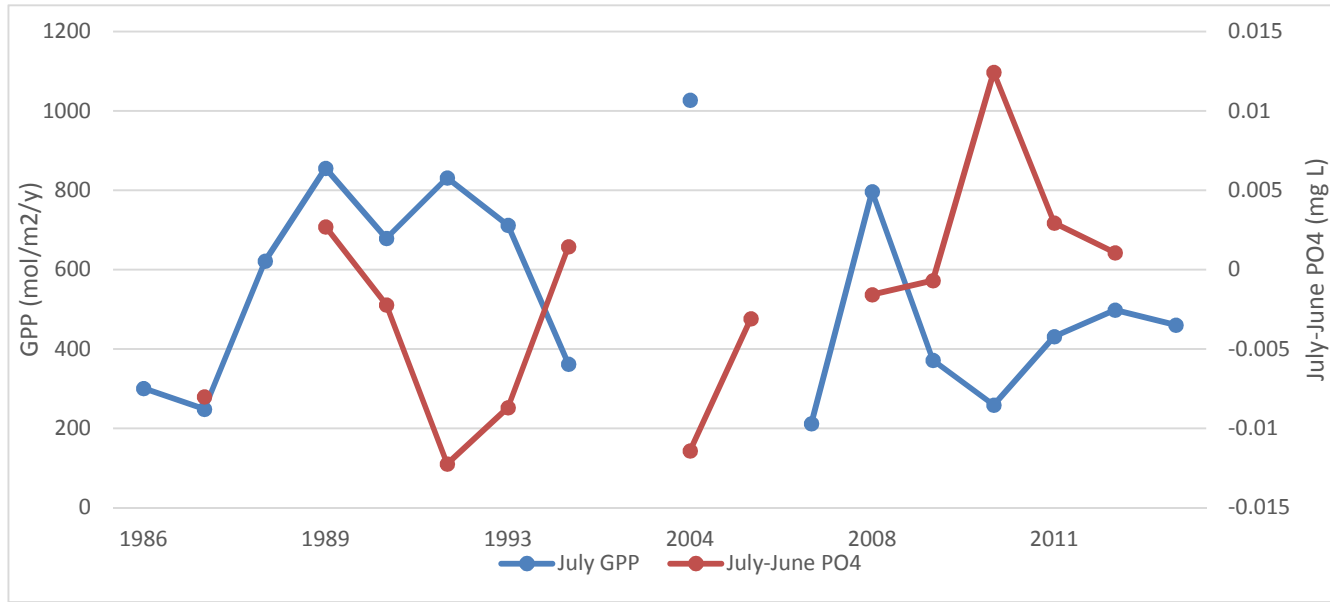
Figure 17: Cumulative net ecosystem production (mol O_2 m-1) for the entire summer (blue line plot) separated by each month's contribution (colored bars).
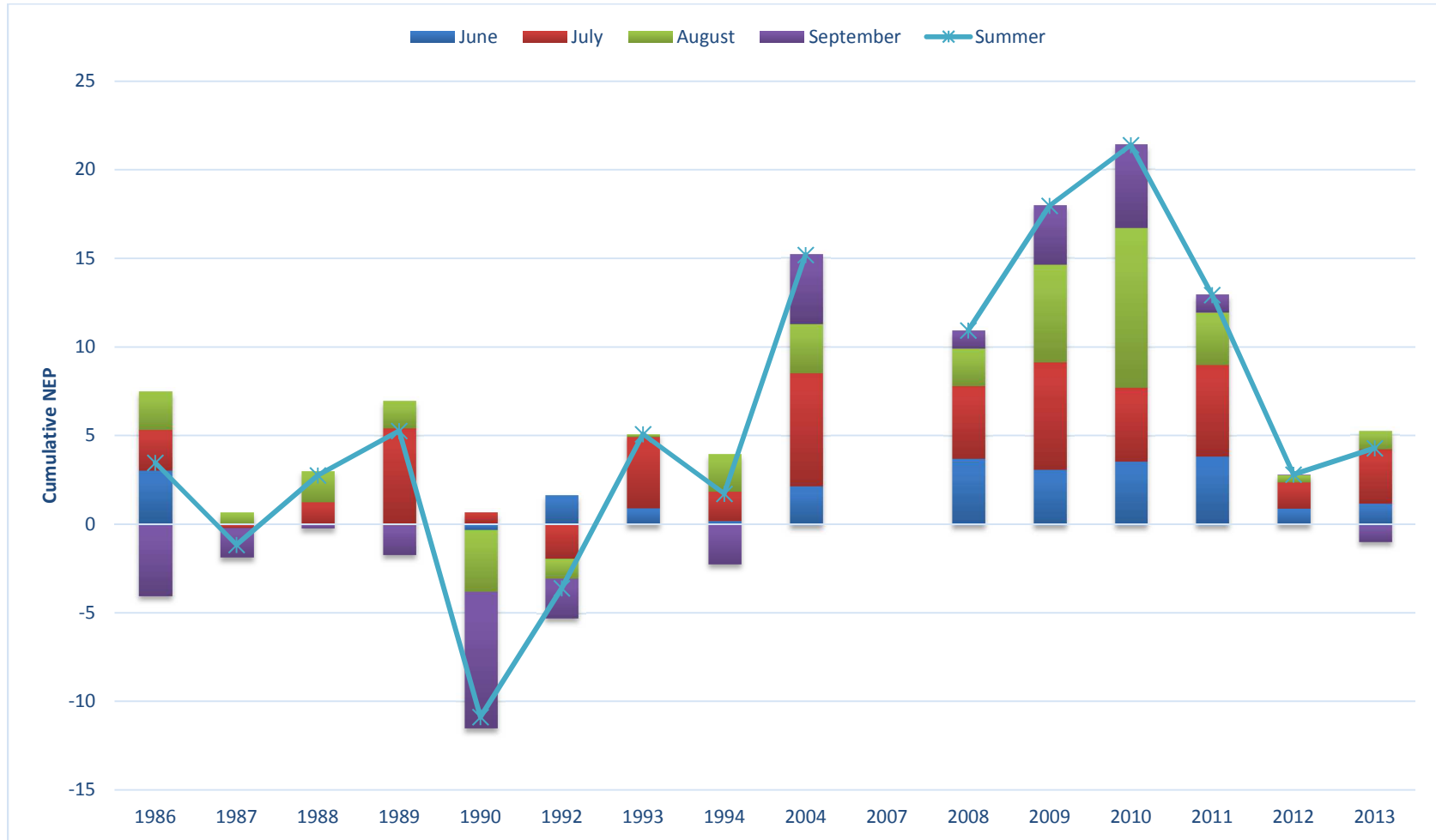
Table 6: Wind speed (m s-1) comparisons for meteorological stations CBRW3 and NOAA45002 over June 1 – September 30 for each of the given years. Data taken from ndbc.noaa.gov.

	Average	SD	Average	SD
	CBRW3		NOAA 45002	
2009	2.675	1.963	4.723	4.514
2010	2.938	1.865	5.405	3.155
2011	3.02	2.275	4.818	4.094
2012	3.007	2.055	5.403	2.813

would be even higher than those presented meaning that respiration would have had to have increased even more.

If the summertime average GPP for each year is compared with the number of low oxygen days in the hypolimnion (Fig. 18a) there are some years that clearly show a relationship between high GPP and increased oxygen consumption in the bottom water, although the statistical relationship is not strong ($r^2 = 0.03$). Summertime net production is a better indicator of low oxygen days, with a $r^2 = 0.20$ between average summer NEP and days <3.0 mg O_2 L^{-1}. The cumulative NEP for each year follows the same trend and relationship as NEP (Fig. 18b). The response of increased oxygen consumption in the bottom with greater amounts of net production is logical because it has been shown that settling organic matter drives hypolimnetic oxygen consumption (Grenz et al. 2000; Renaud et al. 2008). This is also one of the primary mechanisms driving hypoxia suggested by Klump et al. (in prep).

3.4 Conclusions

The Entrance Light data shows that the lower bay is net autotrophic in the summer months. The June-September net production at the Entrance Light was ~2x the net production at the GLOS buoy at GB17 (or station GBMSD63 in Fig. 14). The lower bay region also experiences higher rates of production and respiration than at GB17, which is attributed to closer proximity to the Fox River mouth and its nutrient load.

Comparisons of productivity and phosphate concentrations show a relationship between increased production when phosphate is consumed, which is expected because it is the limiting nutrient in Green Bay. There is also a relationship between net ecosystem production and the

63

number of oxygen depleted days in the season, confirming a linkage between pelagic and benthic processes.

Figure 18a: Summer-averaged gross primary production and days where oxygen concentrations are less than 3 mg L^{-1} and 1 mg L^{-1}. 18b: Summer-averaged net ecosystem production (mol O_2 m^{-2} yr^{-1}), summer cumulative net production (mol O_2 m^{-2}) and days that bottom water oxygen concentrations were less than 3 mg L^{-1}.
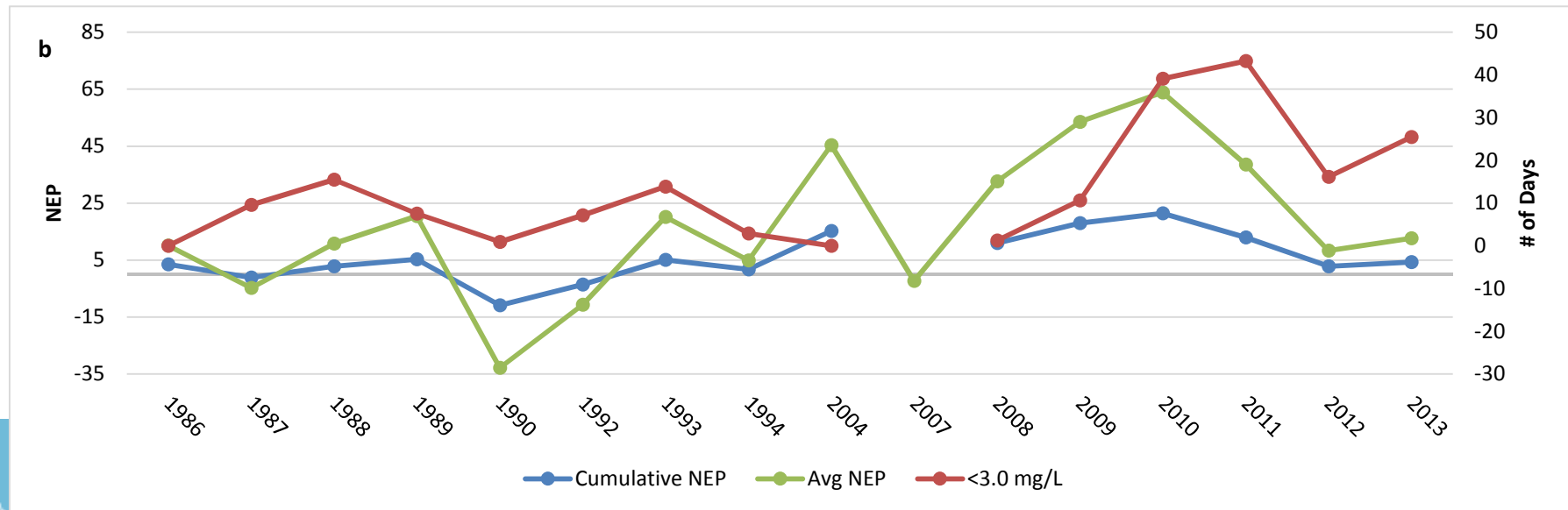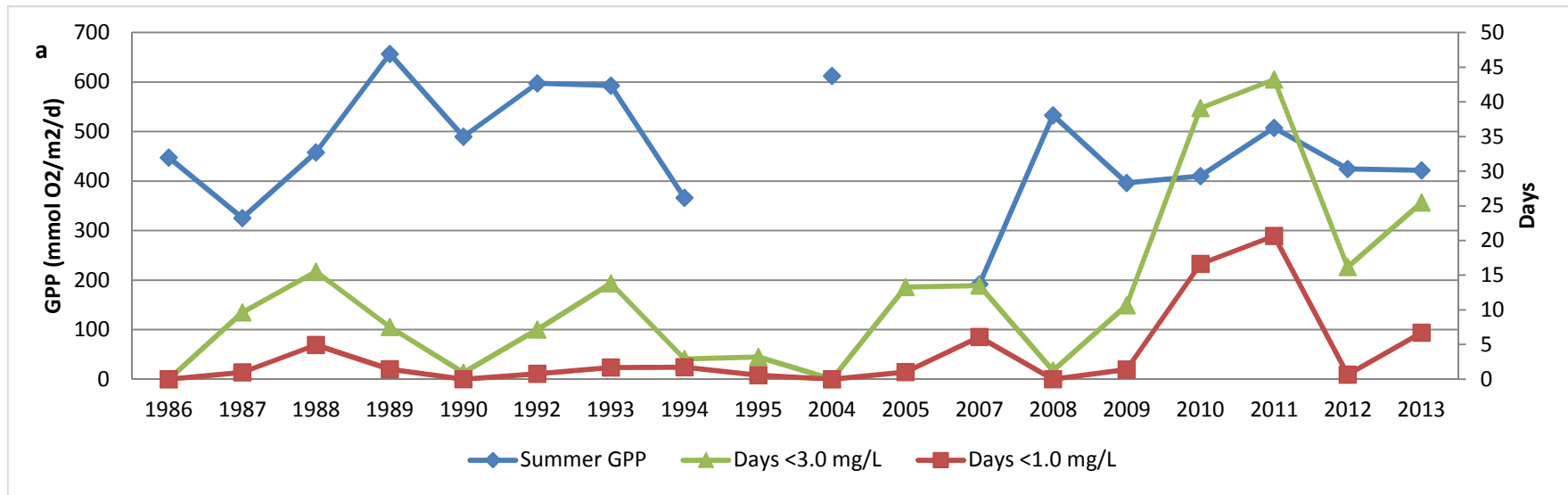
CHAPTER 4: BENTHIC RESPIRATION AND HYPOXIA IN GREEN BAY, LAKE

MICHIGAN

4.1 Introduction

While the occurrence of hypoxic zones is widespread and growing in number with some 400 "dead zones" identified globally (Diaz and Rosenberg 2008), the suite of processes that ultimately lead to oxygen depletion vary substantially, and are controlled, in large part, by a unique combination of local physical dynamics and organic matter loading. Green Bay, Lake Michigan has experienced oxygen depletion for decades (Klump et al in prep).   Early in the 20th century excessive discharges, largely from paper mills on the lower Fox River which empties into Green Bay, often resulted in high biochemical oxygen demand (BOD) and hypoxic conditions within the Fox River and southern portions of the lower bay, including during winter under the ice (Pollution 1939). Following the waste load allocation program under provisions of the Clean Water Act, BOD loadings were substantially reduced in the 1970's, alleviating oxygen depletion within the river and the waters of bay influenced by the river plume. More recently, however, hypoxic conditions have been observed during summer months in portions of the bay remote from the river mouth (Figure 19a). Indications are that oxygen depletion results from respiration of organic debris generated by hyper-eutrophication in combination with thermal stratification, particle deposition and river-lake mixing (Hamidi et al 2015, Klump et al in prep).

Green Bay has long experienced excessive algal blooms that are a result of nutrient runoff from the Fox-Wolf River watershed (Sager and Wiersma 1975; De Stasio et al. 2008). Nearly 1/3 of the total phosphorus load to the entire Lake Michigan basin (~ 500-800 MT/year) enters via the Fox River (Klump et al. 1997a; Robertson and Saad 2011). Bloom-generated organic matter quickly settles to the sediment-water interface and may be resuspended numerous times before finally being permanently buried (Klump et al. 1997a, 2009). Hence oxygen consumption can occur throughout this cycle and the relative contributions of water column and benthic

Figure 19: a: Maps of bottom water dissolved oxygen concentrations (mg L-1) at various stations (black dots) in Green Bay during 3 cruises in 2012. b: Green Bay sampling grid used in this study.
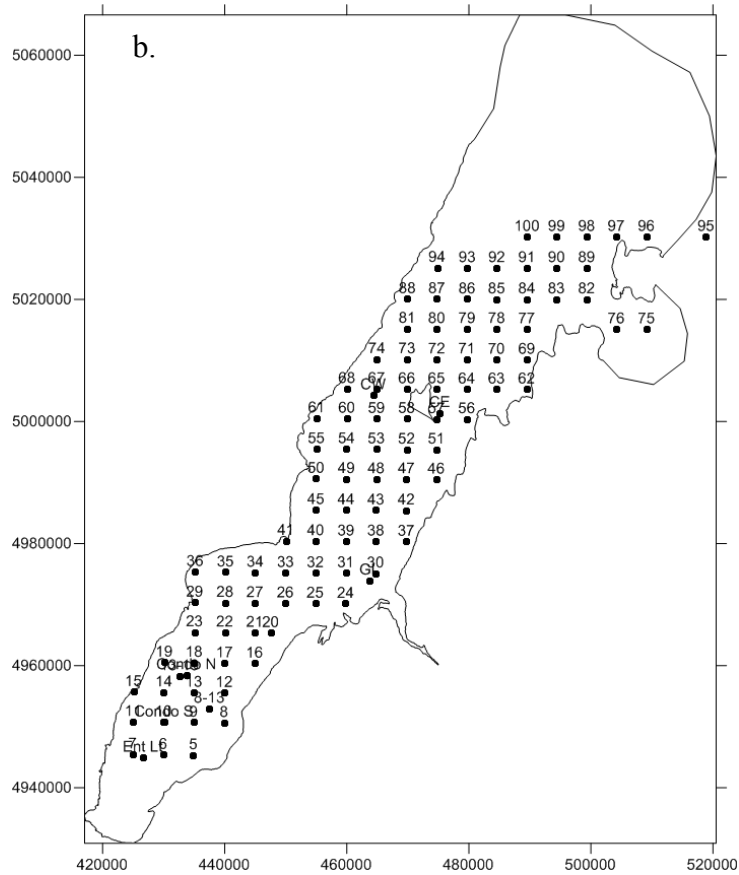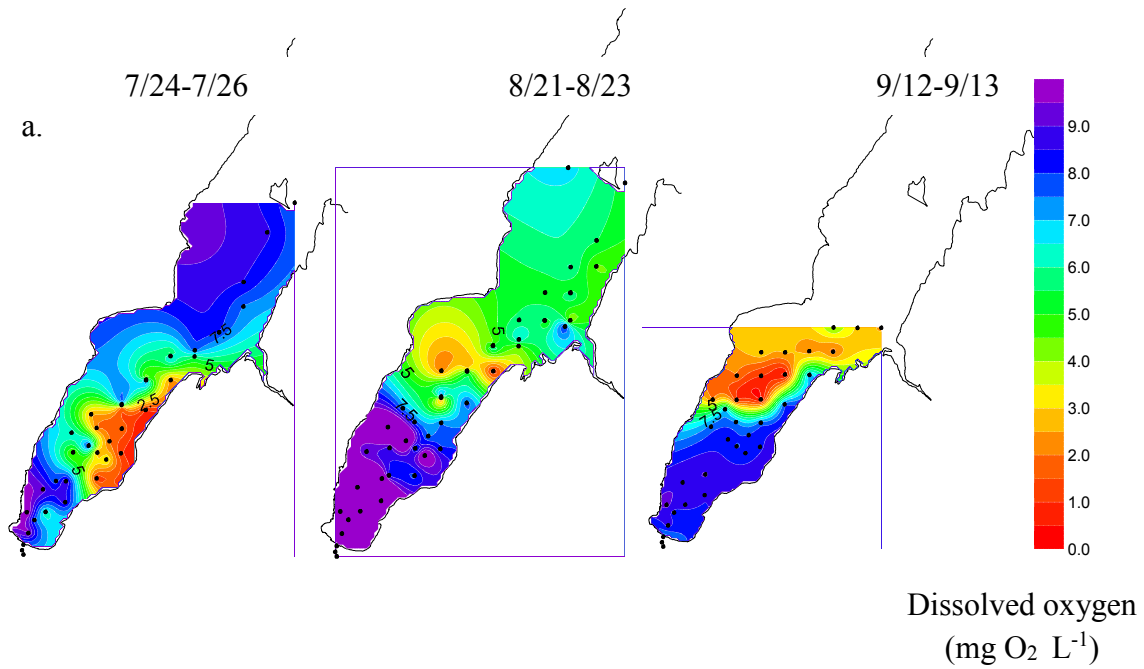
respiration may vary with depth, proximity to the Fox River inputs, and the strength and duration of physical mixing.

Respiratory losses of oxygen consist primarily of water column and benthic respiration. Oxygen consumption within the water column is, for the most part, a response to detrital fallout of decaying algal debris (Findlay and Sinsabaugh 2003; MacPherson et al. 2007). Fitzgerald (1989) showed that phytoplankton decomposition is rapid in Green Bay, with 25% of the biomass respired within a matter of a few hours. Sediment oxygen demand (SOD), on the other hand, can result both from the decomposition of fresh organic matter and from a legacy of organic matter deposition that builds up over time (DiToro 2001; Matzinger et al. 2010). In Green Bay, sediments accumulate rapidly, up to a cm per year, and have an organic carbon content of up to 10% by weight (Klump et al. 2009). These sediments become anaerobic within millimeters (Klump et al. 1997b) and the consumption of oxygen at the benthic boundary is a major component of the oxygen budget for the bay and a major, but previously unquantified, driver of hypoxia.

Many studies and models have been carried out and developed to help understand the formation and occurrence of hypoxia in other systems (Adams et al. 2013; Scully 2016). Biological and physical factors, the major contributors of hypoxia, combine in various ways in different environments to create low oxygen environments. For example, in Chesapeake Bay a model demonstrated that wind speed could explain 50% to 58% of the inter-annual variation in hypoxia during July and August, respectively, because the wind controls mixing and the extent of hypoxic waters especially in later summer (Scully 2016). At the coastal Oregon shelf, seasonal upwelling introduces oxygen poor, nutrient rich waters to the bottom waters which are responsible for lowering oxygen concentrations and stimulating primary production, but also

69

prevent the waters from going fully anoxic through advection and mixing mechanisms (Adams et al. 2013). During summer months in Green Bay a predominant southwest wind drives warm, surface water out of the bay and promotes cooler bottom water from the northern bay and Lake Michigan to replace the lost water, which results in a wind-driven 2-layer flow (Miller and Saylor 1985; Gottlieb et al. 1990; Hamidi et al. 2013). This southerly incursion of cool bottom water during southwest winds, termed cool water intrusions, accentuates thermal stratification and can quickly reestablish a thermocline following intermittent mixing events. The prevailing wind field is important in driving this 2-layer flow and interannual shifts in the wind climate have been shown to reduce the extent of Green Bay-Lake Michigan mixing, causing a subsequent increase in bottom water temperatures and oxygen concentrations from reduced stratification (Waples and Klump 2002). This means that wind speed and direction are important for Green Bay biogeochemical processes, unlike a system such as Lake Erie where only wind speed was a major predictor of inter annual hypoxia (Scully, 2016).

In an estuarine-like circulation pattern, such cold water intrusions have been linked to development of hypoxia in coastal estuaries and can alter fish behavior, fisheries catch, and abundance of prey food (Ludsin et al. 2009; Levin et al. 2009). In Green Bay one such "hypoxic blob" triggered a rare but dramatic fish kill and beaching of tens of thousands of round gobies in August 2005 near the southwest coastline following the shoreward intrusion of a cold, hypoxic water mass (Qualls et al. 2014, WIDNR, unpub).

The primary goal of this study is the quantification of the processes affecting the hypolimnetic oxygen budget in the lower bay (defined as south of Chambers Island) based on empirical measurements. We aim to address this by relating observations of benthic respiration and hypolimnetic oxygen loss to hydrodynamics in the bay quantified by isotopic tracers.

Hypolimnetic water column respiration is also estimated through empirical observations and a hypolimnetic oxygen budget. The relative contributions of benthic respiration and hypolimnetic water column respiration to the oxygen deficit are compared along the depth gradient of Green Bay. These observations are then related to current management strategies for Green Bay to discuss ecosystem responses that may affect management decisions.

4.2 Methods

Study area

Green Bay is the largest freshwater estuary in the world, located in northwest Lake Michigan. This gulf is approximately 190 km in length and 22 km in mean width. The southern end of Green Bay is quite shallow (mean depth <10 m) and it gradually gets deeper towards the north, with a maximum depth of 54 m. The same 5 km x 5 km sampling grid that Klump et al. (2009, 1997a) used was used here for sampling (Fig. 19b). All measurements were taken off of the University of Wisconsin-Milwaukee's R/V Neeskay or Green Bay Metropolitan Sewerage District's R/V Bay Guardian.

The Fox River, which enters at the southern tip of Green Bay, is the largest tributary to the system and delivers 60-70% of the nutrient and sediment loads for the entire bay (Klump et al. 1997a, 2009; Dolan and Chapra 2012). The Lower Fox River watershed is primarily used for agriculture, which has resulted in high nutrient loads to the river and eutrophication of the lower bay (Sager and Wiersma 1972). Mixing between Fox River water (eutrophic) and Lake Michigan water (meso-oligotrophic) creates a gradient within Green Bay, in terms of trophic status (Millard and Sager 1994) and conductivity values (Modlin and Beeton 1970).

Oxygen Depletion

Oxygen depletion in the waters of Green Bay was estimated from changes in measured dissolved oxygen concentrations and inventories collected throughout the summer stratified period. Water column profiles of oxygen were collected approximately monthly during cruises in June, July, August, and September from 2011 to 2014 using YSI (YSI Inc., Yellow Springs, OH) 6600 sondes equipped with temperature, dissolved oxygen, conductivity, turbidity, pH and pressure sensors. Sondes were lowered through the entire water column at a rate slow enough (~2 cm s^{-1}) to capture the sharp thermal gradients present in Green Bay during the summer. Approximately 350 profiles were measured over the study period (all profile data available at *online database* http://fwwa.adc4gis.com/).

Thermoclines in Green Bay typically exhibit a temperature change of 8 to 14 degrees Celsius over a depth interval as narrow as 1 meter. The hypolimnion depth was determined by defining the top of the hypolimnion as the point in the profile, below the thermocline, in which temperature change was less than 1 °C m^{-1} (Quinlan et al. 2005).

In systems which become isolated from contact and exchange with the atmosphere, the loss of oxygen may be estimated from the difference between the measured, *in situ* concentration and the concentration that water mass would have had when initially in equilibrium with the atmosphere – a term referred to as apparent oxygen utilization (AOU). In lakes, this isolation begins at the onset of thermal stratification and is the controlling force that leads to hypoxia. Hypolimnetic AOU was determined using measurements from water column profiles measured in July to September 2009 through 2015 as:

$$AOU = O_2^{obs} - O_2^{sat} \qquad \text{(Eqn. 4.1).}$$

Expressions of oxygen depletion on an areal basis (AOU_{area}) are simply calculated from the apparent loss and the thickness of the hypolimnion (dz) derived from the temperature profile as above for an individual time point, i.e.

$$AOU_{area} = AOU \times dz \qquad \text{(Eqn. 4.2)}.$$

Apparent oxygen utilization is simply the net result of all sources and sinks that lead to the observed depletion. In order to estimate rates of oxygen consumption, oxygen inventories within the hypolimnion, I_{O2}, were calculated for each profile as the sum of the product of the dissolved concentration and depth interval for each layer, z, where Δz was ~ 3 cm:

$$I_{O2} = \sum[DO\ \Delta z] \qquad \text{(Eqn. 4.3)}.$$

An areal hypolimnetic oxygen consumption rate, *HOD*, was then calculated for each station from changes in these inventories over time

$$HOD = (I_{Hypo}^{i} - I_{Hypo}^{j})/\Delta t \qquad \text{(Eqn. 4.4)}$$

where Δt is the difference in time between sampling periods.

Since the hypolimnion is continuously supplied by oxygen transfer from the epilimnion, hypolimnetic consumption rates must be corrected for oxygen diffusion across the thermocline, which was calculated via

$$J_T = -K_z \frac{dO_2}{dz} \qquad \text{(Eqn. 4.5)}$$

where J_T is the diffusive flux of oxygen, K_z is the eddy diffusivity or vertical diffusion coefficient and dO_2/dz is dissolved oxygen concentration gradient across the thermocline. Vertical eddy diffusivities have been estimated using a variety of methods in different environments, e.g. time

series analysis of moored ultrasonic current meters in the shallow (~ 8 m) western basin of Lake Erie (Loewen et al., 2007), tritium tracer diffusion studies in ELA Lakes 224 and 227 (Quay et al. 1980), and micro-profiler temperature gradients in the central basin of Lake Erie (Edwards et al., 2005). Vertical diffusivities are closely related to the dynamic stability of the water column and values range over several orders of magnitude, e.g. $< 10^{-3}$ cm^2 sec^{-1} (Edwards et al. 2005; Loewen et al. 2007), 5.0×10^{-5} cm^2 sec^{-1} and 8.0×10^{-6} cm^2 sec^{-1} (Quay et al. 1980). For the highly stratified, steep thermoclines in Green Bay under relatively calm, stable conditions, values of K_z closer to those measured in the central basin of Lake Erie (Edwards et al. 2005) appear most applicable.

Sediment Core Incubations

Cores for sediment oxygen demand incubations were collected over the course of 18 cruises at a total of 32 Green Bay stations during the summers 2009-2011 and 2013-2015. Using a box corer (surface area 30 cm x 30 cm) sediment cores of up to ~ 80 cm in length were retrieved with a relatively undisturbed sediment-water interface as noted by an intact oxidized surface layer, which in Green Bay is generally less than a few millimeters (Klump et al 2009). Box cores were sub-sampled into quadruplicate 70 cm long, 6.8 cm diameter, plastic core liners leaving > 15 cm head space above the sediment-water interface. Three of these subcores were reserved for each incubation experiment. Sediments and overlying waters were carefully extruded to within ~10 cm of the top of the liner. Subcores were sealed with a poly-carbonate (buna-N) O-ring sealing cap, supporting a mechanical stirrer (paddle = 1.3 cm x5.9 cm, see Fig. 20), 2 luer-loc syringe sampling ports and a port for a polarographic oxygen electrode (Traceable® Digital Oxygen Meters 21800-022). The oxygen sensor was placed at ~5 cm above the sediment-water interface. Triplicate sediment subcores were either placed into a shipboard incubator or wrapped in

74

aluminum foil and incubated in a water bath to maintain temperature. The mechanical stirrers

were operated at 21 rpm which was adequate to mix the overlying water, but slow enough to

avoid visually disturbing the sediment-water interface. The oxygen-sensor

Figure 20: Sediment core incubation set-up with motorized spinners (a, b), oxygen sensors ('c) and sampling ports (d).
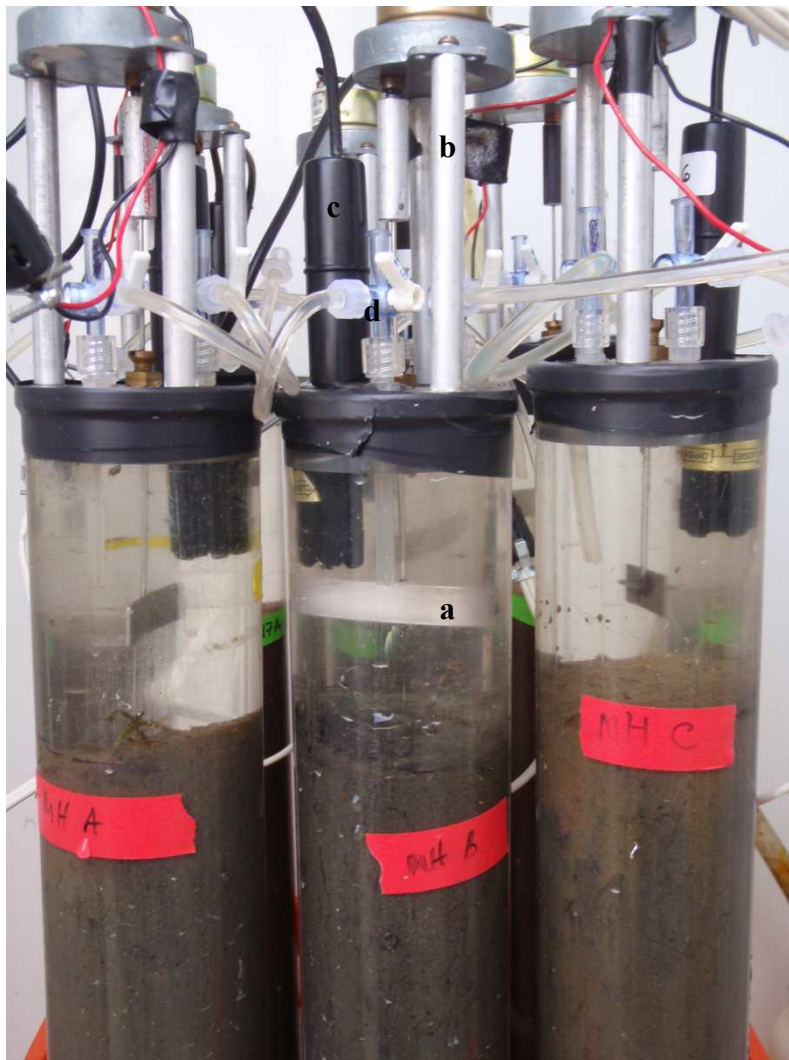
recorded dissolved oxygen concentration and temperature at one second intervals over the course of the incubation. Outputs from the sensors were collected via a software program designed in Visual Basic by T. Hansen (2005) through a multi-port serial card. Up to 9 subcores (3 stations) could be run simultaneously. A total of 86 sediment core incubation experiments were performed in triplicate from June to October in 2009-11 and 2013-15 over 32 stations in southern Green Bay (Table 7). Examples of core incubation results are shown in Figure 21. Oxygen declines were generally linear, and sediment oxygen uptake rates were calculated from regressions of the decreases in oxygen inventories with time. Sensor drift was estimated to be less than 80 mmol O_2 m^{-3} d^{-1} based upon control incubations without sediment, which was considered to be minimal so no corrections were applied. Eight incubations (3%) were discarded because of leakage or loss of an airtight seal.

In most cases, benthic respiration rates were calculated from the onset of the experiment once sensor readings became stable (usually within 30 to 60 minutes) until the concentrations ceased to decline or until the experiment was discontinued, usually within 24-48 hours. In some instances there was a shift in the slope of oxygen inventory decrease over time. For these cases, both an initial rate (typically over a period of < 6 hours) was calculated in addition to a longer term rate which included the entire time course (Fig. 3b). The duration of the experiments varied from 24 hours to 5 days, depending on cruise length and sampling frequency. The 1-second interval oxygen and temperature data were averaged into 3-minute bins for calculations to reduce the number of data points and to remove any abnormal sample points.

Benthic respiration rates, like other biologically driven rates, are temperature dependent. Due to differences between *in situ* and incubation temperatures, the SOD rates were adjusted to ambient temperatures using an Arrhenius function. Klump et al. (2009) conducted whole sediment

76

Table 7: Summary of all sediment oxygen demand experiments and site averaged rates. Rates are in mmol O_2 m^{-2} d^{-1}.

Station	Date	Temperature-Corrected SOD Rate	Station Average	Std Deviation
GBMSD26	9/25/13	31.3	31.3	
GBMSD48	9/25/13	14.0	14.0	
GBMSD50	9/25/13	23.3	23.3	
Ent Light	8/25/15	12.6	12.6	
Mud Hole	7/22/14	18.7	18.7	
2S	8/27/14	32.9	32.9	
5	8/31/10	5.3	39.3	48.0
	9/7/11	73.2		
6	7/29/10	3.5	21.4	13.9
	8/17/11	25.0		
	10/6/11	49.2		
	8/27/13	37.4		
8	9/28/10	10.9	7.0	5.5
	7/20/11	3.2		
9	9/17/09	13.4	21.3	19.3
	7/29/10	1.6		
	6/21/11	9.6		
	8/17/11	32.3		
	7/31/13	49.4		
10	9/28/10	10.4	23.3	18.3
	9/7/11	36.2		
12	7/29/10	3.0	19.9	29.5
	6/21/11	8.1		
	7/20/11	2.3		
	8/17/11	71.9		
	8/27/13	14.3		
13	8/31/10	2.1	6.9	6.5
	9/7/11	14.3		
	8/27/13	4.3		
16	9/1/10	1.3	4.4	2.7
	7/19/11	5.5		
	7/15/15	6.4		
17	7/28/10	2.0	9.1	7.7
	6/22/11	10.8		
	10/6/11	14.5		
	7/31/13	4.8		
	7/24/14	1.8		
	8/25/14	20.9		
18	7/19/11	6.0	6.0	
20	9/28/10	18.6	18.6	
20.5	9/8/11	10.4	10.4	
21	9/17/09	10.4	7.1	3.8
	7/28/10	2.2		
	6/22/11	6.4		
	10/6/11	12.5		
	8/28/14	6.9		
	6/3/15	4.1		
22	9/8/11	10.5	10.5	
25	9/1/10	2.0	2.3	0.6
	7/19/11	3.0		

77

	8/27/15	1.9		
26	9/17/09	7.5	10.9	12.9
	7/28/10	1.8		
	6/22/11	8.9		
	8/18/11	33.5		
	8/26/15	3.0		
27	9/1/10	0.8	5.8	7.0
	9/8/11	10.8		
30X	10/7/11	50.8	28.8	31.2
	7/14/15	6.7		
31	9/16/09	9.6	5.1	4.1
	7/27/10	1.6		
	8/30/10	1.5		
	9/9/11	7.7		
32	9/16/09	7.0	10.4	5.7
	9/29/10	19.0		
	6/23/11	12.9		
	8/18/11	4.8		
	6/3/15	8.2		
33	8/30/10	1.4	4.4	4.3
	7/21/11	7.4		
38	8/30/10	2.3	14.2	20.1
	7/21/11	5.8		
	10/7/11	44.2		
	8/26/15	4.4		
39	7/27/10	1.4	9.1	10.1
	7/21/11	5.4		
	9/9/11	20.6		
42	9/29/10	12.4	12.4	
43	9/16/09	8.5	7.0	1.6
	6/23/11	5.4		
	8/18/11	7.2		
47	7/27/10	1.3	7.9	10.1
	6/23/11	2.9		
	9/9/11	19.5		
48	9/29/10	4.7	13.7	12.7
	10/7/11	22.7		

Figure 21: Examples of oxygen inventory declines over time from cores in one experiment - a) GB8 from July 2011 and b) GB6 from August 2013. Rates are from linear regression analysis of raw data (i.e. non-temperature corrected). Data are averaged into one hour time intervals for clarity.
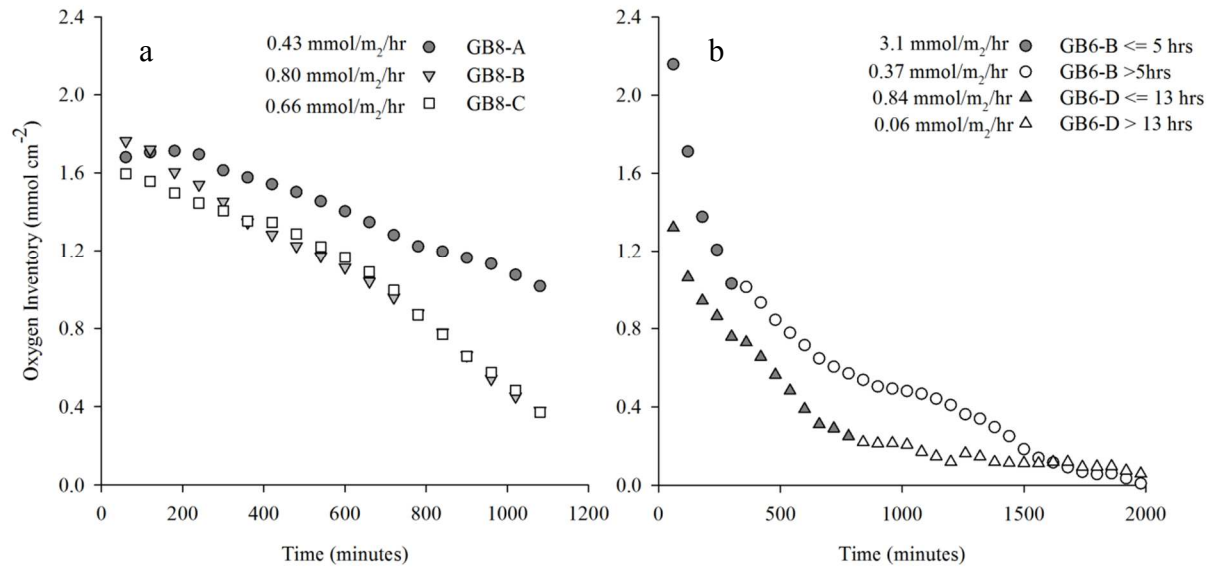
incubations to determine the temperature dependence of carbon and nitrogen remineralization rates in Green Bay sediments over a range of 5 to 15 degrees C. This data fit an Arrhenius function with a characteristic apparent activation energy of 103 kJ mole^{-1}, a value which is typical for organic rich sediments, and equivalent to a Q-10, the factor by which a rate increases for a 10 degree rise in temperature, of approximately 2-3 (Thamdrup et al. 1998). Rates were corrected based on measured *in situ* bottom water temperatures and the average temperature of the overlying water during the course of the experiment. On average, temperature corrections resulted in rate reductions of 38%, or -9.1 ± 14.7 mmol m^{-2} d^{-1}, which represents a temperature difference of $\sim 6.4°$ C.

The spatial distribution of temperature-corrected, observed benthic respiration rates were plotted using Surfer 9® (Golden Software, Golden, CO) using the standard kriging routine and blanking the shoreline to a value of zero. A bay-wide average summertime SOD rate was obtained via the interpolated Surfer 9® function. Incubations were repeated at some stations on as many as 6 individual cruises (GB17); however, most stations were sampled 3 times or less.

$D_2^{18}O$ analysis

Sample volumes of 2 mL to 20 L were collected from the water column at various depths via a submersible pump (flow rate $\approx$ 40 liters per minute) for the analysis of radon-222, methane, $D_2^{18}O$, total suspended solids, and other parameters. Sub-samples for $D_2^{18}O$ analysis were dispensed into thoroughly rinsed triplicate 2-mL Teflon™ sealed glass autosampler vials. Hypolimnetic waters were analyzed from 34 stations between the Fox River inflow and northern Green Bay/Lake Michigan. Fox River water samples were taken off of the pier at the mouth of the river (44.5378°N -87.3788°W). Lake Michigan bottom water samples were taken from

within the Lake Michigan basin or from the northern part of Green Bay near the major connecting channel at Death's Door.

Isotopic analyses were conducted on a Picarro L2130-*i* Analyzer (Picarro Inc., Sunnyvale, CA, USA) to measure isotopic ratios of $^{18}O/$ ^{16}O ($d^{18}O$) and $^{2}H/^{1}H$ ($d^{2}H$) (Gupta et al. 2009). Each individual sample was analyzed 6 times, with the last 3 runs averaged for a sample mean. Three working standards were used at the beginning and end of each run to identify periods of drift or instrument error. The $d^{18}O$ standard values range from -16.8‰ to 0.8‰ and the $d^{2}H$ values range from -124.1‰ to 2.0‰ to bracket an expected large range within samples. These working standards have been calibrated to International Atomic Energy Agency certified standards and the corrections have been applied through ChemCorrect, Picarro's data processing software. The standard deviation of all repeated measurements for the samples were ± 0.02‰ for oxygen and ± 0.09‰ for hydrogen.

4.3 Results and Discussion

River-Lake Mixing

The utility of $D_2^{18}O$ isotopes as natural tracers in aquatic systems has been recognized for studying groundwater recharge (Moya et al. 2016), river exchange (Halder et al. 2013) and estuarine mixing (Wankel et al. 2006). Both Fox River and Lake Michigan waters have distinct isotopic signatures that serve as useful conservative tracers in estimating the relative contributions of each along the gradient from south to north in the bay. Lake Michigan and Fox River waters differ isotopically by about 10.8‰ for $d^{2}H$ and 1.54‰ for $d^{18}O$, an easily detectable difference. A linear relationship between $\delta^{2}H$ values and $\delta^{18}O$ values (Fig. 22a) implies that these two end members make up the majority of the water in the bay, i.e. contributions from

81

other tributaries are undetectable. Additionally, when thermal stratification is present there is a clear difference between surface and bottom water isotopic signatures (Fig. 22b), indicating distinct water masses. These tracers may be used to calculate the fractional contribution or mixing between the Fox River (FR) and Lake Michigan (LM) for individual water masses using

$$C_x = C_{LM}f_{LM} + (1 - f_{LM})C_{FR} \qquad \text{(Eqn. 4.6)}$$

and

$$f_{LM} = (C_x - C_{FR})/(C_{LM} - C_{FR}) \qquad \text{(Eqn. 4.7)}$$

where f is the fraction of the end member present and C is the isotopic signature in per mil.

For both Fox River and Lake Michigan end members, the isotopic variation from month to month within the same year is small relative to the change between end members (Table 8; less

82

Figure 22: D$_2$^{18}O isotope analysis results for a) bottom water sites ranging from the Fox River mouth to GB100 and b) water column profiles at deeper stations.
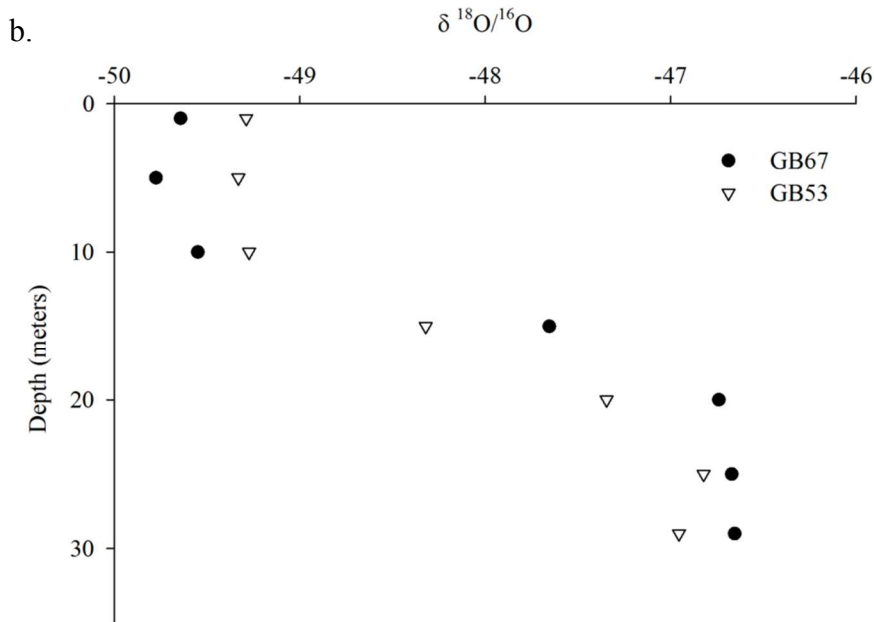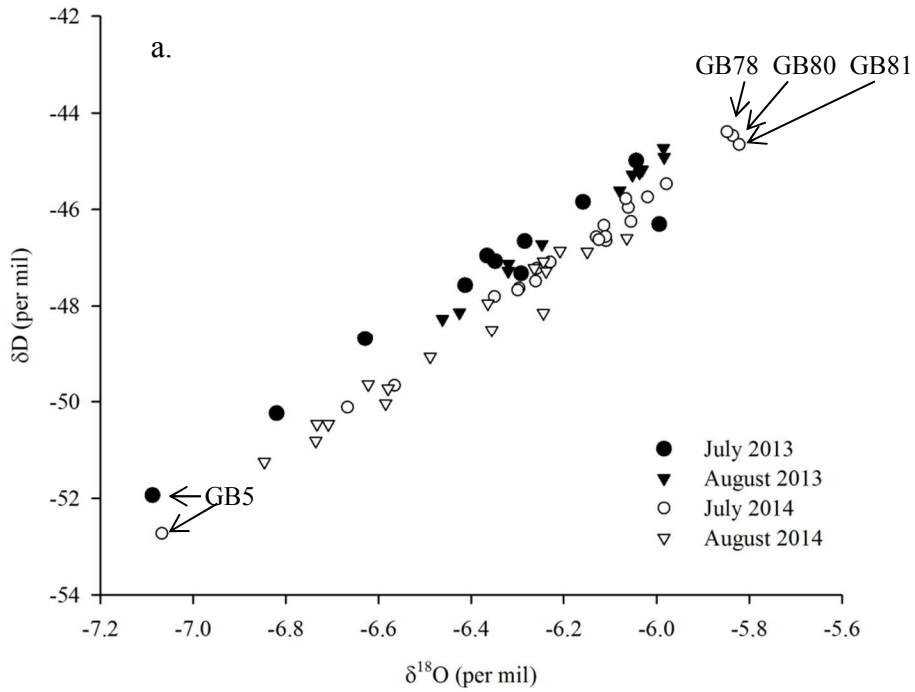
Table 8: Summary of $D_2{}^{18}O$ end members values (in ‰) that were collected in 2013 and 2014. FR= mouth of the Fox River.

	Station	Sample Depth	Date	Average $d^{18}O$	Average d^2H
River-End Members	GB5	1	7/31/2013	-7.13	-52.02
	GB6	1	8/27/2013	-6.65	-49.69
	FR	1	7/25/2014	-7.53	-55.50
	FR	1	8/25/2014	-7.40	-55.09
Lake Michigan End Members	GB100	32	7/30/2013	-6.04	-44.99
	GB83	30	8/28/2013	-5.99	-44.73
	Lake Michigan	53	7/21/2014	-5.74	-43.80

than 0.07, 0.2 ‰ for $\delta^{18}O$, δ^2H, respectively). Month to month differences in bottom water signatures at individual stations are remarkably small and both ^2H and ^{18}O ratios give similar results in calculating the average fractions of Lake Michigan water present, for example in August 2013 indicating 0.70 and 0.71, respectively.

Surface waters are characterized by a higher fraction of Fox River water (>0.65) a result presumably of the relative buoyancy and propagation of the warmer river plume (Miller and Saylor 1985; Hamidi et al. 2013). The fraction of Lake Michigan water in the hypolimnion ranges from 100% to 1% (Fig. 23), along a coherent gradient from north to south. Deeper northern bay waters tend to remain stratified throughout the summer preserving the Lake Michigan isotopic signature and inputs to hypolimnetic waters in the southern bay. The Lake Michigan signature is diluted by surface water from the Fox River through entrainment of surface water via vertical diffusion and mixing. For example, GB31, which is 24 meters deep and ~60 km from the Fox River mouth, generally does not mix during the summer season due to strong thermal stratification and the fraction of Lake Michigan present can range from 0.66 to 0.86. At GB 12, 11 meters deep, 30 km from the Fox River, and prone to mixing, isotopic values reveal that Lake Michigan water constitutes much less of the total hypolimnetic water mass, from 0.33 (August 2013) to 0.44 (August 2014).

These elevated proportions of isotopically labeled Lake Michigan water in the hypolimnion also support the conclusion that the cold water intrusions in southern Green Bay are composed of primarily of northern, cool Green Bay/Lake Michigan bottom water (Grunert, 2013; Kennedy, 1982; Klump et al. 2013). Thermistor string data from NOAA Buoy 45014 show periodic water column mixing during the stratified season followed by restratification within a period of hours to days during the summers of 2013-14 (Fig. 24a, b). In Figure 24b there is a mixing event at day

85

Figure 23: Fraction of bottom water with a Lake Michigan signal, based on d^{18}O isotopes at sites varying distance from the Fox River mouth.
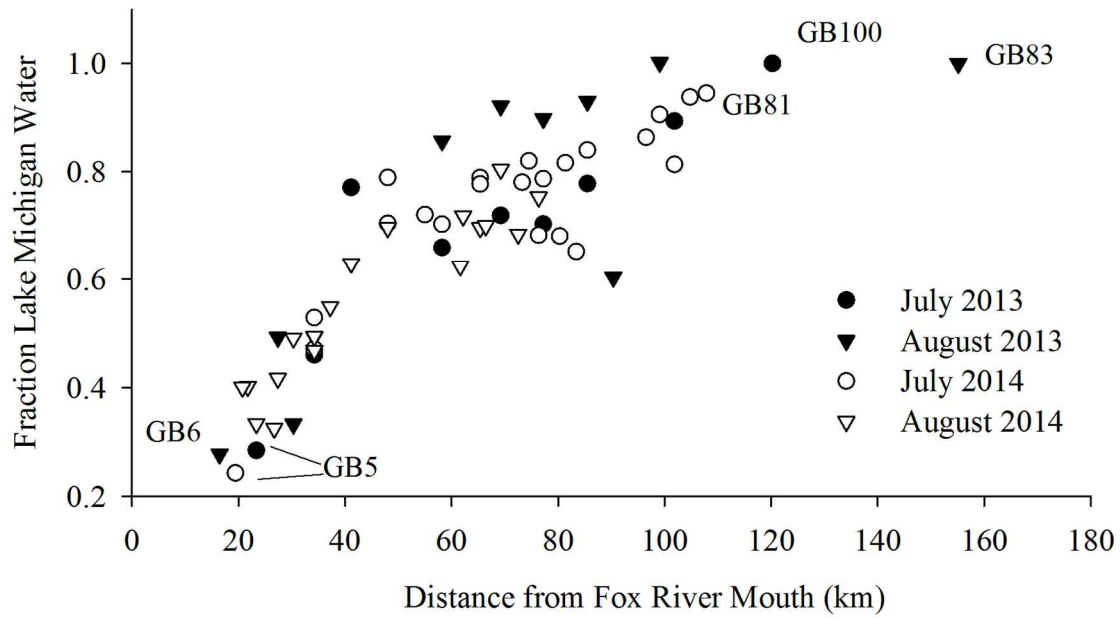
Figure 24: GB17 thermal structure for a) 2013 and b) 2014 based on thermistor data from NOAA45014 with concurrent c) bottom water oxygen (black) and temperature (gray) data from 2014 collected at a sonde on an adjacent mooring at 13 meters depth. White lines indicate monthly breaks, with the first line representing July 1st for each year.
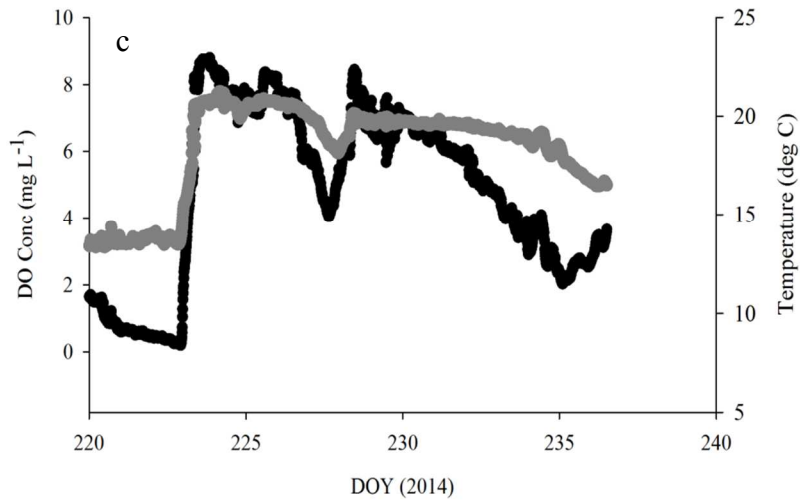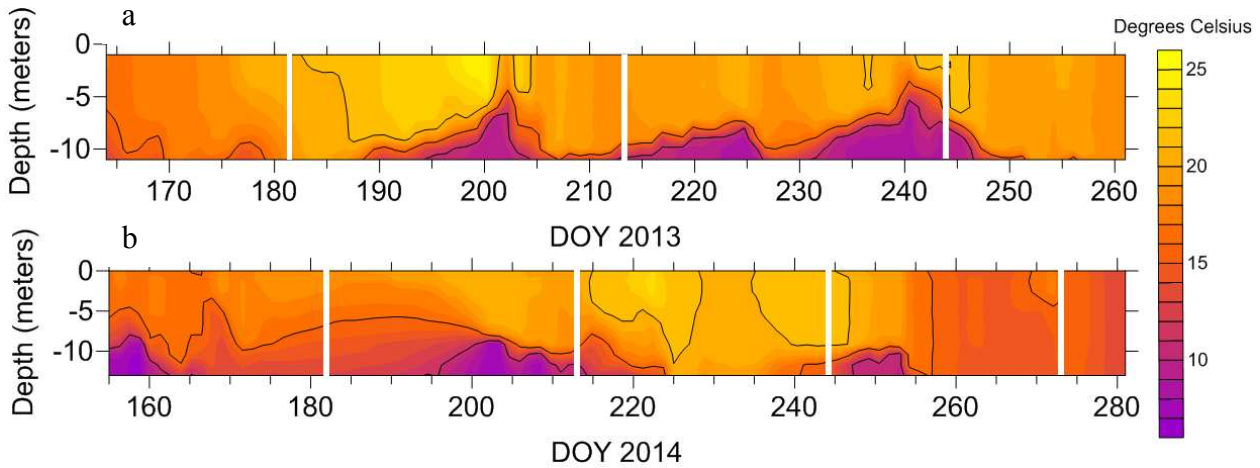
225, then at day 229 the bottom water slightly cools and the oxygen drops (Fig. 24c). As the bottom water at NOAA45014 continued to cool (day 237 = 17.6 °C, day 239 = 16.9°C) the $d^{18}O$ signal increased from -6.622‰ to -6.579‰, suggesting that the incoming water mass is sourced from the northern bay. These cool water intrusions and the two layer flow in the bay can result in rapid set-up of thermal stratification and restratification following mixing, a process which appears to accelerate hypoxia in shallow water by delivering oxygen concentrations that are already substantially depleted.

Oxygen Depletion

Hypolimnetic oxygen deficits have been used in a variety of ways, including to compare trophic states of lakes, to evaluate responses in nutrient load reductions, and to predict potential responses to climate change (Walker 1979; Matthews and Effler 2006; Jankowski et al. 2006). . Both volumetric and areal hypolimnetic deficits have been utilized (Davis et al. 1987; Burns 1995; Quinlan et al. 2005; Matzinger et al. 2010), with the latter useful in comparing to water column respiration and benthic respiration (SOD) rates. Table 9 summarizes the different methods used to calculate and describe oxygen deficiencies, inventories and rates in this study.

The depletion of oxygen from its saturation state, or apparent oxygen utilization (AOU), has been widely used in estuarine and marine environments, including to infer respiration of organic matter and to calculate the composition of that organic material (Ito et al. 2004; Zhu et al. 2011; Hu et al. 2016). Other applications include determination of N_2O production pathways (Kock et al. 2016) and evaluation of shifts in ocean circulation (Joos et al. 2003). Hypolimnetic oxygen depletion results predominately from respiration of particulate and dissolved organic matter within the water column and of settling particulate organic matter reaching the sediment-water interface. The relative contribution of water column vs. sediment respiration depends largely on

88

Table 9: Description of various acronyms used to describe oxygen condition within Green Bay.

Acronym/Term	Definition	Data used to calculate	Units
AOU	Apparent oxygen utilization	BW Oxygen saturation and concentration	mmol O_2 m^{-3} d^{-1}
AOU_{area}	Apparent oxygen utilization over area	BW Oxygen saturation, concentration, hypolimnetic thickness	mmol O_2 m^{-2} d^{-1}
OLR	Oxygen Loss Rate	AOU_{area}, length of stratification	mmol O_2 m^{-2} d^{-1}
HOD	Hypolimnetic oxygen deficit	Oxygen profiles in subsequent months, hypolimnetic thickness	mmol O_2 m^{-2} d^{-1}
I_{O2}	Inventory of oxygen	Oxygen concentration, hypolimnetic thickness	mmol O_2 m^{-2}
SOD	Sediment oxygen demand	Oxygen uptake in sediment over time	mmol O_2 m^{-2} d^{-1}
R_H	Hypolimnetic water column respiration	HOD and SOD	mmol O_2 m^{-2} d^{-1}

temperature, depth of the water, inputs of labile organic matter, and the residence time of this material within the water column. The relative influence of each tends to differ by system and even within systems (Cornett and Rigler 1980; Müller et al. 2012; Bouffard et al. 2013).

In Green Bay, hypolimnetic AOU, increases, in general, from north to south in the bay, -50 mmol O_2 m^{-3} in the northern bay to -283 mmol O_2 m^{-3} in the lower bay (avg = -147 ± 75 mmol O_2 m^{-3}) as southern stations progressively experience increasingly oxygen depleted hypolimnia to the point of hypoxia (Fig 25). On an areal basis, however, the region of greatest oxygen loss appears to be the mid bay region in water depths of 20-30 meters (Fig. 26). This region represents the greatest oxygen sink in the bay, even though it does not experience hypoxia to the

89

extent of that in shallower waters to the south, the more common "dead zone" region. Hypoxia, therefore, appears to be driven by both biological respiration and a compression of the hypolimnion in shallow water, where depletion occurs more rapidly due to a smaller reservoir of dissolved oxygen.

A relationship between AOU and stratification stability is suggested when making yearly comparisons. When thermal stratification was stronger in 2013 average bottom water temperatures were 12.6 ± 4.8 degrees C at 11 m depth (n = 3283) versus in 2014 when average temperatures were 15.1 ± 3.9 degrees C (n = 3169), nearly 2.5 degrees C warmer. This corresponded to increased oxygen utilization of 25% in the cooler year, 2013, (-128 ± 75 mmol O_2 m^{-3}, n=22) than for 2014 (-106 ± 64 mmol O_2 m^{-3}, n=40).

Hypolimnetic Oxygen Deficits and the onset of Hypoxia

While AOU is a measure of the loss of oxygen from its atmospheric equilibrium concentration, hypolimnetic oxygen depletion rates (HOD) may be estimated from time series measurements of

Figure 25: Apparent oxygen utilization (mmol O$_2$ m^{-3}) for bottom waters during July through September of 2011-14.
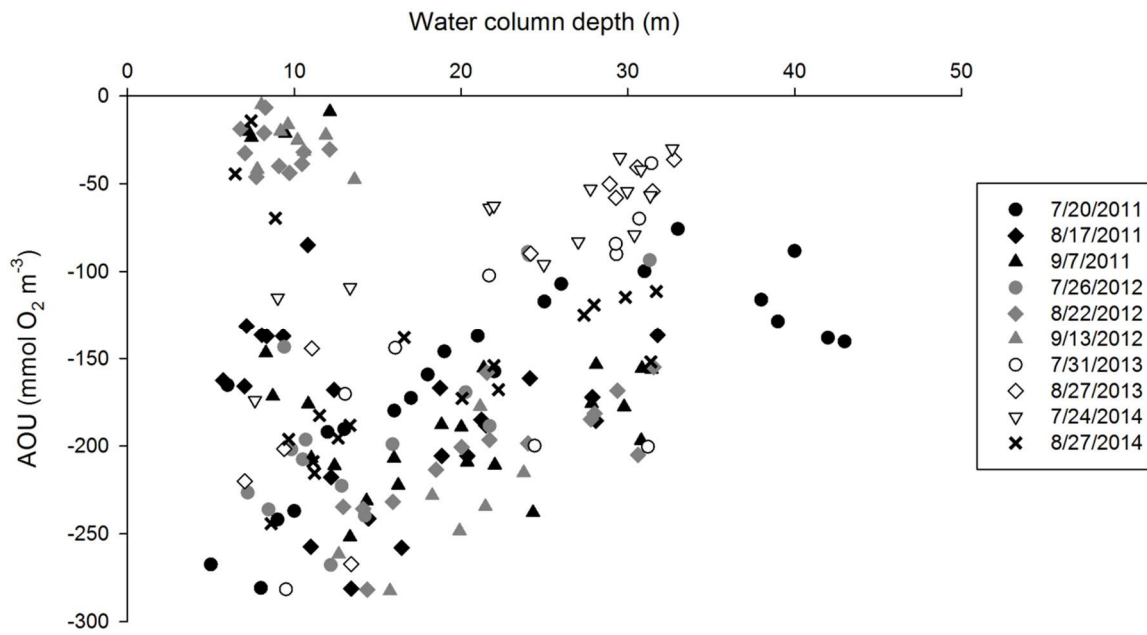
Figure 26: Areal based AOU values (AOUarea = AOU * hypolimnion thickness) for bottom waters in Green Bay during July through September of 2011-14.
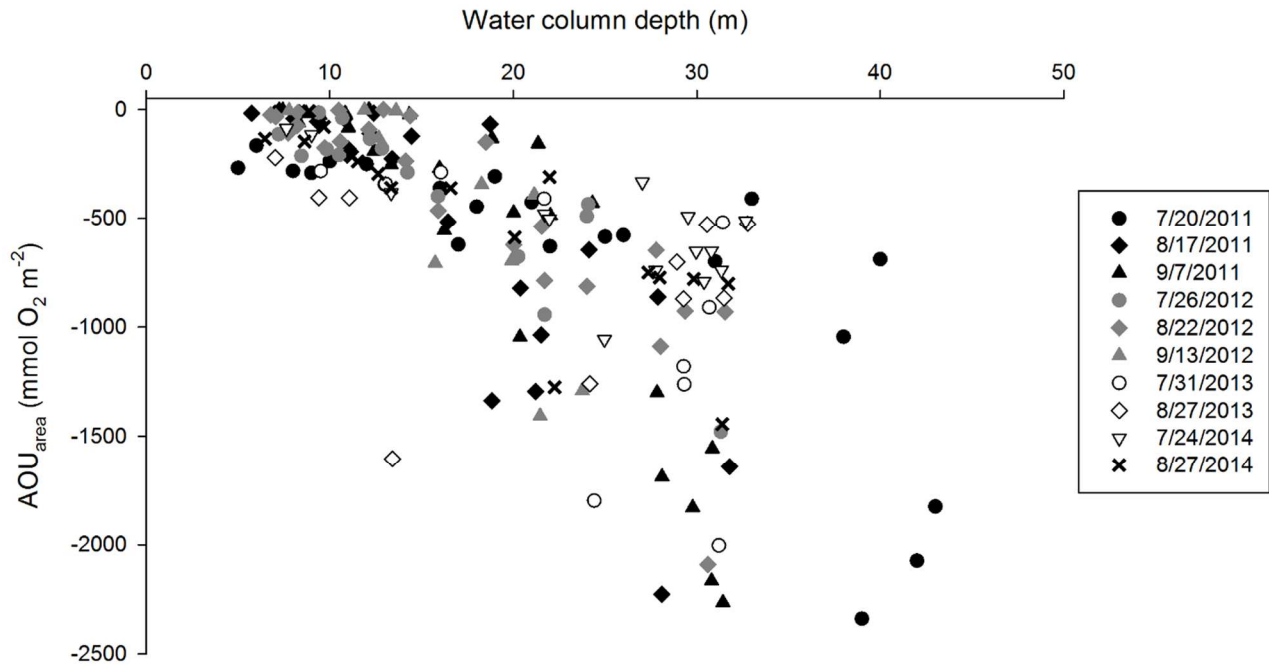
the change in the inventory of oxygen in the hypolimnion after the onset of stratification (Eqn. 4.4).

HOD rates were calculated from 13 sites in lower Green Bay that demonstrated continuous stratification during an approximate 2 month period in 2010-2014 (Table 10). Values ranged from -1.0 to -48.8 mmol O_2 m^{-2} d^{-1} with an average of -18.3±15.7 mmol O_2 m^{-2} d^{-1} (n=10). These are similar to HODs estimated by Valenta (2013) over a larger region of southern Green Bay with an average of -16.5 mmol O_2 m^{-2} d^{-1} (-0.4 to –61.2 mmol O_2 m^{-2} d^{-1}), as well as those from two formerly eutrophic lakes of Switzerland (-16 to -31 mmol O_2 m^{-2} d^{-1}; Matzinger et al., 2010). Studies in other eutrophic systems (i.e. central Lake Erie and Onondaga Lake) measured HOD rates ranging from -14 to -64 mmol O_2 m^{-2} d^{-1} (Edwards et al., 2005; Matthews and Effler, 2006), which also agree with values measured in the eutrophic lower Green Bay. In general for Green Bay greater HOD values correspond with thicker hypolimnia (Valenta 2013) .

A first-order hypolimnetic oxygen mass-balance model may be constructed from the sum of all sinks and sources of oxygen:

$$HOD = J_T + WOD + SOD \pm A \qquad \text{(Eqn. 4.8)}$$

where J_T is vertical diffusion across the thermocline (Eqn. 3), A is horizontal advection, SOD is sediment oxygen demand, and WOD is the hypolimnetic water column oxygen demand, or the net result of hypolimnetic primary production (P_H) and hypolimnetic respiration (R_H) i.e.

$$WOD = P_H\text{-}R_H \qquad \text{(Eqn. 4.9)}.$$

Hypolimnetic waters in Green Bay receive little to no light due to the high turbidity of surface waters (Grunert 2013; Qualls et al., 2013, 2007) and show very limited to no diel fluctuations in

93

Table 10: Hypolimnetic oxygen depletion (mmol O_2 m^{-2} d^{-1}) calculations for various stations in Green Bay based on loss of oxygen inventory (mmol O_2 m^{-2}) from the hypolimnion (I) between two time periods. Months in italics represent values from Valenta (2013) where full profile data was not available to fill in the table. Thermocline diffusion (mmol O_2 m^{-2} d^{-1}) of oxygen is given for profiles from this study and is based on the oxygen concentration (mmol O_2 m^{-3}) gradients between epilimnetic and hypolimnetic waters and diffusivities.

Months	Site	Year	I_1 at t1	I_2 at t2	Δt	HOD	Hypolimnion Thickness	Avg. Epi. DO	Avg. Hypo. DO	Average dz	Thermocline Diffusion
July-August	17	2011	504	32	28	-16.9	1.8	269	94	3.0	2.77E-01
July-August	22	2011	746	64	28	-24.4	2.5	268	151	2.0	1.94E-01
August-September	22	2011	64	40.6	23	-1.0	0.6	276	157	1.9	2.02E-01
July-August	43	2011	3422	2443	28	-35.0	12.9	278	234	11.2	1.15E-02
July-August	21	2012	249.7	214.3	26	-1.4	2.0	274	142	3.1	1.77E-01
August-September	21	2012	214.3	97.1	22	-5.3	2.3	266	120	1.5	2.94E-01
August-September	32	2012	654.7	544	21	-5.3	3.0	263	179	5.0	5.68E-02
July-August	26	2014	1960	106	38	-48.8	3.0	287	242	8.7	9.89E-03
July-August 25	17	2014	1059.7	179	35	-25.2	2.2	285	248	2.0	5.80E-02
July-August 27	17	2014	1059.7	311.7	37	-20.2	2.1	285	269	1.7	3.82E-02
July-August	6	2011	69.6	60	27	-0.4	1.1				
July-August	10	2011	93.5	51.4	27	-1.6	3.2				
July-August	12	2011	222.9	128.9	27	-3.5	1.6				
August-September	12	2011	128.9	27.6	21	-4.8	0.4				
July-August	17	2011	535.7	60	27	-17.6	3.7				
July-August	18	2011	420.1	17.4	27	-14.9	2.7				
July-August	21	2011	686.1	181.3	27	-18.7	3.7				
July-August	22	2011	766.3	67.2	27	-25.9	4.6				
August-September	22	2011	67.2	25.9	21	-2.0	1.0				
July-August	26	2010	1616.7	1215	30	-13.4	6.2				
July-August	26	2011	1530.9	1054.6	27	-17.6	6.4				
August-September	26	2011	1054.6	517.3	21	-25.6	5.0				
July-August	31	2010	2225.7	1579.9	30	-21.5	9.3				

July-August	31	2011	2437.9	1767.1	27	-24.8	10.0
August-September	31	2011	1767.1	481.2	21	-61.2	6.3
July-August	38	2010	2483.8	2125.1	30	-12.0	11.1
July-August	39	2010	2737	2307	30	-14.3	12.1

oxygen concentrations that would indicate photosynthetic production (LaBuhn and Klump 2016). Oxygen profiles occasionally show a small subthermocline peak in dissolved oxygen, but these peaks are quite variable and on the order of 0.5 to 1.0 mg/L or less. This suggests that primary production within the hypolimnion for most of the bay is relatively minor and net water column oxygen balance may be simplified to the respiration term alone $WOD = R_H$. Ignoring advection for the moment (i.e. $A_{in} \approx A_{out}$), WOD and SOD are the two primary components of oxygen depletion in the hypolimnion (Burns and Ross 1972; Lehman 1988; Bouffard et al. 2013).The resulting mass balance is then:

$$HOD = J_T + SOD + R_H \qquad \text{(Eqn. 4.10).}$$

Oxygen diffusion into the hypolimnion across the thermocline is estimated to be 2.7×10^{-3} to 3.3×10^{-1} mmol O_2 m^{-2} d^{-1}, for a range of diffusivities and concentration gradients (Table 10). These cross-thermocline fluxes of oxygen typically corresponded to 0.02% to 1.94% of the total hypolimnetic oxygen consumption rate, and hence contribute relatively little to the oxygen mass balance of the hypolimnion in Green Bay, consistent with observations in other strongly stratified systems (Edwards et al. 2005; Matzinger et al. 2010; Rucinski et al. 2010). In 20% of the cases in Green Bay, where relatively low HOD values were observed (<1.5 mmol O_2 m^{-2} d^{-1}), diffusion from the epilimnion could have contributed more than 10%, and as much as 18%, of the total estimated oxygen consumption. By way of contrast, vertical mixing contributions observed by Burns and Ross (1987) in Lake Erie (12%) and Matthews and Effler (2006) in Onondaga Lake (15-37%) were within the same range.

Benthic respiration in Green Bay

96

Benthic respiration or sediment oxygen demand from both aerobic metabolism of labile organic material and anaerobic reoxidation of reduced substances is often the major process controlling hypolimnetic oxygen depletion especially in shallow water (Davis et al. 1987; Gelda et al. 1995; Matthews and Effler 2006; Müller et al. 2012). In Green Bay, temperature corrected SOD rates have been directly quantified via sediment core incubations.

A total of 236 individual cores over 86 experiments were conducted during the course of this study (Table 7). The average rate of SOD estimated from this data is -12.9 ± 14.9 mmol O_2 m^{-2} d^{-1}. This agrees reasonably well with other oxygen flux estimates from the southern to mid bay, including oxygen microelectrode measured pore water gradients across the sediment-water interface from 1995 (-11.9 ± 5.6 mmol O_2 m^{-2} d^{-1}; Klump et al. 2009) and eddy covariance experiments (-10.1 ± 11.5 mmol O_2 m^{-2} d^{-1}) from 2014-15 (discussed more below; Koopmans et al. 2016). These benthic respiration rates in Green Bay are also within the range of previously measured rates in similar environments (Table 11), such as Chesapeake Bay (-3.1 to -26.9 mmol O_2 m^{-2} d^{-1}; Cowan and Boynton, 1996) and Mobile Bay (-3.1 to -39.1 mmol O_2 m^{-2} d^{-1}; Cowan et al., 1996).

The distribution of SOD does not match patterns of sediment deposition or surface sediment organic carbon content (Fig. 27), but is focused in the southern portion of the bay consistent with the distribution of the most commonly observed region of hypoxia (Fig. 19.1a). The combination of high organic matter loading and algal production with rapid deposition in shallow water presumably fuels benthic respiration at rates higher that in sediments further north. The average spatially integrated benthic respiration rate for the region south of Chambers

Table 11: Comparisons of benthic respiration (mmol O_2 m^{-2} d^{-1}) across different environments. Results from this study are bolded.

Water Body	Benthic Respiration Rate	Technique Used	Source
Central Lake Erie	-9.4	Benthic chambers	Snodgrass and Fay, 1987
Central Lake Erie	-6.4	Whole core incubations	Smith and Matisoff, 2008
Chesapeake Bay	-3.1 to -26.9	Whole core incubations	Cowan and Boynton, 1996
Crimean Shelf, Black Sea	-6	Eddy covariance	Holtappels et al. 2013
Green Bay	**-0.8 to -73**	**Whole core incubations**	**This study**
Green Bay	-31 to -220	Whole core incubations	Gardiner et al. 1984
Green Bay	-5 to -28	Microprofiles	Klump et al. 1997b
Green Bay	-10.1	Eddy covariance	Koopmans et al. unpub
Mobile Bay	-3.1 to -39.1	Whole core incubations	Cowan et al. 1996
Monterey Bay	-5.4	Eddy covariance	Johnson et al. 2011
Monterey Bay	-8.5	Whole core incubations	Johnson et al. 2011
Oregon Continental Shelf	-3.2 to -9.8	Eddy covariance	Reimers et al. 2012
Oregon Continental Shelf	-1.1 to -2.7	Microprofiles	Reimers et al. 2012
San Francisco Bay	-26 to 0	Whole core incubations	Grenz et al. 2000

Figure 27: Maps showing kriged values of a) sediment oxygen demand and b) organic carbon content of the sediment (Klump et al. unpub). Circles designate the location of SOD experiments.
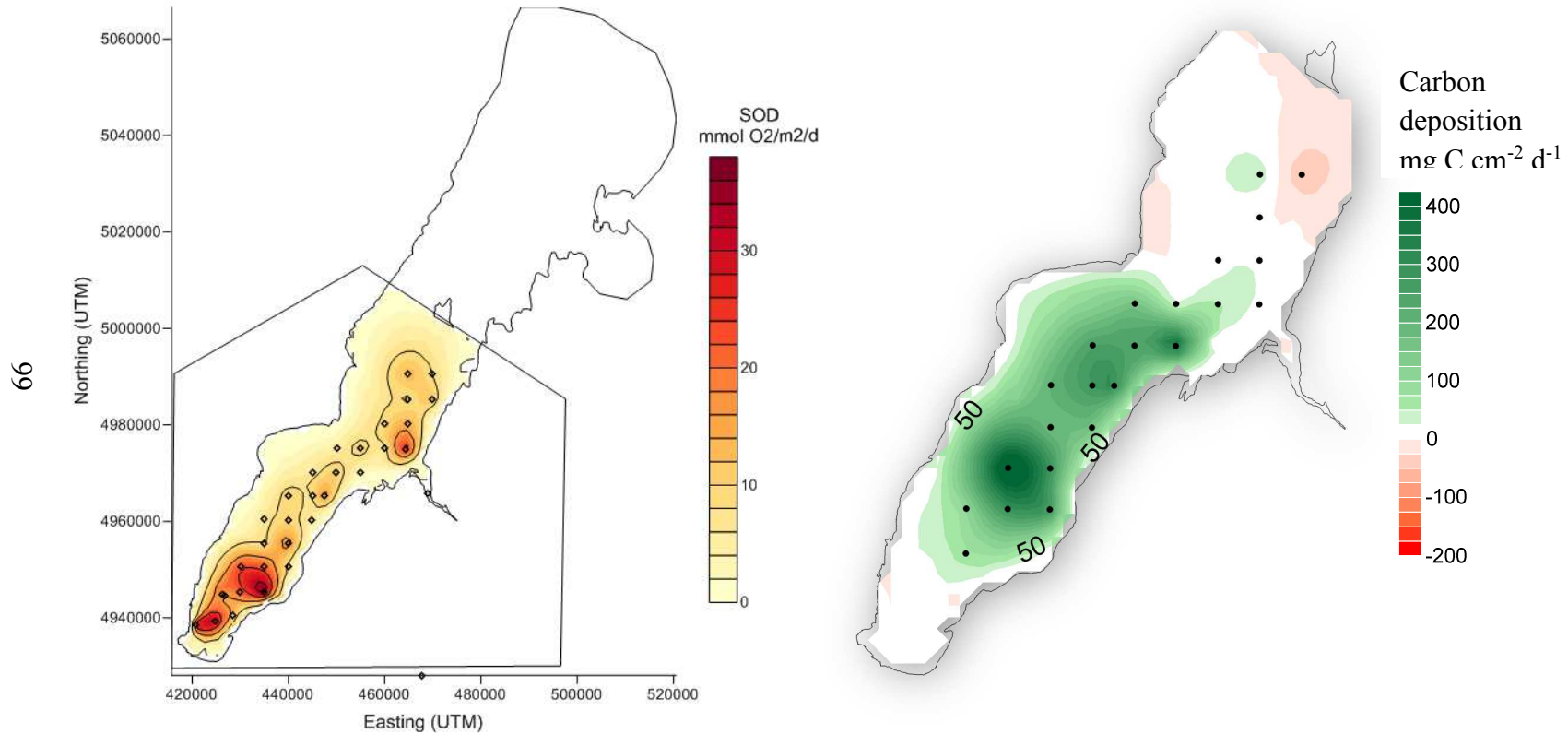
Island is ~-7.9 mmol O_2 m^{-2} d^{-1}. The two regions along the main axis – the lower bay and the mid-lower bay (Fig. 27a) -- where SOD is focused and where rates exceed 10 mmol O_2 m^{-2} d^{-1} represent only 25% of the surface area of lower Green Bay, but account for ~53% of the total benthic oxygen consumption.

Selective decomposition of the more labile fractions of organic matter can fuel rapid rates of respiration within the water column.   Benthic respiration, on the other hand, is fueled both by rapidly deposited labile material and by the diagenesis of the more refractory components that accumulate on the bottom over periods of months to years.

Eddy covariance and core incubation comparisons

Aquatic eddy covariance (EC), based on atmospheric eddy covariance, is a non-invasive technique to measure benthic respiration that has become increasingly popular since its introduction (Berg et al. 2003) due to its ability to track temporal variations in benthic fluxes and has been used in a number of environments and applications, including to measure groundwater discharge, benthic oxygen exchange over shelf sediments, and stream oxygen production and respiration (Crusius et al. 2008; Reimers et al. 2012; Koopmans and Berg 2015). Past studies have demonstrated that traditional methods, such as core incubations and *in-situ* chambers, to measure benthic metabolism result in a general offset of rates from those measured by EC due to lack of natural hydrodynamic effects (Berg et al. 2003; Kuwae et al. 2006; Reimers et al. 2012). For these reasons, EC was used in Green Bay as a check on oxygen uptake rates measured by sediment core incubations. Koopmans et al. (2016) gives an overview of the methods and calculations used in the study.

There were 8 successful EC deployments during 2014 and 2015 within Green Bay. These EC deployments represent the first application of eddy covariance in the Laurentian Great Lakes. The average oxygen fluxes calculated from EC data indicate uptake by the sediments (i.e. negative fluxes), even during daylight periods when benthic oxygen production could be occurring. The likely reason for this lack of production is that a vast majority of the solar irradiance is absorbed in the turbid surface waters. The average EC flux for the successful deployments was -6.78 ± 3.92 mmol O_2 m^{-2} d^{-1} and the minimum and maximum average fluxes were from the two longest deployments (Table 12).

Sediment oxygen demand experiments were performed simultaneously with EC deployments to allow for comparisons between rates. The comparisons were between experiments and deployments made at the same site with overlapping dates. There was one exception for the EC 2014 Entrance Light sample. The 2014 and 2015 fluxes had the same average, so the sediment core incubations from the Entrance Light in 2015 were also compared to the 2014 data. Eddy covariance oxygen fluxes were generally smaller than core incubation fluxes (Fig. 28; Table 13), but the eddy covariance measurements matched overall patterns observed with core incubations. This lends confidence to the measurements made with core incubations from 2009-15. The average SOD:EC ratio over the 8 comparisons was 1.27. Greater rates measured by core incubations could be explained by compression of the diffusion boundary layer by the continuous stirring, which allows for enhanced oxygen diffusion across the sediment-water interface. Natural conditions within Green Bay have a seiche effect that changes bottom current directions, which means the water speed over the sediments is much more variable than within

101

Table 12: Site details and in situ conditions for successful eddy covariance deployments. Water depth and mean water temp, flow speed and O_2 were calculated from instruments on the eddy frame. EC fluxes are reported as negative values to represent oxygen consumption by the sediments. The number of half-hour intervals in the mean EC flux are reported as *n* and errors as standard error. Table from (Koopmans et al. 2016).

Site	Sample date	Water depth (m)	Temperature (°C)	Flow Speed (cm s^{-1})	[O_2] (µmol l^{-1})	Peak PAR (µmol m^{-2} s^{-1})	EC O_2 flux (mmol m^{-2} d^{-1})	*n*	EC flux *s.e.*
GB 17	25-Aug-2014	13.5	16.6	2.72	101	< 10	-11.5	84	0.72
GB 21	27-Aug-2014	16	12.5	2.06	166	< 10	-5.28	23	0.48
GB EL	16-Sep-2014	7.8	15.6	4.23	296	< 10	-10.8	14	1.44
GB 16	15-Jul-2015	11.5	14.4	3.45	60	< 10	-2.40	20	0.48
GB EL	25-Aug-2015	7.8	8.7	3.08	273	< 10	-10.8	8	2.16
GB 26	25-Aug-2015	23	10.1	3.41	318	< 10	-4.08	23	0.48
GB 38	26-Aug-2015	28	6.6	1.22	332	< 10	-7.44	18	1.68
GB 25	27-Aug-2015	21	6.7	3.58	325	< 10	-1.92	44	0.24

Figure 28: Comparisons of average oxygen fluxes measured at the same site using sediment core incubations and eddy covariance. Error bars are standard errors of the eddy covariance data. The line represents the linear regression plot, with the equation given.
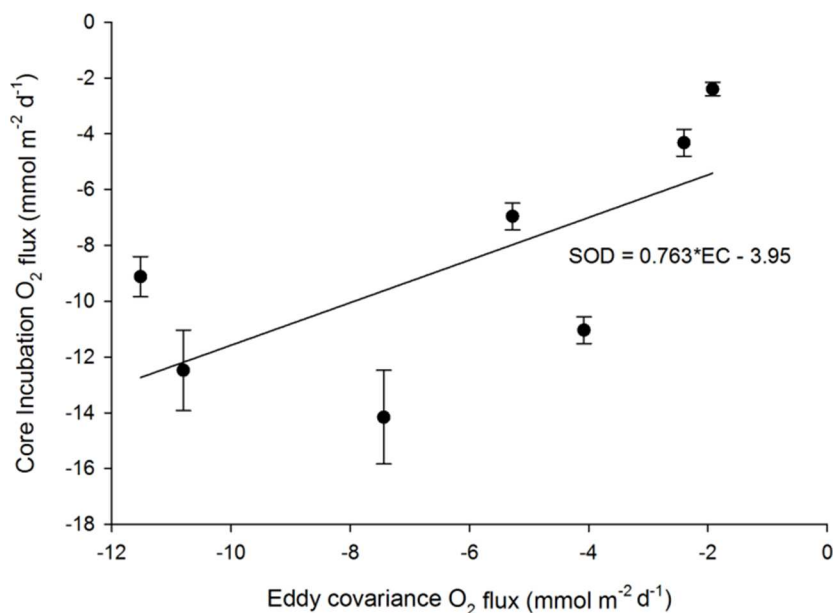
Table 13: Fluxes used to create Figure 28, with standard errors also provided for the eddy covariance fluxes. Eddy covariance fluxes calculated by D. Koopmans. All fluxes and errors are in units of mmol O_2 m^{-2} d^{-1}.

Site	Date of EC	EC Flux	EC Std. Error	Core Incubation Flux
GB17	8/25/2014	-11.52	0.72	-20.9
GB21	8/27/2014	-5.28	0.48	-6.9
GB EL	9/16/2014	-10.8	1.44	-12.6
GB16	7/15/2015	-2.4	0.48	-6.4
GB EL	8/25/2015	-10.8	2.16	-12.6
GB26	8/25/2015	-4.08	0.48	-2.9
GB38	8/26/2015	-7.44	1.68	-3.0
GB25	8/27/2015	-1.92	0.24	-1.9

103

the cores. Therefore, *in-situ* conditions experience a much more dynamic diffusive boundary layer thickness than in the cores and a smaller uptake rate.

Sediment oxygen demand vs. water column respiration

While SOD dominates in some systems, other studies have shown that water column respiration is a significant contributor to hypolimnetic oxygen depletion (Bouffard et al., 2013; Burns and Ross, 1972; Cornett and Rigler, 1979). Hypolimnetic water column respiration rates (R_H) may be estimated using Eqn. 6, via the difference in the observed hypolimnetic deficit (HOD) plus thermocline diffusion (J_T) and the site-averaged SOD (Table 14). The average R_H (for cases where SOD < HOD + J_T) is 16.5 ± 13.4 mmol O_2 m^{-2} d^{-1} (n = 17) and represents 59% of the total oxygen loss in the hypolimnion (R_H/HOD*100). By way of comparison, average epilimnetic respiration rates calculated from diel oxygen cycles at GB17 (LaBuhn and Klump 2016) translates to -7.6 mmol O_2 m^{-2} d^{-1} when corrected for the cooler hypolimnetic temperatures (14 °C vs 22 °C), a value similar to those calculated via the mass balance of Eqn. 6.

Advection of oxygen depleted waters is an important mechanism to set-up hypoxia within Green Bay and helps explain the prevalence of hypoxia in the shallow southern portions of the bay. The apparent residence time of oxygen in the hypolimnion may be estimated via the expression:

$$T_{res} = AOU_{area}/HOD \qquad \text{(Eqn. 4.11)}$$

and represents the time it would take to deplete a fully saturated volume of water in equilibrium with the atmosphere to the measured loss through the combined processes of water column and benthic respiration.

Less time is required to deplete oxygen (i.e. shorter oxygen residence time) in the shallower waters of Green Bay, which is also the general area that hypoxia is usually observed (Fig. 29). The oxygen drawdown takes less time at shallow depths because the initial oxygen inventories (Fig. 30) in that region are smaller due to both the smaller volume of the hypolimnion and an initial "pre-depleted' condition as a consequence of oxygen consumption as bottom waters flow over anoxic sediments found in "upstream" areas as bottom waters move southward. An estimate of how far a water mass would need to travel while the oxygen was being consumed can be determined by:

$$Distance = \frac{I_{O_2}}{HOD} * V_h$$
(Eqn. 4.12)

where V_h is the velocity of the hypolimnetic water. For an initial oxygen inventory (in the mid-bay ~1000 mmol O_2 m^{-2}), an oxygen depletion rate (average of all HOD = -17.2 mmol O_2 m^{-2} d^{-1}), and average flow speed of the bottom water (1.8 km d^{-1}, Hamidi et al. 2015), the hypolimnion would be anoxic within 58 days and hypoxic (~250 mmol m^{-2} in 4 meter hypolimnion) within 44 days. As the hypolimnion compresses the time to depletion obviously becomes shorter. The water mass would have traveled 78 to 105 kilometers, which is the approximate distance from the upper-bay region to the dead zone.

Table 14: Values used to calculate hypolimnetic water column respiration (R_H) include the hypolimnetic oxygen deficit (HOD), sediment oxygen demand (SOD) and thermocline diffusion rate (J_T) when available. Values in italics are uncorrected for thermocline diffusion. All rates are in units of mmol O_2 m^{-2} d^{-1}. Positive values indicate that SOD > HOD + J_T.

Site	HOD	HOD + J_T	SOD	R_H
6	*-0.4*	*-0.36*	-24	*23.64*
10	*-1.6*	*-1.56*	-23.3	*21.74*
12	*-3.5*	*-3.48*	-19.9	*16.42*
12	*-4.8*	*-4.82*	-19.9	*15.08*
17	-16.9	-16.58	-9.1	-7.48
17	-25.2	-25.10	-9.1	-16.00
17	-20.2	-20.18	-9.1	-11.08
17	*-17.6*	*-17.62*	-9.1	*-8.52*
18	*-14.9*	*-14.91*	-6	*-8.91*
21	-1.4	-1.18	-7.1	5.92
21	-5.3	-5.03	-7.1	2.07
21	*-18.7*	*-18.70*	-7.1	*-11.60*
22	-24.4	-24.16	-10.5	-13.66
22	-1.0	-0.82	-10.5	9.68
22	*-25.9*	*-25.89*	-10.5	*-15.39*
22	*-2.0*	*-1.97*	-10.5	*8.53*
26	-48.8	-48.78	-10.9	-37.88
26	*-13.4*	*-13.39*	-10.9	*-2.49*
26	*-17.6*	*-17.64*	-10.9	*-6.74*
26	*-25.6*	*-25.59*	-10.9	*-14.69*
31	*-21.5*	*-21.53*	-5.1	*-16.43*
31	*-24.8*	*-24.84*	-5.1	*-19.74*
31	*-61.2*	*-61.23*	-5.1	*-56.13*
32	-5.3	-5.21	-10.4	5.19
38	*-12.0*	*-11.96*	-14.2	*2.24*
39	*-14.3*	*-14.33*	-9.1	*-5.23*
43	-35.0	-34.95	-7	-27.95

106

Figure 29: Time to deplete oxygen, or residence time of oxygen, versus water depth.
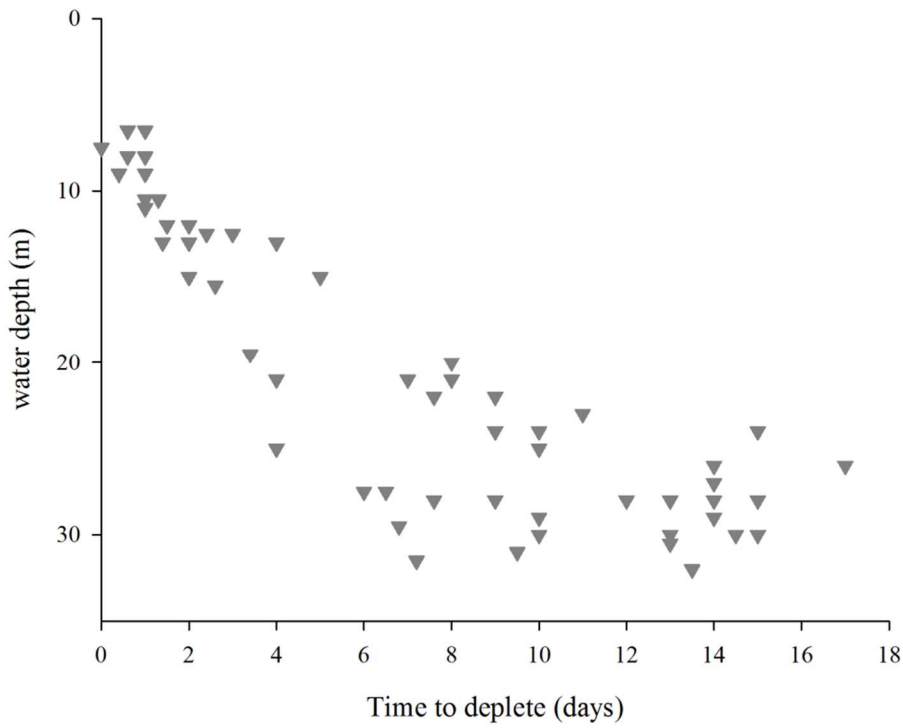
Figure 30: Hypolimnetic oxygen inventories for stations in Green Bay versus water column depth.

107
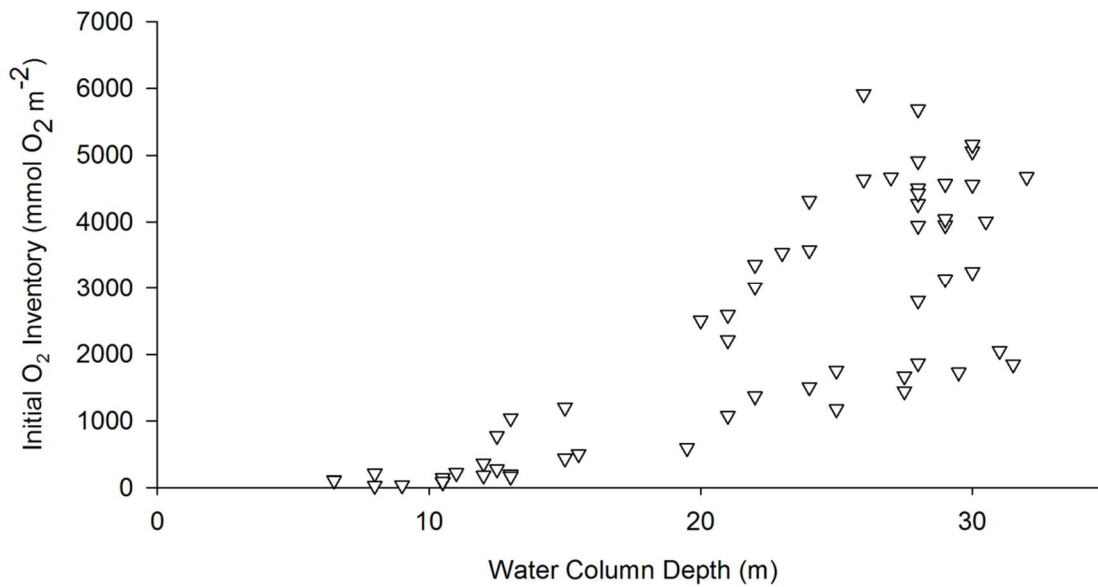
Oxygen depletion rates may also be estimated from the AOU_{area} by calculating the magnitude of depletion since the onset of stratification determined from the thermistor string data at the GLOS monitoring buoy (NOAA 45014), i.e.:

$$OLR = AOU_{area}/\Delta t \qquad \text{(Eqn. 4.13)}$$

where OLR is the apparent oxygen depletion rate and Δt is the time since stratification has developed. These OLRs are complimentary to the HODs calculated above, but also provide a larger set of data since calculations may be made each individual profile. OLRs for lower Green Bay range from -2.0 to -80 mmol O_2 m^{-2} d^{-1} (Fig. 31). The average OLR (-14.9 ± 16.7 mmol O_2 m^{-2} d^{-1}, n = 43) agrees well with the average HOD rate calculated above. Comparisons between OLR and SOD make it clear that SOD is the dominant oxygen consumer in waters less than 10 m deep. There is also a general decrease in the role of SOD for total hypolimnetic oxygen loss at increasing water depths can be explained by greater importance of water column respiration (R_H). For example, a water mass moving from station GB31 to GB17, a distance of ~24 km with a travel time of 13 days, assuming a flow rate of 1.8 km d^{-1}, would experience an oxygen loss of 168 mmol O2 m^{-2} due to SOD alone. This is only 15% of the observed loss (~1150 mmol m^{-2}) indicating the importance of water column respiration and hypolimnion compression in the hypolimnetic oxygen budget of deeper waters.

4.4 Conclusions

Most management strategies to reduce hypoxia involve addressing eutrophication through nutrient load reductions (Mee et al. 2005; McCrackin et al. 2016). Some coastal systems where nutrient reductions have been implemented have had a relatively fast response in chlorophyll

108

concentrations and productivity rates. In almost all systems, however, there is a much slower response, if at all, in the hypolimnion oxygen concentrations. This has been attributed to natural interannual variability, lack of ecosystem resilience, and climate change factors. Climate change factors included lengthened stratification by extended periods of warm conditions and increased respiration rates through warmer temperatures.

In Green Bay, the remedial action plan calls for phosphorus load reductions by 40-60% from the Fox River Watershed (WIDNR 2011), which should favor hypoxia abatement through reduced algal production. A decline in algal production should lead to less respiration, both in the epilimnion and hypolimnion, because there will be less organic matter to consume. Sediment responses will be much slower, however, due to both decades of high nutrient loading and the efficient trapping of phosphorus in Green Bay sediments as observed by Klump et al. (1997a).

Conversely, climate change projections for the Green Bay region predict increased temperatures which could lengthen stratification by up to 6 weeks (WICCI, 2011). Longer periods of stratification would likely increase the probability of low oxygen conditions simply by extending the amount of time the bottom water is separated from the atmosphere, essentially masking any benthic response to reduced nutrient loads. Therefore, to evaluate the progress of Green Bay recovery to nutrient load reduction, monitoring efforts of potential responses, such as water column oxygen demand, should primarily be water-column based. The monitoring should cover a large spatial extent in the bay, as opposed to only in the lower bay, where problems are the worst.

Water column respiration and oxygen consumption by the sediments resulting from organic matter decomposition are the two major sink terms of the oxygen budget of Green Bay. The

Figure 31: Oxygen loss rates (OLR; black dots) and SOD:OLR comparisons (white diamonds) versus water column depth.
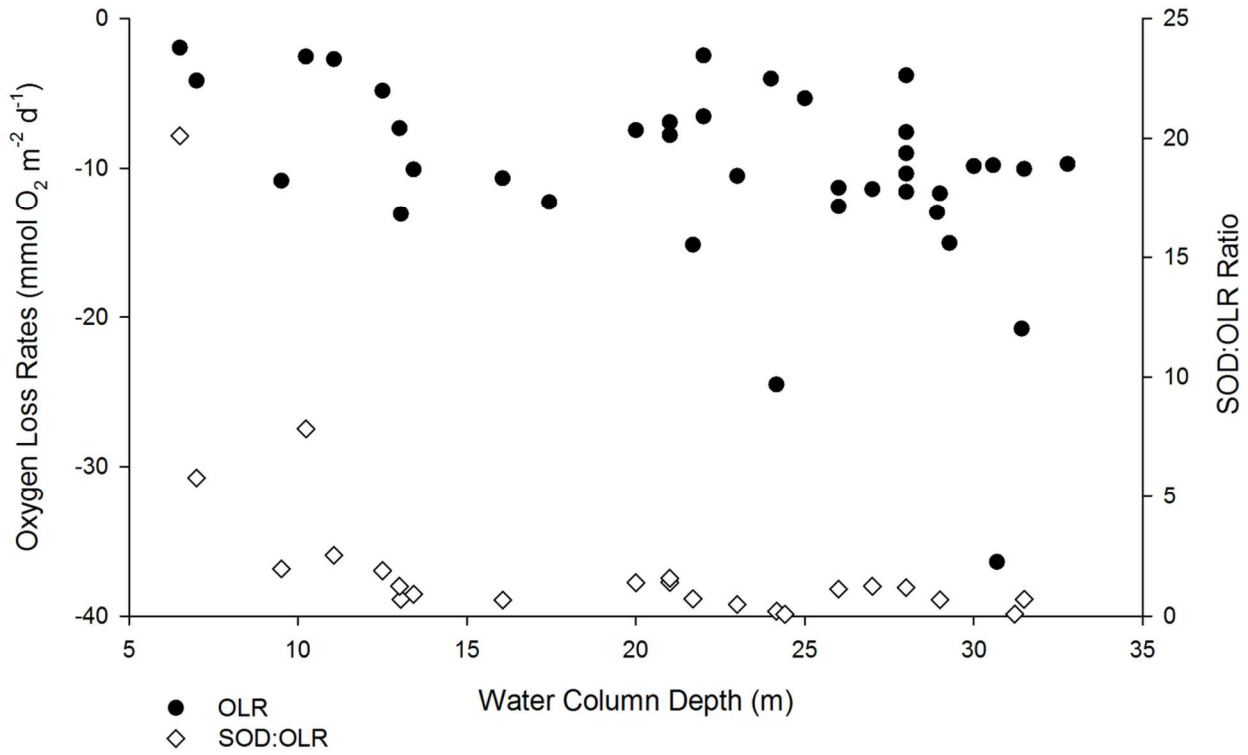
relative influence of each is affected by hypolimnetic thickness (i.e. water depth) and presumably the delivery of respirable organic matter which is heavily skewed to the southern portion of the bay by nutrient and organic matter loading from the Fox River. SOD, therefore, tends to be focused in the southern bay near this riverine source at shallow depths (< 15 meters) that corresponds to the area where deposition of fresh algal material is at its highest.

Hypoxia in Green Bay today is a summertime phenomenon that responds to prolonged thermal stratification and is also strongly influenced by wind driven currents (Waples and Klump 2002) and its estuarine-like circulation. Cool bottom waters originating from northern Green Bay and Lake Michigan flow southward under prevailing southwest winds and become increasingly depleted of oxygen as the pass over the organic-rich sediments of the mid bay. It is here where much of the oxygen depletion appears to occur.

Climate change projections for this region call for warmer temperature and a summer lengthened by as much as 6 weeks (WICCI, 2011). Such a shift would most likely increase the likelihood of hypoxia in the absence of countervailing processes, simply through the sequestration of bottom water over longer periods.

CHAPTER 5: EVALUATION OF TRANSPORT IN GREEN BAY VIA NATURAL

TRACERS

5.1 Introduction

Studies have shown that physical processes can have major influence over biogeochemical activities in aquatic and marine systems. For example, wind patterns influence water mass circulation and can affect stratification intensity. These dynamics, in turn, alter oxygen dynamics, such as reduced availability to the hypolimnia which can lead to enhanced methane production (Breitburg 1990; Waples and Klump 2002; Fujiwara et al. 2002; Scully 2010, 2016). Physical exchanges within the benthic boundary layer, such as advection of groundwater into coastal systems, can contribute limiting nutrients that drive a system eutrophic (Corbett et al. 2000; Shaw et al. 2013) and anoxic water that reduce biological habitat in bottom waters (Edwards et al. 2009; Koopmans and Berg 2015).

The movements of water masses, both horizontally and vertically, in Green Bay can also play a strong role in biogeochemical processes, including benthic metabolism, nutrient cycling, particle transport and the onset, duration and spatial extent of hypoxia (Waples and Klump 2002; Hamidi et al. 2015). In Green Bay it has been hypothesized that cool bottom water from Lake Michigan may form cold water intrusions that pass over organic-rich sediments (up to 10% organic matter by wt.) and turn into "hypoxic blobs" that flow into the lower bay (Kennedy, 1982; Klump et al. in prep). While general circulation patterns of Green Bay are relatively well constrained (Miller and Saylor 1985; Gottlieb et al. 1990; Hamidi et al. 2015), more specific information regarding the water exchanges between Lake Michigan, the rivers and Green Bay would improve both biogeochemical and hydrodynamic models of the bay and improve our understanding of the influences these may have on dissolved oxygen conditions in the summer. Furthermore, few studies have been performed to constrain benthic boundary exchange rates and diffusion rates

113

within Green Bay (Klump et al. 1997a, 2009). Additional studies would provide valuable ranges of sediment-water exchange rates to help understand how the benthos affect biogeochemical cycles with gaseous components.

Within any given system there are many physical processes that could be studied with a variety of techniques, although one of the most preferred methods is utilization of natural tracers. The application of natural tracers to study physical processes is useful because they are present throughout the environment with no need to be added to the system. This type of tracer is also preferable because it is natural part of the biogeochemical and physical cycles, meaning that the tracer will not cause any unwanted interactions and there is no waiting time needed for the tracer to equilibrate to the environment. Examples of natural tracers include $D_2^{18}O$, ^{222}Rn and methane (CH_4).

Stable isotopes of oxygen (^{18}O and ^{16}O) and hydrogen (^2H and ^1H) can be used to differentiate waters of various origins, examine mixing relationships and understand processes that have affected the water since it was formed (Harvey et al. 1997). Drever (1988) quantified the natural, average ratio of ^{18}O to ^{16}O as 1:1500 and of ^2H (or deuterium, D) to ^1H as 1:6700. Processes like evaporation or ice formation can alter the isotopic signature which makes these stable isotopes valuable for studying regional hydrologic cycles (Lessels et al. 2016; Wang et al. 2016). In the absence of fractionation or over short time scales, the isotopic signature of waterbodies may be used as a conservative tracer for estimating source waters (e.g. rivers vs. lake vs. ground water) and water mass mixing.

^{222}Rn is a naturally occurring radionuclide ($t_{1/2}$ = 3.82 d) produced from the alpha-decay of ^{226}Ra ($t_{1/2}$ = 1622 yr) within the ^{238}U decay series. ^{226}Ra accumulates in the sediments, which results in

114

relatively high ^{222}Rn activities in sediment porewater compared to the water column (Broecker and Peng 1982). Radon is also a noble gas, meaning that it does not undergo biological or chemical reactions and behaves conservatively during diffusive and advective processes. This, combined with a short half-life, make it an ideal natural tracer for studying exchange processes across the sediment-water interface (Key et al. 1979; Martens et al. 1980). ^{222}Rn was initially used to study vertical eddy diffusivity in the deep sea (Broecker, 1965). Since then, ^{222}Rn has been successfully used in coastal systems to estimate groundwater and porewater influences on the overlying water column (Klump and Martens 1981; Lambert and Burnett 2003; Cable and Martin 2008), particularly as a tracer of gas emanation. Advection rates can also be estimated for sites where water column inventories greatly exceed porewater diffusion supported fluxes (Corbett et al. 2000; Smith et al. 2008). It has also been suggested that ^{222}Rn could be used to determine bottom water movements (Broecker, 1965).

Another gas commonly used to track water-sediment fluxes and vertical diffusion is methane. In aquatic systems one of the primary sources of methane is production in anoxic sediments from methanogens that reduce organic matter to CH_4 (Sansone et al. 2004; Naqvi et al. 2010), Pulses of groundwater can also act as a natural source of methane to bottom waters (Moya et al. 2016). Unlike ^{222}Rn and $D_2^{18}O$, methane is biogeochemically reactive. Methane oxidation occurs in oxic conditions, typically in the upper layers of sediment by bacterial activity. Once CH_4 enters the water column, oxidation may be very low or even non-detectable (Kuivila et al. 1989; Geprägs et al. 2016). Waples (1998) has suggested that in Green Bay methane oxidation is very low (Fig. 32) and that methane may be considered as a tracer of gas exchange. Therefore, it is possible that

115

Figure 32: Water column profile of methane at Green Bay station 38 on 8/26/2014.
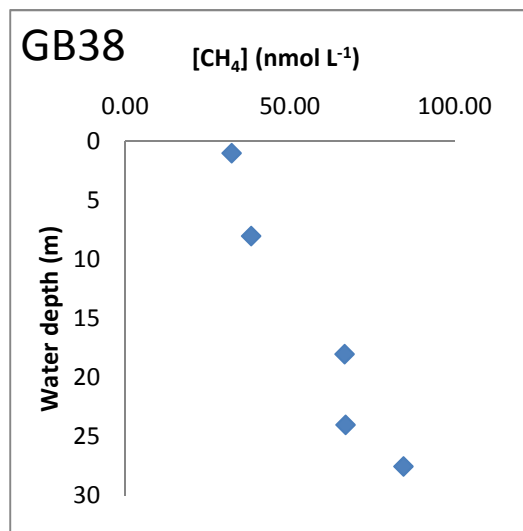
methane could also be used as a tracer of horizontal water movements in areas where

hypolimnetic CH_4 concentrations are in excess of water column averages.

Three major goals were developed for the application of natural tracers in Green Bay, Lake

Michigan. The first was to evaluate water flow paths, intrusion distance, and potentially mixing

rates using $D_2^{18}O$. The second goal was to estimate sediment-water exchange rates of in the

benthic boundary layer using ^{222}Rn and CH_4. The final goal was to examine the utility of ^{222}Rn

and CH_4 as tracers of horizontal bottom water transport in northern Green Bay.

5.2 Methods

Horizontal Tracers

Two to 20 liter samples of bulk water for analysis of ^{222}Rn, methane, total suspended solids, etc.

were collected from the water column via a submersible pump (~ flow rate 30 liters per minute)

during field studies of July, August and September of 2012-2015. Samples for $D_2^{18}O$ from surface and bottom waters were stored in thoroughly rinsed triplicate 2-mL Teflon™ sealed glass autosampler vials. Bottom waters were analyzed from a total of 34 stations along the length of the bay from the Fox River inflow to northern Green Bay/Lake Michigan.

Isotopes were analyzed by wavelength-scanned cavity ring-down spectroscopy using a Picarro L2130-*I* Analyzer with a Vaporization module AO211 and an autosampler (Picarro Inc., Sunnyvale, CA, USA) to measure isotopic ratios of $^{18}O/ ^{16}O$ ($\delta^{18}O$) and $^2H/^1H$ (δD) (Gupta et al. 2009). Each individual triplicate sample was analyzed 6 times, with the last 3 runs averaged for a sample mean. Three standards were used at the beginning and end of each run to identify periods of drift or instrument error. The three working standards- over a range of values- have been standardized to IAEA standards. Working standards are kept in stainless steel barrels under 10 psi of N_2.

In general, delta values (δ), given as *per mil*, are used to represent relative differences in isotopic species in parts per thousand and are calculated using

$$\delta\ (‰) = \left[\frac{R_{sample} - R_{std}}{R_{std}}\right] x 1000 \qquad \text{(Eqn. 5.1)}$$

where R is the isotopic ratio. For oxygen and hydrogen, R is $^{18}O/^{16}O$ and $^2H/^1H$, respectively, while R_{std} is the ratio of Vienna Standard Mean Ocean Water (VSMOW2). VSMOW2 reference values are 0.0 and 0.00 for δ^2H and $\delta^{18}O$, respectively, with expanded uncertainties of 0.3 and 0.02 (Wise and Watters 2011).

Vertical Tracers

117

To sample porewater from sediment, bulk sediment was collected in a 30 x 30 cm (900 cm^2) box corer and was then sub-cored into four standard 7.5cm benthos core liners. The sub core with the most intact sediment-water interface, as determined by visual inspection, was transferred to a whole-core squeezer as described by Jahnke (1988). Depth profiles of porewater were obtained by collecting samples from 0 to 12 cm at known 1 to 2 cm intervals. Porewater was collected by inserting porous polyethylene Porex® filter rods (70 μm matrix) attached to stopcocks and cleaned 10mL syringes into the sampling ports (Figure 33). Two different methods of obtaining filtration were employed. The primary sample method was sediment compression by applying pressure to the top and bottom core ends that slowly forced porewater through the porous rods into the syringes, until 10 mL of sample was reached or until sample stopped being collected. The second method was a vacuum approach in which a vacuum was essentially created by extruding the plunger of the syringe, drawing porewater into the syringe until sufficient sample was collected. In this method headspace was included in the sample for extraction.

Porewater was immediately held in a shipboard refrigerator until analysis, usually within hours for ^{222}Rn. Samples for ^{222}Rn were transferred to a 100-mL glass syringe with enough N$_2$ gas to reach 100 mL total volume and stripped for 30 to 60 seconds. The measured stripping efficiency is 80% determined by repeated stripping of samples. The head space was transferred to an evacuated Lucas type scintillation cell that was then placed in an alpha counting chamber (Mathieu et al. 1988). Samples were counted for a minimum of 3 hours.

Methane porewater samples were analyzed shipboard as soon as possible after collection. A volume of helium equal to that of the water sample was added to the syringe and shaken

118

vigorously for 30 seconds, then the head space gas was analyzed with a Hach Carle F.I.D. gas chromatograph (Buchhloz et al. 1995).

Water column profiles of ^{222}Rn and methane were collected using a submersible pump (flow rate ~40 liters per minute). For ^{222}Rn, a 20-L glass carboy was flushed with water at least 5 times, allowed to fill, drained to acquire ~1L of headspace and was then sealed using custom-made fittings. Within 48 hours of sample collection the samples were processed according to Mathieu et al. (1988). Briefly, the sample was stripped for radon by circulating helium through the sample and radon was collected on a charcoal column trap using a dry ice and propanol slurry (-40 °C). The column was then flushed with helium and gases were transferred to an evacuated Lucas scintillation cell for alpha counting. Select samples were re-measured after >1 month to determine radium supported radon activities.

Figure 33: An example of porewater collection occurring at Station GB31 in August 2013. Porex® was fitted to luer-lock attachments and inserted into holes at 1 cm intervals. Clean 10-mL plastic syringes were fitted with 3-way stop cock, then attached to the exposed luer-lock fitting as quickly as possible. In this particular case, the core was slowly squeezed using the ratchet wrench located at the bottom of the core. Porewater is expelled through the Porex®. Up to 10 mL of porewater was collected per depth.
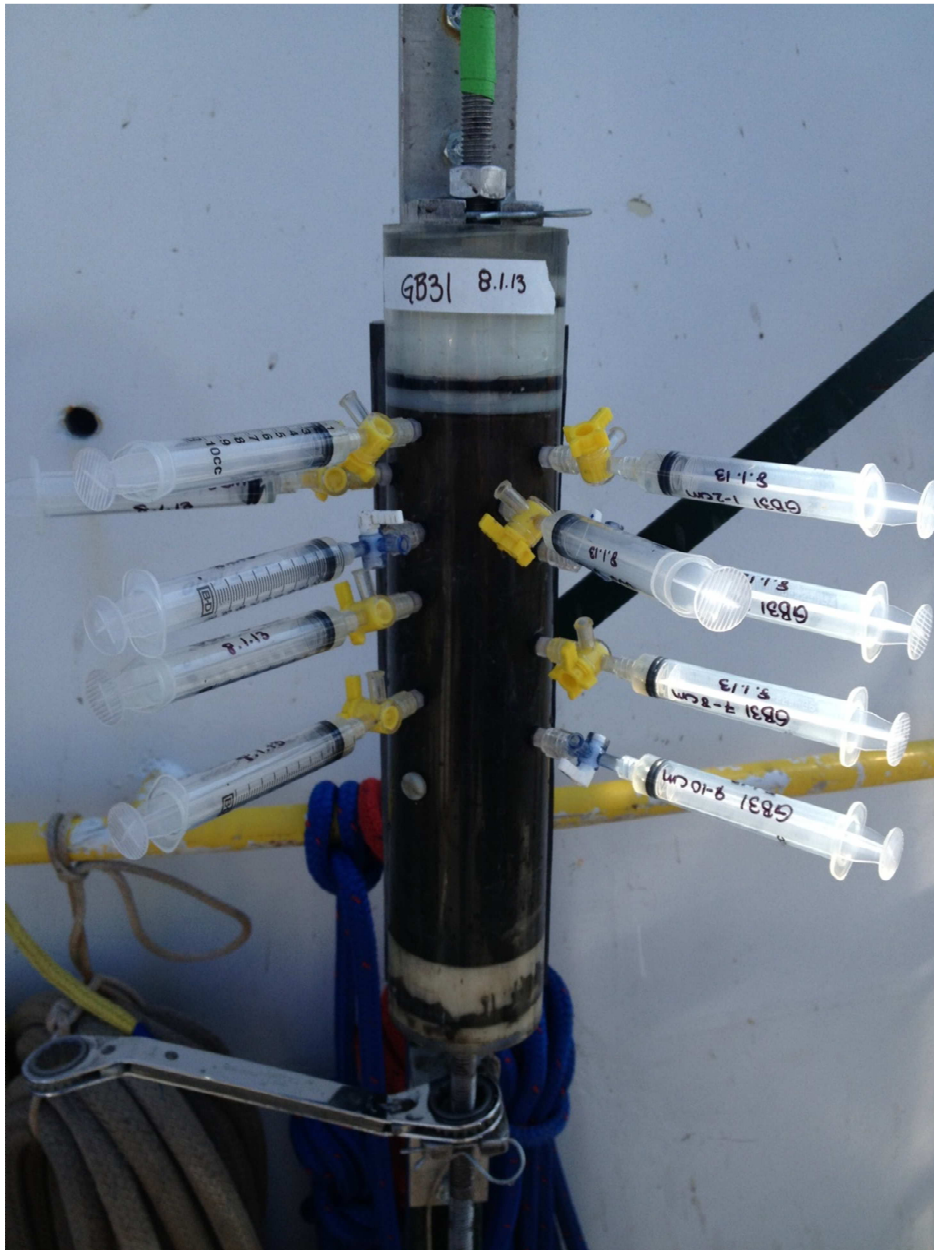
Methane samples were collected in 50 mL glass jar with etched glass stoppers after being rinsed a minimum of 5 times. Methane oxidation was effectively inhibited by adding 1 mL of 1.5M $CuSO_4 \cdot 5H_2O$. 20 mL of sample was stripped in 5 mL of N_2 then the gas was injected into a flame-ionization gas chromatograph (Stainton 1973).

For all ^{222}Rn samples the measured alpha counts were converted to an activity in disintegrations per minute per liter (dpm L^{-1}) using a spreadsheet developed by G. Kipphut based on Key et al. (1979) and Mathieu et al. (1988). The background signal of the counting cell and counter-cell efficiencies were included in calculations.

Benthic fluxes (J) of ^{222}Rn and methane supported by concentration gradients are calculated using Fick's first law (Berner 1980):

$$J = -\emptyset D_s(dC/dz) \qquad \text{(Eqn. 5.2)}$$

where ϕ is the sediment porosity ($cm_{pw}^3 \, cm_{sed}^{-3}$) and D_s is the whole sediment diffusion coefficient ($cm^2 \, s^{-1}$; Klump and Martens, 1981). Gradients of these gases are present due to fractions of the gases escaping the sediment, where they are sourced, to the overlying water column. The overlying water column concentrations are approximately two orders of magnitude lower than sediment concentrations and a gradient is created across the sediment-water interface (Broecker, 1965; Hammond and Fuller, 1979).

The upward migration of radon results in a sediment deficiency, or an activity ratio of Rn:Ra less than one (Hammond and Fuller, 1979). At depth in the sediments a secular equilibrium, C_{eq}, is reached where Rn:Ra approaches 1 (Fig. 34). To calculate benthic fluxes steady-state is assumed (Broecker 1965; Hammond and Fuller 1979) and horizontal advection is generally considered

121

Figure 34: Example of the radon-222 distribution at Green Bay station 43 during 2013. Blue area represents water column radon inventory supported from sediment. Red area shows radon deficiency in sediment due to diffusion. The dotted line indicates the radon:radium equilibrium that occurs with depth.

122
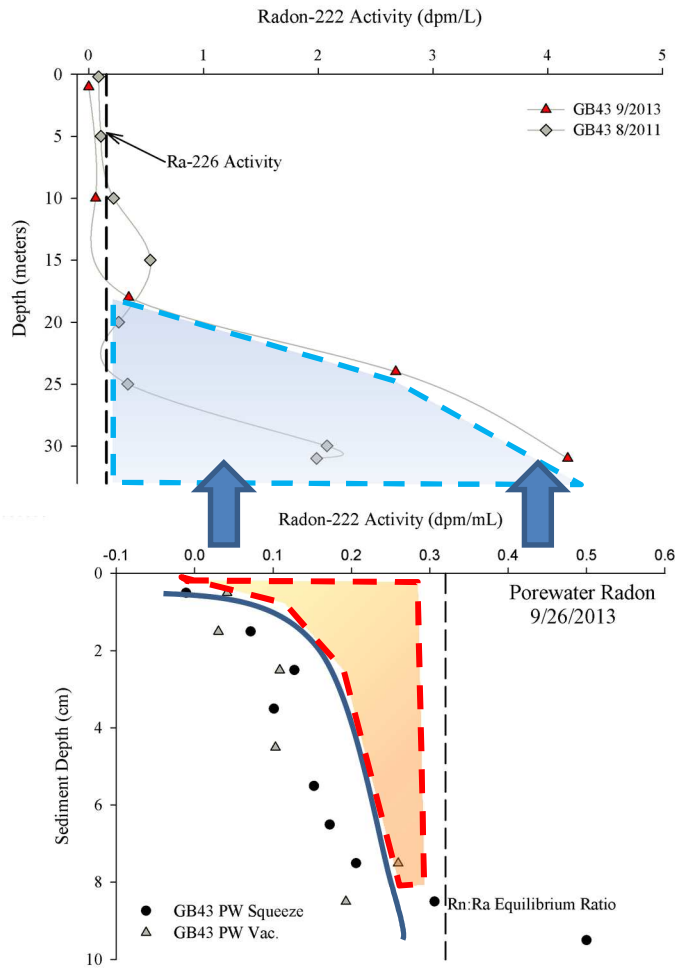
negligible for short-lived radioisotopes (Key et al. 1979). In the case where molecular diffusion is the only transport process of radon, the distribution in sediments can be described by (Kipphut and Martens 1982):

$$J_{PW} = (D_s\lambda)^{\frac{1}{2}} * (C_{eq} - C_0) \qquad \text{(Eqn. 5.3)}$$

where C_0 is the ^{222}Rn activity at the sediment surface (dpm m^{-3}), C_{eq} is the ^{222}Rn supported by ^{226}Ra (dpm m^{-3}) and λ is the decay constant for ^{222}Rn (0.182 d^{-1}). D_s can be approximated by $D_s \sim \phi^2 D_m$, where D_m is the molecular diffusion coefficient in the aqueous phase (Klump and Martens 1981).

Methane porewater fluxes are taken from Klump et al. (2009) and are discussed briefly below.

Hypolimnetic ^{222}Rn inventories (I_{hypo}) were calculated for as

$$I_{hypo} = \sum_{z=b}^{z=t} \bar{A}\,\Delta z \qquad \text{(Eqn. 5.4)}$$

where A is the mean non-supported water column activity (dpm m^{-3}) between depths, Δz, and these are summed between the bottom-most sample, b, and the bottom of the thermocline, t. In cases where a measured radon activity was not available at two depths in the hypolimnion, the measured supported ^{222}Rn value was applied at the 1-meter interval directly below the bottom of the thermocline. For example, if the bottom of the thermocline was calculated to be 10.4 meters, the supported ^{222}Rn value was applied for z=11 m. The bottom of the thermocline was calculated as the first depth in the water column not exceeding a 1 degree Celsius change over one meter.

123

5.3 Results and Discussion

Horizontal Water Transport

Stable isotopes were measured over a large spatial distribution in Green Bay during 2013 and 2014. Isotopic signatures (δ^{18}O, δ^{2}H) of the two end-members varied somewhat from month to month-- for the Fox River and for Lake Michigan (Table 15). Differences in the surface water (i.e. Fox River) throughout the summer (e.g. 6/26/13 δ^{18}O = -7.06‰ vs 8/29/13 δ^{18}O = -6.57‰) are attributed to evaporation (Gat 1996), which increases the abundance of ^{18}O and ^{2}H, and changes in δ^{18}O/^{16}O and δ^{2}H/^{1}H values of precipitation as a function of season (Dansgaard 1964). The ratios of surface water isotopes can also be affected by watershed activities, such as increases in the heavier isotope through increased evaporation caused by plant interception and surface retention (Gat and Tzur 1967).

After the isotopic sample means were calculated, the mixing at each site was computed by assuming the surface sample from the Fox River mouth was 100% Fox River water and the bottom sample that was farthest north was 100% Lake Michigan water. The other working assumption for these calculations was that water in Green Bay is only from either the Fox River (FR) or Lake Michigan (LM), which have been previously shown to be the major sources within the system (Modlin and Beeton 1970; Hamidi et al. 2015). For a majority of the months, there was a true Fox River water sample taken off of the pier at the Fox River Mouth (FR) from the University Bay Boat Launch (44.538°N, -88.004°W).

Table 15: Stable isotope values (per mil) for samples used as end members within Green Bay during July and August 2013 and 2014.

	Station	Sample Depth	Date	Average O18/O16	Average D/H
River-End Members	FR	1	7/25/2014	-7.53	-55.50
	FR	1	8/25/2014	-7.40	-55.09
Lake Michigan End Members	GB100	32	7/30/2013	-6.04	-44.99
	GB83	30	8/28/2013	-5.99	-44.73
	Lake Michigan	53	7/21/2014	-5.74	-43.80
	Lake Michigan		*Used for August 2014*	-5.74	-43.80

Differences in bottom water isotopic signatures are smaller and they are possibly due to differences in sampling location from month to month or groundwater inputs. It is recognized that our end-member samples were not taken from the same location in northern Green Bay, let alone Lake Michigan. However, when we compare the percentage of Lake Michigan water calculated for mid-bay stations from the true Lake Michigan sample (65%-83%) and the northern Green Bay samples (66%-90%) they are very similar.

There is a linear relationship between δ^2H values and δ^{18}O values, which indicates that these two end members make up a large majority of the water in the bay (Fig. 35). When thermal stratification is present there is a clear difference between surface and bottom water isotopic signatures, indicative of two different water sources (Fig. 36). Fox River water generally dominates the surface water component of the samples during the summer months, which is expected because it is warmer and therefore, more buoyant (Miller and Saylor 1985; Hamidi et al. 2013). The average fraction of Lake Michigan water in the hypolimnion is 0.65($\pm$ 0.23) over the July and August 2013 and 2014 (Fig. 37; Table 16). There was no consistency in this dataset to determine if July or August had a greater fraction of LM. The average ($\pm$SD) Lake Michigan bottom water fraction was greater in 2013 (0.68$\pm$ 0.27) than 2014 (0.63$\pm$ 0.20), but it was not significant. There was a substantial Lake Michigan signal in the bottom water at GB12, only 30 km from the mouth of the Fox River, with values ranging from 33% (August 2013) to 44% (August 2014) of the total bottom water inventory. This supports the hypothesis (Miller and Saylor 1985; Grunert 2013) that benthic, cold water intrusions from Lake Michigan do occur in this

Figure 35: The distribution of isotopic signatures from samples collected in July and August 2013-14. The station numbers of the lightest and heaviest samples are noted.
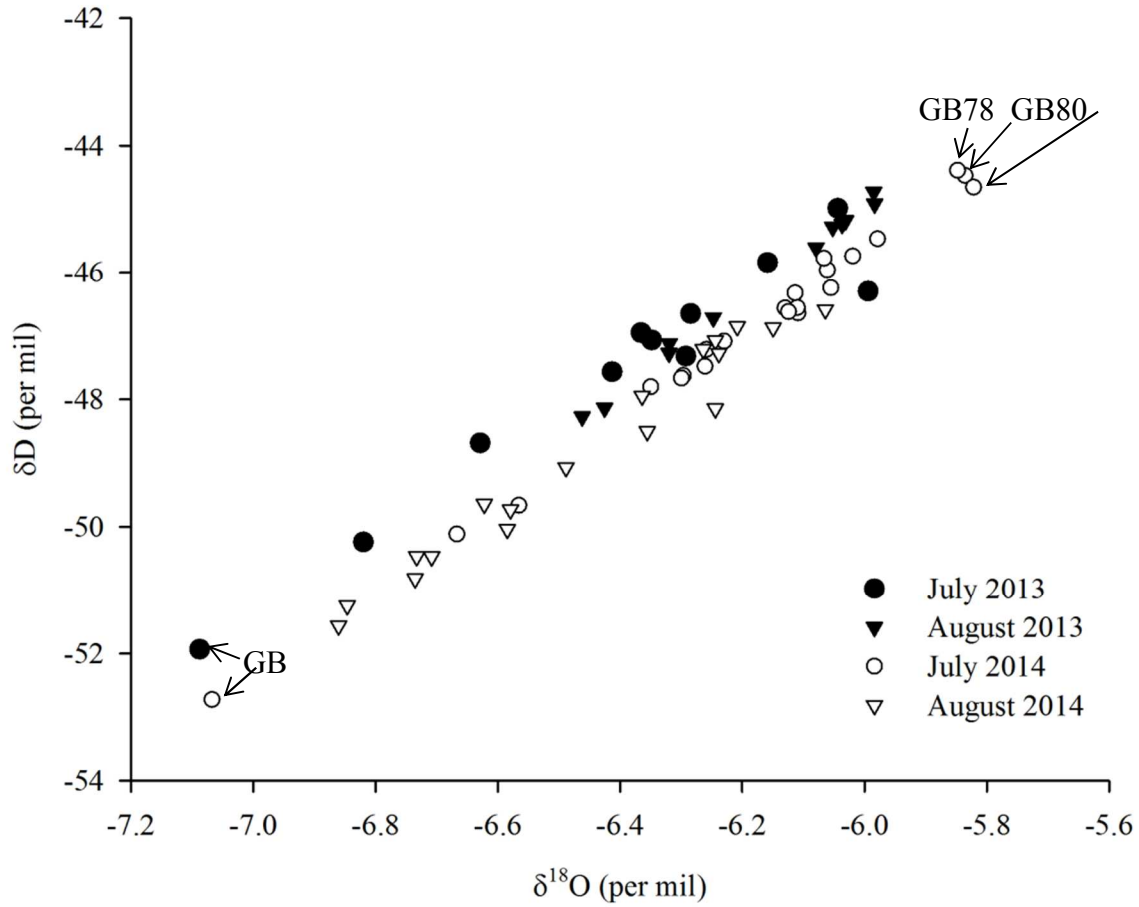
Figure 36: Isotopic signatures from samples of two water column profiles in mid-Green Bay.
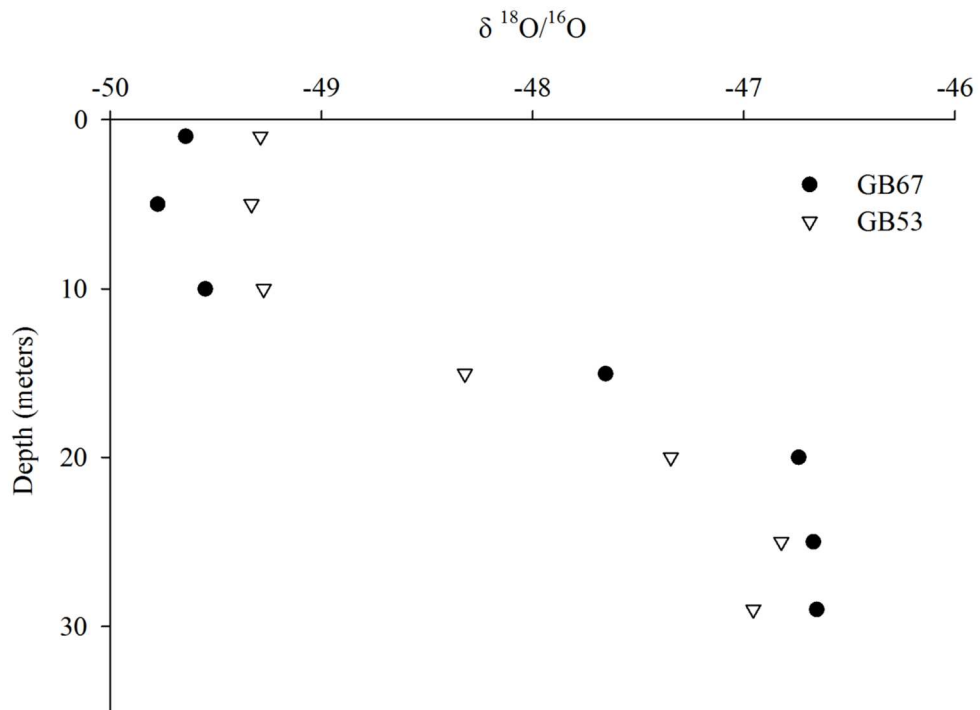
Figure 37a: D218O results were used to calculate the fraction of Lake Michigan water present at the different sites. Surface (left) and bottom (right) results for July 2013 are given with the same scale.
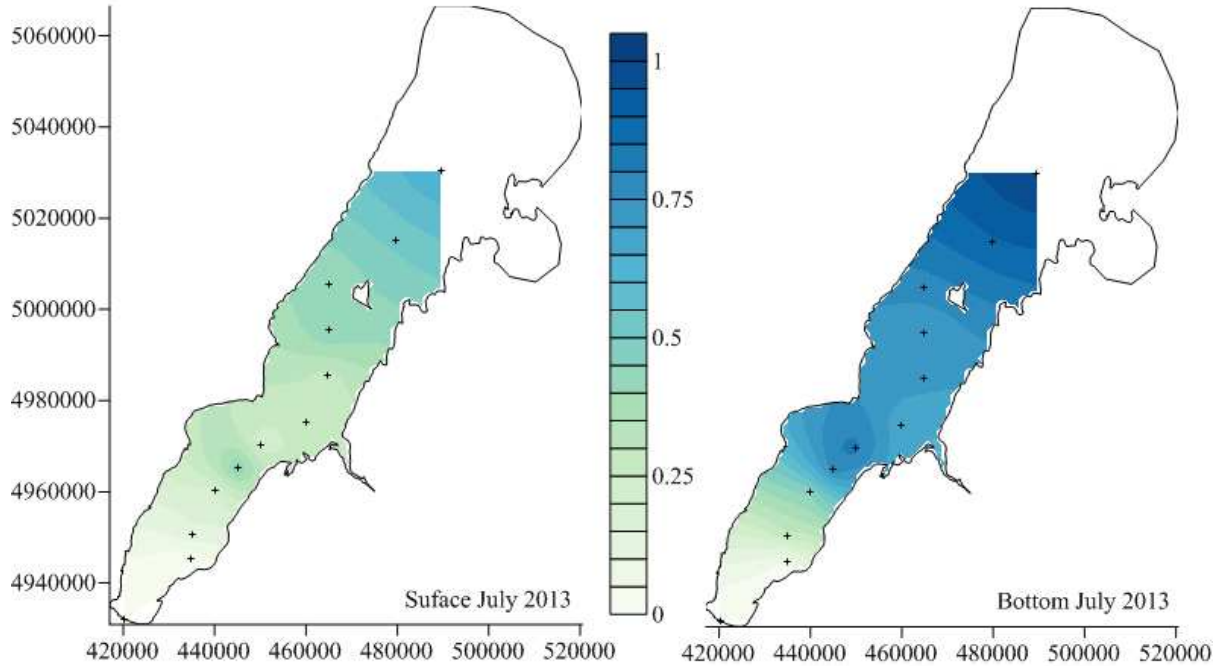
Figure 37b: Same scale as Fig. 37a, but with results for August 2013.

129
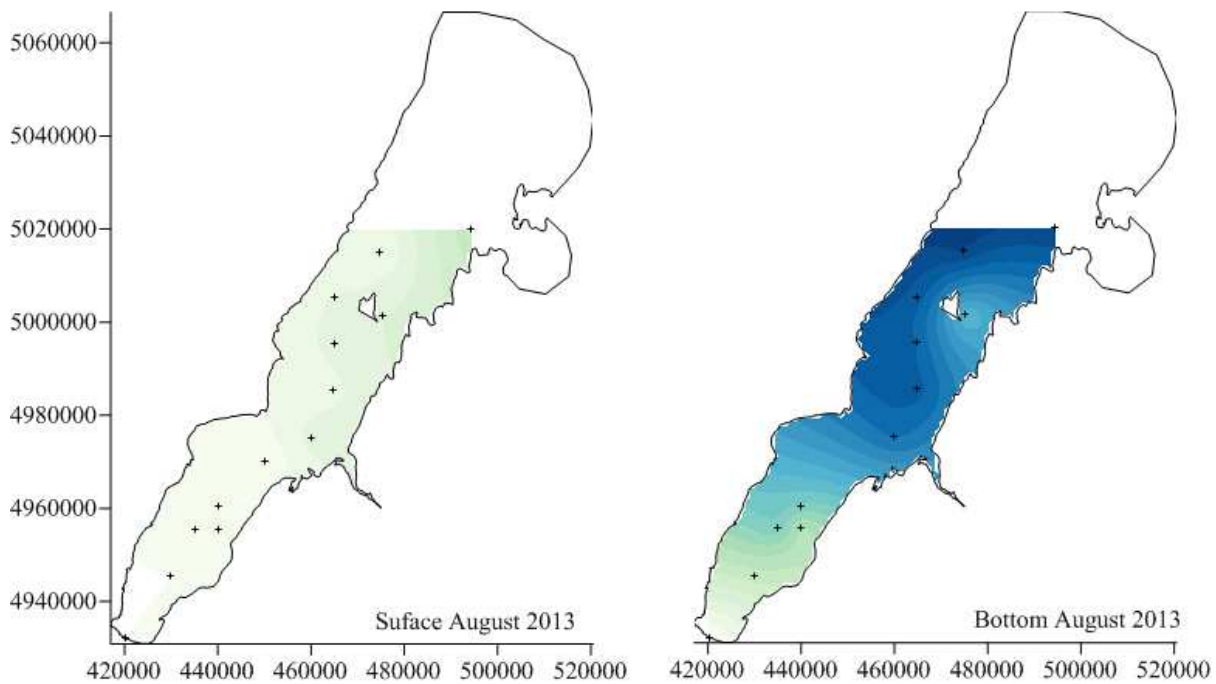
Figure 37c: Same scale as 37a, but with results for July 2014.
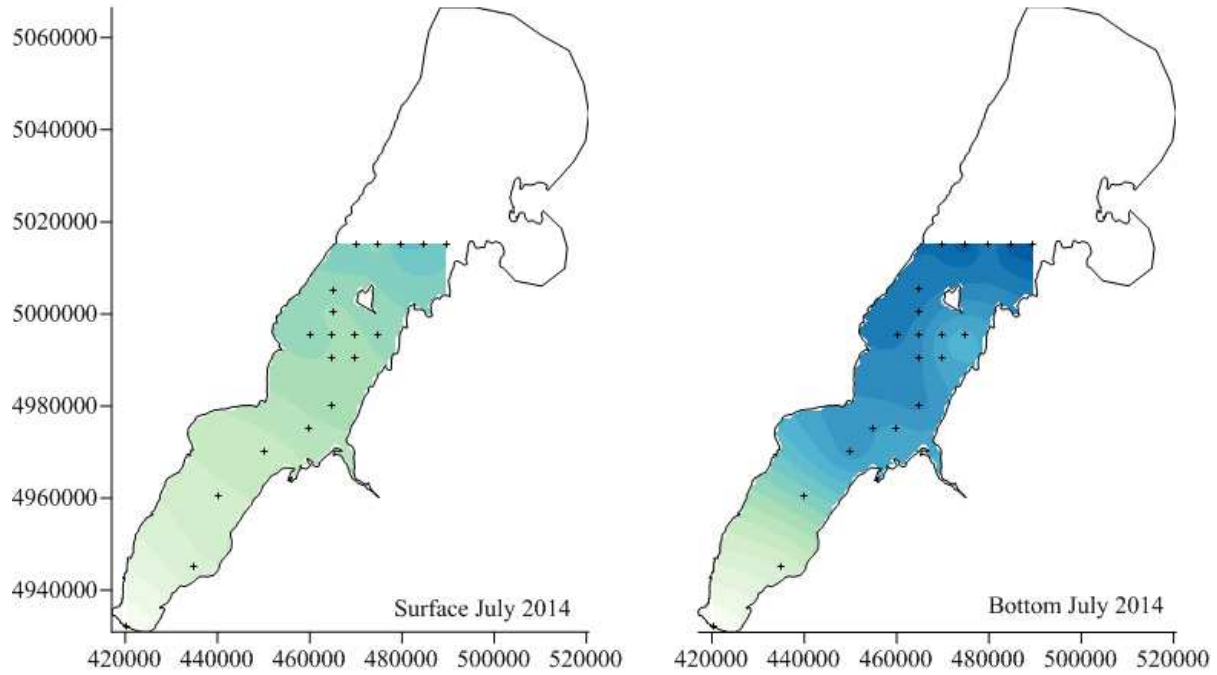
Figure 37d: Sample scale as Fig. 37a, but results for August 2014.
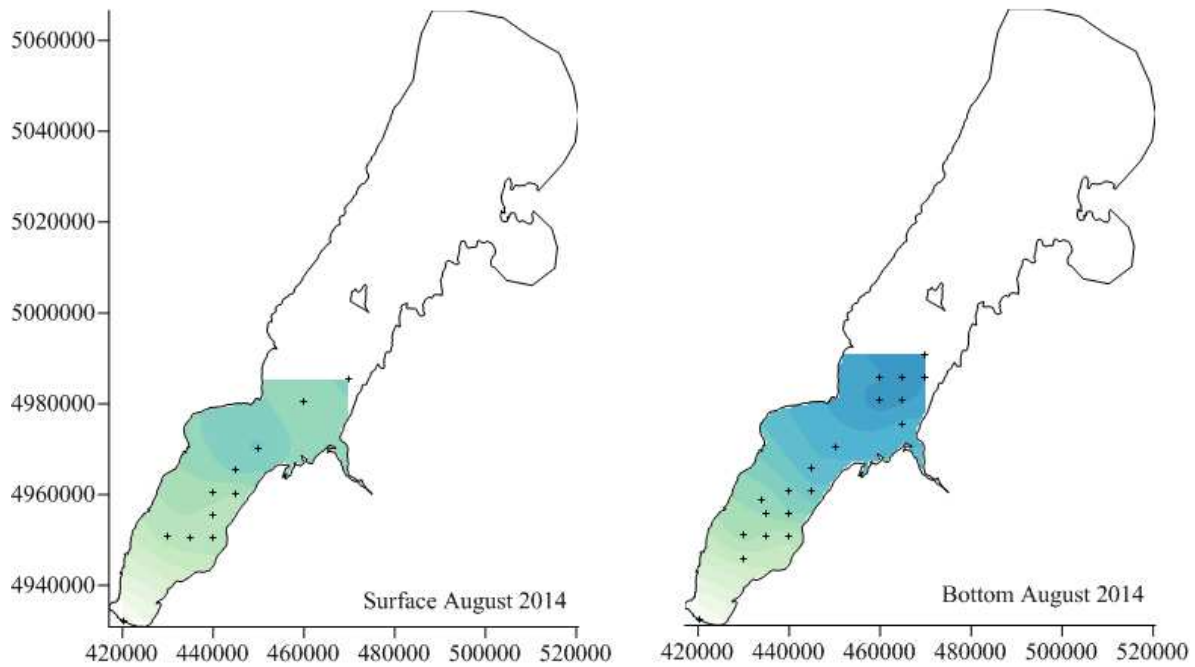
system. Elevated Lake Michigan isotope ratios to the west of Chambers Island demonstrate that the circulation of bottom water is clockwise, which agrees with previous studies in the system (Gottlieb et al., 1990; Hamidi et al., 2015; Miller and Saylor, 1985).

Sediment diffusive fluxes

23 cores were analyzed for ^{222}Rn activity in porewater from September 2012 to August 2015. Of these, 19 were collected using the compression technique and 4 were collected using the vacuum technique. Sediment-water radon fluxes were calculated using Eqn. 5.3. The porosity values were taken from the site closest to the sample site and ranged from 0.889 to 0.992 cm^3 cm^{-3} (Klump et al. 1997a). The molecular diffusion value was 1.14×10^{-5} cm^2 sec^{-1} (Klump and Martens 1981), resulting in D_s values ranging from 9.0×10^{-6} to 1.1×10^{-5} cm^2 sec^{-1}.

The benthic flux for ^{222}Rn from porewater diffusion, J_{PW}, in Green Bay ranged from 140 to 2.6×10^4 dpm m^{-2} d^{-1}, with an average of 1830 ± 5300 dpm m^{-2} d^{-1} (Fig. 38, Table 17). The largest fluxes were measured north of the Sturgeon Bay inlet, with the exception of one flux from the southern part of the bay. A geological survey of sediments in Green Bay from the 1970s found higher amounts of manganese nodules in sediments located north of Sturgeon Bay (Fig. 38a; Moore et al., 1973), near zones that match areas of high radon porewater fluxes (Fig. 38b). This is in accordance with studies that have shown that ^{226}Ra accumulates near manganese deposits (Todd et al. 1988), due to accumulation and enrichment of ^{230}Th, the parent isotope of ^{226}Ra, within manganese nodules (Baturin 1988).

131

Table 16: Results of the mixing equation applied to isotopic signatures within Green Bay given as fraction of Lake Michigan (LM) water present. Each sampling cruise is noted in the first column and distance to the Fox River (FR) is in kilometers.

Sampling Cruise	Site	FR Distance (km)	Surface Fraction LM	Bottom Fraction LM
Jul-13	GB5	18	0.000	0.012
7/30 – 8/1	GB9	23	0.111	0.254
	GB17	34	0.189	0.474
	GB21	41	0.320	0.668
	GB26	48	0.204	0.813
	GB31	58	0.226	0.633
	GB43	69	0.261	0.704
	GB53	77	0.388	0.720
	GB67	85	0.338	0.763
	GB79	102	0.465	0.879
	GB100	120	0.604	1.000
Aug-13	GB6	16	0.000	0.287
8/27 – 8/29	GB12	30	0.050	0.314
	GB13	27	0.064	0.487
	GB17	34	0.085	0.517
	GB26	48	0.056	
	GB31	58	0.148	0.823
	GB43	69	0.119	0.898
	GB53	77	0.155	0.888
	GB67	85	0.104	0.909
	GB80	99	0.108	0.963
	GB83	115	0.303	1.000
	Chamber's East	90	0.160	0.600
Jul-14	GB5	19	0	0.250
7/21 – 7/24	GB17	34	0.261	0.487
	GB17	34	0.228	0.528
	GB26	48	0.236	0.802
	GB26	48	0.299	0.750
	GB31	58	0.342	0.726
	GB32	55	-	0.762
	GB38	65	0.389	0.810
	GB38	65	0.381	0.810

132

	GB47	76	0.396	0.713
	GB48	73	0.390	0.804
	GB51	83	0.432	0.697
	GB52	80	0.402	0.709
	GB53	77	0.401	0.831
	GB54	75	0.438	0.838
	GB59	81	0.411	0.865
	GB67	85	0.456	0.885
	GB77	108	0.521	1.000
	GB78	105	0.576	1.007
	GB79	102	0.588	0.882
	GB80	99	0.443	0.957
	GB81	97	0.523	0.909
Aug-14	GB6	16	0.201	-
8/25 – 8/28	GB8	27	0.272	0.312
	GB9	23	0.321	0.340
	GB10	21	0.328	0.379
	GB12	30	0.303	0.448
	GB16	37	0.339	0.533
	GB17	34	0.339	0.475
	GB17	34	0.367	0.482
	GB21	41	0.396	0.583
	GB26	48	0.383	0.615
	GB39	62	0.418	0.729
	GB42	72	0.470	0.697

133

Table 17: ^{222}Rn porewater fluxes (dpm m^{-2} d^{-1}) calculated using Eqn. 5.3 based on profiles from Fig. 38. **Indicates that the porosity from GB48 was used for calculations.

Site	Method	Sample Date	Jpw Rn-222 (dpm m^{-2} d^{-1})
GB6	Squeeze	6/4/2014	613
GB9	Squeeze	9/25/2103	227
GB9	Vacuum	9/25/2013	356
GB13	Squeeze	8/27/2013	260
GB17	Squeeze	7/31/2013	142
GB21	Vacuum	8/26/2015	196
GB26	Squeeze	7/21/2014	818
GB31	Squeeze	8/29/2013	244
GB31	Squeeze	9/12/2012	281
GB31	Vacuum	8/29/2013	468
GB31	Squeeze	8/1/2013	488
GB38	Squeeze	7/24/2014	686
GB39	Squeeze	8/26/2014	710
GB43	Vacuum	9/26/2013	692
GB43	Squeeze	9/26/2013	1552
GB47	Squeeze	8/26/2014	1973
GB48	Squeeze	6/5/2014	730
GB48	Squeeze	7/22/2014	815
GB48	Squeeze	8/27/2015	959
GB67**	Squeeze	6/5/2014	26060
GB73**	Squeeze	6/5/2014	2546
GB79**	Squeeze	7/30/2013	519
GB80	Squeeze	7/23/2014	704

Figure 38: Porewater profiles of ^{222}Rn.
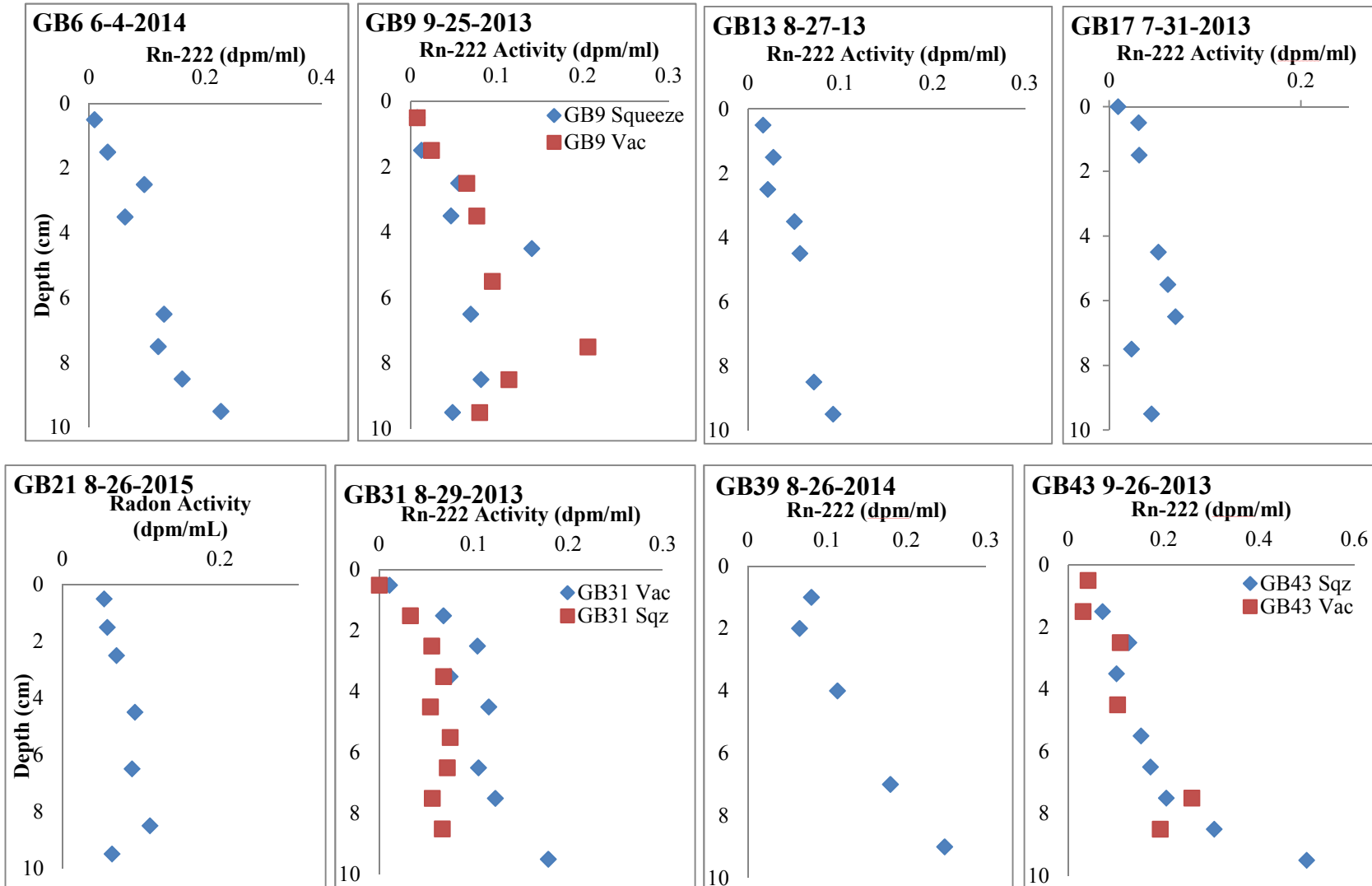
Figure 38 (cont.)
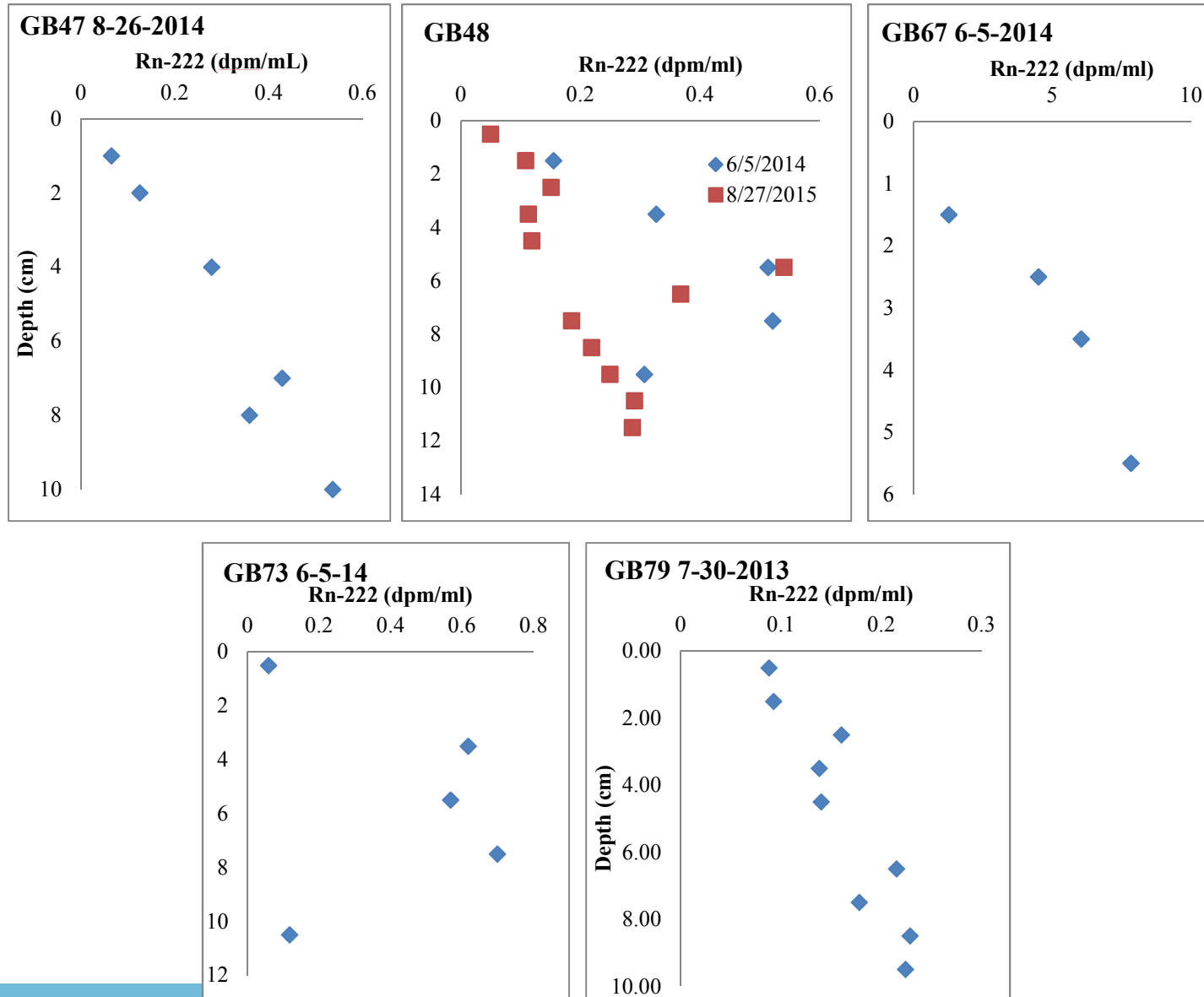
Figure 39: Manganese nodule distribution in Green Bay (left, from Moore et al. 1973) versus station averaged (red diamonds) ^{222}Rn porewater fluxes (right).

(Moore et al. 1973)
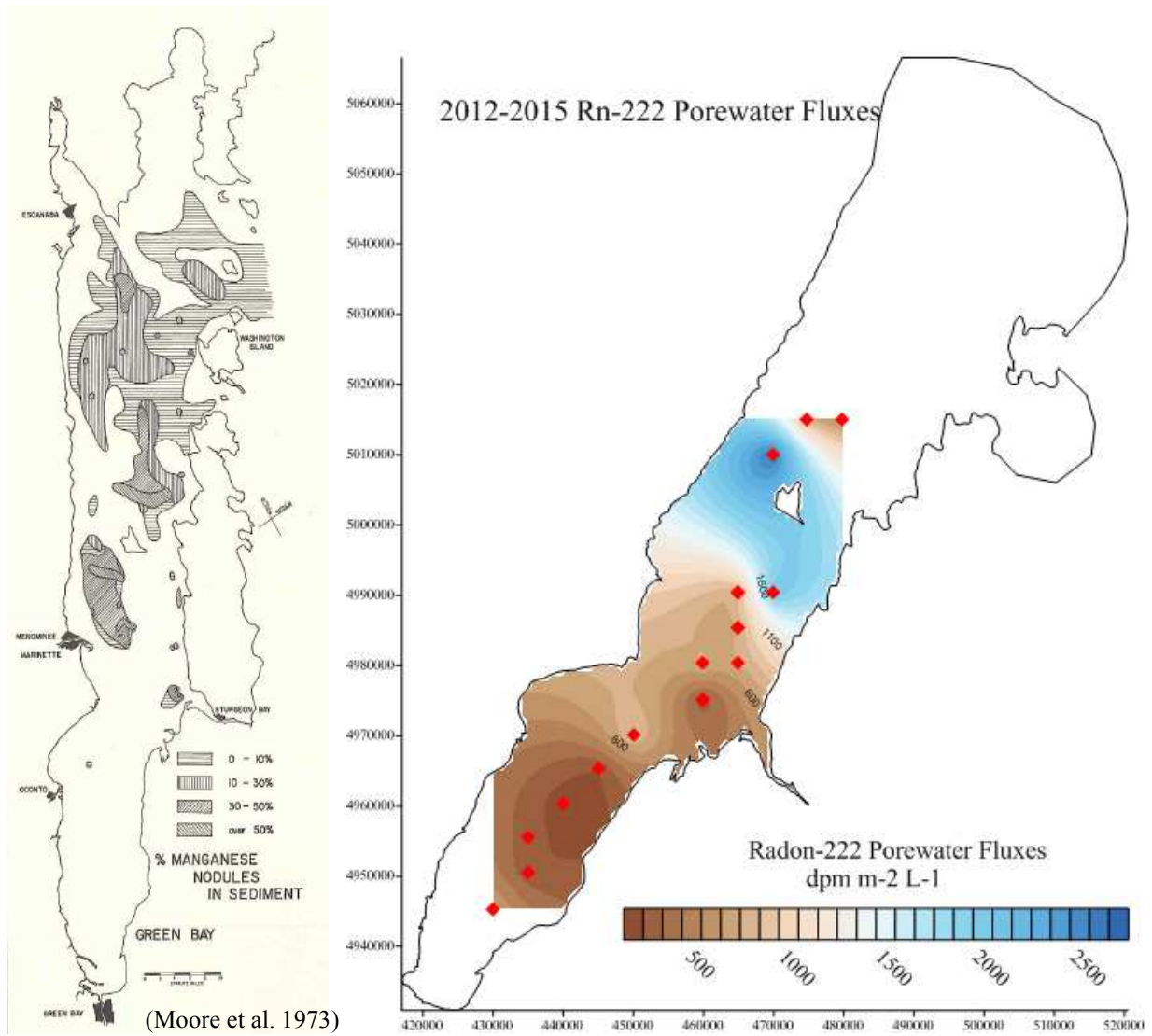
Methane porewater measurements for southern Green Bay were made by Bucholz et al. (1995). The average J_{PW} for all porewater methane profiles was 5.75×10^5 nmol CH_4 m^{-2} d^{-1} (Klump et al. 2009). A more specific lower-bay J_{PW-CH4} value from GB17 is 2.5×10^5 nmol m^{-2} d^{-1}. CH_4 porewater fluxes decrease away from the Fox River (Klump et al. 2009), although there is much less spatial coverage so there is more uncertainty than with radon-222 fluxes. The measured decrease with increasing distance from the Fox River is likely due to decreased organic matter present in the sediment (Klump et al. 2009, 1997) resulting in less anaerobic bacterial activity to produce CH_4 (Manahan 2010).

Water column Rn and CH$_4$

Since 2005, there have been ~70 discrete samples of ^{222}Rn collected as either a single bottom water samples or as part of a full water column profile. All data was corrected for the ^{226}Ra supported values. Over the course of our study the supported ^{222}Rn activity was 0.097 ± 0.033 dpm L^{-1} (n=6), with the exception of one supported value measured in the northern bay (GB79) that was 0.154 dpm L^{-1}. Therefore, 0.097 was used at all of the sites south of GB79 and 0.154 was applied to sites north of GB79.

The bottom water activities and hypolimnetic inventories are the most relevant in determining hypolimnetic advective flow. ^{222}Rn bottom water activities are highest in the mid to upper bay (Fig. 40). The activities of bottom water samples collected since 2011 range from 506 to 1.67×10^4 dpm m^{-3} with an average of 3940 dpm m^{-3}. The hypolimnetic inventories (I_{hypo}) for all sites averaged $2.16 \times 10^4 \pm 2.3 \times 10^4$ dpm m^{-2} (n=32), with a range of 1160 to 8.79×10^4 dpm m^{-2}. Similar to the distribution of ^{222}Rn benthic fluxes, the highest water column ^{222}Rn hypolimnetic inventories (Fig. 41) were found in deeper waters north of the Sturgeon Bay inlet (Table 18).

138

Table 18: Measured bottom water (BW) activities (dpm m^{-3}) and hypolimnetic inventories (I$_{hypo}$; dpm m^{-2}) of 222Rn at a series of stations in Green Bay during 2011-2013. Hypolimnetic flux (dpm m^{-2} d^{-1}) is calculated as Flux$_{hypo}$ = I$_{hypo}$*λ. Depth (m) corresponds to sample depth of the BW and hypolimnetic thickness (m) was determined from thermal profiles. If the thickness was less than 1, a value of 1 was used.

Site	Date	Depth (m)	BW Activity (dpm m^{-3})	Hypolimnion Thickness (m)	I$_{hypo}$ (dpm m^{-2})	Flux$_{hypo}$ (dpm m^{-2} d^{-1})
9	7/30/2013	9	16678	1	8340	1520
9	8/27/2014	9	4284	1	2140	390
12-13	8/28/2014	10.5	2504	1	1250	228
13	8/27/2013	11	1164	2	1160	212
16	8/28/2014	12	3574	1	1790	325
17	8/27/2013	13	1001	6	4280	779
17	7/21/2014	13	3034	3	7165	1305
26	7/22/2014	22	994	6	4640	845
31	7/21/2011	24	1034	8	5470	995
31	9/9/2011	23.8	945	3.8	3535	644
31	10/8/2011	24	1062	2	2140	389
31	8/1/2013	24	507	9	3025	551
31	8/26/2015	24.5	516	8.5	11350	2065
32	7/22/2014	22	754	4	1510	274
38	7/22/2014	26	4864	12	29180	5310
43	8/18/2011	31	1954	11	9230	1680
43	9/26/2013	31	4175	7	15570	2835
47	7/22/2014	29.5	5498	11.5	69400	12630
48	7/23/2014	28	7763	9	64410	11720
48	8/27/2015	31	4991	14	45740	8325
52	7/22/2014	25	4544	3	6815	1240
53	8/28/2013	28	8071	14	87935	16005
53	7/22/2014	28	6320	8	47870	8710
54	7/23/2014	22	5184	7	18140	3300
67	7/23/2014	28	3022	12	18130	3300
78	7/23/2014	22	1329	6	3985	725
79	7/30/2013	30	5022	10	50220	9140
79	7/23/2014	30	4051	16	32410	5900
80	7/23/2014	26	3647	16	29175	5310
81	7/23/2014	24	5523	9	24850	4250
83	8/28/2013	30	4456	10	28870	5255
100	7/30/2013	32	7661	12	50400	9170

Figure 40: Average bottom water 222Rn activity measured at a number of stations (black squares) around Green Bay..

Rn-222 Activity (dpm m-3)
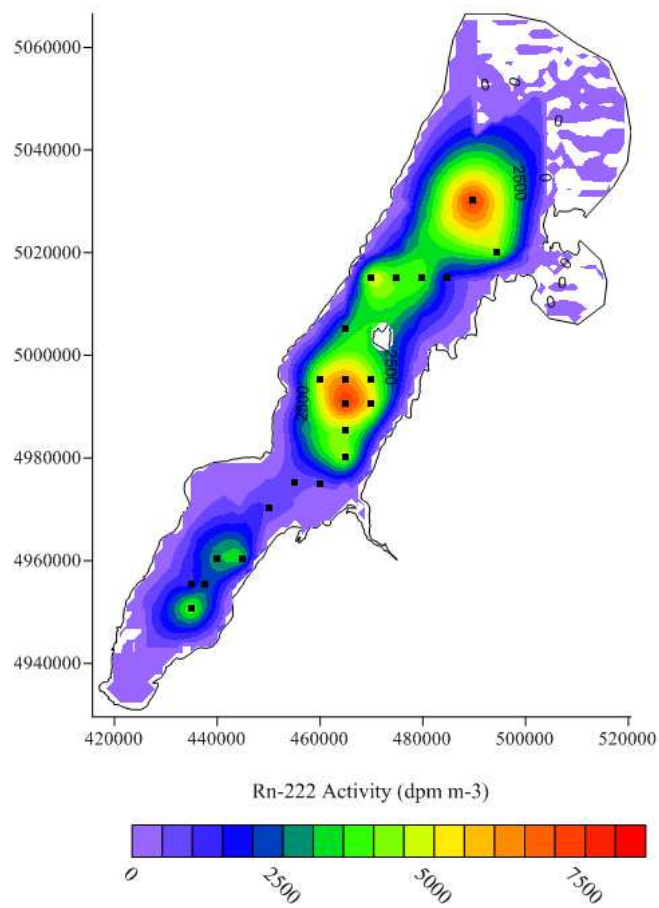
Figure 41: Hypolimnetic 222Rn inventories as a function of water depth.
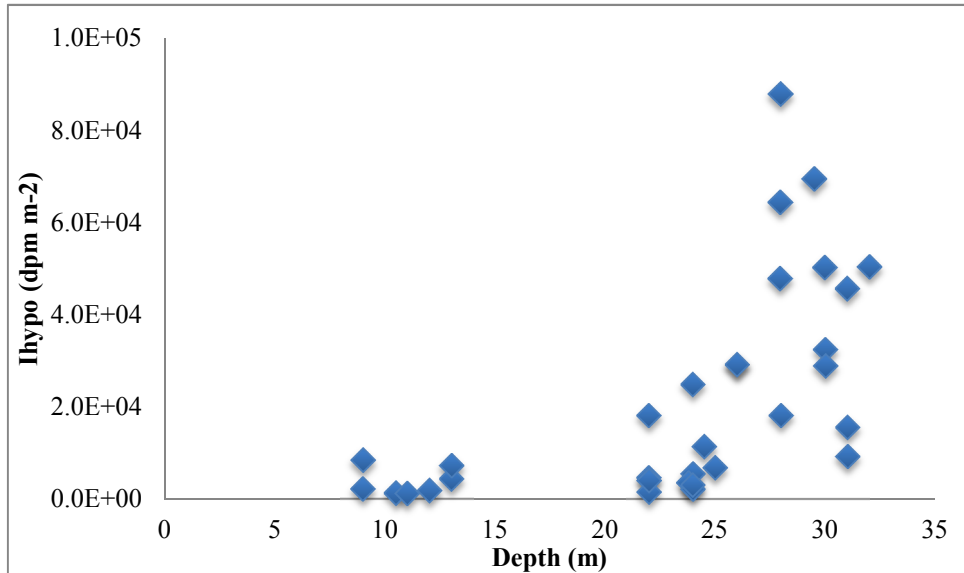
From 2013-2015 there were 62 sites sampled for water column CH_4 concentrations. The average ($\pm SD$) water column CH_4 concentration was 92 ± 127 nmol L^{-1} (n=282). Bottom water CH_4 concentrations ranged from 25 to 1209 nmol L^{-1}, with an average ($\pm SD$) of 151 ± 217 nmol L^{-1} (n=52; Table 19). Hypolimnetic CH_4 concentrations exceeded epilimnetic concentrations in the area south of GB31 (~Sturgeon Bay; Fig. 42). This is attributed to high algal production in the southern regions of Green Bay (Qualls et al. 2007), which corresponds to higher organic matter loading to the sediment and greater amounts of anaerobic respiration producing CH_4 (Sansone et al. 2004; Naqvi et al. 2010).

Excesses of hypolimnetic methane concentrations relative to epilimnetic concentrations means that methane data can be related to previously presented oxygen data (Chapter 4) through an "Apparent Methane Production" calculation, similar to the apparent oxygen utilization (AOU) calculations. It is known that as oxygen is consumed, methane is produced within the sediments. Therefore, it could be hypothesized that as O_2 concentrations decrease, CH_4 concentrations will increase. Water column concentrations can be compared because water column oxidation of

141

methane has been shown to be negligible in Green Bay (Waples, 1998 The apparent methane production term, or AMP, can be calculated as:

$$AMP = CH_{4\ Obs}^{\ BW} - CH_{4\ equil}^{\ atm} \qquad \text{(Eqn. 5.5)}$$

where CH_{4obs}^{BW} is the observed bottom water methane concentration and $CH_{4\ equil}^{atm}$ is the concentration of methane in the water that is in equilibrium with the atmosphere (60 μmol L^{-1}; Waples, 1998). An areal AMP value can also be estimated by compensating for the hypolimnetic depth, z_h, or

$$AMP_{area} = AMP * z_h \qquad \text{(Eqn. 5.6).}$$

AMP and AMP$_{area}$ results are listed in Table 19. Methane production was highest in the shallow waters (Fig. 43), which agrees with AOU results of lowest oxygen concentrations in the same region. (Fig. 25). The AMP values that are negative indicate that bottom water concentrations do not exceed the atmospheric equilibrium concentration. All of the negative AMP values were found in waters deeper than 20 meters. When the hypolimnetic thickness was considered, the methane production did not follow a strong trend (Fig. 44). The values that are greater than zero tend to be evenly distributed throughout different water depths.

Determining advective flow

One of the goals of the water column ^{222}Rn and CH$_4$ analysis was to evaluate the usefulness of these naturally occurring species as tracers for advective flow, either together or separately. ^{222}Rn and CH$_4$ have been used as tracers in several studies

Table 19: CH$_4$ bottom water concentrations of samples collected in Green Bay from 2013-2015 and apparent methane production values based on Eqns.5.5 and 5.6.

Site	Date	Depth (meters)	CH4 (μmol m^{-3})	AMP (μmol m^{-3})	Hypo Thickness (m)	AMP$_{areal}$ (μmol m^{-2})
5	Jul 2014	6	81.4	21	0.5	11
6	Aug 2013	6	213.6	154	1	154
8	Jul 2014	7	113.7	54	1	54
8	Aug 2014	7.5	143.7	84	0.1	8
9	Aug 2014	9	469.9	410	0.4	164
10	Aug 2014	8	1073.0	1013	0.6	608
12	Aug 2013	10.5	172.4	112	2.7	303
12	Aug 2014	10.5	213.0	153	1	153
13	Aug 2013	11	220.4	160	2.8	449
13	Aug 2014	10.5	154.9	95	1	95
16	Aug 2014	12	208.7	149	1	149
17	Aug 2013	13	148.3	88	1.5	133
17	Aug 2014	13	322.5	262	6	1575
17	Aug 2014	12.5	170.9	111	1.5	166
21	Aug 2014	15	85.2	25	1.5	38
21	Aug 2015	16	102.3	42	2.6	110
26	Jul 2013	21	187.7	128	2.6	332
26	Aug 2013	21	108.9	49	4	195
26	Aug 2013	21	187.7	128	11.3	1443
26	Jul 2014	21	109.6	50	7.5	372
26	Aug 2014	22	122.2	62	7.6	472
30	Aug 2014	19.5	92.2	32	3.4	109
31	Jul 2013	24	152.6	93	9	834
31	Aug 2013	24	75.6	16	14	218
31	Aug 2015	24	34.8	-25	11	-277
32	Aug 2014	22	213.0	153	2	306
38	Jul 2014	26	54.2	-6	14	-81
38	Aug 2014	27.5	84.4	24	6	146
39	Aug 2014	27.5	42.6	-17	6.5	-113
42	Aug 2014	31	140.4	80	9.5	764
43	Jul 2013	31	55.5	-5	10	-45
43	Aug 2013	31	32.8	-27	16	-435
43	Sep 2013	31	102.5	42	11	467
43	Aug 2014	31.5	85.9	26	7.2	187
44	Aug 2014	28	76.2	16	6.6	107
47	Jul 2014	29	82.4	22	10	224
47	Aug 2014	29.5	96.4	36	6.8	248
48	Aug 2015	31	24.7	-35	10	-353
52	Jul 2014	25	60.1	0	4	0
53	Jul 2013	29	39.1	-21	14	-292
53	Aug 2013	28	49.9	-10	15	-151
53	Jul 2014	28	48.6	-11	12	-137
67	Jul 2013	29	38.4	-22	14	-302
67	Aug 2013	29	41.2	-19	14	-263
77	Jul 2014	28	54.6	-5	14	-75

143

78	Jul 2014	22	53.9	-6	10	-61
79	Jul 2013	30.5	33.8	-26	13	-341
80	Aug 2013	32	46.5	-13	14.5	-195
80	Jul 2014	26	66.7	7	17	114
83	Aug 2013	30	28.0	-32	13	-416
100	Jul 2013	32	26.9	-33	13.5	-447
CN	Aug 2014	10.5	1208.5	1149	1.3	1493

Figure 42: Bottom water methane concentrations in Green Bay during July and August 2013-14.
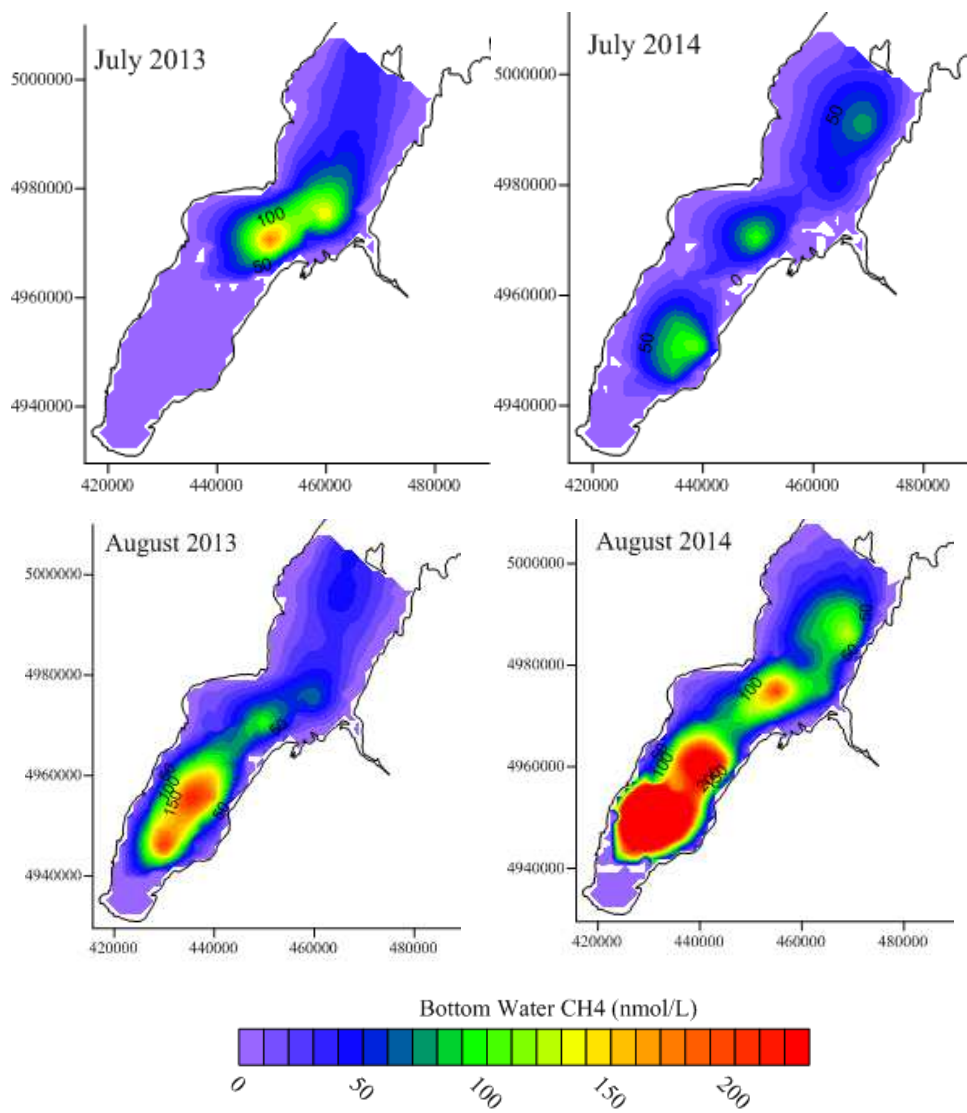
Figure 43: Apparent methane production values at different depths in Green Bay calculated using Eqn. 5.5.
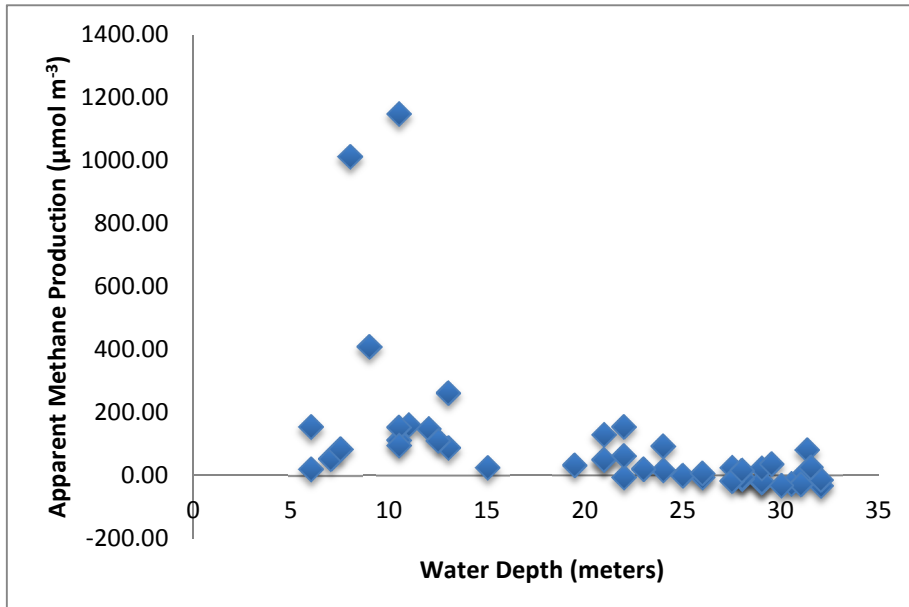
Figure 44: Areal apparent methane production values, calculated using Eqn. 5.6.

145
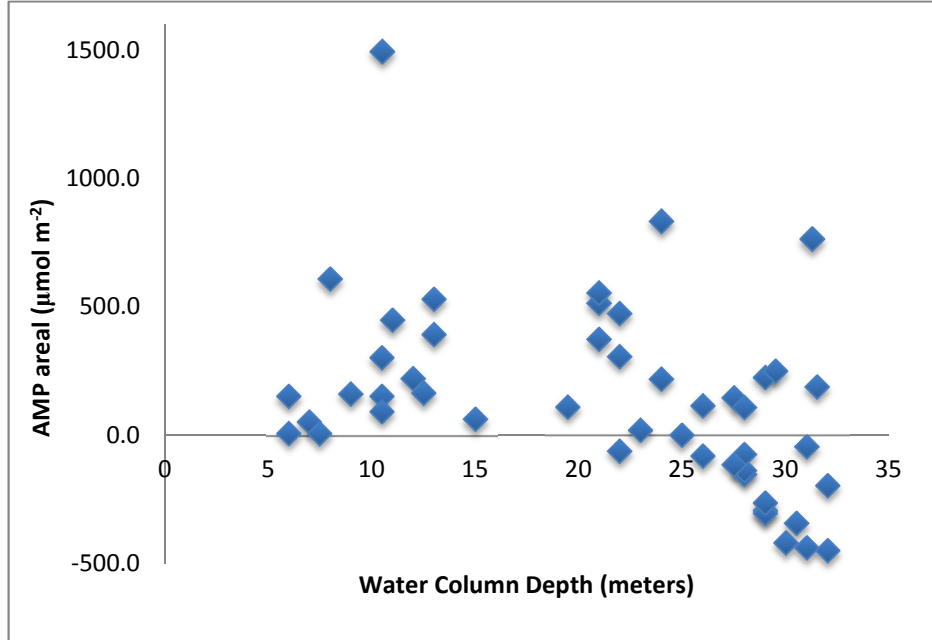
(Klump and Martens 1981; Lambert and Burnett 2003; Moya et al. 2016); however, in Green Bay we chose not to use them together due to differences in concentration maxima (Figs. 40 and 42). While both radon and methane are sourced from the sediments, through [226]Ra decay and anaerobic organic carbon remineralization respectively, their dominant sediment sources are spatially separated. This results in maximum methane concentrations found in southern Green Bay and maximum [222]Rn activities are found in northern Green Bay. [222]Rn and CH4 samples were not always taken simultaneously, so this would make it more difficult to use the two tracers together. In general, there were fewer methane samples collected than radon samples and methane porewater fluxes have not been measured in the last 5 years. For these reasons, it was preferable to evaluate the use of [222]Rn as a natural tracer for advective flow. It is recognized, though, that CH4 may also be an adequate natural tracer (assuming lack of water column respiration).

One approach to determine whether [222]Rn is a suitable natural tracer for advection was to use a box-model. A mass balance for [222]Rn in the hypolimnion can be considered as:

$$I_{hypo}\lambda = J_{PW} - J_{Thermo} + J_{In} - J_{Out}$$ (Eqn. 5.7)

where I_{hypo} is the non-supported inventory from Eqn. 5.4, λ is the decay constant, J_{Thermo} is the flux through the thermocline, and A is the product of concentration and flow, both incoming, J_{In}, and outgoing, J_{Out}. J_{Thermo} is estimated as the difference between epilimnetic and hypolimnetic activities over depth, dz, and is expressed as:

$$J_{Thermo} = \frac{dA}{dz} * k$$ (Eqn. 5.8)

146

where k is the vertical diffusion rate. The k value used here was 4.32E-4 m^2 d^{-1}, which is based on tritium tracer tests in the thermocline of two inland lakes (Quay et al. 1980). Diffusion of radon out of the hypolimnion through the thermocline is quite small (-0.03 to -0.17 dpm m^{-2} d^{-1}), so it is considered negligible.

The measured radon activity beyond what is supported by the sediments can be calculated as

$$JAdv_{hypo,ex} = I_{hypo}\lambda - J_{PW} \qquad \text{(Eqn. 5.9)}$$

where $J^{Adv}_{hypo,ex}$ is referred to as the excess radon flux from advection. This advection-supported radon can be used in a two-box model to determine what water velocities are necessary to transport "upstream" radon activities to the site in time to still be useful as a natural tracer. If the water moves too slowly, the ^{222}Rn signal will decay below detection. The two-box model is pictured in Fig. 45, where it is assumed that

$$A_{in} = A_{up}exp^{-\lambda t} \qquad \text{(Eqn. 5.10)}$$

where t is the time it takes a water mass to travel a certain distance from the "upstream" location to the site of interest. For calculation purposes, the distance is set as 10 km. Therefore, if it is assumed that incoming and outgoing velocities are the same, then Eqn. 5.7 can be solved A_{up} as

$$A_{up} = (JAdv_{hypo,ex} + A_{out})/(\frac{x}{t} * exp^{-\lambda t}) \qquad \text{(Eqn. 5.11)}.$$

Advective hypolimnetic excesses were calculated for 32 sites where bottom water inventories were available. The excesses ranged from -96 dpm m^{-2} d^{-1} to 1.5x10^4 dpm m^{-2} d^{-1}, with an average of 3225 dpm m^{-2} d^{-1} (Table 20). Three of these excess values and corresponding bottom water activities were used with a series of time values to calculate possible upstream radon activities that could provide realistic A_{in} activities for the 2nd box. For an activity to be

147

considered realistic it had to be close in magnitude to the A_{out} activity of the 2nd box, since it is likely that the activity will not decay significantly over the time it would take the water mass to transverse the box. A velocity was calculated using the 10 km distance divided by the varying time factor and plotted against results of Eqn. 5.11 in Figure 46. With the exclusion of GB9 bottom water activity in 2013, which is 2x greater than any other measured bottom water activity, the largest measured activity is ~8000 dpm m^{-3}, so the plot is constrained to 10,000 dpm m^{-3} to only show realistic activities. Upstream activities that are near the highest observed activities would require a water velocity of 2 to 10 km d^{-1} to decay to the observed bottom water activity. This range of velocities is realistic for Green Bay, especially considering that H. Bravo (UWM) has observed velocities of 1.8 km d^{-1} at GB31 (pers. comm.). This means that ^{222}Rn could be a sufficient natural tracer under natural flow conditions within short enough distances between locations.

To make a more specific comparison- consider GB38 and GB48 results from July 2014. The observed activity at GB48 on 7/22/14 was ~7760 dpm m^{-3}. At GB38, 10 km away, the bottom water activity was ~4860 dpm m^{-3} and the advective supported flux was 4625 dpm m^{-2} d^{-1}. If the incoming bottom water at GB38 was flowing from GB48, the water speed would be ~3.5 km d^{-1} based on Figure 46. This is a reasonable value and shows usefulness of ^{222}Rn as a natural tracer of advective flow.

Figure 45: Two-box model of advectively supported 222Rn in bottom waters that have activities exceeding what is supported by the sediments.
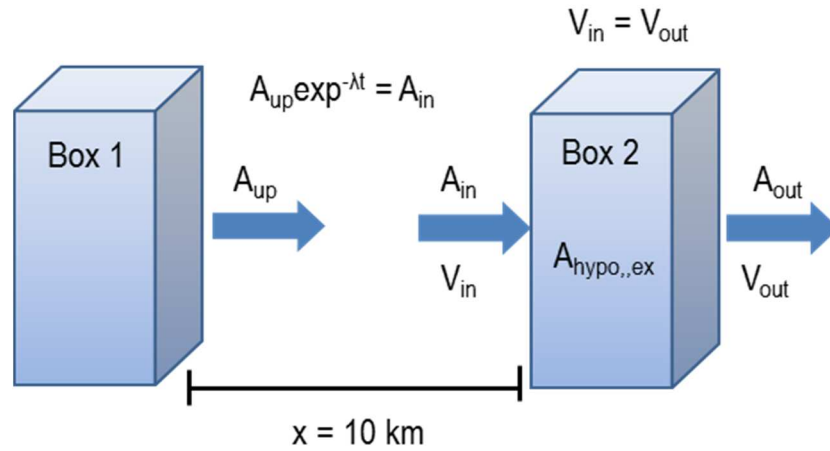
Figure 46: "Upstream" ^{222}Rn activities necessary to supply the observed "downstream" activity over varying velocities.
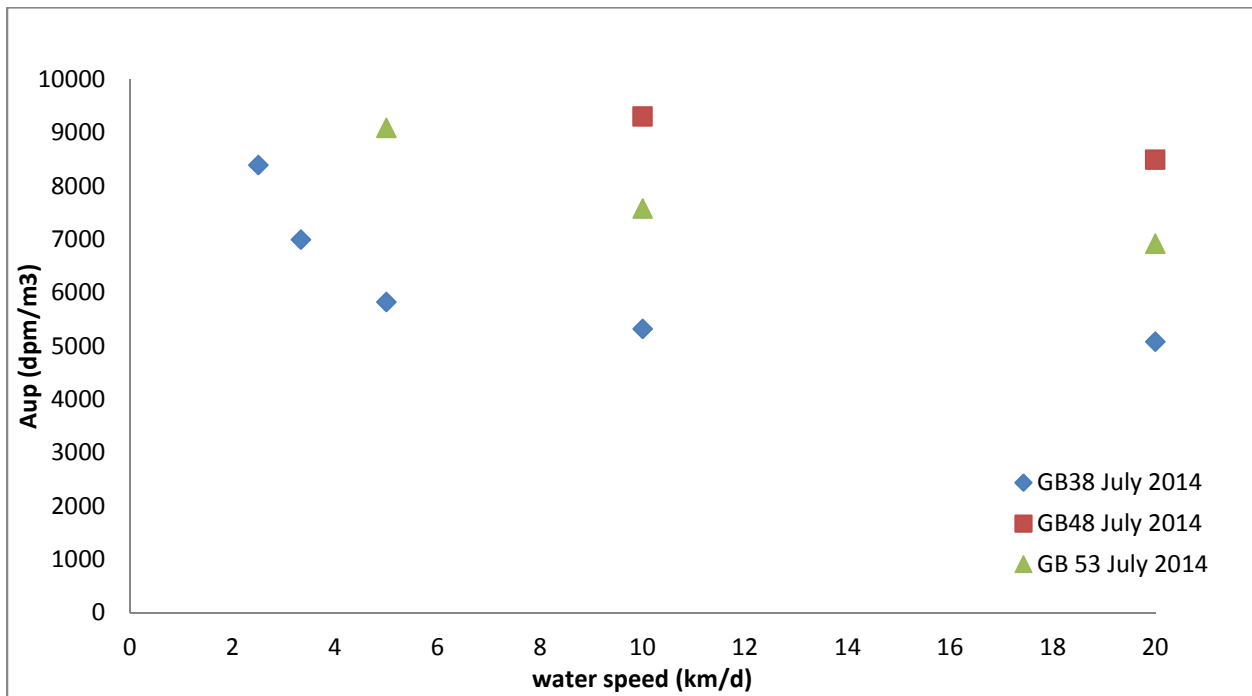
Table 20: The difference between the hypolimnetic radon flux and the porewater-supported radon is the advectively-supported excess radon. This excess can be used to estimate the necessary upstream activities that could support the observed activity (A_{obs}) at a station for a certain velocity.

Station	Date	Hypo Rn Flux $I*\lambda$ = dpm/m2/d	Jpw dpm/m2/d	Advective Hypo Excess dpm/m2/d	A_{obs} (A_{out}) dpm/m3
GB9	8/27/14	390	227	163	4283.5
GB9	7/30/13	1518	227	1290	16677.5
GB12-13	8/28/14	228	260	-32	2503.5
GB13	8/27/13	212	260	-49	1163.5
GB16	8/28/14	325	142	183	3573.5
GB17	7/21/14	1304	142	1162	3033.5
GB17	8/27/13	779	142	637	1000.5
GB26	7/22/14	845	818	27	993.5
GB31	8/1/13	551	370	180	506.5
GB31	7/21/11	995	370	625	1033.5
G-31	9/9//11	644	370	273	944.5
GB31	10/8/11	389	370	19	1061.5
GB31	8/26/15	2066	370	1696	515.5
GB32	7/22/14	274	370	-96	753.5
GB38	7/22/14	5311	686	4625	4863.5
GB43	9/26/13	2834	1122	1712	4174.5
GB43	8/18/11	1680	1122	558	1953.5
GB47	7/22/14	12631	1973	10658	5497.5
GB48	7/23/14	11723	835	10888	7762.8
GB48	8/27/15	8325	835	7490	4990.5
GB52	7/22/14	1240	1119	121	4543.5
GB53	7/22/14	8713	1119	7594	6319.5
GB53	8/28/13	16004	1119	14885	8070.5
GB54	7/23/14	3302	1119	2183	5183.5
GB67	7/23/14	3299	2546	754	3021.5
Gb78	7/23/14	725	519	206	1328.5
GB79	7/23/14	5898	519	5379	4051
GB79	7/30/13	9140	519	8621	5022
GB80	7/23/14	5310	704	4606	3647
GB81	7/23/14	4523	704	3819	5523
GB83	8/28/13	5254	704	4550	4456
GB100	7/30/13	9173	704	8470	7661

5.4 Conclusions

Three natural tracers were used in Green Bay to evaluate horizontal and vertical transport of water masses and gases. Two-layer flow in Green Bay during stratified periods was confirmed using $D_2^{18}O$, which is a novel approach for this system, although similar to an earlier effort using conductivity (Modlin and Beeton 1970). $D_2^{18}O$ was also used to quantify the fraction of Lake Michigan water present at various locations in Green Bay. The average percentage of bottom water was 65%, with a strong gradient along the main axis.

Methane concentrations in the bottom water were greatest in the southern bay, where there is greatest amount of organic matter deposition. The concentrations ranged from 25 nmol L^{-1} at GB48 to 1208 nmol L^{-1} at Condo North (44.776°N -87.837°W), west of GB11, and could be potentially useful for future studies looking at this potent greenhouse gas. An "apparent methane production" calculation was also used to show that methane production is greatest where oxygen utilization is also the highest.

The highest ^{222}Rn activities were found in the northern bay, where manganese nodules that contain elevated levels of ^{226}Ra have accumulated (or formed). ^{222}Rn porewater fluxes were used to estimate gas flux from the sediment. Highest fluxes were also found in the northern bay, due to the presence of manganese nodules. The porewater fluxes and hypolimnetic inventories were utilized to determine that ^{222}Rn is a useful tracer in Green Bay under natural flow conditions and observed activities. Radon can be used to estimate advective flow if enough samples are taken spatially over a small time period, such as in July 2014. This flow can then be applied to mass balances for biogeochemically important gases, such as dissolved oxygen, CO_2 and CH_4, to help constrain sources and sinks within Green Bay.

CHAPTER 6: BIOGEOCHEMICAL MODELING OF GREEN BAY

6.1 Introduction

Ecosystem modeling has become a key tool to understand the functioning of a system, help make management decisions and identify expected changes under future climate scenarios. These models are extremely diverse in their complexity, simulated processes and available outputs (e. g. Patterson et al., 1985; Scully, 2010; Zhou et al., 2014). This means there are many options available to researchers, depending on the questions they want to answer and the available empirical data.

A focus of recent studies in Green Bay, Lake Michigan has been the occurrence of seasonal hypoxia with an emphasis on developing a modeling framework that will inform management on the potential efforts needed to reduce both excess algal blooms and the resulting hypoxia, under both current and future conditions. Future climate change projections predict warmer and wetter conditions for the region (www.wicci.wisc.edu, WICCI), 2011), both of which have the potential to exacerbate seasonal oxygen depletion via extended stratification and increased nutrient runoff. The hydrodynamics within Green Bay are very dynamic (Miller and Saylor 1985; Hamidi et al. 2013, 2015) and can be strongly influenced by shifts in climate variables, such as wind fields (Waples and Klump 2002), which alters interannual circulation patterns and material trapping in the bay.

There have been a number of previous models created for Green Bay. Mortimer (1978) described the hydrodynamics within the bay with a simple horizontal flow model based on conductivity mixing of bay water that captured the general trends, but lacked in describing mixing processes and details of circulation patterns. More thorough physical models have been created to understand major nutrient dynamics, including the influence of primary production on the organic carbon budget (Auer and Canale 1986) and phosphorus exchange along the major axis of

153

Green Bay (Maccoux et al. 2013). While all of these models are still useful, there have been none that include watershed land-use changes, climate change projection scenarios and their effects on hypoxia.

The major processes required for the model include nutrient cycling, phytoplankton dynamics and sediment oxygen demand (SOD), as well as the response of these variables to loading reductions and climate change. Due to the complexity of the hydrodynamics within Green Bay and the potential for climate change to impact these dynamics, a linked hydrodynamic-biogeochemical model was also desired.

The hydrodynamic model, Environmental Fluid Dynamics Code (EFDC), is a state-of-the-art finite difference model that has the ability to simulate water and sediment dynamics in three dimensions (Tech and Place 2007). EFDC, developed in the 1980s and 1990s, is an open source model and is currently maintained with support from the USEPA. The water quality model is a modified framework from the Row-Column AESOP (RCA) model that was developed by HydroQual, Inc.as part of the "Advanced Ecological Systems Modeling Program" (AESOP) (HydroQual 2004). This modified framework is known as the "Advanced Aquatic Ecosystem Model," or A2EM. A2EM was created by LimnoTech to represent Great Lakes specific water quality components, such as sub-models for simulating bioenergetics of *Dreissenid* mussels and *Cladophora* (DePinto et al. 2009). The water quality model receives linkage files from the EFDC results (Fig. 47) and has the ability to simulate nearly 30 state variables, including dissolved oxygen, organic and inorganic nutrients and multiple algal classes (DePinto et al. 2009; Verhamme et al. 2016). There was no separate

Figure 47: The modeling framework of EFDC and A2EM used for the GBHYP ecosystem model. Sections in grey were not used in this model, although the capability is available. Figure from E. Verhamme, LimnoTech.
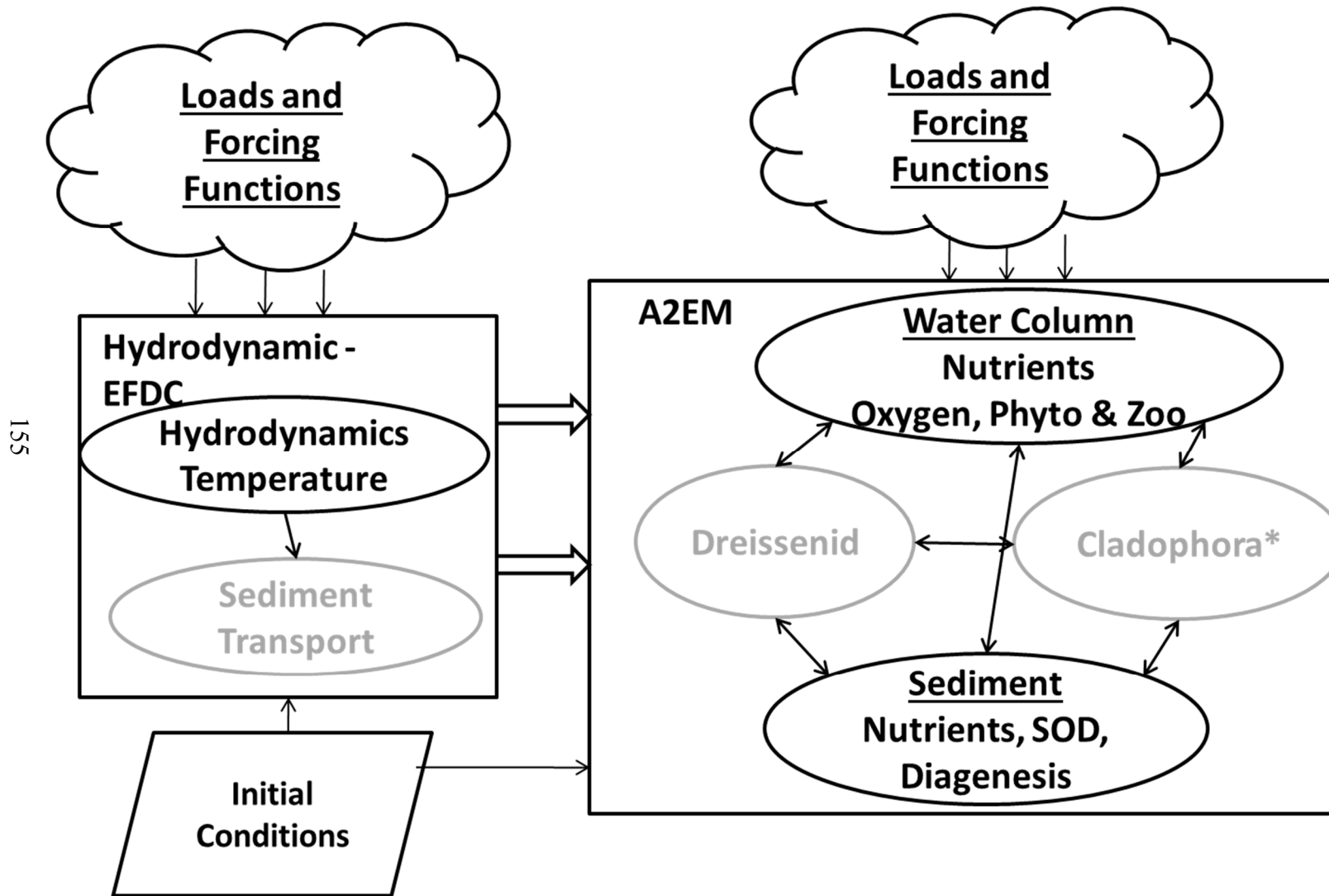
sediment-transport component to this model, although it is an additional option that will be explored in the future. EFDC-A2EM has been used in several systems around the Laurentian Great Lakes and in the Mississippi River. In Saginaw Bay, Lake Huron the model was adapted to examine the effects of Dreissenids on local nutrient cycling (Bierman et al. 2005). A more extensive project was undertaken for western Lake Erie in collaboration with the ANNEX4 working group to develop a phosphorus load-cyanobacteria response relationship to help assess what nutrient loading criteria should be implemented (Verhamme et al. 2016). Similarly, EFDC-A2EM was adapted to help the Minnesota Pollution Control Agency determine appropriate total maximum daily loads (TMDLs) for total phosphorus and chlorophyll *a* in the Upper Mississippi River and its watershed (DePinto et al. 2009).

In addition to the Green Bay EFDC-A2EM linked model, named GBHYP, a watershed model and regional climate models were used to create a more comprehensive assessment of impacts of the Fox-Wolf watershed on nutrient and sediment loading to Green Bay and how best management practices (BMPs) and climate change could affect the watershed's influence on Green Bay (Fig. 48). The SWAT model, supported by USDA, was refined for this particular system and run by Dr. Paul Baumgart. David Lorenz, Ph.D., from University of Wisconsin-Madison worked to develop a series of "downscaled" regional climate models for Green Bay based on global climate change scenarios. Lorenz provided outputs from 13 regional climate models, of which two were selected to be used in EFDC-A2EM climate change simulations for 2011 and 2012, respectively. The 4 models (i.e. watershed, climate/atmospheric, hydrodynamic and biogeochemical) are collectively known as the Green Bay Ecosystem Model (GBEM, Fig. 48).

6.2 Methods

GBHYP model development

A spatial grid for Green Bay, south of Chambers Island, was developed by H. Bravo and S. Hamidi using SeaGrid, an application for Matlab 5.2+ (woodshole.er.usgs.gov). This area was chosen because it contains the region that experiences seasonal hypoxia, is influenced by Fox River water, and the Chambers Island transect represents a natural divide between northern and southern Green Bay. In the horizontal direction, the grid transitioned from a cell size of 200 meters at the southern-most end of the bay to 2 km at the northern boundary for a total of 4006 cells (Fig. 49). A fine grid in the southern end was required to adequately capture the hydrodynamics of the Fox River interacting with Long Tail Point and the newly reconstructed Cat Island Chain. The outer edge boundary of the model domain was drawn from northwest to southeast, crossing through Chambers Island. Four main tributaries to Green Bay also had open cells to allow for exchange. These rivers include the Fox, Oconto, Peshtigo, and Menominee Rivers.

The vertical grid was created using a "generalized vertical coordinate" system, which allows for a variable number of vertical layers across the horizontal grid locations (Tech and Place 2007). The number of layers in a given cell correspond to the depth at that particular location. If a location was less than or equal to 10 meters deep then the number of layers in that cell corresponded to the whole number depth so each layer represented 1 meter, with the depth rounded down (i.e. 7.6 m received 7 layers). If the location was deeper than 10 meters, the

157

Figure 48: The integrated model framework and process that was followed (generally) for the Green Bay Ecosystem Model.
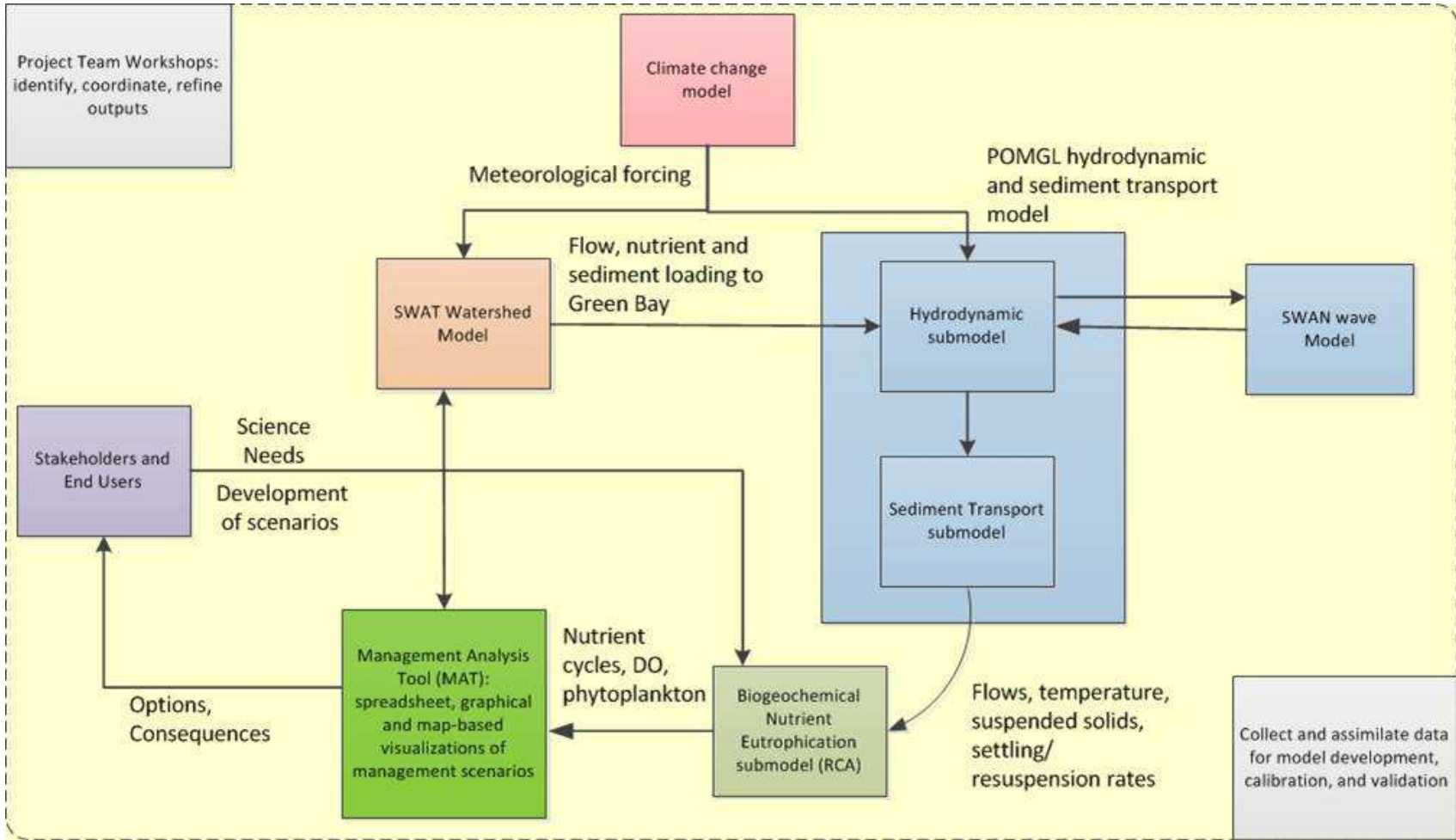
number of layers remained equal to 10, but the representative thickness increased. For example, one layer at a 20-meter deep site would represent 2 meters.

Model Inputs

The selected simulation years for the baseline model were 2011, 2012 and 2013. Each experienced different physical conditions in terms of temperature, precipitation and river discharge (Table 21) and were well monitored. Initial conditions for EFDC and A2EM were created. EFDC input files were primarily created by Dr. Sajad Hamidi and are briefly discussed here and throughout this chapter. Initial water temperatures within Green Bay were set at 4 degrees C, since this system fully mixes every fall and freezes over every winter. EFDC boundary conditions for the outer edge of Green Bay near Chambers Island were adapted from a nested Green Bay FORTRAN model that Hamidi et al. (2012, 2013) had previously developed. The nested model was created by running the Princeton Ocean Model for Great Lakes (POMGL; Schwab and Bedford, 1994) and using that output at the Green Bay-Lake Michigan border as a boundary condition for the Green Bay-nested model. Temperature and flow outputs from the Green Bay FORTRAN model were converted and used as the boundary condition files (tser.inp and qser.inp, respectively) at the Chambers Island boundary. The temperature and flow boundary conditions for the tributaries were obtained from USGS daily gauge data on each of the rivers. Meteorological inputs, such as wind and atmospheric pressure (wser.inp, pser.inp), were built from data collected at 11 land based meteorological stations around Lake Michigan and converted to over-water values (Sajad Hamidi, personal communication), although during periods that Green Bay was iced over the wind speed over the water was set to 0 m s^{-1}.

Table 21: Weather conditions for the years of model development. Precipitation and temperature data was collected from the National Climate Data Center (ncdc.noaa.gov) station at Green Bay Austin Straubel International Airport. Discharge data is from the USGS gauge "Fox River at Oil Tank Depot at Green Bay, WI."

	March-May Total Precip. mm	June-Sep. Total Precip. mm	June-Sept. Mean Temp. degrees C	March-May Avg. Discharge Cfs	June-Sept. Avg. Discharge cfs
2011	308	424	19.25	11450	4715
2012	204	317	20.233	7520	1715
2013	231	333	19.15	9350	3815

160

All A2EM input files, including the initial and boundary conditions were prepared as part of this phase of the modeling effort. Initial conditions for the water column parameters within A2EM were based on the earliest grab sample data collected from Green Bay, which occurred on 5-8-2013 by GBMSD. Sediment conditions, including nutrient concentrations and porosity values, were converted from extensive work by Klump et al. (1997, 2009) on a 5 km x 5 km grid to model inputs for the 4006 cells. Briefly, major nutrient classes considered were total and organic carbon, total nitrogen and total phosphorus. Site-specific nutrient concentrations were kriged in ArcMap (ArcGIS 10, Esri, Redlands, CA), then extracted to the GBHYP model grid locations. The nutrient concentrations were divided into 3 reactivity classes- G1, G2 and G3, with G1 being most labile and G3 being most refractory.

Boundary conditions for the tributaries in A2EM were created from USGS river gauge data and GBMSD monitoring data. Fox River data from USGS Water Quality Program at site USGS 040851385 was available for 2011-13 in approximately weekly intervals. GBMSD measurements were made at 3 sites in the Fox River (i.e. stations 7, 13 and 16), so these data were averaged together for one Fox River value for each ~weekly sampling period. All data was converted to have consistent units (e.g. SRP in mg/L as P) then interpolated to daily values. Additionally, the first sample of the year was applied to every day prior in that calendar year and the last sample collected was applied to every remaining day in that calendar year. GBMSD effluent data was also added to the model domain at the Fox River boundary cell as a point source of TSS and TP.

Boundary conditions for the other tributaries in the model domain (i.e. the Peshtigo, Oconto and Menomonie Rivers) were created from historical USGS monitoring data, despite there not being samples taken from each river during the model period (201-13). The Menominee River was the

only river sampled over the model period (2011-2015), although it was also sampled in 1993-95 and 2003. The Peshtigo River was sampled in 1991-94, 2003 and 2008 and the Oconto was only sampled in 2008-09. Based on knowledge of minimal land use and land cover changes within the watersheds since 2003, it was assumed that any changes in watershed nutrient loadings and ratios between different watersheds would be minimal. Adequate data for the boundary conditions of these three tributaries could then be obtained through a series of data manipulations. First, in 2003 the Peshtigo and Menominee Rivers had 6 shared sampling dates- once a month from May to October. From these 6 dates a series of ratios for the available were calculated (Table 22) and applied to available 2011-13 Menominee River data to essentially convert it to Peshtigo River data. The Oconto and Peshtigo Rivers shared 5 sampling dates in 2008- June, August, September, November and December. Similarly, ratios were calculated for the available parameters and then used on the Peshtigo River data (converted from Menominee River data) to convert it to Oconto River data. For consistency with the model input requirements- orthophosphate values from the USGS were used as SRP and specific conductivity was used as a surrogate for chloride. There was no TKN data available for comparisons between tributaries, therefore, it was assumed that nitrate and TKN acted similarly.

Boundary condition data for the Lake Michigan boundary was taken from GBMSD monitoring efforts. At station GBMSD75 (GridNo = 3558) there were bi-weekly samples taken during summer months in a suite of parameters that was not available elsewhere. Concentrations at GBMSD75 were presumed to be similar enough to the conditions near Chambers Island, although it is recognized that this is not ideal. Surface samples were used in the epilimnion and bottom samples were applied to the hypolimnion. These values were then interpolated to daily concentrations.

162

Previous modeling parameters from a recent Western Lake Erie model (Verhamme et al. 2016) were initially applied as the coefficients in this model. A series of ratios were used to simulate 29 commonly measured state variables computed by the model. The most commonly measured parameters include suspended solids (SS), total phosphorus (TP), soluble reactive phosphorus (SRP), nitrate and nitrite (NO23), total Kjeldahl nitrogen (TKN) and chloride. The ratios for the major conversions are given in Table 23. Several other model coefficients were also used from Verhamme et al. 2016. The phosphorus cycle and its components are presented in Figure 50. A selection of phytoplankton coefficients from the L_Constants database are given in Table 24 as an example. Additional nutrient and phytoplankton cycles and suggested parameter values are available in HydroQual (2004), but are not presented here. They are discussed at depth in several LimnoTech reports, as well as Verhamme et al. 2016.

Figure 49: The EFDC/A2EM model grid for GBHYP, with boundaries and tributaries marked. Base figure from E. Verhamme, LimnoTech.
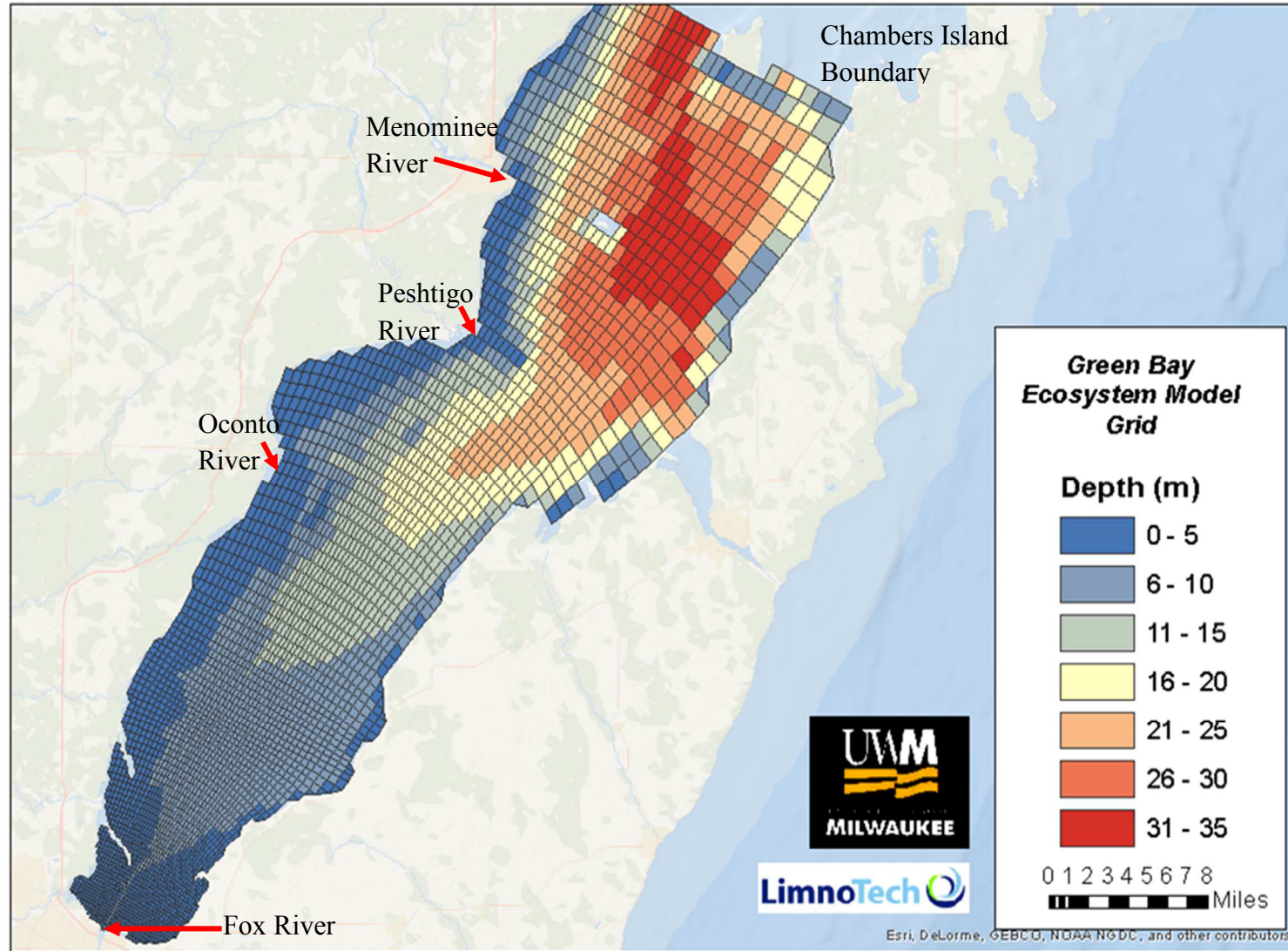
Figure 50: A box model diagram of the phosphorus nutrient dynamics ran in GBHYP. The colored arrows track algal growth (green) and death (red). Figure from E. Verhamme, LimnoTech.
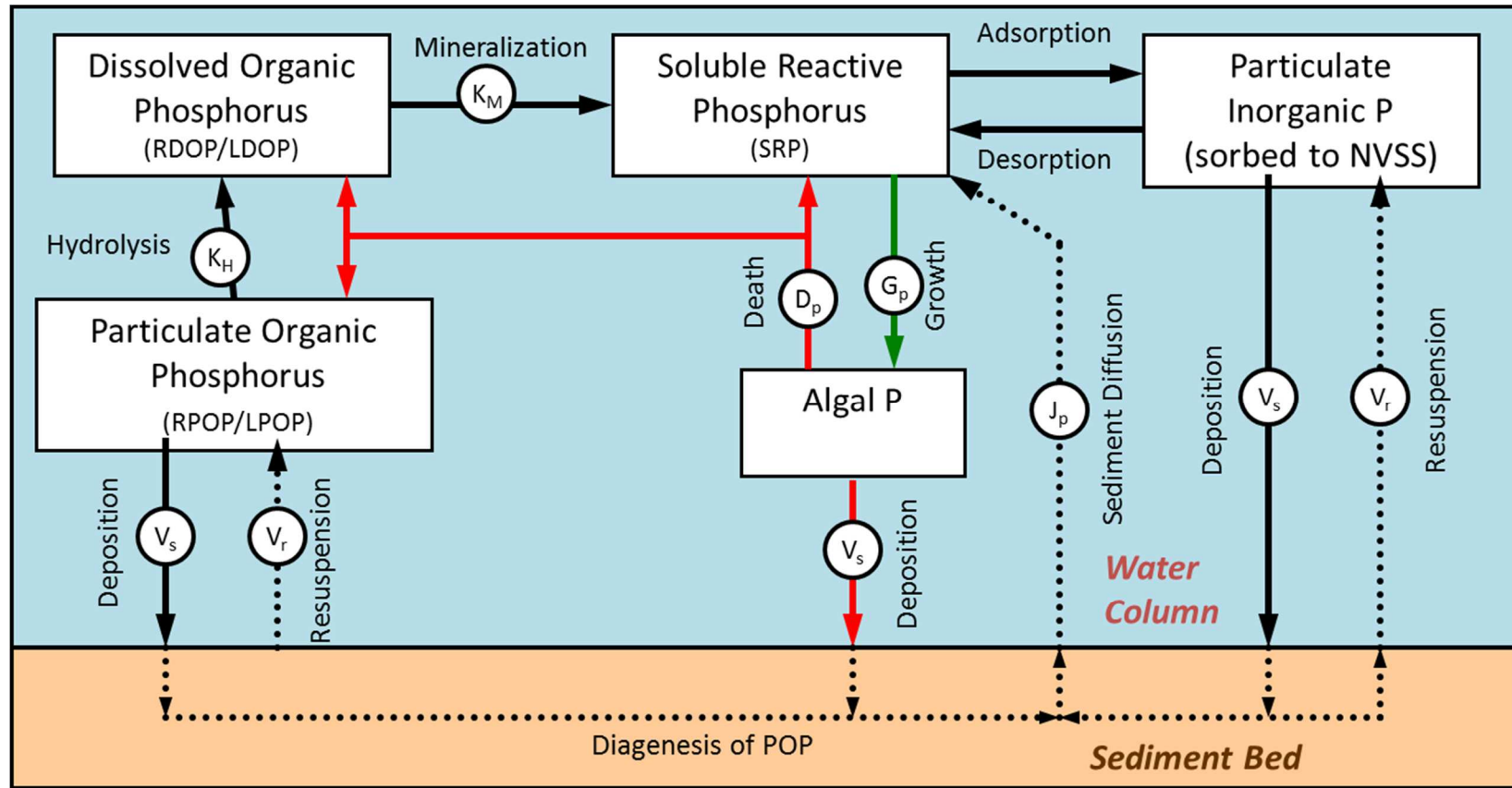
Table 22: Conversion values used for the Menominee (M), Peshtigo (P) and Oconto (O) rivers to create boundary condition data. The ratios are based on USGS monitoring data from the same dates. A value in italics indicates that no data was available for this time period because it was typically during the winter months, so a value of 1 was applied to represent similar activity across all watersheds.

Rivers	Parameter	Average Ratio	Ratio SD	Months Applied
P:M	NO23, TKN	20.1	11.7	Aug - Oct
		2.4	2.7	May - July
		1		Nov - Apr
	TP, SRP	0.64	0.3	All
	SpCond/Cl	1.9	0.2	All
	TSS	0.63	0.3	All
O:P	NO23, TKN	0.26	0.2	May-Sept
		4.6	2.7	Oct-Dec
		1		Jan-Apr
	TP	1.6	0.6	May-Aug
		0.57	0.2	Sept-Dec
		1		Jan-Apr
	SRP	1.03	0.7	May-Dec
		1		Jan-Apr
	Cl	1.1	0.2	May-Dec
		1		Jan-Apr
	TSS	*1*		All

166

Table 23: Factors used to transform measured parameters into model input variables, given as both acronyms and spelled out.

Variables affected	Variables affected	Value	Units
NH$_4$	Ammonium	0.01	mg L^{-1}
POC:SS	Particulate organic carbon: suspended solids	0.1	Ratio
DKN:TKN	Dissolved Kjedhal nitrogen	0.75	Ratio
PKN:TKN	Particulate Kjedhal nitrogen	0.2	Ratio
DOC	Dissolved organic carbon	5	mg L^{-1}
SIT		3	mg L^{-1}
TOP	Total Organic Phosphorus		
= P – SRP			
DOP:TOP	Dissolved organic phosphorus	0.5	Ratio
POP:TOP	Particulate organic phopshorus	0.5	Ratio
	Refractory: Total	0.85	Ratio
	Labile:Total	0.15	Ratio

Table 24: A selection of parameters and coefficients for different classes of phytoplankton, found in card L_Constants. ly = Langley.

	Class 1: Blue Greens	Class 2: Diatoms	Class 3: Greens
Saturating light intensity	300 ly/day	150 ly/day	150 ly/day
Base settling rate	-0.5 m/day	0.25 m/day	0.1 m/day
Nutrient stressed settling rate	-0.1 m/day	0.1 m/day	0.05 m/day

A2EM Corroboration

Data for model corroboration was obtained from a number of *in-situ* water quality monitoring programs including those maintained by GBMSD, University of Wisconsin-Milwaukee (UWM), University of Wisconsin- Green Bay, and USGS (Table 25). GBMSD and UWM have the most extensive datasets, both in terms of spatial extent and number of samples. For this reason, the data was split into two groups- one for model development and one for model testing, in accordance with the "Hold out method" for calibration (Bennett et al. 2013), or in this case- corroboration. The observations were assigned a parameter number that corresponded with the applicable ParamterID. For example, dissolved oxygen concentrations were assigned a parameter number of 2, which corresponds to the dissolved oxygen ParameterID.

Model validation was done according to methods used by Verhamme et al. (2016) with recommendations from Bennett et al. (2013). The model output was visually compared with measurements made at different locations within the bay. The model performance for three state variables was statistically quantified using linear regression to calculate the coefficient of determination, or r^2, using

$$r^2 = SS_{regression}/SS_{total} \qquad \text{(Eqn. 6.1)}$$

where $SS_{regression}$ is the sum of squares for regression and SS_{total} is the total sum of squares (Whitlock and Schluter 2009). This is one of the simplest methods to determine whether the model produces results that agree with observational data (Bennett et al. 2013).

It should be noted that this iteration of the model is not the final version, but rather a beta version. The A2EM model coefficients were not adjusted specifically for GBHYP. Further

discussion about calibration suggestions and other possible considerations to better tune the model follows the results section.

6.3 Results

Model Calibration and Corroboration

Early runs for EFDC had trouble simulating the strong temperature gradient at the Lake Michigan boundary. This was overcome by smoothing the wind data using a running average technique. This reduced variability and allowed for adequate stratification to be captured in the model. Another problem with initial runs of EFDC was a violation of mass balance for the water-essentially the incoming and outgoing water masses from the Chambers Island boundary were not equal which resulted in large fluctuations of the water column depth. Adjustments were made to the POM model to better equalize the mass exchanges (S. Hamidi, personal communication). Dr. S. Hamidi performed model validation on the EFDC model by comparing model outputs with observations including current profiler data and temperature data from both profiles and moorings.

The final runs of EFDC were able to adequately replicate temperature data within Green Bay. Figures 51 and 52 show good correlation between daily measurements and daily model results for the summer season both in timing and magnitude of change. The strong agreement between observations and model results indicate that EFDC is well calibrated within GBHYP and is not responsible for weak comparisons present in A2EM (see below).

169

Table 25: List of all sources of data available to develop GBHYP A2EM. Sources in italics were not utilized in this model iteration. Acronyms: GBMSD= Green Bay Metropolitan Sewearage District (now NEW Water), GB = Green Bay, TP = Total Phosphorus, SRP = Soluble Reactive Phosphorus (also Ortho-Phosphate), TKN = Total Kjedahl Nitrogen, TSS = Total Suspended Solids, TS= Total Solids, VS = Volatile Solids.

Source, Parameters	Location(s)	Sampling Frequency	Duration/History
GBMSD: temp, DO, conductivity	Mouth of Fox River, Entrance Light Station	15 min.	Since 1988, April-October
GBMSD: TP, SRP, NO2, NO3, NH4, TKN, TSS, TS, VS, Turbidity, ChlA, DO, Temp, Secchi	2 depths @ 4 Fox River sites, 12 lower GB, 6 mid GB	~Weekly	1986-Present, April – October
UWM: temp (profile and mooring), DO (profile and mooring), conductivity, turbidity	Many locations on 5x5km sampling grid	~Monthly	2010-2015, May-October
UWM-GLOS Buoy, air temp, relative humidity, air pressure, wind speed and direction, wave height, surface water temp, turbidity, DO, pH	GB-17	30 min.	2012-present
USGS, Discharge, water temp, TP, SRP, NO2, NO3	Mouth of Fox River, Oconto, Peshtigo and Menominee Rivers	Instantaneous	~1950's to present
GBMSD, Phytoplankton abundance and type	6-8 sites in Fox River, lower and mid-GB	Weekly	2011-present
WDNR/UWGB,TSS, VSS, ChlA, wave velocity, light extinction	Leeward and windward sides of Cat Island Chain	Weekly	Summer 2013

170

Figure 51: Temperature comparisons between model results (blue line) and observations (various colored points) at GB17 during 2012 (top) and 2013 (bottom).
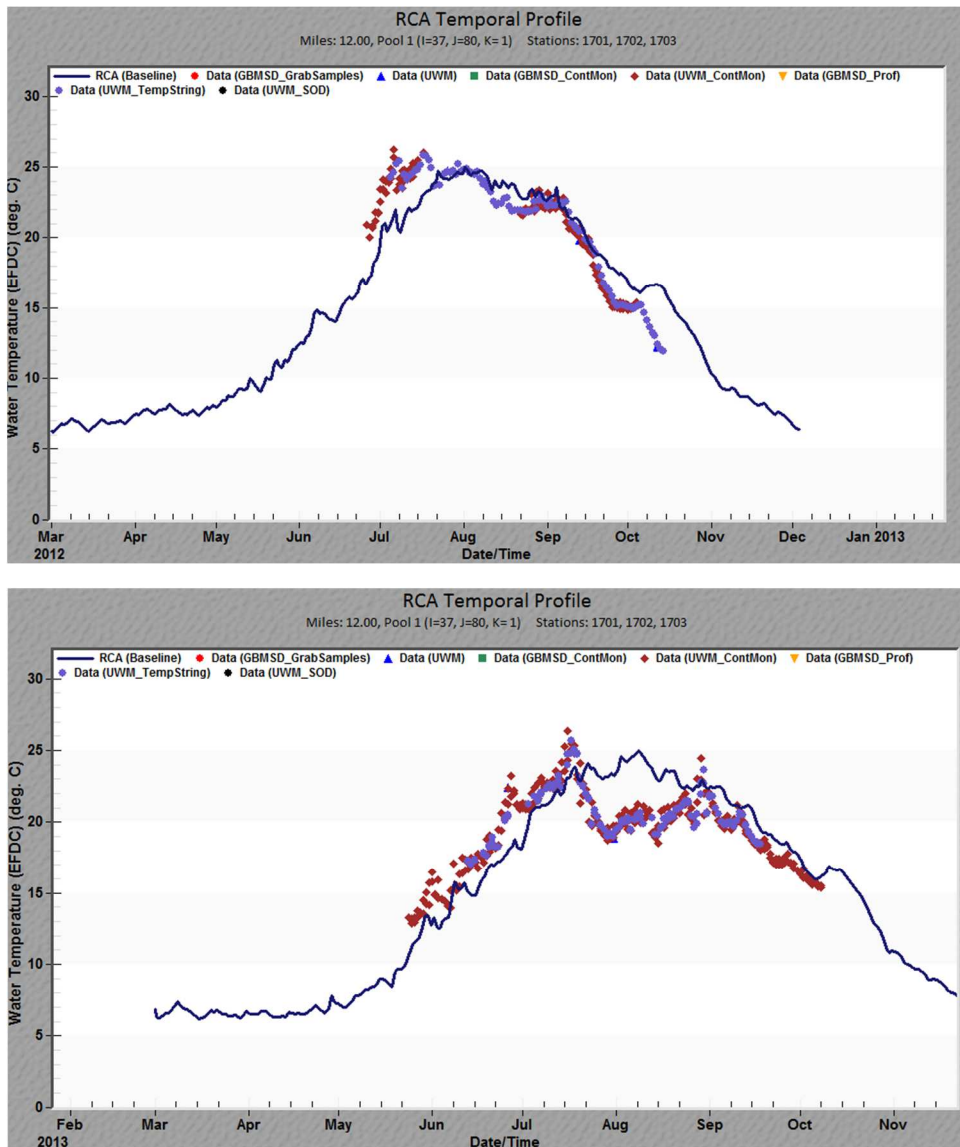
Figure 52: Temperature comparisons between model output (blue line) and observations (various colored points) at GB30 during 2011 (top) and GB38 during 2011, 2012 and 2013 (bottom).
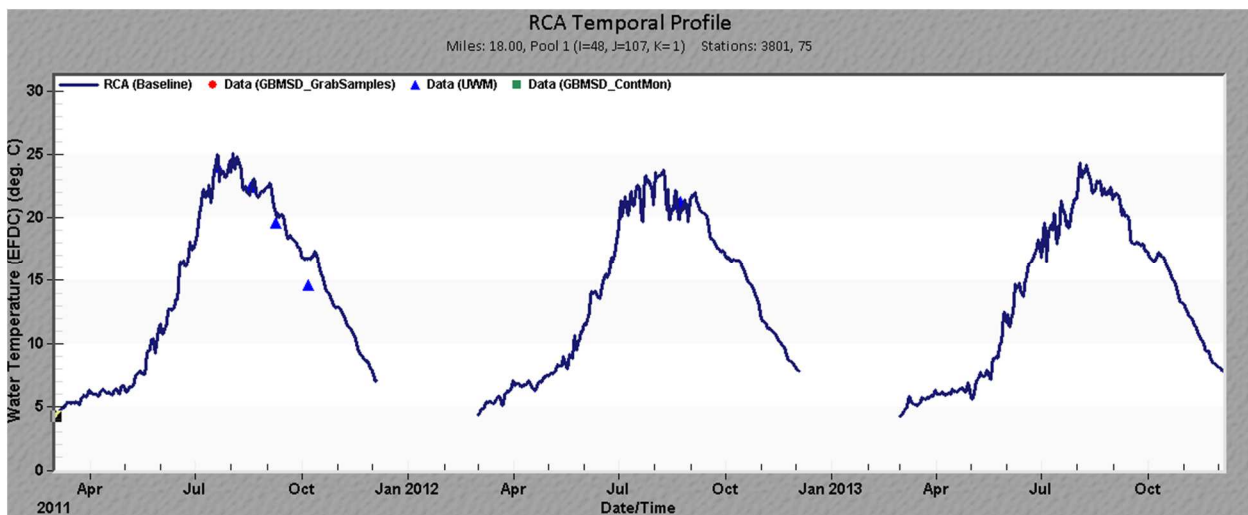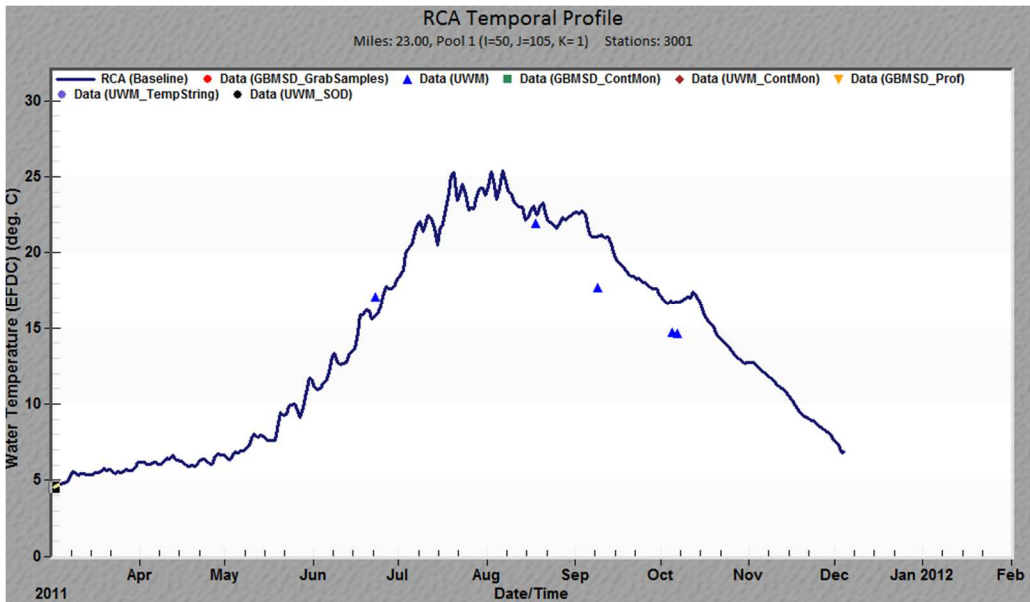
Within the A2EM framework, many adjustments had to be made to the initial model values to get successful runs. One of the largest adjustments was sediment nutrient concentrations and the division between three designations of lability- G1 to G3. Early model runs often produced excessive dissolved oxygen depletion. This was attributed to high benthic respiration, resulting from excess amounts of very labile organic matter (G1 class) in surface sediments. Alterations to the labile fraction of organic carbon were conducted by holding the total organic carbon content the same and simply changing the fraction of organic carbon that goes into the G1 class. Originally, one percent of all organic carbon was entered into the G1 class, which is the most labile. However, based on Be-7 deposition (Klump et al. unpub) it is known that some areas more rapidly acquire fresh organic matter, meaning that not all sediments should have the same fraction of G1 organic carbon. A gradient of one to three percent organic carbon was applied to sites to mimic the Be-7 map (Fig. 53).

Once the model was running TP, SRP and Chl-*a* outputs from the model were compared to measured values. First, visual comparisons were made across a gradient of stations. TP and SRP were reasonably well simulated at stations that were close to the Fox River mouth (Fig. 54a and 54b). Farther out into the open bay this "beta" version of the model failed to produce realistic concentrations in keeping with observations One possible contributing factor is the use of slow settling rates, which would result in not adequately removing the organic matter and nutrients from surface waters at rates that are observed (3-6 m d^{-1} within the hypolimnion during stratified periods, Eadie et al., 1991). Another possible error is lack of coefficient calibration in the phosphorus cycle. For example, partitioning of phosphorus between the different classes may have to be adjusted. Chl*a* was better simulated at GBMSD station 51 than phosphorus (Fig.

54c), but the model still over-predicted the variability and magnitude of concentrations, which

should be addressed in future iterations.

Figure 53: Short-term organic carbon deposition (mg C cm-2 d-1) to the sediments determined from Beryllium-7 measurements in Green Bay. Figure from V. Klump.
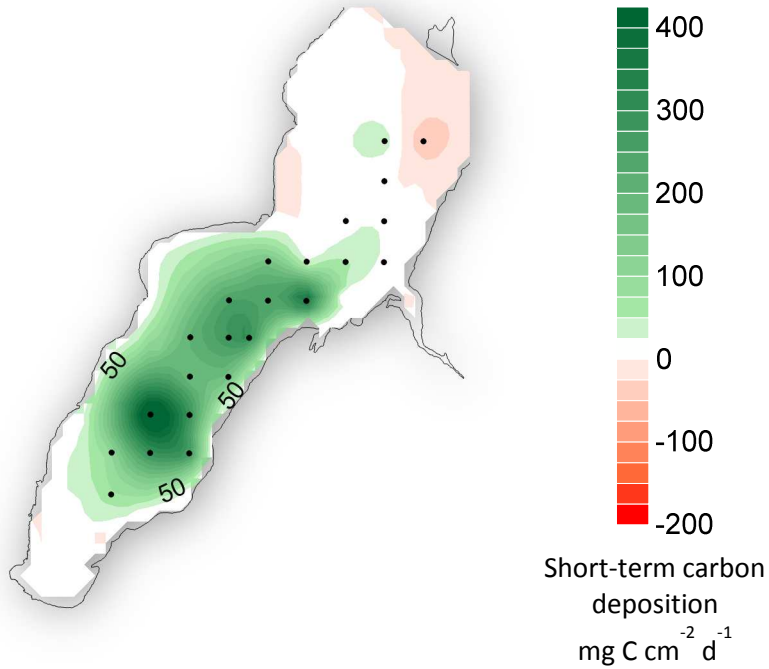
Figure 54a: Total phosphorus (mg P L^{-1}) model results (blue line) and monitoring data (red dots) for 2011-13 at station GBMSD 22.
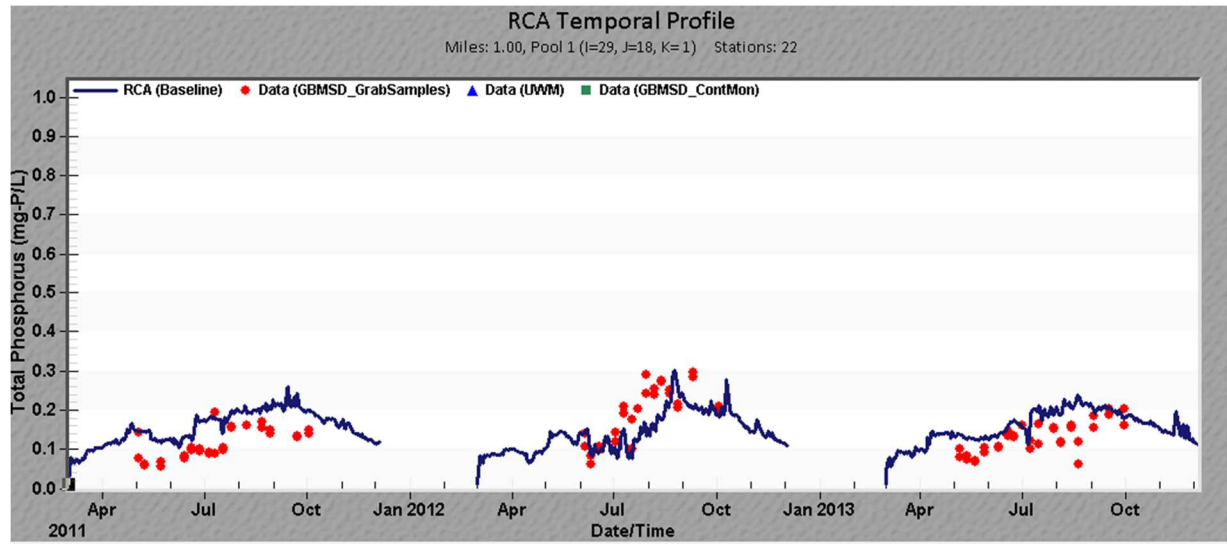
Figure 54b: The same as 54a, except for dissolved phosphorus, which is equivalent to SRP.
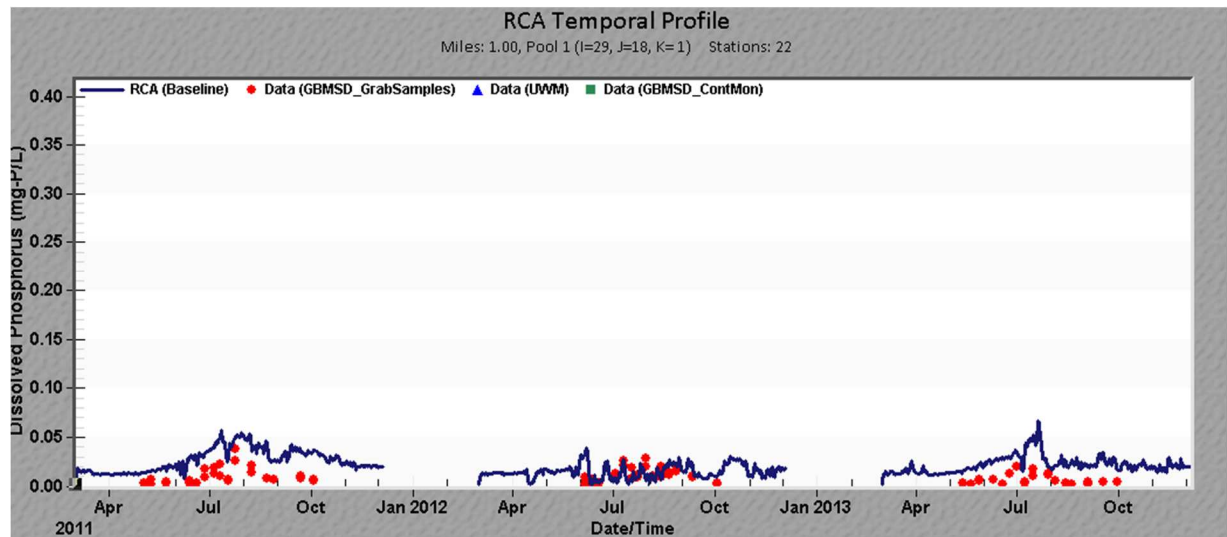
Figure 54c: The same as Figure 54a, except for chlorophyll-*a*.
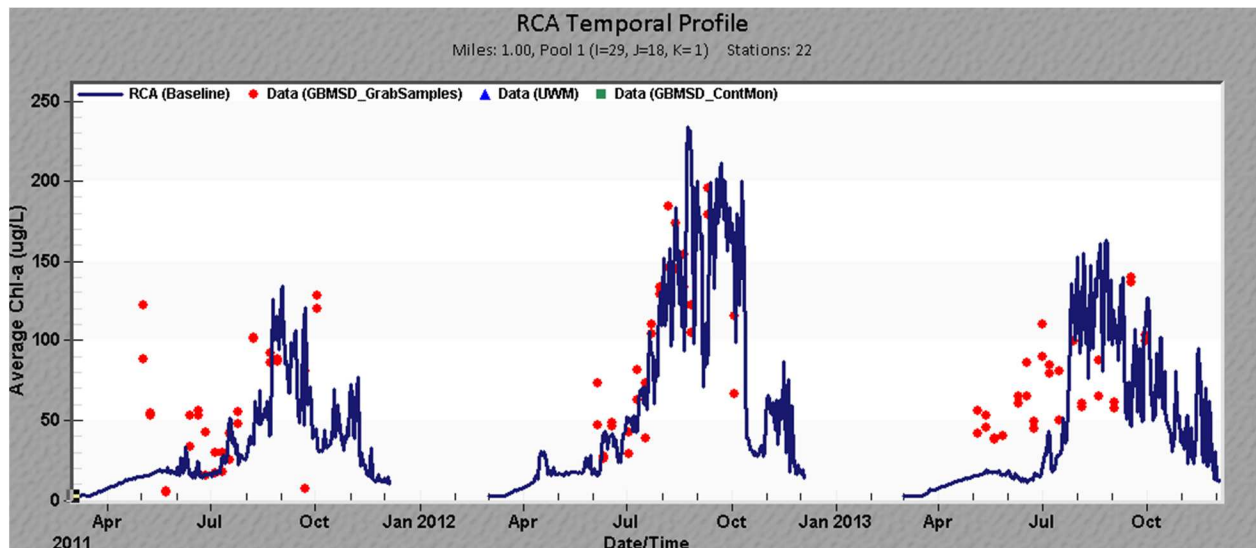
Comparisons between the means and standard deviations of the model results and observations shows that the model over predicts concentrations of key state variables by more than double (Table 26). The performance of A2EM was statistically quantified using the coefficient of determination, although it was not expected that the coefficients would show strong predictability of the model. First, all of the observational data for TP, SRP and NO23 was used to calculate r^2 values of 0.0017, 6E-6, and 0.0077 (Table 27), respectively. These results indicate that the model can reproduce less than one percent of the empirical data, meaning the model is poorly calibrated. This is unsurprising given the results shown Figure 55 and the suggestion from Bennett et al. (2013) that evaluation for spatially and temporally complex models may not be accomplished using simple methods. Next, r^2 values were calculated at specific sites to evaluate whether the seemingly better model performance at GBMSD22 relative to GBMSD51 or GBMSD65 could be quantified. Indeed, the model performed much better at the site closest to the Fox River than at sites farther into Green Bay (Table 27). Due to time and financial

176

limitations, further calibration efforts to improve model results remain to be attempted and is the subject of ongoing efforts. Recommendations for future model users would include using 2 years of model data to calibrate the model, then using the remaining year to validate.

Possible Improvements to A2EM

The GBHYP A2EM model performed quite poorly, especially in the outer bay, and this will need to be addressed during future work with this model. Due to time restraints, there was no coefficient adjustment done in this first effort and all of the coefficients reflect those used by Verhamme et al. (2016) for the Lake Erie model. While the coefficients used in this rendition of the model are realistic for aquatic environments in general, considerable variability undoubtedly occurs in Green Bay and developing a Green Bay- specific set of coefficients might significantly improve model performance. Specific coefficients to consider adjusting initially include settling velocities of phytoplankton classes, partitioning of nutrients between these classes, and evaluation of whether or not the Class 4 and 5 phytoplankton should remain excluded.

Another possible model parameter to evaluate is whether the sediment class designations are accurate. Organic carbon deposition maps of Green Bay show that most rapid deposition occurs within the southern bay, so these sediments should have larger fractions of G1 carbon, nitrogen, and phosphorus. Klump et al.'s (2009) estimations of organic carbon content in southern bay sediments to be 10 to 25% should be used as a check on values in the model. Conversely, in the middle of Green Bay, near GB31, there is the highest rate of long-term deposition, which would mean that G2 and G3 classes of nutrients should be higher in the northern bay in proportion to the southern bay. It was noticed that the model predicts oxygen concentrations to be much lower in the mid-bay than is observed, which could be a result of too much labile carbon introduced. It was also suggested by E. Verhamme that the sediments should be allowed to run for several

177

years to reach an equilibrium (of sorts) within the model domain. This is another possible route to help correct the model's function.

An additional add-on model feature within the EFDC-A2EM capabilities is a sediment-wind-wave model, known as SWAN. This can more accurately simulate sediment conditions by inducing resuspension events during high winds and changing shear stress at the bottom. This is a separate model that can be ran in tandem with EFDC, then applied to A2EM. It was recognized at the onset of this project that using SWAN would be very beneficial, but it was ultimately decided to not employ SWAN to leave more resources for other components.

5.4 Model Application and Discussion

An eventual goal of the modeling effort is to simulate a series of nutrient loading reduction and climate change scenarios. After the model's performance has been improved, these scenarios should be repeated to obtain useful results for stakeholders, managers, and scientists, but the basic framework of that scenario testing is developed here.

Reduction Scenario Framework

The major management goal within the Fox River watershed is reduction of non-point nutrient run-off through implementation of BMPs on agricultural lands. To simulate how those nutrient reductions would affect biogeochemistry within Green Bay and response time of different variables, a series of nutrient load reductions scenarios were constructed and implemented within the modeling framework (Table 28). In Scenarios 1, 2, and 3 the A2EM system variable inputs for the Fox River were globally scaled by an appropriate factor. For example, the 25% reduction scenario received a scale factor of 0.75. Only Fox River inputs were affected because that is the

impaired watershed of interest. For Scenario 4, only the soluble reactive phosphorus was scaled to 50% to mimic phosphate specific management efforts that could be implemented.

Test results for loading reduction scenarios (25, 50 and 75% TP reductions) for TP, SRP and Chl*a* are given in Figure 55. The S1-S3 scenarios result in the same general dynamics of the given variables, but at a smaller scale. In the lower bay (i.e. GBMSD22) the Chl*a* response falls

Table 26: Mean and standard deviation values for selected observed (O) and simulated (S) parameters.

Parameter	n	O_{mean}	O_{SD}	S_{mean}	S_{SD}
SRP	617	0.003	0.003	0.049	0.081
TP	629	0.05	0.049	0.182	0.14
NO23	583	0.027	0.036	0.779	0.778

Table 27: Coefficient of determination (r2) results for the parameters listed in Table 26.

Parameter	All Data	GBMSD22	GBMSD51	GBMSD65
SRP	0.002	0.078	0.040	0.034
TP	6E-6	0.161	0.066	0.011
NO23	0.008	0.091	0.017	0.008

Table 28: List of scenarios ran using GBHYP and the corresponding changes made.

Scenario	Scenario Description	Boundaries Affected	Point Source Affected	Changes Made	Scenario Years
S1	25% Reduction	Fox	Yes	Global scale factor = .75	2011-13
S2	50% Reduction	Fox	Yes	Global scale factor = .50	2011-13
S3	75% Reduction	Fox	Yes	Global scale factor = .25	2011-13
S4	50% SRP Reduction	Fox	No	PO4T factor=.5	2011-13
S5	Climate change MRI	All, except Lake Michigan	No	Applied scaling factors to TSS (1.17), TP and OP (1.14) from P. Baumguart	2011
S6	Climate change ECHO	All, except Lake Michigan	No	Applied scaling factor to TSS, TP and OP (.97) from P. Baumguart	2012
S7	MRI + 50% Reduction	All, except Lake Michigan Reductions only to Fox	Yes	Scale factor = 0.5 for everything	2011
S8	ECHO + 50% Reduction	All, except Lake Michigan. Reductions only to Fox	Yes	Scale factor= 0.5 for everything	2012

between the baseline and the 25% reduction scenario. The largest responses to nutrient load reductions occur closest to the mouth of the Fox River. This could be due to "cold starting" the model, or essentially starting each model year with the same conditions regardless of how the previous year ended. This would minimize the response farther out from the Fox River mouth area because every year the parameters are re-set. A response within the water column after nutrient load reductions has been shown to take a season or two (Riemann et al. 2016), so it would be beneficial to "hot start" the model in future runs in order to elicit a response. A "hot start" uses the outputs from the end of the previous year to start the current year. The lack of response in the more open bay could also be contributed to inadequate simulation of processes there, as was suggested for the baseline runs.

Hypolimnetic parameters, such as sediment nutrients, are not shown here but they are important to evaluating the recovery of the ecosystem. The response of sediment nutrient concentrations to the scenarios is not shown because it could take decades to occur, especially in environments with a long history of hypoxia and eutrophication (Steckbauer et al. 2011). For this reason, a response in sediment conditions over the 3 years of model runs would be attenuated, even if a "hot start" was used for the model. The best solution to this issue is to allow the model to run for several years to allow the sediments to properly respond to loading reductions.

Figure 55a: Total phosphorus responses to 25%, 50%, and 75% global reduction scenarios (green, yellow, and aqua lines respectively) and a 50% SRP reduction scenario (orange line) at GBMSD22. The blue line and red dots represent the baseline model results and observation data, respectively.
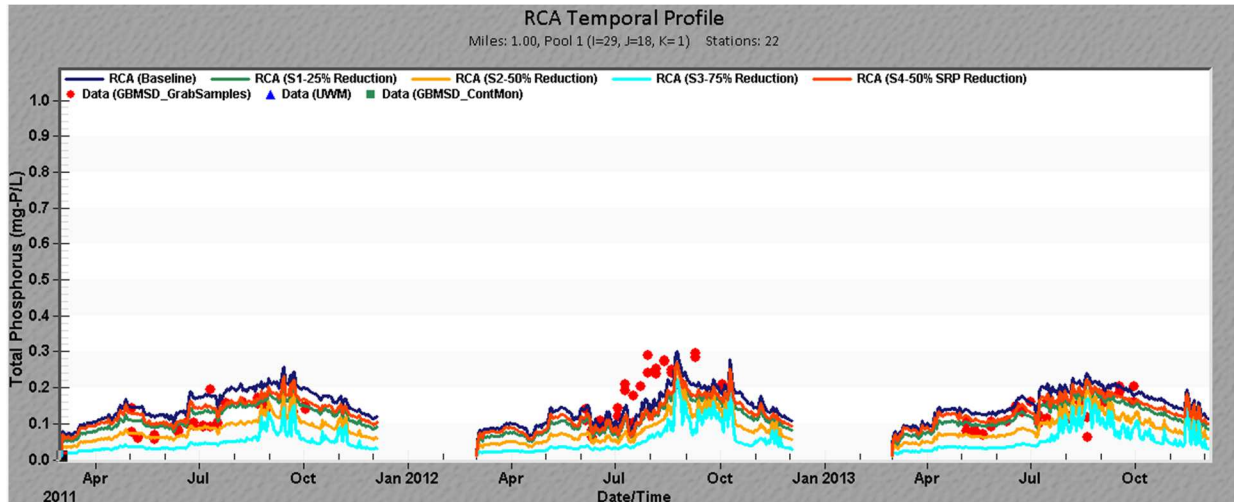
Figure 55b: Soluble reactive phosphorus responses to the 4 nutrient load reduction scenarios listed above at GBMSD 22.

183
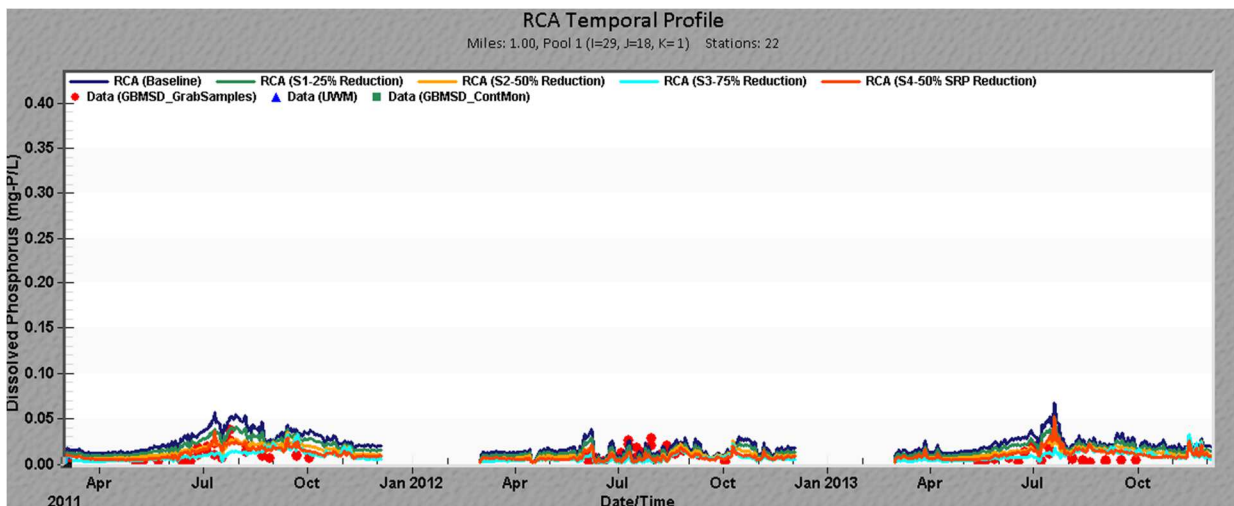
Figure 55c: Chlorophyll-*a* responses to the 4 nutrient load reduction scenarios from 55a at GBMSD 22.
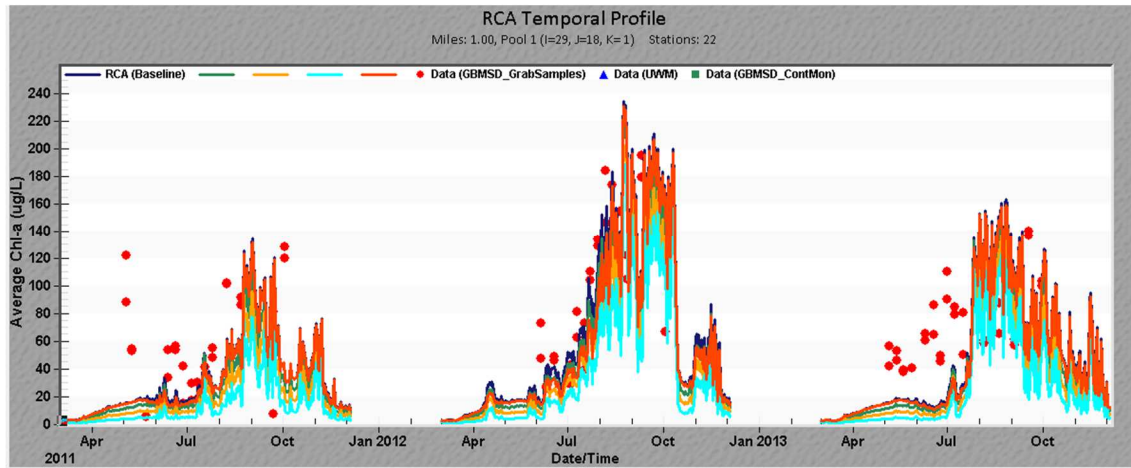
Climate Change Scenarios

Another management concern is whether or not the BMPs that are implemented today will be sufficient under future climate conditions. The load limits that are being set currently may suffice to alleviate seasonal hypoxia now, but will they also be adequate in the next 50 years as the climate changes? To answer this, 13 global climate models were downscaled using a statistical technique selected by Dr. David Lorenz (pers. communication). The increments in monthly air temperature predicted by the 13 climate change models, with respect to the 2011-2013 baseline years were computed. The climate change model predictions closest to the 90th percentile and 10th percentile increments, 2012 ECHO and 2011 MRI respectively, were selected to represent the years with warmest and coldest air temperature predictions as initial test cases.

The appropriate MRI and ECHO outputs from the downscaled climate model and the POMGL model runs were used in the SWAT and EFDC models to simulate watershed and hydrodynamic changes, respectively. Of particular interest in the watershed was how magnitude and timing of nutrient loading would change with regards to shifting storm events and shortened winters. Dr. Paul Baumgart (UW-GB) performed these SWAT model runs and provided scaling factors for discharge, TS, TP and SRP loads. Fox River-specific scaling factors were calculated, while scaling factors from the Wolf River (upstream of the Fox River) were used as surrogates for the Oconto, Menominee and Peshtigo Rivers. It was assumed that the Wolf River watershed is similar enough to the other watersheds that it could be used in lieu of performing additional (and separate) SWAT model runs. The scaling factors for TS, TP and SRP are given in Table 30.

The climate change scenarios (S5 and S6 for MRI and ECHO, respectively) for EFDC were performed using the temperature, dew point temperature and wind data from the downscaled climate models. The river discharge from the SWAT model climate scenarios was used to create

185

new flow inputs. Chambers Island boundary conditions were taken from the POMGL results. Outputs from EFDC for S5 and S6 were used in A2EM, as were the scaling factors from Table 5. Other factors, such as initial conditions within Green Bay, remained unchanged. As a final step, a 50% nutrient reduction scenario for both MRI and ECHO projections was performed, as S7 and S8. The same method used in S2-S4 in applying a 0.5 global scale factor was used for S7 and S8.

The responses to MRI and ECHO climate change scenarios were quite different. MRI predictions included less precipitation and cooler temperatures than ECHO (Fig. 56). This resulted in total phosphorus concentrations near the baseline for S5 and higher concentrations than baseline for S6 (Fig. 57a). SRP concentrations followed a similar trend, although at times the SRP in S5 also exceeded baseline conditions at the outer stations (Fig. 57b). Scenarios 7 and 8 followed the same trend as noted before in terms of response to nutrient reductions. The

Figure 56: Temperature model predictions for MRI (yellow line) and ECHO (green line) regional climate models at GBMSD22.
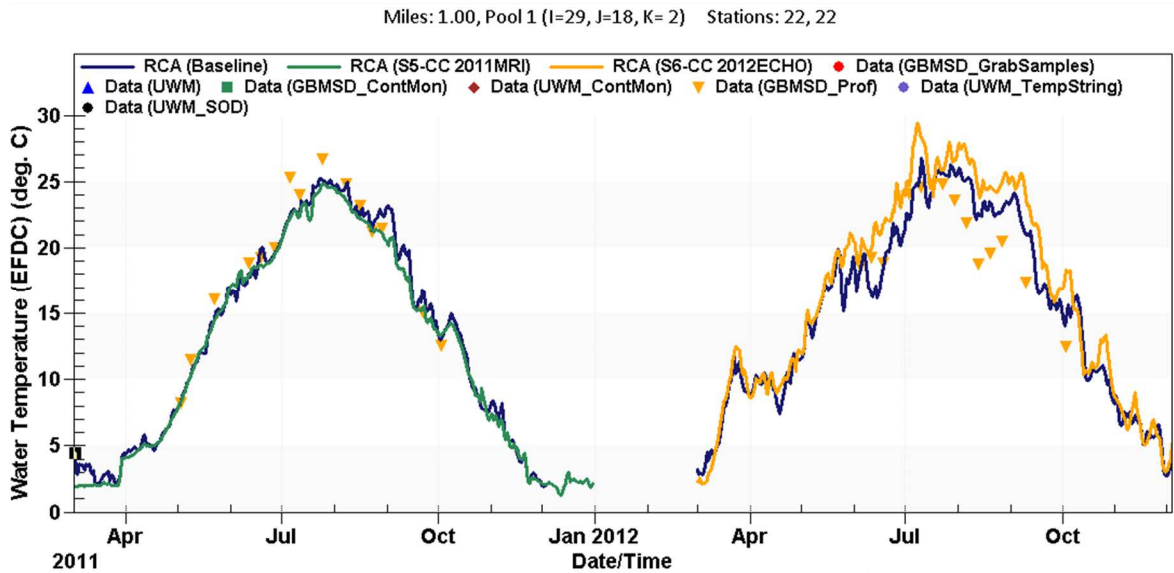
Figure 57a: Response of total phosphorus for two climate change scenarios at GBMSD22.
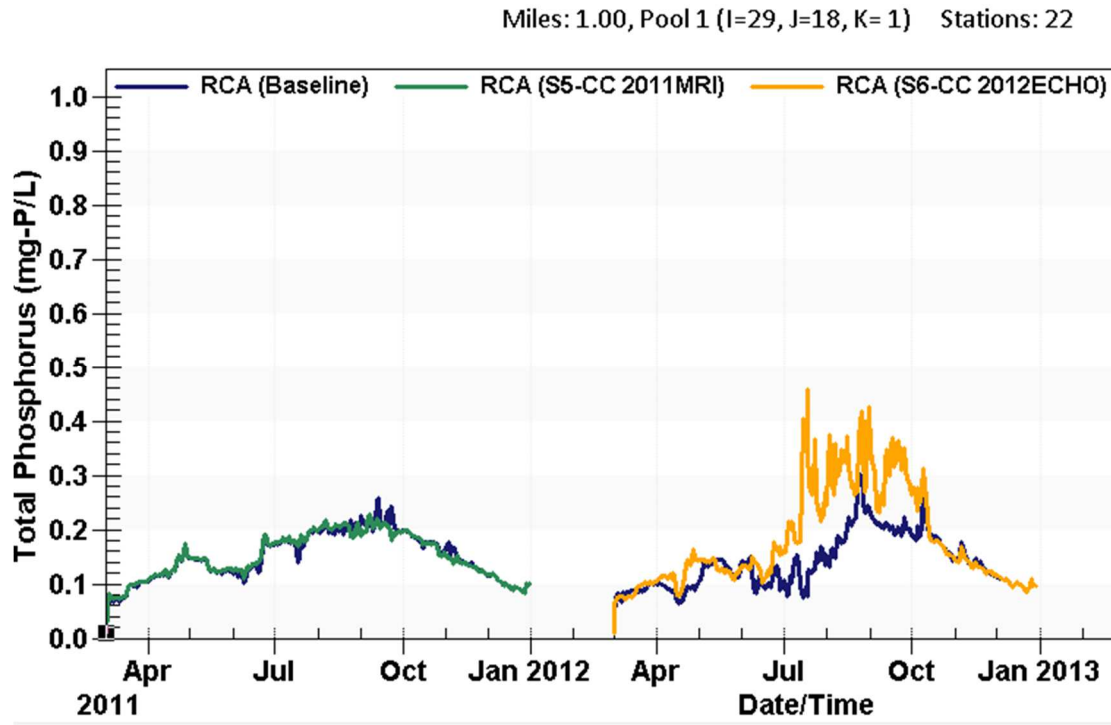
Figure 57b: Response of dissolved phosphorus (or SRP) for two climate change scenarios at GBMSD22.
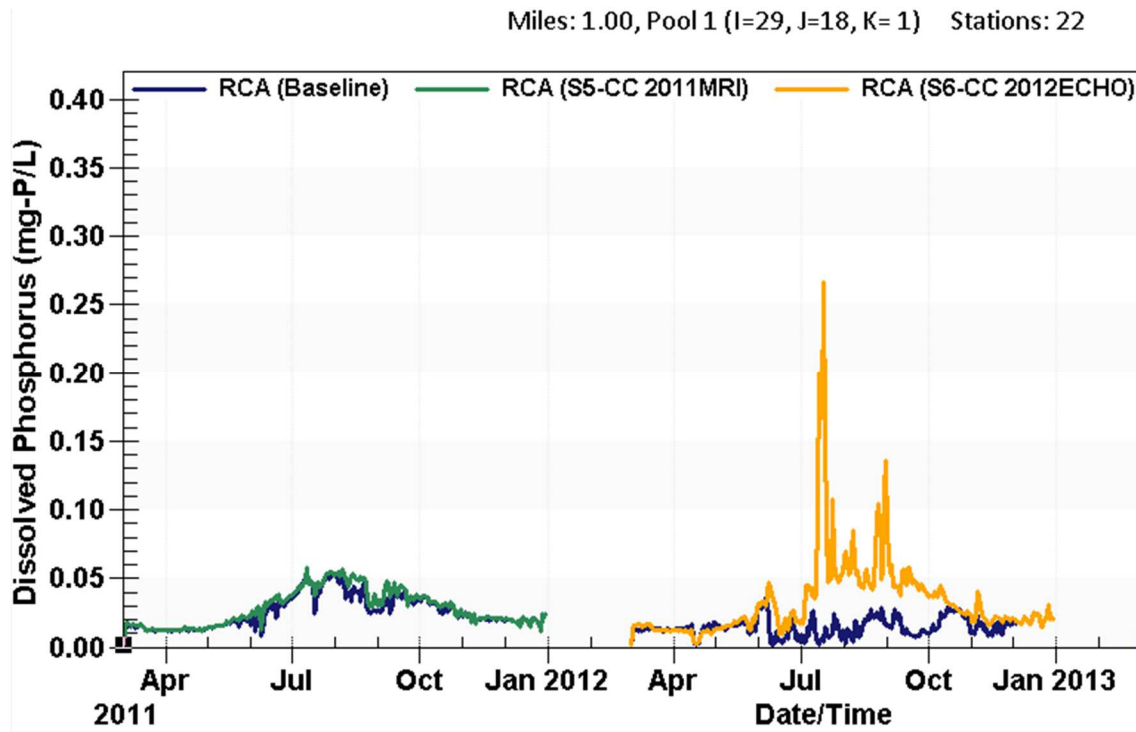
Figure 57c: Response of chlorophyll-*a* for two climate change scenarios at GBMSD22.
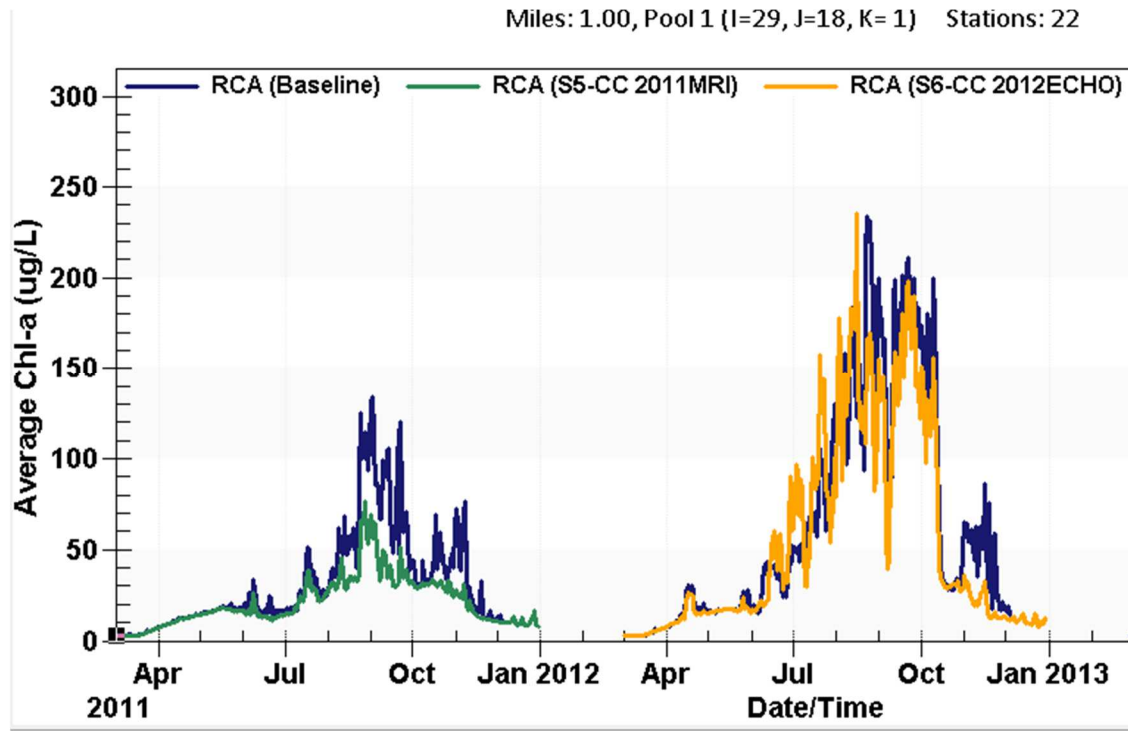
response seemed to be more pronounced for S7 than S8. One potential explanation for this could be the warmer water temperatures of S8 counteracted nutrient reductions by increased growth rates and stronger stratification. These processes have been proposed as mechanisms for why Danish coastal systems with reduced nutrient loads did not experience improved water quality conditions of the same scale (Riemann et al. 2016).

5.5 Management Analysis Tool

WinModel will eventually provide a useful tool for visualizing and comparing all of the modeling results, but it is not practical for an environmental manager or stakeholder to learn to use this program. As an alternative, LimnoTech has developed a management analysis tool, or MAT, framework in which model results are summarized and synthesized into a usable format. The end goal is that the MAT could be distributed to local stakeholders and environmental managers so they can explore how different watershed changes affect water quality within Green Bay.

There are many options for user-specified outputs within the MAT. For example, Green Bay has been separated into different regions (Fig. 58) so a user could evaluate how nutrient load reductions near the mouth of the Fox River affects chlorophyll concentrations farther into Green Bay (Fig. 59). A screenshot of the MAT "Metric Comparison" tab (Fig. 59) shows some of the many features available with the tool, including 14 metrics to compare between 9 different zones. The scenario results for different parameters can be compared with water quality criteria for Green Bay (Fig. 60). All of the criteria that are signified within the tool are from total maximum daily load (TMDL) or CWA standards.

189

One of the unique features to the MAT designed for GBHYP is the inclusion of a "hypoxic area"

variable. This area was specified over a specific depth region where hypoxia is known to

Figure 58: Zone specifications for Green Bay within the GBHYP Management Analysis Tool.

190
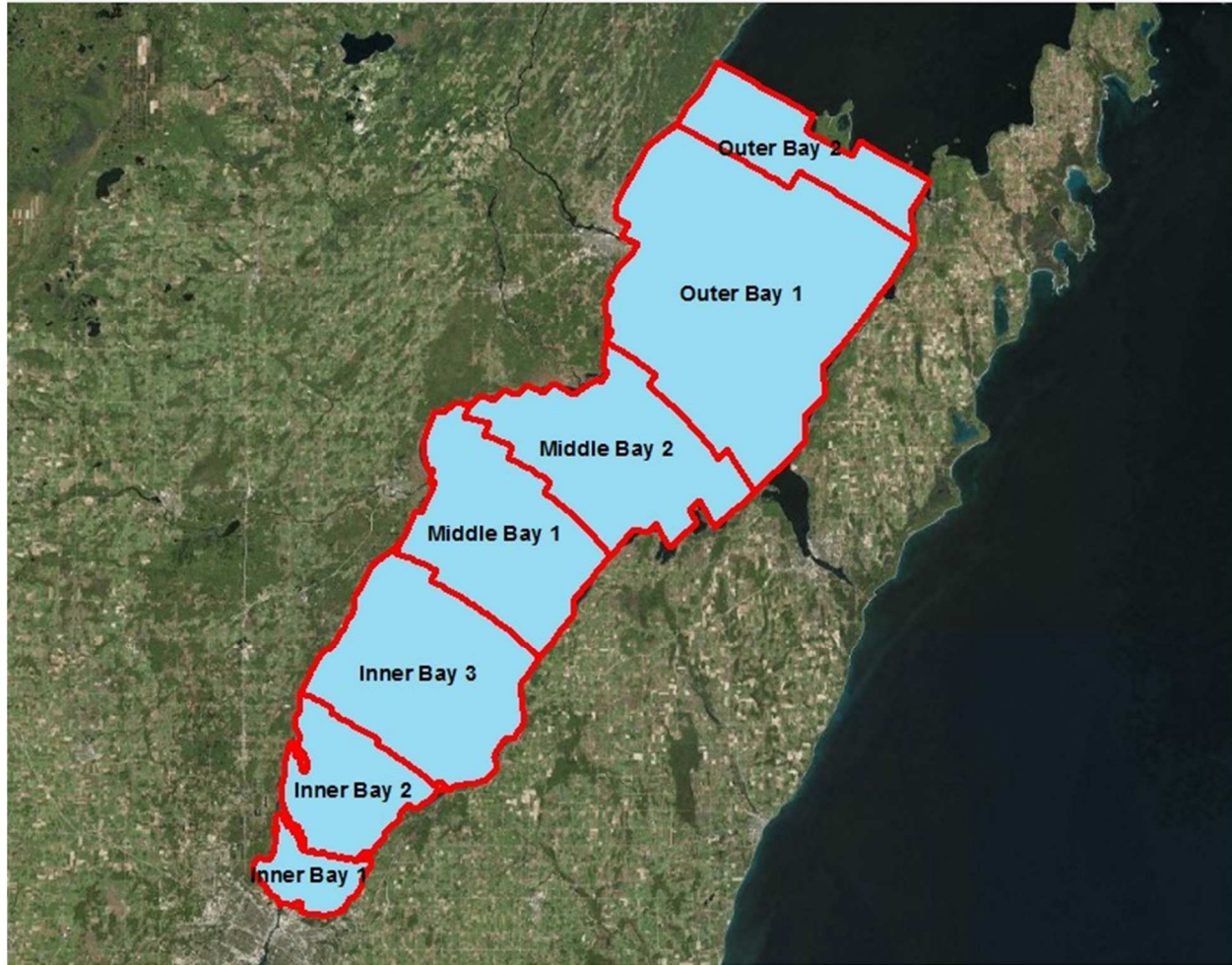
Figure 59: Example of the metric comparison tool with the MAT.
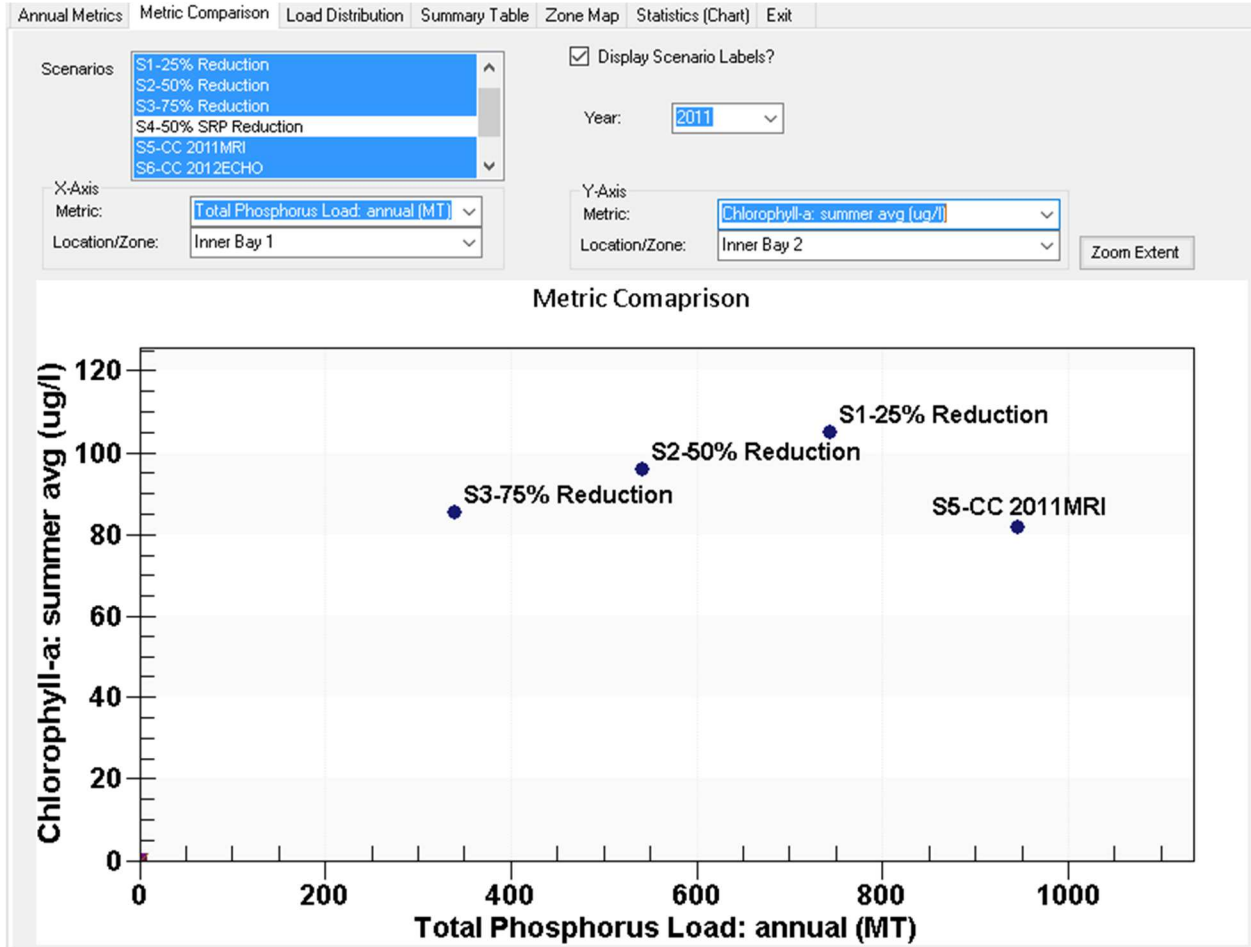
Figure 60: Reduction scenario results across the 3 years of the model and the comparison to water quality criteria for Green Bay.
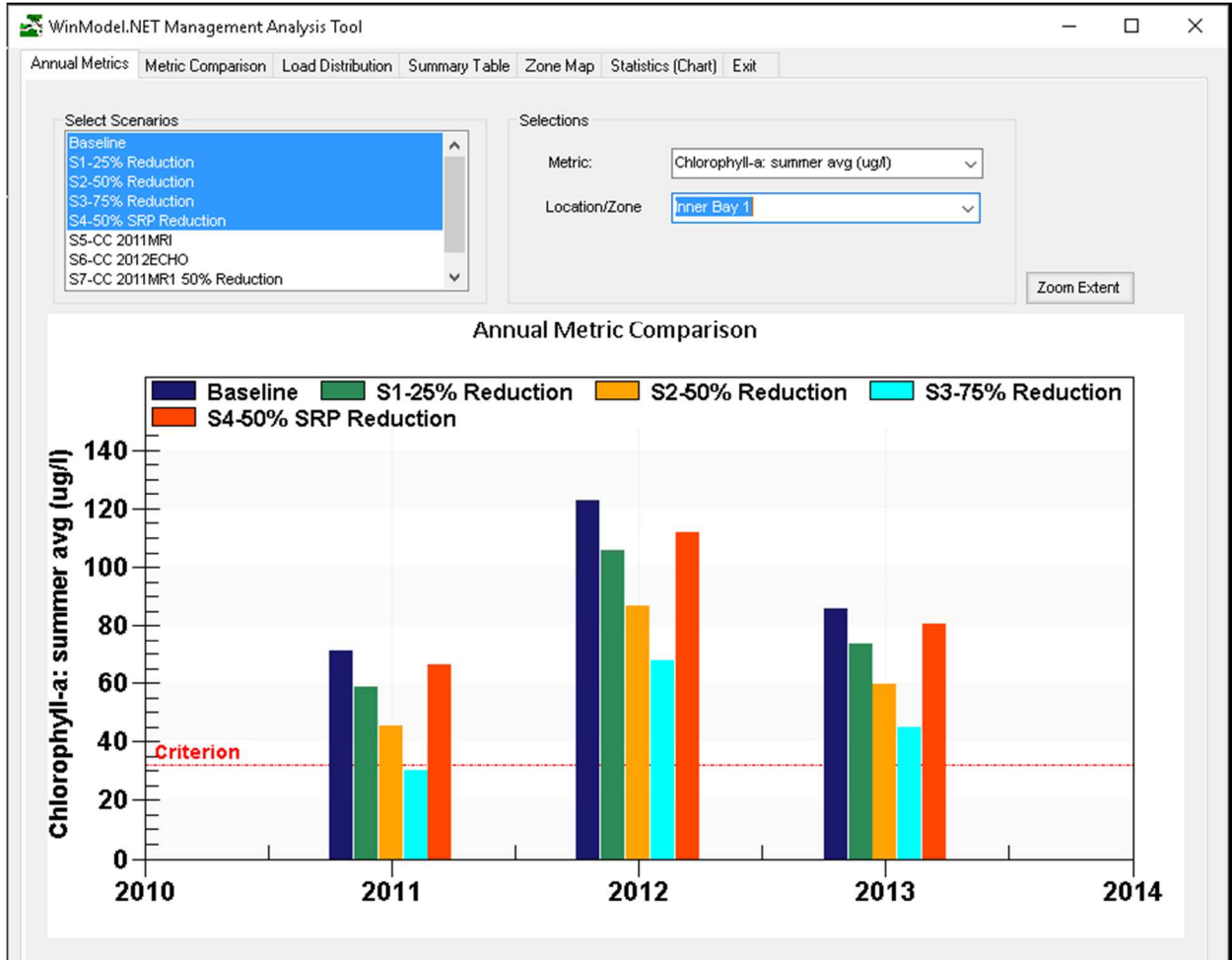
form. This feature will be critical to answering one of the fundamental questions of this study: What nutrient load from the Fox River watershed adequately reduces hypoxia in Green Bay? From 2009-2015 the hypoxic area in Green Bay varied from 0-100 km^2 and the area that experienced oxygen concentrations less than 5 mg L^{-1} varied from 150-600 km^2. With this iteration of the model, the extent of hypoxia, like that for TP and Chl concentrations, is over-predicted. To get an idea of changes that would occur under various scenarios, the magnitude and direction of changes that the model can generate can still be compared. For example, a nutrient load reduction of 50% would reduce the hypoxic area by only 10 km^2 (330 down to 320 km^2 for 2013) to 18 km^2 (548 down to 530 km^2 for 2011). These cliate change scenarios predict little change in the hypoxic area (i.e. 100 km^2) under MRI scenario to an increase up to 810 km^2 for the ECHO scenario. A 50% reduction in nutrient loads under MRI and ECHO climate change conditions project hypoxic area decreases of 25 km^2 and 20 km^2, respectively. While these reductions are larger than under S1-S3 scenarios, the ECHO-predicted hypoxic area is still more than 200 km^2 larger than under current conditions. It is important to note that these results will undoubtedly change as the model becomes better calibrated, and the results given here are only in illustration of the model's current responsiveness.

One of the modeling components that was not discussed in details is the simulation of BMPs applied to the watershed and how they affect nutrient loading to the system. Paul Baumgart has run several iterations of the watershed model to evaluate effects of varying BMPs, both in type and percent coverage, and presented the results at the modeling workshop (discussed in 5.7). The results of the BMPs have yet to be integrated into the MAT, but it will eventually strengthen the applicability of the tool by allowing users to determine what BMP type and intensity could produce a change within Green Bay.

5.6 Outreach

A major component of the integrated modeling project was to connect stakeholders and environmental managers, receive feedback, and make adjustments in the future. This connection between the science and stakeholders was facilitated by a hands-on modeling workshop at UW-Green Bay in September 2015. At this workshop the model development was explained and the participants were able to practice using the MAT, ask questions to the scientists and engineers, and provide feedback on the tool. Participants represented a variety of stakeholder and management groups including agricultural representatives, farmers, DNR, and non-profits.

The feedback was thoroughly considered and used to make revisions. The updated model was presented via a webinar, facilitated through UW-Extension (Chad Cook). The webinar was viewed by more than 40 people, with an opportunity for question and answer. The presentations were summarized and uploaded to a website that provides information and fact sheets about the project (fyi.uwm.edu/gbem/).

Members of the modeling team also presented the results at the 9th Biennial State of Lake Michigan conference in October 2015. An entire session, titled "Restoring the health of the Green Bay ecosystem under a changing climate: modeling land use, management, and future outcomes," was designated to introduce the various components of the GBEM to the attendees and to generate feedback on the approach and results thus far.

5.8 Conclusions and Future Work

The GBEM was able to combine 4 different models to evaluate the nutrient reductions that are necessary to decrease hypoxia in Green Bay and ultimately improve water quality. The major products developed here included the biogeochemical model (GBHYP) and a management

194

analysis tool. The biogeochemical model was created using a suite of monitoring data from a variety of sources- including University of Wisconsin-Milwaukee and Green Bay Metropolitan Sewerage District (now NEW Water). This model is able to simulate several processes of interest, although this iteration of GBHYP has simply established a modeling framework only and requires further development, calibration and parameterization. For example, the model can generate a hypoxic zone, but overestimates in and places it in the upper bay. This is consistent with over-predicting mid and upper bay concentrations of nearly every parameter, including phosphorus, chlorophyll a and nitrogen. Suggestions for improved performance include increasing settling rates within the lower bay and improving sediment nutrient class designation. The model also shows somewhat realistic responses to load and climate changes, which will be very useful once the baseline runs are better calibrated. The MAT is a useful interface that stakeholders can use to evaluate how changes in the watershed affect water quality in Green Bay.

Ecosystem models need constant revisions, as processes are better understood, monitoring improves and management questions change. GBEM is no exception. The primary need for this set of models is for the biogeochemical model to be better calibrated and confirmed. One suggested way to accomplish this is to use two years of data to calibrate the various coefficients and optimize the simulation. Then, the 3rd year of data can be used to confirm the model, both visually and statistically. The secondary need for GBEM is to integrate the results from the best management practices for the Fox River watershed into the MAT. This will better help managers understand the required changes that need to occur within the watershed to accomplish a certain water quality goal or goals. These improvements will create a scientifically accurate model that will allow environmental managers to make well-informed policy decisions that can improve and protect the integrity of Green Bay. It would also be useful to collect samples during or

195

immediately after storm events to make sure the model correctly replicates the affects a storm has on Green Bay biogeochemistry.

Overall, the modeling team was successful in producing a first-round integrated ecosystem model that can eventually be used to determine what necessary changes have to be made now, and under future climate projections, to reduce hypoxia. Several stakeholders were brought into the project to provide feedback on the first iteration of the model and to help with future iterations. Improvements will need to be made to better replicate observations, but GBHYP will undoubtedly be a valuable tool for both scientists and environmental managers once it is fully calibrated.

CHAPTER 7: CONCLUSIONS

7.1 Summary

To better understand the development of hypoxia in Green Bay a series of studies were performed to answer a series of questions about the sources and sinks of oxygen in Green Bay and to develop an oxygen mass balance for the system. These questions, also presented in the introduction, include:

1) Are surface waters net sources or sinks of autochthonous organic matter?
2) What are the major biogeochemical processes responsible for oxygen consumption in the hypolimnion?
3) Does cool, bottom water from the northern bay contribute substantially to hypoxia?
4) What level of nutrient load reductions from the watershed will result in acceptable decrease of hypoxia?
   a. Will this amount of reduction be adequate in the future?

First, the epilimnetic oxygen dynamics were evaluated using continuous data collected on seasonal buoys. Buoy NOAA45014, located at GB17, collected all of the necessary data for diel oxygen cycle calculations including oxygen, temperature, wind speed, and solar irradiance. During the summer months of 2013-15, GB17 surface waters were typically slightly autotrophic, with gross primary production exceeding respiration by a few percent. Farther south in Green Bay, at the Entrance Light, a longer time series of continuous oxygen data were analyzed with wind data from NOAA45002 and CBRW3. This station was also autotrophic, although the magnitudes of production and respiration were greater than at GB17 consistent with the generally larger algal biomass observed at this station. Continuous bottom water oxygen

observations at the Entrance Light also allowed for comparisons to be made between net ecosystem production and days of depleted oxygen, with a correlation coefficient of 0.20. Therefore, to answer Question1, the epilimnion in lower Green Bay is a net source of carbon and organic matter, which can contribute to oxygen consumption in the hypolimnion.

Quantifying hypolimnetic oxygen depletion rates was accomplished through sediment core incubations, eddy covariance flux estimates, and calculations of total oxygen loss rate by both inventory depletions and apparent oxygen utilizations. 86 separate sediment core incubations were carried out in triplicate at several stations around lower Green Bay. The average observed sediment oxygen uptake (or SOD) rate was 12.9 mmol O_2 m^{-2} d^{-1}. The non-invasive aquatic eddy covariance technique was used to determine if the incubation rates adequately captured the oxygen uptake rate, despite lacking natural hydrodynamic processes. The core incubation rates were always somewhat higher than what the eddy covariance system measured, but the same spatial trends were followed for both techniques. Site specific sediment oxygen demands were then subtracted from oxygen inventory loss rates (i.e. HOD) to estimate hypolimnetic water column respiration (R_H) rates. Overall, R_H accounts for ~59% of the oxygen consumption within the hypolimnion, although this percentage varies as a function of depth. In response to Question 2- sediment oxygen demand and hypolimnetic water column respiration are the two major oxygen consuming processes within Green Bay. SOD is the greatest oxygen consumer in shallow waters and R_H is the primary consuming process in deeper waters of the mid-bay, although the dynamics between the two processes are complicated by bottom water mixing processes.

To evaluate the influence of advection within the hypolimnion, a series of natural tracers were used to study movement processes and extents of mixing. Due to a naturally occurring gradient of isotopic signature between the Fox River and Lake Michigan, the stable isotopes ^2H and ^{18}O

198

were used to calculate percent mixing of these two water sources. There is a strong distinction between surface water and bottom water signatures, with surface waters dominated by Fox River signature (~65% Fox River signature) and bottom water signatures ranging from 100% Lake Michigan near the gap to 30% at GB6. This strong distinction between water masses contributes to a strong thermal gradient that is observed within Green Bay. Furthermore, with continuous temperature and dissolved oxygen measurements at the bottom water, a link between incoming pulses of cool water from the northern bay and drops in oxygen concentration was made. Next, to estimate the magnitude of advective flow, the applicability of two sediment-based natural tracers-- ^{222}Rn and CH_4—were evaluated. The bottom water inventories of each gas were calculated across Green Bay and it was determined that ^{222}Rn was better suited to estimating advection because its hypolimnetic inventories and benthic fluxes were greatest in the northern bay and decreased southward, which is the direction of flow. The most realistic advective flow rate estimated by ^{222}Rn is ~10 m d^{-1}, approximately two order of magnitude lower than the modeled velocity of bottom water. The answer to Question 3 is that yes, bottom water from the northern bay contributes to hypoxia by setting up strong thermal stratification and pushing low-oxygen water from the mid-bay to the southern bay, where it goes hypoxic.

All of these results help fill in the oxygen mass balance (see section 8.2), but to get an idea of what watershed management practices can do to help reduce hypoxia a biogeochemical model was initiated for Green Bay as part of an integrated modeling effort. The biogeochemical model, A2EM, was part of a linked hydrodynamic-biogeochemical model called GBHYP. Observations made by the Green Bay Metropolitan Sewerage District, University of Wisconsin-Milwaukee, and the US Geological Survey were primarily used to create boundary conditions and initial conditions for the model. Despite needing further calibration and parameterization, the model

199

promises to a useful tool for adaptive management in Green Bay. A series of reduction scenarios were developed to evaluate how various phosphorus loads from the Lower Fox River would affect water quality in Green Bay. Reductions of 25 to 75% elicit a significant model response, but an answer to question 4 remains an open one pending further model refinements.

7.2 Oxygen Mass Balance

One of the overarching goals of this thesis was to produce a summertime oxygen mass balance for Green Bay. A box model representation of the balance was presented in Chapter 1 and is filled in here with summertime values (Fig. 61). Due to the difference in hypolimnetic oxygen consuming processes as the bay gets deeper, there were two different zones considered for the final balance. In a 2-dimensional case, advection is not included, but it does play a role in the spatial distribution of dissolved oxygen within the bay. For Zone 1, the sediment oxygen demand consumes all of the oxygen during the stratified season and is a probable driver of the high recycling rates noted by Klump et al. (2009). In Zone 2, oxygen consumption within the hypolimnion is divided between the water column and the sediments. This is attributed to the deeper depth, which allows more time for organic matter decomposition to occur within the water column.

The balance has been well constrained, with the exception of advection terms. These rates are all specific to the stratified season in Green Bay, which is usually late June through early September. Within the epilimnion, oxygen is generally supersaturated and lost to the atmosphere during stratification.

Figure 61: The completed summertime oxygen mass balance for lower Green Bay with all rates given in units of mmol O2 m-2 d-1. Zone 1 is south of the GB12-14 station line and Zone 2 is south of Sturgeon Bay to Zone 1. Atmospheric fluxes are in italics because they are incorporated into the GPP and R calculations. Production in the hypolimnion was considered negligible (neg.) and was also not calculated.
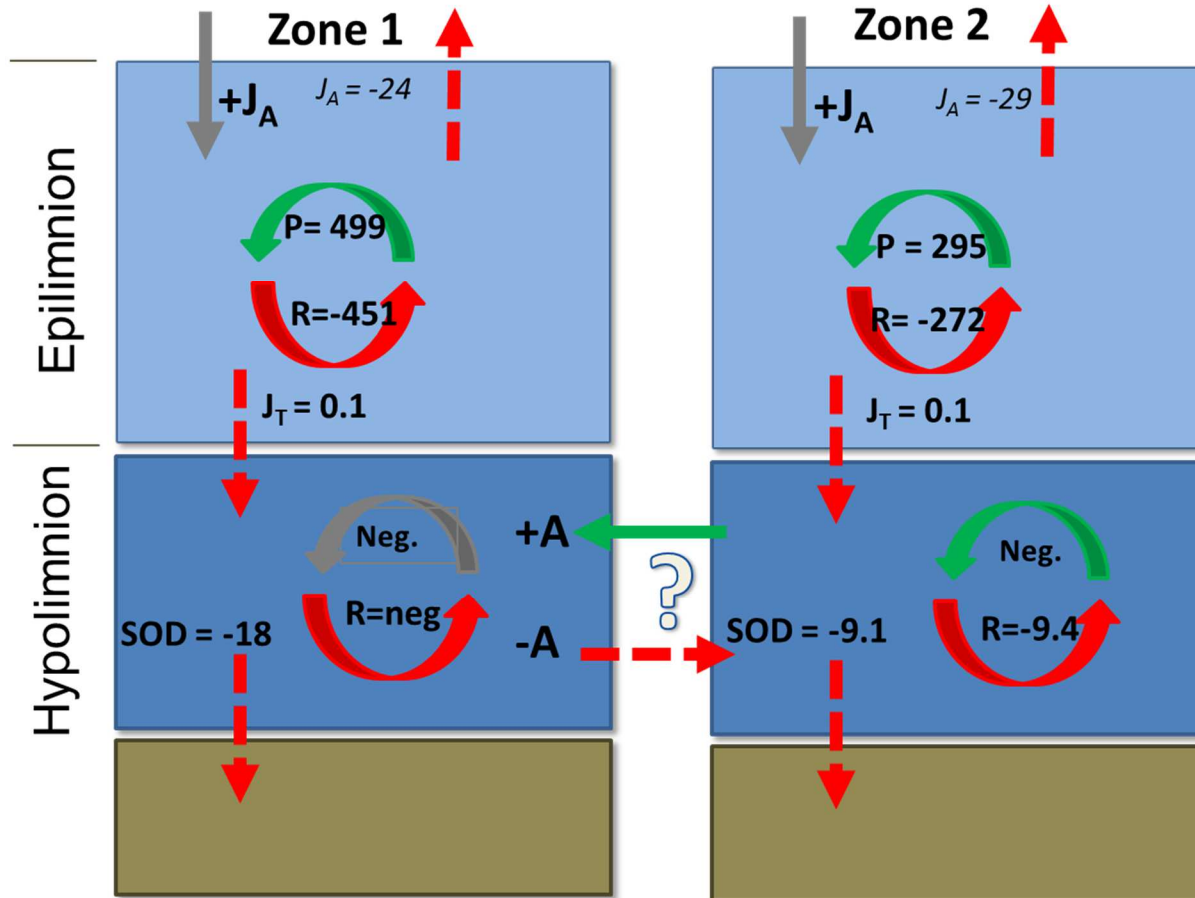
stratified. Occasional mixing events cause surface waters to mix with oxygen depleted hypolimnetic waters, resulting in under-saturated conditions and an oxygen influx to the water column. Similar observations were not obtained for the hypolimnion, although fall overturn has been shown to cause a release of carbon, in the forms of CH_4 and CO_2, to the atmosphere (Waples, 1998). While Green Bay may be a net sink of carbon during the stratified period, the non-stratified period is very different, and on an annual basis is observed to be net heterotrophic (Waples 1998, Klump et al. 2009).

7.3 Conclusions

There are biological and physical causes of seasonal hypoxia within Green Bay. The physical drivers of hypoxia, including 2-layer mixing and strong thermal gradients, cannot be managed. The value of models is that both nutrient management plans and water quality improvement expectations can be placed in the context of realistic system responses. Internal recycling processes also contribute to oxygen consumption and can effect nutrient loading reduction efforts. For these reasons, it is important to consider a number of response parameters to evaluate recovery progress for Green Bay. Suggestions include primary production both at the inner and mid bay, hypolimnetic water column respiration, and invertebrate recolonization. Yearlong studies would also be valuable to get a better understanding of seasonal effects that were not captured within this study.

REFERENCES

Adams, K. A., J. A. Barth, and F. Chan. 2013. Temporal variability of near-bottom dissolved oxygen during upwelling off central Oregon. J. Geophys. Res. Ocean. **118**: 4839–4854.

Aku, P. M. K., L. G. Rudstam, and W. M. Tonn. 1997. Impact of hypolimnetic oxygenation on the vertical distribution of cisco (Coregonus artedi) in Amisk Lake, Alberta. Can. J. Fish. Aquat. Sci. **54**: 2182–2195.

Althouse, B., S. Higgins, and M. J. Vander Zanden. 2014. Benthic and planktonic primary production along a nutrient gradient in Green Bay, Lake Michigan, USA. Freshw. Sci. **33**: 487–498.

Andersen, J. H., L. Schlüter, and G. Ærtebjerg. 2006. Coastal eutrophication: Recent developments in definitions and implications for monitoring strategies. J. Plankton Res. **28**: 621–628.

Auer, M., and R. Canale. 1986. Mathematical Modelling of Primary Production in Green Bay (Lake Michigan, USA), A Phosphorus and Light-Limited System. Hydrobiol. Bull. **20**: 195–211.

Baturin, G. N. 1988. The geochemistry of manganese and manganese nodules in the ocean, D. Reidel Publishing Company.

Bender, M., K. Grande, K. Johnson, J. Marra, P. J. L. Williams, J. Sieburth, M. Pilson, C. Langdon, G. Hitchcock, J. Orchando, and C. Hunt. 1987. A comparison of four methods for determining planktonic community production. Limnol. Oceanogr. **32**: 1085–1098.

Bennett, N. D., B. F. W. Croke, G. Guariso, J. H. A. Guillaume, S. H. Hamilton, A. J. Jakeman, S. Marsili-Libelli, L. T. H. Newham, J. P. Norton, C. Perrin, S. A. Pierce, B. Robson, R. Seppelt, A. A. Voinov, B. D. Fath, and V. Andreassian. 2013. Characterising performance of environmental models. Environ. Model. Softw. **40**: 1–20.

Berg, P., H. Røy, F. Janssen, V. Meyer, B. B. Jørgensen, M. Huettel, and D. De Beer. 2003. Oxygen uptake by aquatic sediments measured with a novel non-invasive eddy-correlation technique. Mar. Ecol. Prog. Ser. **261**: 75–83.

Berner, R. A. 1980. Early Diagenesis: A Theoretical Approach, Princeton University Press.

Bierman, V. J., J. Kaur, J. V Depinto, T. J. Feist, and D. W. Dilks. 2005. Modeling the Role of Zebra Mussels in the Proliferation of Blue-green Algae in Saginaw Bay, Lake Huron. J. Great Lakes Res. **31**: 32–55.

Van de Bogert, M. C., S. R. Carpenter, J. J. Cole, and M. L. Pace. 2007. Assessing pelagic and benthic metabolism using free water measurements. Limnol. Oceanogr. Methods **5**: 145–155.

Bouffard, D., J. D. Ackerman, and L. Boegman. 2013. Factors affecting the development and dynamics of hypoxia in a large shallow stratified lake: Hourly to seasonal patterns. Water

Resour. Res. **49**: 2380–2394.

Bravo, H. R., S. A. Hamidi, J. V. Klump, and J. T. Waples. 2015. Currents and heat fluxes induce stratification leading to hypoxia in Green Bay, Lake Michigan. *E-proceedings of the 36th IAHR World Congress*. IAHR. 1–10.

Breitburg, D. L. 1990. Near-shore hypoxia in the Chesapeake Bay: Patterns and relationships among physical factors. Estuar. Coast. Shelf Sci. **30**: 593–609.

Brock, T. D. 2012. A Eutrophic Lake: Lake Mendota, Wisconsin, Springer Science & Business Media.

Broecker, W. S. 1965. An application of natural radon to problems in ocean circulation. *Symposium on diffusion in oceans and fresh waters*.

Broecker, W. S., and T.-H. Peng. 1982. Tracers in the sea, 1st ed. Lamont-Doherty Geological Observatory, Columbia University.

Buchhloz, L. A., J. V Klump, M. L. P. Collins, C. A. Brantner, and C. C. Remsen. 1995. Actvity of methanotrophic bacteria in Green Bay sediments. Methane, Bact. Porewater, **16**: 1–8.

Burns, N. M. 1995. Using hypolimnetic dissolved oxygen depletion rates for monitoring lakes. New Zeal. J. Mar. Freshw. Res. **29**: 1–11.

Burns, N. M., and C. Ross. 1972. Project Hypo: An intensive study of the Lake Erie central basin hypolimnion and related surface water phenomena, Ottawa: Information Canada.

Cable, J. E., and J. B. Martin. 2008. In situ evaluation of nearshore marine and fresh pore water transport into Flamengo Bay, Brazil. Estuar. Coast. Shelf Sci. **76**: 473–483.

Cadmus, G. 2012. Total Maximum Daily Load and Watershed Management Plan for Total Phosphorus and Total Suspended Solids in the Lower Fox River Basin and August 2011 Prepared for : Oneida Tribe of.

Caffrey, J. M. 2004. Factors Controlling Net Ecosystem Metabolism in U . S . Estuaries. Estuaries **27**: 90–101.

Carstensen, J., D. J. Conley, J. H. Andersen, and G. Aertebjerg. 2006. Coastal eutrophication and trend reversal: A Danish case study. Limnol. Oceanogr. **51**: 398–408.

Cole, J. J., and N. F. Caraco. 1998. Atmospheric exchange of carbon dioxide in a low-wind oligotrophic lake measured by the addition of SF6. Limnol. Oceanogr. **43**: 647–656.

Collins, J. R., P. a. Raymond, W. F. Bohlen, and M. M. Howard-Strobel. 2013. Estimates of New and Total Productivity in Central Long Island Sound from In Situ Measurements of Nitrate and Dissolved Oxygen. Estuaries and Coasts **36**: 74–97.

Conley, D. J. 1983. Limnological characteristics of Green Bay, Lake Michigan. University of Wisconsin-Green Bay.

Conley, D. J., J. Carstensen, G. Ærtebjerg, P. B. Christensen, T. Dalsgaard, J. L. S. Hansen, and

A. B. Josefson. 2007. Long-term changes and impacts of hypoxia in Danish coastal waters. *Ecological Applications*. Ecological Society of America. S165–S184.

Consi, T. R., T. F. Hansen, and J. V. Klump. 2007. GLUCOS: The Great Lakes Urban Coastal Observing System. Sea Technol. **48**: 39–53.

Corbett, D. R., K. Dillon, W. Burnett, and J. Chanton. 2000. Estimating the groundwater contribution into Florida Bay via natural tracers, 222 Rn and CH 4. Limnol. Oceanogr. **45**: 1546–1557.

Cornett, R. J., and F. H. Rigler. 1979. Hypolinimetic Oxygen Deficits: Their Prediction and Interpretation. Science (80-.). **205**: 580–581.

Cornett, R. J., and F. H. Rigler. 1980. The areal hypolimnetic oxygen deficit: An empirical test of the model. Limnol. Oceanogr. **25**: 672–679.

Cowan, J. L. W., and W. R. Boynton. 1996. Sediment-water oxygen and nutrient exchanges along the longitudinal axis of Chesapeake Bay: Seasonal patterns, controlling factors and ecological significance. Estuaries **19**: 562–580.

Cowan, J. L. W., J. R. Pennock, and W. R. Boynton. 1996. Seasonal and interannual patterns of sediment-water nutrient and oxygen fluxes in Mobile Bay, Alabama (USA): Regulating factors and ecological significance. Mar. Ecol. Prog. Ser. **141**: 229–245.

Crusius, J., P. Berg, D. J. Koopmans, and L. Erban. 2008. Eddy correlation measurements of submarine groundwater discharge. Mar. Chem. **109**: 77–85.

D'Avanzo, C., J. N. Kremer, and S. C. Wainright. 1996. Ecosystem production and respiration in response to eutrophication in shallow temperate estuaries. Mar. Ecol. Prog. Ser. **141**: 263–274.

Dansgaard, W. 1964. Stable isotopes in precipitation. Tellus **16**: 436–468.

Davies, J.-M., and R. E. Hecky. 2005. Initial Measurements of Benthic Photosynthesis and Respiration in Lake Erie. J. Great Lakes Res. **31**: 195–207.

Davis, W. S., L. A. Fay, and C. E. Herdendorf. 1987. Overview of USEPA/CLEAR Lake Erie Sediment Oxygen Demand Investigations During 1979. J. Great Lakes Res. **13**: 731–737.

DePinto, J. V, H. Holmberg, T. Redder, E. Verhamme, W. Larson, N. Senjem, and H. Munir. 2009. Linked hydrodynamic-sediment transport-water quality model for support of the Upper Mississippi River-Lake Pepin TMDL.

Diaz, R. J., and R. Rosenberg. 1995. Marine benthic hypoxia: A review of its ecological effects and the behavioural responses of benthic macrofauna. Oceanogr. Mar. Biol. - an Annu. Rev. **33**: 245–303.

Diaz, R. J., and R. Rosenberg. 2008. Spreading dead zones and consequences for marine ecosystems. Science (80-.). **321**: 926–929.

DiToro, D. M. 2001. Sediment Flux Modeling, Wiley-Interscience.

Dolan, D. M., and S. C. Chapra. 2012. Great Lakes total phosphorus revisited: 1. Loading analysis and update (1994-2008). J. Great Lakes Res. **38**: 730–740.

Eadie, B. J., G. L. Bell, and N. Hawley. 1991. Sediment Trap Study in the Green Bay Mass Balance Program: Mass and Organic Carbon Fluxes, Resuspension, and Particle Settling Velocities.

Edwards, W. J., J. D. Conroy, and D. a. Culver. 2005. Hypolimnetic Oxygen Depletion Dynamics in the Central Basin of Lake Erie. J. Great Lakes Res. **31**: 262–271.

Edwards, W. J., F. M. Soster, G. Matisoff, and D. W. Schloesser. 2009. The effect of mayfly (Hexagenia spp.) burrowing activity on sediment oxygen demand in western Lake Erie. J. Great Lakes Res. **35**: 507–516.

Fahnenstiel, G. L., G. A. Lang, T. F. Nalepa, and T. H. Johengen. 1995. Effects of Zebra Mussel (Dreissena polymorpha) Colonization on Water Quality Parameters in Saginaw Bay, Lake Huron. J. Great Lakes Res. **21**: 435–448.

Fahnenstiel, G., S. Pothoven, H. Vanderploeg, D. Klarer, T. Nalepa, and D. Scavia. 2010. Recent changes in primary production and phytoplankton in the offshore region of southeastern Lake Michigan. J. Great Lakes Res. **36**: 20–29.

Fee, E. 1973. A numerical model for determining integral primary production and its application to Lake Michigan. J. Fish. Board Canada **30**: 1447–1468.

Findlay, S. E. G., and R. L. Sinsabaugh. 2003. Aquatic Ecosystems: Interactivity of Dissolved Organic Matter, J.H. Thorp [ed.]. Academic Press.

Fujiwara, T., T. Takahashi, A. Kasai, Y. Sugiyama, and M. Kuno. 2002. The Role of Circulation in the Development of Hypoxia in Ise Bay, Japan. Estuar. Coast. Shelf Sci. **54**: 19–31.

Funkey, C. P., D. J. Conley, N. S. Reuss, C. Humborg, T. Jilbert, and C. P. Slomp. 2014. Hypoxia sustains cyanobacteria blooms in the Baltic Sea. Environ. Sci. Technol. **48**: 2598–2602.

Gat, J. 1996. Oxygen and hydrogen isotopes in the hydrologic cycle. Annu. Rev. Earth Planet. Sci. **24**: 225–262.

Gat, J. R., and Y. Tzur. 1967. Modification of the isotopic composition of rainwater by processes which occur before groundwater recharge. *Isotopes in hydrology*. 49–60.

Gelda, R. K., M. T. Auer, and S. W. Effler. 1995. Determination of sediment oxygen demand by direct measurement and by inference from reduced species accumulation. Mar. Freshw. Res. **46**: 81–88.

Geprägs, P., M. E. Torres, S. Mau, S. Kasten, M. Römer, and G. Bohrmann. 2016. Carbon cycling fed by methane seepage at the shallow Cumberland Bay, South Georgia, sub-Antarctic. Geochemistry, Geophys. Geosystems **17**: 1401–1418.

del Giorgio, P. A., and R. H. Peters. 1993. Balance between Phytoplankton Production and

Plankton Respiration in Lakes. Can. J. Fish. Aquat. Sci. **50**: 282–289.

Gottlieb, E. S., J. H. Saylor, and G. S. Miller. 1990. NOAA Technical Memorandum ERL GLERL-73 Currents and water temperatures observed in Green Bay, Lake Michigan Part I : Winter 1988 -1989 Part II: Summer 1989.

Grenz, C., J. E. Cloern, S. W. Hager, and B. E. Cole. 2000. Nutrient and Oxygen Fluxes During a Spring Phytoplankton bloom in South San Francisco Bay (USA). Mar. Ecol. Prog. Ser. **197**: 67–80.

Grunert, B. 2013. Evaluating the Summer Thermal Structure of Southern Green Bay, Lake Michigan. University of Wisconsin-Milwaukee.

Gupta, P., D. Noone, J. Galewsky, C. Sweeney, and B. H. Vaughn. 2009. Demonstration of high-precision continuous measurements of water vapor isotopologues in laboratory and remote field deployments using wavelength-scanned cavity ring-down spectroscopy (WS-CRDS) technology. Rapid Commun. Mass Spectrom. **23**: 2534–2542.

Halder, J., L. Decrouy, and T. W. Vennemann. 2013. Mixing of Rhine River water in Lake Geneva (Switzerland-France) inferred from stable hydrogen and oxygen isotope profiles. J. Hydrol. **477**: 152–164.

Hamidi, S. A., H. R. Bravo, and J. V. Klump. 2013. Evidence of multiple physical drivers on the circulation and thermal regime in the Green Bay of Lake Michigan. *World Environmental and Water Resources Congress*. 1719–1726.

Hamidi, S. A., H. R. Bravo, J. V. Klump, D. Beletsky, and D. J. Schwab. 2012. Hydrodynamic Model for Green Bay, Lake Michigan. *World Environmental and Water Resources Congress 2012@ Crossing sBoundaries*. 2814–2822.

Hamidi, S. A., H. R. Bravo, J. Val Klump, and J. T. Waples. 2015. The role of circulation and heat fluxes in the formation of stratification leading to hypoxia in Green Bay, Lake Michigan. J. Great Lakes Res. **41**: 1024–1036.

Hammond, D. E., and C. Fuller. 1979. The use of Radon-222 to estimate benthic exchange and atmospheric exchange rates in San Francisco Bay, p. 213–230. *In* American Association for the Advancement of Science- Pacific Division.

Hansen, T. F. 2005. Sediment oxygen demand data logger.

Hanson, P. C., D. L. Bade, S. R. Carpenter, and T. K. Kratz. 2003. Lake metabolism: Relationships with dissolved organic carbon and phosphorus. Limnol. Oceanogr. **48**: 1112–1119.

Hanson, P. C., S. R. Carpenter, N. Kimura, C. Wu, S. P. Cornelius, and T. K. Kratz. 2008. Evaluation of metabolism models for free-water dissolved oxygen methods in lakes. Limnol. Oceanogr. Methods **6**: 454–465.

Hotchkiss, E. R., and R. O. J. Hall. 2014. High rates of daytime respiration in three streams: Use of $\delta^{18}OO_2$ and O_2 to model diel ecosystem metabolism. Limnol. Oceanogr. **59**: 798–810.

Howarth, R., F. Chan, D. J. Conley, J. Garnier, S. C. Doney, R. Marino, and G. Billen. 2011. Coupled biogeochemical cycles: eutrophication and hypoxia in temperate estuaries and coastal marine ecosystems. Front. Ecol. Environ. **9**: 18–26.

Howarth, R. W., R. Marino, R. Garritt, and D. Sherman. 1992. Ecosystem Respiration and Organic-Carbon Processing in a Large, Tidally Influenced River - the Hudson River. Biogeochemistry **16**: 83–102.

Howmiller, R. P., and A. M. Beeton. 1971. Biological evaluation of environmental quality Green Bay Lake, Michigan. J.Wat.Poll.Contr.Fed. **43**: 123–133.

Hu, X., W.-J. Cai, N. N. Rabalais, and J. Xue. 2016. Coupled oxygen and dissolved inorganic carbon dynamics in coastal ocean and its use as a potential indicator for detecting water column oil degradation. Deep Sea Res. Part II Top. Stud. Oceanogr. **129**: 311–318.

HydroQual. 2004. User's Guide for RCA (Release 3.0).

Ito, T., M. J. Follows, and E. A. Boyle. 2004. Is AOU a good measure of respiration in the oceans? Geophys. Res. Lett. **31**: 1–4.

Jahnke, R. A. 1988. A simple, reliable, and inexpensive pore-water sampler. Limnol. Oceanogr. **33**: 483–487.

Jankowski, T., D. M. Livingstone, H. Bührer, R. Forster, and P. Niederhauser. 2006. Consequences of the 2003 European heat wave for lake temperature profiles, thermal stability, and hypolimnetic oxygen depletion: Implications for a warmer world. Limnol. Oceanogr. **51**: 815–819.

Joos, F., G.-K. Plattner, T. F. Stocker, A. Körtzinger, and D. W. R. Wallace. 2003. Trends in marine dissolved oxygen: Implications for ocean circulation changes and the carbon budget. Eos, Trans. Am. Geophys. Union **84**: 197.

Jurtshuk Jr., P. 1996. Bacterial Metabolism, *In* Medical Microbiology. University of Texas Medical Branch at Galveston.

Keister, J. E., E. D. Houde, and D. L. Breitburg. 2000. Effects of bottom-layer hypoxia on abundances and depth distributions of organisms in Patuxent River, Chesapeake Bay. Mar. Ecol. Prog. Ser. **205**: 43–59.

Kennedy, J. 1982. Water-Mass Structures and Exchanges in Green Bay, Lake Michigan. University of Wisconsin-Milwaukee.

Key, R. M., N. L. Guinasso, and D. R. Schink. 1979. Emanation of radon-222 from marine sediments. Mar. Chem. **7**: 221–250.

Kipphut, G. W., and C. S. Martens. 1982. Biogeochemical cycling in an organic-rich coastal marine basin—3. Dissolved gas transport in methane-saturated sediments. Geochim. Cosmochim. Acta **46**: 2049–2060.

Klump, J. V., D. N. Edgington, P. E. Sager, and D. M. Robertson. 1997a. Sedimentary

phosphorus cycling and a phosphorus mass balance for the Green Bay (Lake Michigan) ecosystem. Can. J. Fish. Aquat. Sci. **54**: 10–26.

Klump, J. V., S. A. Fitzgerald, and J. T. Waples. 2009. Benthic biogeochemical cycling, nutrient stoichiometry, and carbon and nitrogen mass balances in a eutrophic freshwater bay. Limnol. Oceanogr. **54**: 692–712.

Klump, J. V., and C. S. Martens. 1981. Biogeochemical cycling in an organic rich coastal marine basin—II. Nutrient sediment-water exchange processes. Geochim. Cosmochim. Acta **45**: 101–121.

Klump, J. V., R. Paddock, D. Lovalvo, M. Doroodchi, C. E. Reimers, J. Waples, R. MacKenzie, S. Wroczynski, and D. Vande Slundt. 1997b. Real-Time Studiesof Benthic-Pelagic Interactions Using BESS: An ROV Driven Benthic Shuttle System. Mar. Technol. Sci. **31**: 21–33.

Kock, A., D. L. Arevalo-Martinez, C. R. Loscher, and H. W. Bange. 2016. Extreme N2O accumulation in the coastal oxygen minimum zone off Peru. Biogeosciences **13**: 827–840.

Kocum, E., D. B. Nedwell, and G. J. C. Underwood. 2002. Regulation of phytoplankton primary production along a hypernutrified estuary. Mar. Ecol. Prog. Ser. **231**: 13–22.

Koopmans, D. J., and P. Berg. 2015. Stream oxygen flux and metabolism determined with the open water and aquatic eddy covariance techniques. Limnol. Oceanogr. **60**: 1344–1355.

Koopmans, D. J., S. L. LaBuhn, and J. V. Klump. 2016. Benthic respiration in Green Bay: Traditional sediment core incubations versus novel aquatic eddy covariance.

Kuivila, K. M., J. W. Murray, A. H. Devol, and P. C. Novelli. 1989. Methane production, sulfate reduction and competition for substrates in the sediments of Lake Washington. Geochim. Cosmochim. Acta **53**: 409–416.

Kuwae, T., K. Kamio, T. Inoue, E. Miyoshi, and Y. Uchiyama. 2006. Oxygen exchange flux between sediment and water in an intertidal sandflat, measured in situ by the eddy-correlation method. Mar. Ecol. Prog. Ser. **307**: 59–68.

LaBuhn, S. L., and J. V. Klump. 2016. Estimating summertime epilimnetic primary production via in situ monitoring in an eutrophic freshwater embayment, Green Bay, Lake Michigan. J. Great Lakes Res. , doi:10.1016/j.jglr.2016.07.028

Lambert, M. J., and W. C. Burnett. 2003. Submarine groundwater discharge estimates at a Florida coastal site based on continuous radon measurements. Biogeochemistry **66**: 55–73.

Lehman, J. T. 1988. Hypolimnetic metabolism in Lake Washington: Relative effects of nutrient load and food web structure on lake productivity1. Limnol. Oceanogr. **33**: 1334–1347.

Lessels, J. S., D. Tetzlaff, C. Birkel, J. Dick, and C. Soulsby. 2016. Water sources and mixing in riparian wetlands revealed by tracers and geospatial analysis. Water Resour. Res. **52**: 456–470.

Levin, L. A., W. Ekau, A. J. Gooday, F. Jorissen, J. J. Middelburg, S. W. A. Naqvi, C. Neira, N. N. Rabalais, and J. Zhang. 2009. Effects of natural and human-induced hypoxia on coastal benthos. Biogeosciences **6**: 2063–2098.

Loewen, M. R., J. D. Ackerman, and P. F. Hamblin. 2007. Environmental implications of stratification and turbulent mixing in a shallow lake basin. Can. J. Fish. Aquat. Sci. **64**: 43–57.

Lohrenz, S. E., G. L. Fahnenstiel, D. G. Redalje, G. A. Lang, M. J. Dagg, T. E. Whitledge, and Q. Dortch. 1999. Nutrients, irradiance, and mixing as factors in regulating primary production in coastal waters impacted by the Mississippi River plume. Cont. Shelf Res. **19**: 1113–1141.

Ludsin, S. A., X. Zhang, S. B. Brandt, M. R. Roman, W. C. Boicourt, D. M. Mason, and M. Costantini. 2009. Hypoxia-avoidance by planktivorous fish in Chesapeake Bay: Implications for food web interactions and fish recruitment. J. Exp. Mar. Bio. Ecol. **381**: S121–S131.

Maccoux, M. J., D. M. Dolan, and S. C. Chapra. 2013. Chloride and total phosphorus budgets for Green Bay, Lake Michigan. J. Great Lakes Res. **39**: 420–428.

MacPherson, T. A., L. B. Cahoon, and M. A. Mallin. 2007. Water column oxygen demand and sediment oxygen flux: Patterns of oxygen depletion in tidal creeks. Hydrobiologia **586**: 235–248.

Malkin, S. Y., S. a. Bocaniov, R. E. Smith, S. J. Guildford, and R. E. Hecky. 2010. In situ measurements confirm the seasonal dominance of benthic algae over phytoplankton in nearshore primary production of a large lake. Freshw. Biol. **55**: 2468–2483.

Manahan, S. E. 2010. Environmental chemistry, CRC Press.

Martens, C. S., G. W. Kipphut, and J. V. Klump. 1980. Sediment-water chemical exchange in the coastal zone traced by in situ Radon-222 flux measurements. Science (80-.). **208**: 285–288.

Mathieu, G. G., P. E. Biscaye, R. A. Lupton, and D. E. Hammond. 1988. System for measurement of 222Rn at low levels in natural waters. Health Phys. **55**: 989–992.

Matisoff, G., E. M. Kaltenberg, R. L. Steely, S. K. Hummel, J. Seo, K. J. Gibbons, T. B. Bridgeman, Y. Seo, M. Behbahani, W. F. James, L. T. Johnson, P. Doan, M. Dittrich, M. A. Evans, and J. D. Chaffin. 2016. Internal loading of phosphorus in western Lake Erie. J. Great Lakes Res. **42**: 1–14.

Matthews, D. A., and S. W. Effler. 2006. Long-term changes in the areal hypolimnetic oxygen deficit (AHOD) of Onondaga Lake: Evidence of sediment feedback. Limnol. Oceanogr. **51**: 702–714.

Matzinger, A., B. Müller, P. Niederhauser, M. Schmid, and A. Wüest. 2010. Hypolimnetic oxygen consumption by sediment-based reduced substances in former eutrophic lakes. Limnol. Oceanogr. **55**: 2073–2084.

210

McCrackin, M. L., H. P. Jones, P. C. Jones, and D. Moreno-Mateos. 2016. Recovery of lakes and coastal marine ecosystems from eutrophication: A global meta-analysis. Limnol. Oceanogr. , doi:10.1002/lno.10441

McNair, J. N., L. C. Gereaux, A. D. Weinke, M. R. Sesselmann, S. T. Kendall, and B. A. Biddanda. 2013. New methods for estimating components of lake metabolism based on free-water dissolved-oxygen dynamics. Ecol. Modell. **263**: 251–263.

Mee, L., J. Friedrich, and M. Gomoiu. 2005. Restoring the Black Sea in Times of Uncertainty. Oceanography **18**: 100–111.

Millard, E., and P. Sager. 1994. Comparison of phosphorus, light climate, and photosynthesis between two culturally eutrophied bays: Green Bay, Lake Michigan, and the Bay of Quinte, Lake Ontario. Can. J. Fish. … **51**: 2579–2590.

Miller, G. S., and J. H. Saylor. 1985. Currents and temperature in Green Bay, Lake Michigan. J. Great Lakes Res. **11**: 97–109.

Mitsch, W. J., J. W. Day, J. W. Gilliam, P. M. Groffman, D. L. Hey, G. W. Randall, and N. Wang. 2001. Reducing nitrogen loading to the Gulf of Mexico from the Mississippi River basin: Strategies to counter a persistent ecological problem. Bioscience **51**: 373–388.

Modlin, R. F., and A. M. Beeton. 1970. Dispersal of Fox River Water in Green Bay, Lake Michigan. *Proceedings of the 13th Conference of Great Lakes Research*. 468–476.

Moore, J. R., R. P. Meyer, and C. L. Morgan. 1973. Investigation of the sediments and potential manganese nodule resources of Green Bay, Wisconsin, University of Wisconsin, Sea Grant College Program,.

Mortimer, C. 1978. Water Movement, Transport and Mixing in Green Bay, Lake Michigan.

Moya, C. E., M. Raiber, M. Taulis, and M. E. Cox. 2016. Using environmental isotopes and dissolved methane concentrations to constrain hydrochemical processes and inter-aquifer mixing in the Galilee and Eromanga Basins, Great Artesian Basin, Australia. J. Hydrol. **539**: 304–318.

Müller, B., L. D. Bryant, A. Matzinger, and A. Wüest. 2012. Hypolimnetic oxygen depletion in eutrophic lakes. Environ. Sci. Technol. **46**: 9964–71.

Naqvi, S. W. A., H. W. Bange, L. Farias, P. M. S. Monteiro, M. I. Scranton, and J. Zhange. 2010. Marine hypoxia/anoxia as a source of CH4 and N2O. Biogeosciences **7**: 2159–2190.

Nixon, S. W. 1995. Coastal marine eutrophication: a definition, social causes, and future concerns. Ophelia **41**: 199–219.

Odum, H. T. 1956. Primary production in flowing waters. Limnol. Oceanogr. **1**: 102–117.

Odum, H. T. 1957. Trophic Structure and Productivity of Silver Springs, Florida on JSTOR. Ecol. Monogr. **27**: 55–112.

Ostrom, N. E., H. J. Carrick, M. R. Twiss, and L. Piwinski. 2005. Evaluation of primary

production in Lake Erie by multiple proxies. Oecologia **144**: 115–124.

Patterson, J. C., B. R. Allanson, and G. N. Ivey. 1985. A dissolved oxygen budget model for Lake Erie in summer. Freshw. Biol. **15**: 683–694.

Pearson, T. H., and R. Rosenberg. 1978. Macrobenthic succession in relation to organic enrichment and pollution of the marine environment. Oceanogr. Mar. Biol. - an Annu. Rev. **16**: 229–311.

Persson, L., V. Harris, C. Lukas, J. Christie, H. J. Harris, L. Meyers, J. Sullivan, P. Allen, and R. Baba. 1988. Lower Green Bay Remedial Action Plan.

Petticrew, E. L., and J. M. Arocena. 2001. Evaluation of iron-phosphate as a source of internal lake phosphorus loadings. *Science of the Total Environment*. 87–93.

Pollution, W. S. C. on W. 1939. Investigation of the pollution of the Fox and East Rivers and of Green Bay in the vicinity of the City of Green Bay.

Qualls, T., H. J. B. Harris, and V. Harris. 2013. The State of the Bay The Condition of the Bay of Green Bay / Lake Michigan 2013.

Qualls, T. M., D. M. Dolan, T. Reed, M. E. Zorn, and J. Kennedy. 2007. Analysis of the Impacts of the Zebra Mussel, Dreissena polymorpha, on Nutrients, Water Clarity, and the Chlorophyll-Phosphorus Relationship in Lower Green Bay. J. Great Lakes Res. **33**: 617–626.

Quay, P. D., W. S. Broecker, R. H. Hesslein, and D. W. Schindler. 1980. Vertical diffusion rates determined by tritium tracer experiments in the thermocline and hypolimnion of two lakes. Limnol. Oceanogr. **25**: 201–218.

Quinlan, R., A. M. Paterson, J. P. Smol, M. S. V Douglas, and B. J. Clark. 2005. Comparing different methods of calculating volume-weighted hypolimnetic oxygen (VWHO) in lakes. Aquat. Sci. **67**: 97–103.

Rabalais, N. N., W.-J. Cai, J. Carstensen, D. J. Conley, B. Fry, X. Hu, Z. Quiñones-Rivera, R. Rosenberg, C. P. Slomp, R. E. Turner, M. Voss, B. Wissel, and J. Zhang. 2014. Eutrophication-driven deoxygenation in the coastal ocean. Oceanography **27**: 172–183.

Read, J., V. Klump, T. Johengen, D. Schwab, K. Paige, S. Eddy, E. Anderson, and C. Manninen. 2010. Working in Freshwater: The Great Lakes Observing System Contributions to Regional and National Observations, Data Infrastructure, and Decision Support. Mar. Technol. Soc. J. **44**: 84–98.

Redfield, A. C., B. H. Ketchum, and F. A. Richards. 1963. The influence of organisms on the composition of sea water, p. 26–77. *In* The sea. Wiley.

Reimers, C. E., H. T. Özkan-Haller, P. Berg, A. Devol, K. McCann-Grosvenor, and R. D. Sanders. 2012. Benthic oxygen consumption rates during hypoxic conditions on the Oregon continental shelf: Evaluation of the eddy correlation method. J. Geophys. Res. Ocean. **117**.

Renaud, P. E., N. Morata, M. L. Carroll, S. G. Denisenko, and M. Reigstad. 2008. Pelagic–benthic coupling in the western Barents Sea: Processes and time scales. Deep Sea Res. Part II Top. Stud. Oceanogr. **55**: 2372–2380.

Renaud, P. E., A. Riedel, C. Michel, N. Morata, M. Gosselin, T. Juul-Pedersen, and A. Chiuchiolo. 2007. Seasonal variation in benthic community oxygen demand: A response to an ice algal bloom in the Beaufort Sea, Canadian Arctic? J. Mar. Syst. **67**: 1–12.

Richey, J. E., R. C. Wissmar, a H. Devol, G. E. Likens, J. S. Eaton, R. G. Wetzel, W. E. Odum, N. M. Johnson, O. L. Loucks, R. T. Prentki, and P. H. Rich. 1978. Carbon flow in four lake ecosystems: a structural approach. Science **202**: 1183–6.

Riemann, B., J. Carstensen, K. Dahl, H. Fossing, J. W. Hansen, H. H. Jakobsen, A. B. Josefson, D. Krause-Jensen, S. Markager, P. A. Stæhr, K. Timmermann, J. Windolf, and J. H. Andersen. 2016. Recovery of Danish Coastal Ecosystems After Reductions in Nutrient Loading: A Holistic Ecosystem Approach. Estuaries and Coasts **39**: 82–97.

Rigosi, A., P. Hanson, D. P. Hamilton, M. Hipsey, J. A. Rusak, J. Bois, K. Sparber, I. Chorus, A. J. Watkinson, B. Qin, B. Kim, and J. D. Brookes. 2015. Determining the probability of cyanobacterial blooms: the application of Bayesian networks in multiple lake systems. Ecol. Appl. **25**: 186–199.

Robertson, D. M., and D. A. Saad. 2011. Nutrient Inputs to the Laurentian Great Lakes by Source and Watershed Estimated Using SPARROW Watershed Models. J. Am. Water Resour. Assoc. **47**: 1011–1033.

Robertson, D. M., D. A. Saad, D. E. Christiansen, and D. J. Lorenz. 2016. Simulated impacts of climate change on phosphorus loading to Lake Michigan. J. Great Lakes Res. **42**: 536–548.

Rucinski, D. K., D. Beletsky, J. V. DePinto, D. J. Schwab, and D. Scavia. 2010. A simple 1-dimensional, climate based dissolved oxygen model for the central basin of Lake Erie. J. Great Lakes Res. **36**: 465–476.

Sager, P. E., and J. H. Wiersma. 1972. Nutrient discharges to Gren Bay, Lake Michgian from the lower Fox River. *Proceedings of the 15th Conference of Great Lakes Research*. 132–148.

Sager, P. E., and J. H. Wiersma. 1975. Phosphorus Sources for Lower Green Bay, Lake Michigan. Water Pollut. Control Fed. **47**: 504–514.

Sansone, F. J., A. W. Graham, and W. M. Berelson. 2004. Methane along the western Mexican margin. Limnol. Oceanogr. **49**: 2242–2255.

Schindler, D. E., and M. D. Scheuerell. 2002. Habitat Coupling in Lake Ecosystems. Oikos **98**: 177–189.

Schraufnagel, F. H., L. A. Montie, L. A. Leuschow, J. Lissack, & Karl, G., and J. R. McKersie. 1968. Report on an investigation of the pollution in the lower Fox River and Green Bay made during 1966 and 1967.

Schwab, D. J., and K. W. Bedford. 1994. Initial implementation of the Great Lakes forecasting

system: A real-time system for predicting lake circulation and thermal structure. Water Pollut. Res. J. Cananda **29**: 203–220.

Scully, M. E. 2010. Wind Modulation of Dissolved Oxygen in Chesapeake Bay. Estuaries and Coasts **33**: 1164–1175.

Scully, M. E. 2016. The contribution of physical processes to inter-annual variations of hypoxia in Chesapeake Bay: A 30-yr modeling study. Limnol. Oceanogr. , doi:10.1002/LNO.10372

Shaw, G. D., E. S. White, and C. H. Gammons. 2013. Characterizing groundwater–lake interactions and its impact on lake water quality. J. Hydrol. **492**: 69–78.

Smith, C. G., J. E. Cable, J. B. Martin, and M. Roy. 2008. Evaluating the source and seasonality of submarine groundwater discharge using a radon-222 pore water transport model.

Smith, P. L., R. A. Ragotzkie, A. W. Andren, and H. J. Harris. 1988. Estuary rehabilitation: The Green Bay story. Oceanus **31**: 12–20.

Smith, S. V. 1985. Physical, chemical and biological characteristics of CO2 gas flux across the air-water interface. Plant, Cell Environ. **8**: 387–398.

Staehr, P. A., D. Bade, M. C. Van de Bogert, G. R. Koch, C. Williamson, P. Hanson, J. J. Cole, and T. Kratz. 2010a. Lake metabolism and the diel oxygen technique: State of the science. Limnol. Oceanogr. Methods **8**: 628–644.

Staehr, P. A., K. Sand-Jensen, A. L. Raun, B. Nilsson, and J. Kidmose. 2010b. Drivers of metabolism and net heterotrophy in contrasting lakes. Limnol. Oceanogr. **55**: 817–830.

Stainton, M. P. 1973. A Syringe Gas-Stripping Procedure for Gas-Chromatographic Determination of Dissolved Inorganic and Organic Carbon in Fresh Water and Carbonates in Sediments. J. Fish. Res. Board Canada **30**: 1441–1445.

De Stasio, B. T., M. B. Schrimpf, A. E. Beranek, and W. C. Daniels. 2008. Increased chlorophyll a, phytoplankton abundance, and cyanobacteria occurrence following invasion of Green Bay, Lake Michigan by dreissenid mussels. Aquat. Invasions **3**: 21–27.

Steckbauer, A., C. M. Duarte, J. Carstensen, R. Vaquer-Sunyer, and D. J. Conley. 2011. Ecosystem impacts of hypoxia: thresholds of hypoxia and pathways to recovery. Environ. Res. Lett. **6**: 25003.

Sterner, R. W. 2010. In situ-measured primary production in Lake Superior. J. Great Lakes Res. **36**: 139–149.

Strayer, D. 1988. On the limits to secondary production. Limnol. Oceanogr. **33**: 1217–1220.

Taft, J. L., W. R. Taylor, E. O. Hartwig, and L. Randy. 1980. Seasonal Oxygen Depletion in Chesapeake Bay. Estuaries **3**: 242–247.

Tech, T., and E. Place. 2007. The Environmental Fluid Dynamics Code User Manual. 231.

Thamdrup, B., J. W. Hansen, and B. B. Jørgensen. 1998. Temperature dependance of aerobic

respiration in a coastal sediment. FEMS Microbiol. Ecol. **25**: 189–200.

Tobias, C. R., J. K. Böhlke, and J. W. Harvey. 2007. The oxygen-18 isotope approach for measuring aquatic metabolism in high productivity waters. Limnol. Oceanogr. **52**: 1439–1453.

Todd, J. F., R. J. Elsinger, and W. S. Moore. 1988. The distributions of uranium, radium and thorium isotopes in two anoxic fjords: Framvaren Fjord (Norway) and Saanich Inlet (British Columbia). Mar. Chem. **23**: 393–415.

United States - Canada. 2013. Great Lakes Water Quality Agreement.

Valenta, T. 2013. Oxygen Depletion in Green Bay. University of Wisconsin- Green Bay.

Vaquer-Sunyer, R., and C. M. Duarte. 2008. Thresholds of hypoxia for marine biodiversity. Proc. Natl. Acad. Sci. U. S. A. **105**: 15452–15457.

Vaquer-Sunyer, R., and C. M. Duarte. 2010. Sulfide exposure accelerates hypoxia-driven mortality. Limnol. Oceanogr. **55**: 1075–1082.

Verhamme, E., T. Redder, D. Schlea, J. Grush, J. Bratton, and J. DePinto. 2016. Development of the Western Lake Erie Ecosystem Model (WLEEM): application to connect phosphorus loads to cyanobacteria biomass. J. Great Lakes Res. **in review**, doi:10.1016/j.jglr.2016.09.006

Walker, W. W. 1979. Use of hypolimnetic oxygen depletion rate as a trophic state index for lakes. Water Resour. Res. **15**: 1463–1470.

Wang, S., M. Zhang, Y. Che, F. Chen, and F. Qiang. 2016. Contribution of recycled moisture to precipitation in oases of arid central Asia: A stable isotope approach. Water Resour. Res. **52**: 3246–3257.

Wankel, S. D., C. Kendall, C. A. Francis, and A. Paytan. 2006. Nitrogen sources and cycling in the San Francisco Bay Estuary: A nitrate dual isotopic composition approach. Limnol. Oceanogr. **51**: 1654–1664.

Wanninkhof, R. 1992. Relationship Between Wind Speed and Gas Exchange. J. Geophys. Res. **97**: 7373–7382.

Waples, J. T. 1998. Air-water gas exchange and the carbon cycle of Green Bay, Lake Michigan. University of Wisconsin-Milwaukee.

Waples, J. T., and J. V. Klump. 2002. Biophysical effects of a decadal shift in summer wind direction over the Laurentian Great Lakes. Geophys. Res. Lett. **29**, doi:10.1029/2001GL014564

Watras, C. J., K. A. Morrison, N. R. Lottig, and T. K. Kratz. 2015. Comparing the diel cycles of dissolved organic matter fluorescence in a clear-water and two dark-water Wisconsin lakes: potential insights into lake metabolism. Can. J. Fish. Aquat. Sci. **73**: 65–75.

Weiss, R. F. 1970. The solubility of nitrogen, oxygen and argon in water and seawater. Deep Sea

Res. Oceanogr. Abstr. **17**: 721–735.

Wetzel, R. G. 2001. Limnology: Lake and River Ecosystems, 3rd ed. Academic Press.

Whitlock, M. C., and D. Schluter. 2009. Regression and correlation, p. 431–512. *In* The Analysis of Biological Data. Roberts and Company Publishers.

WIDNR. 2011. Stage 2 remedial action plan update for the Lower Green Bay and Fox River area of concern.

Williamson, J. E., and J. M. Carter. 2001. Water-Quality Characteristics in the Black Hills Area, South Dakota.

Wisconsin Department of Natural Resources. 1993. Lower Green Bay remedial action plan 1993 update for the Lower Green Bay and Fox River Area of Concern.

Wisconsin Initiative on Climate Change Impacts (WICCI). 2011. Wisconsin's changing climate: Impacts and adaptation.

Wise, S. A., and R. L. Watters. 2011. Report of investigation: Reference material 8535a VSMOW2 Vienna Standard Mean Ocean Water.

Woodwell, G. M., and R. H. Whittaker. 1968. Primary Production in Terrestrial Ecosystems. Am. Zool. **8**: 19–30.

Zhou, Y., D. R. Obenour, D. Scavia, T. H. Johengen, and A. M. Michalak. 2013. Spatial and temporal trends in Lake Erie hypoxia, 1987-2007. Environ. Sci. Technol. **47**: 899–905.

Zhou, Y., D. Scavia, and A. M. Michalak. 2014. Nutrient loading and meteorological conditions explain interannual variability of hypoxia in the Chesapeake Bay. Limnol. Oceanogr. **59**: 373–384.

Zhu, Z.-Y., J. Zhang, Y. Wu, Y.-Y. Zhang, J. Lin, and S.-M. Liu. 2011. Hypoxia off the Changjiang (Yangtze River) Estuary: Oxygen depletion and organic matter decomposition. Mar. Chem. **125**: 108–116.

APPENDIX: Phosphate release from anoxic sediments

This section provides evidence of phosphate release from sediment cores when the oxygen is depleted. The nutrient samples were collected through the sampling ports of the core tops used in the incubation experiments. Samples were analyzed on a SEAL auto-analyzer at the School of Freshwater Sciences. Provided dissolved oxygen concentrations are recorded from the oxygen meter immediately preceding the collection of sample water.

Table 29: Dissolved oxygen and phosphate concentration data for triplicate sediment core incubation experiments that showed signs of phosphate release under sustained anoxic conditions. *** indicates that no data was available at that sample period for the given parameter.

Site	Date/Time of Sample	Sample Number	Dissolved oxygen (mg/L)			Phosphate (µmol/L)		
			Core 1	Core 2	Core 3	Core 1	Core 2	Core 3
GB17	7/31/2013 15:03	1	7.3	4.3	4.3	0.37	0.51	0.27
	7/31/2013 16:40	2	6.8	4.2	5.8	0.34	0.52	0.45
	7/31/2013 19:47	3	6.0	4.0	5.1	0.27	0.11	0.46
	7/31/2013 21:31	4	5.5	3.9	4.9	0.31	0.38	0.09
	8/1/2013 7:39	5	4.6	1.8	3.0	0.57	0.13	0.88
	8/1/2013 11:25	6	4.2	1.9	2.5	0.40	0.67	0.79
	8/1/2013 14:45	7	3.6	1.8	2.4	0.32	0.54	0.79
	8/1/2013 17:18	8	3.2	1.6	2.4	0.39	0.33	0.16
	8/5/2013 10:27	9	0.0	0.0	0.0	9.26	8.10	8.62
GB9	7/31/13 16:45	1	8.3	8.2	7.3	0.28	0.24	0.11
	7/31/13 19:54	2	3.4	3.5	3.0	0.31	0.41	0.45
	7/31/13 21:38	3	3.5	3.4	2.9	0.38	0.06	0.12
	8/1/13 7:46	4	2.7	1.4	4.0	0.29	0.24	0.36
	8/1/13 11:29	5	2.7	0.8	2.7	0.53	0.76	0.49

	8/1/13 14:52	6	2.4	0.5	1.9	0.55	0.92	0.59
	8/1/13 17:22	7	2.1	0.3	1.7	0.20	0.50	0.22
	8/5/13 10:33	8	1.1	0.0	0.0	1.72	14.34	6.83
GB6	8/27/13 17:05	1	8.6	8.8	4.8	0.31	0.55	1.01
	8/27/13 21:52	2	3.9	4.6	2.5	1.10	0.57	0.67
	8/28/13 7:48	3	1.9	5.5	0.7	0.52	0.50	0.56
	8/28/13 13:09	4	1.5	5.8	0.4	0.43	0.92	1.14
	8/28/13 18:44	5	0.6	5.8	0.3	0.72	0.75	0.69
	8/28/13 22:27	6	0.2	5.2	0.4	0.22	0.65	0.59
	8/29/13 8:35	7	0.1	5.3	0.0	0.88	1.07	1.07
	8/29/13 15:43	8	0.1	4.9	0.1	0.58	0.33	0.86
	8/31/13 10:54	9	0.2	5.4	0.1	5.73	1.16	7.17
	9/1/13 11:18	10	0.1	6.0	0.2	10.60	***	12.30
	9/3/13 16:01	11	***	***	***	21.56	***	25.19
	9/4/13 10:04	12	0.5	6.4	0.1	24.78	2.49	27.68
	9/4/13 17:53	13	0.2	***	0.1	23.56	***	25.67
	9/5/13 9:29	14	0.0	6.3	0.0	25.74	3.09	24.83
	9/5/13 16:28	15	0.7	6.4	0.1	24.21	4.21	27.84
	9/6/13 8:36	16	0.1	6.9	0.0	26.41	3.31	30.68
GB12	8/27/13 19:05	1	4.7	4.0	5.1	0.58	0.31	0.43
	8/27/13 21:55	2	5.5	4.7	2.9	0.23	0.69	0.39
	8/28/13 7:51	3	4.0	2.4	1.3	0.40	1.09	0.97
	8/28/13 13:12	4	3.4	1.7	1.2	0.41	1.32	0.70
	8/28/13 18:47	5	2.5	0.8	0.9	0.66	1.15	0.68
	8/28/13 22:31	6	1.9	0.6	0.9	0.49	0.94	0.29
	8/29/13 8:38	7	1.0	0.2	0.9	0.82	0.57	0.64
	8/29/13 15:48	8	0.5	0.0	0.0	1.09	1.25	1.19
	8/31/13 10:57	9	0.1	0.0	0.6	1.23	2.79	1.58
	9/1/13 11:05	10	0.0	0.0	0.3	1.04	3.79	1.37

	9/3/13 16:05	11	***	***	***	5.18	11.58	3.97
	9/4/13 10:09	12	0.1	0.1	0.0	4.91	15.34	6.48
	9/4/13 17:56	13	0.1	0.1	0.0	3.40	15.60	7.95
	9/5/13 9:35	14	0.0	0.0	0.3	2.80	16.42	11.02
	9/5/13 16:32	15	0.1	0.1	0.0	2.62	18.46	12.15
	9/6/13 8:39	16	0.0	0.0	0.4	3.21	20.18	***
GB13	8/27/13 15:42	1	7.5	4.6	5.7	1.19	0.46	0.68
	8/27/13 21:49	2	5.1	3.4	4.4	0.49	0.87	0.65
	8/28/13 7:45	3	3.2	1.9	2.1	0.45	0.94	0.91
	8/28/13 13:07	4	2.2	1.5	1.5	1.21	1.52	1.08
	8/28/13 18:41	5	1.1	0.6	0.8	1.10	1.00	1.31
	8/28/13 22:23	6	0.7	0.3	0.6	1.06	1.00	0.76
	8/29/13 8:32	7	0.0	0.0	0.1	1.44	1.53	1.07
	8/29/13 15:39	8	0.0	0.0	0.2	1.65	1.41	0.62
	8/31/13 10:50	9	0.0	0.1	0.1	7.30	8.23	5.12
	9/1/13 11:27	10	0.0	0.0	0.0	13.93	13.91	10.45
	9/3/13 15:55	11	***	***	***	30.07	31.79	23.01
	9/4/13 10:00	12	0.0	0.0	0.1	35.82	36.58	27.36
	9/4/13 17:49	13	0.0	0.0	0.1	29.82	28.96	24.85
	9/5/13 9:24	14	0.0	0.0	0.1	31.98	29.02	28.09
	9/5/13 16:22	15	0.0	0.0	0.1	34.56	31.75	29.35
	9/6/13 8:31	16	0.0	0.0	0.1	32.78	35.26	30.88
GBMSD26	9/25/13 16:13	1	9.1	8.6	8.4	1.02	0.27	0.56
	9/25/13 17:57	2	7.8	7.6	6.8	0.33	0.04	0.28
	9/25/13 20:45	3	6.6	5.9	5.1	0.41	0.14	0.80
	9/26/13 7:56	4	1.3	0.2	0.7	0.85	0.72	0.83
	9/26/13 13:25	5	0.8	0.0	0.8	0.86	0.74	0.76
	9/27/13 15:30	6	0.5	0.2	0.3	1.51	1.72	0.99
	9/28/13 16:56	7	0.0	0.0	0.1	2.36	2.49	1.49

	Date & Time							
	9/30/13 9:09	8	0.0	0.0	0.2	4.41	3.56	3.62
	9/30/13 10:18	9	0.0	0.0	0.1	7.13	3.92	5.83
GBMSD50	9/25/13 16:07	1	8.3	7.7	8.1	0.48	0.70	1.01
	9/25/13 18:02	2	6.9	7.0	6.9	0.40	0.84	0.74
	9/25/13 20:49	3	6.0	6.2	6.1	0.71	0.41	0.05
	9/26/13 8:01	4	3.2	3.0	5.5	0.05	0.35	0.12
	9/26/13 13:31	5	2.1	2.3	4.4	0.15	0.26	0.30
	9/27/13 15:30	6	0.5	0.2	3.7	0.04	0.25	0.11
	9/28/13 17:03	7	0.0	0.0	2.3	1.71	0.90	0.36
	9/30/13 9:10	8	0.0	0.0	1.8	5.23	3.48	0.27
	9/30/13 10:22	9	0.0	0.1	3.4	8.91	7.31	0.26

CURRICULUM VITAE

SHELBY LABUHN
600 E. Greenfield Ave., Milwaukee, WI 53204
(906) 440-0224   sllabuhn@uwm.edu

EDUCATION

Ph.D. Freshwater Sciences   University of Wisconsin-Milwaukee   *Fall 2016*
   Dissertation: *A multi-faceted biogeochemical approach to analyzing hypoxia in Green Bay, Lake Michigan*

B.S. Environmental Chemistry, *magna cum laude*   Lake Superior State University
      May 2011
   Senior Thesis: *A Pilot Study to Determine an Effective Technology to Remove Geosmin and 2-Methylisoborneol for the City of Fairmont*

EXPERIENCE

Great Lakes WATER Institute/School of Freshwater Sciences   Milwaukee, Wisconsin
Graduate Research Assistant   June 2011-present
- Design dissertation research goals, design and perform experiments to gather results and utilize historical datasets to study system changes
- Develop necessary inputs of data from multiple sources to utilize in EFDC-RCA models for studying Green Bay dynamics over differing watershed and climate scenarios
- Analyze collected water samples for radon-222, $D_2^{18}O$ and methane to evaluate water transport and mixing; analyze phosphorus, nitrogen, and TSS to determine water quality condition
- Collect and process sediment samples for oxygen uptake experiments, porewater extraction for nutrients and sediment-water gas exchange, core sectioning for depositional studies
- Participation in monthly research cruises includes deployment of GLOS buoy and long-term moorings with data loggers and YSI Sondes to measure water quality, take vertical profiles with YSI Sondes and Seabird CTD, data entry, organization and analysis
- Perform managerial duties of students during 2 study abroad-research trips to Laguna Bacalar, Mexico, perform community outreach to promote the School of Freshwater Sciences

R/V Oceanus, Oregon State University, Newport, Oregon
Assistant Scientist   July 2013

221

- Deploy eddy correlation and microelectrode profiler landers to study sediment-water processes of coastal Pacific sediments
- Perform mircoelectrode preparation, maintenance, and calibration
- Assist with multicorer and CTD deployments/recovery, provide other help as needed, 10 days of ship experience

R/V New Horizon, Scripps Institution of Oceanography, San Diego, California
Chief Scientist Training Cruise Participant   November 2012
- Design research plan for 7-day cruise and coordinate efforts with 12 scientists across U.S.
- Attend 2-day UNOLS workshop on chief scientist preparations and execute cruise plan including mobilization, sample collection and demobilization, assist with a variety of research tasks

R/V Ronald H. Brown, National Oceanic and Atmospheric Administration (NOAA), USA
Assistant Scientist   July-August 2011
- Operate underway-CTD (uCTD), CTD and XBT, collect CTD samples for oxygen and salinity
- Assist in repairs of scientific equipment including uCTD, CTD, and XBT
- Assist in ozone sonde launches, provide other meteorological experiment help as needed
- 34 days of ship experience from Charleston, South Carolina to Cape Town, South Africa

Atlantic Oceanographic and Meteorological Lab, NOAA, Miami, Florida
Ernst F. Hollings Intern   June-August 2010
- Assist in establishing an *in-situ* data monitoring system with a linked time-lapse photography of Biscayne Bay to evaluate baseline conditions before Port of Miami expansion
- Participate in routine nutrient monitoring of Florida Bay and Gulf of Mexico, including 5 days aboard R/V Savannah and 4-day small boat operation

Environmental Analysis Lab, LSSU, Sault Ste Marie, Michigan
Student Technician   June 2009-May 2011
- Analyze samples for various water quality parameters including coliform/E-coli., taste and odor compounds by SPME GC-MS, anions by IC, Total P by UV/VIS
- Perform algal toxin (microcystin) analysis by HPLC and ELISA
- Help to develop standard lab methods for SPME GC-MS

Learning Center, LSSU, Sault Ste Marie, Michigan
Chemistry Tutor and Supplemental Instructor   September 2008-
May 2011
- Assist students with questions as necessary, offer support during practice problems and homework, clarify material, provide pre-exam preparation quizzes
- Prepare educational material related to in-class lectures

222

- Front Desk Receptionist and Manager for 2 semesters each

AWARDS

- CILER Graduate Fellowship, 2015-16
- UWM Distinguished Dissertator Graduate School Fellowship, 2014-15
- UWM Distinguished Graduate School Fellowship, 2013-14
- UNOLS/NSF/ONR Annual Meeting Early Career Scientist Participant, March 2014
- ASLO Student Travel Award Participant, February 2014
- UNOLS Early Career Chief Scientist Training Program Participant, November 2012
- Oceans and Human Health NOAA Fellowship, 2011-2012
- School of Freshwater Sciences Watertech Scholarship, October 2012
- Ernest F. Hollings NOAA Scholarship, 2009-11
- Commencement Student Respondent, May 2011
- LSSU Undergraduate Research Grant Recipient, February 2011
- Alpha Chi National Honor Society, 2010-11
- LSSU Faculty Association Scholarship, January 2011
- West Michigan Air and Waste Management Association Scholarship, April 2009
- President's Distinguished Scholarship, 2007-11
- John Lehman Chemistry Scholarship, 2007-08

PUBLICATIONS

- LaBuhn, S. and Klump. J.V. 2016. Journal of Great Lakes Research. Estimating summertime primary production via *in-situ* monitoring in an eutrophic freshwater embayment, Green Bay, Lake Michigan."

PRESENTATIONS

- LaBuhn, S., Wilcox, E., Valenta, T., Qualls, T., Klump, J., and Kennedy, J. 2016. Estimating summertime primary production via *in-situ* monitoring in Green Bay, Lake Michigan. International Association for Great Lakes Research Annual Meeting. Guelph, Ontario.
- LaBuhn, S., Koopmans, D., Berg, P. and Klump, J. 2015. Constructing an oxygen budget for Green Bay, Lake Michigan. Association of Sciences for Limnology and Oceanography Aquatic Sciences Meeting. Granada, Spain.
- LaBuhn, S, Klump, J., Anderson, P. 2014. Identifying horizontal and vertical mixing in Green Bay, Lake Michigan with two natural tracers- radon-222 and D218O. Ocean Sciences Meeting. Honolulu, HI.
- LaBuhn, S. and Klump, V. Natural tracers of water movements and gas fluxes. 2013. Lake Michigan: State of the Lake and Great Lakes Beach Association Joint Conference. Sheboygan, WI.

- Grunert, B., LaBuhn, S. and Klump, V. Climate and the aquatic environment: Green Bay, Lake Michigan. 2013. International Association for Great Lakes Research Annual Meeting. West Lafayette, IN.
- LaBuhn, S., Grunert, B., Waples, J. and Klump, V. Comparative potential effects of climate on Green Bay stratification. March 2013. Recent Changes in the Biogeochemistry of the Great Lakes System Workshop. Detroit, MI.
- LaBuhn, S.L., Maas, M., Klump, V. and Kaster, J. Limnological Survey of Hydrochemical Parameters within Laguna Bacalar, Quintana Roo, Mexico. 2013. Association of Sciences for Limnology and Oceanography Aquatic Sciences Meeting. New Orleans, LA.
- Klump, J.V., Waples, J.T., Valenta, T, LaBuhn, S.L., Anderson, P., Weckerly, K. and Szmania, D. Hypoxia and Climate in Green Bay, Lake Michigan. 2012. Oceans and Human Health Gordon Conference. Biddeford, ME.
- LaBuhn, S., C. Burrows, C. Groff, N. Neureuther, S. Schaal, and J. Volk, Ana Flores Cupul, Ana Beatriz Martinez Dominguez, Milagros Medina Poot. Chemistry and preliminary microbial communities in Laguna Bacalar, Yucatan Peninsula, Mexico. 2012. International Stromatolite Symposium. Bacalar, Mexico.
- LaBuhn, S. and Westrick, J. A pilot study to determine an effective technology to remove geosmin and methylisoborneol for the City of Fairmont. 2011. Borchardt Conference: Advancements in Water and Wastewater. Ann Arbor, MI.
- LaBuhn, S., Carsey, T.P. and Stamates, J. A spatial characterization of Biscayne Bay. 2010. NOAA's Office of Education Summer Symposium. Silver Spring, MD.

ACTIVITIES

- Student Rep on Academic Planning and Curriculum Committee September 2015-August 2016
- Harborside Academy Middle School Science Presenter, UWM
  January 2014-16
  Present information about School of Freshwater Sciences, discuss current research occurring at SFS, answer questions about career paths and freshwater research
- Girl Scout Freshwater Sciences Demonstrator, UWM   March 2015
  Lead Girl Scouts around Freshwater Sciences School, demonstrate research done on R/V Neeskay, map reading exercises, discuss careers in science
- Regional Ocean Science Bowl Session Moderator, UWM   February 2015
  Act as head individual in competition room for high school students, read aloud and accept/reject student responses to questions, set pace of game.
- Science Leader, UWM American-Indian Summer Research Cruise   July 2014
  Collaborate and design research plan for 1-day cruise with high school summer program, teach students how to perform variety of sampling skills, serve as science expert, initiate discussions on present water issues.

- National Ocean Science Bowl Chief Science Judge, UWM   April 2013
    Evaluated challenge questions; identified other possible acceptable answers; interpreted, reviewed and accepted/rejected challenged verbal answers
- Science Olympiad Event Supervisor, UWM   April 2013
    Assist in developing exam and rubric for "Water Resources" section of WI Science Olympiad, serve as test room moderator and exam grader, rank teams by final score, help set-up and teardown exam room.
- Sturgeon Bowl Tour Guide, School of Freshwater Sciences
        February 2013
- WATER Council, University of Wiscsonsin-Milwaukee   September 2011-Present
    Volunteer within the community to promote water resource protection, assist with mini-grant proposal to SWWT Water for rain barrel distribution and support with distribution efforts, served at the Global Water Center grand opening.
- Chemistry Club, LSSU   September 2007-May 2011
    o President- Organize meetings and group events, attend Presidents Council, chair Standards Board, organize fundraisers, organize community outreach events, enforce by-laws and address member ideas and concerns
    o Vice President- Organize fundraisers, assist in running meetings, plan trips and group activities, coordinate high school outreach events

- Varsity Women's Track and Field, LSSU   September 2007-May 2008

SKILLS

- YSI Sonde calibration, deployment and troubleshooting
- PO_4 and NO_3 analysis via colorometric and automated sampler analyses
- Instrument knowledge of GC-MS, HPLC, Picarro Isotope Analyzer
- Software usage of SigmaPlot, Surfer, R and ArcGIS 9.x/10
- Microsoft Office Software, including Word, Excel, PowerPoint and Access
- Student managerial experience
- Beginning to intermediate Spanish

CERTIFICATIONS

- OSHA Hazwoper 40-Hour Certification, April 2011
- PADI Open Water Scuba Diving, October 2009